Dissertation

Holocene human impact, climate and environment in the northern Central Alps:

A geochemical approach on mountain peatlands

–

Thesis in fulfilment of a Doctor of Natural Sciences (Dr. rer. nat.) as part of a binational doctoral degree procedure (cotutelle)

between

Institut National Polytechnique de Toulouse (France)

and

The Faculty of Mathematics and Natural Sciences at

Christian-Albrechts-Universität zu Kiel (Germany)

submitted by

Clemens von Scheffer

2019

Supervisors:

Dr. Gaël Le Roux (Toulouse INP)

Prof. Dr. Ingmar Unkel (Kiel University)

Date of Disputation: 03.07.2019

Examination chairperson: Prof. Dr. Rainer Duttmann

External reviewer 1: Dr. habil. Anne-Véronique Walter-Simonnet

External reviewer 2: Dr. Karin Koinig

Place of Disputation: Kiel

"We are all part of the same compost heap"

T. *Durden*

Abstract (English)

Since the last deglaciation the European Alps have experienced several phases of human colonisation from different directions and societies. However, the interaction of climate, human impact and environment is still not fully understood in this high mountain region. In particular, information on the time and scale of human impact in the northern Central Alps (NCA) during the Holocene is missing. This study fills this gap by using geochemical, pollen and radiocarbon analyses in comparison to regional archaeological and historical data. Mires in three areas of the NCA were selected as study sites: Kleinwalser Valley (Vorarlberg, Austria), Piller Mire (Tyrol, Austria) and upper Fimba Valley (Grisons, Switzerland), situated in an altitudinal range of 1100 to 2400 m a.s.l.

These mires were cored and analysed. The use of geochemical proxies (lithogenic elements, trace metals) in peat is a well-established method to detect mineral input, erosion or metallurgical activities. Despite an advantage of a fast sample preparation and measurement, applying portable X-Ray-Fluorescence analysis (pXRF) on mountain mires is an uncommon approach, mainly due to limitations by low count rates, matrix effects or lacking calibrations for organic materials. By calibrating pXRF with measurements of quantitative Inductively Coupled Plasma – Mass Spectrometry (ICP-MS), these issues could be overcome, showing that, Ti, Pb, Sr, Zn, K, S, Fe, V, Zr, and - to some extent - Rb, Ca and Mn, can be successfully calibrated and used as palaeoenvironmental proxies in peat. These proxies allow the following conclusions:

At high elevations, periglacial processes influence the deposition processes in the mires. Around 8200 and in the late 7th millennium BP, wetter and colder climate conditions prevail in the region. The earliest land use is recorded in the Kleinwalser Valley around 5500 cal BP, with fire clearings, pastoralism and hints at previously undetected regional metallurgy. Just before the Bronze Age (c. 4300 cal BP), centuries before mining districts in the Eastern Alps boomed, metallurgy around the Piller Mire is detected. The possibly strongest human land use in prehistoric times affects all sites from the Mid to Late Bronze Age (3500-3000 cal BP), as shown by elevated erosion and significant landscape alteration – from forests to agro-pastoral systems. Potential metal enrichments are, however, masked by high mineral inputs. This period is followed by a phase of lower land use, reaching well into the late Roman period (2800 cal BP to 250 cal CE). However, a strong Pb enrichment factor (Pb EF) in the Kleinwalser Valley is recorded around 2700 cal BP. Human impact increases in north-western Tyrol around 2400 cal BP. Periods of mining and metallurgy are indicated by increased Pb EF in all mires during the Roman Empire but also right after its collapse. Intensive human activities rise again with the fading Roman power after 250

cal CE in the Kleinwalser Valley but are interrupted by a climate deterioration after 500 cal CE (Late Antique Little Ice Age). At the sites in higher elevations, land use intensification does not take place before the High Middle Ages and is accompanied by rising Pb EF, indicating mining activities after 1000 cal CE. While Pb EF keeps rising due to mining, industrialisation and leaded fuel until 1980 cal CE, fluctuating human impact (deforestation, pasture management, drainage) can be linked to a varying impact of climatic, cultural and demographic factors. Over the last century, growing tourism and infrastructure construction increase erosion, but land use change leads to a recovery of the studied mires in Kleinwalser Valley and Tyrol.

The results of this study add a new dimension to archaeological and historical data, by showing the wider extent of human land use and its links to climate. Moreover, previously unknown periods of prehistoric mining or metallurgy in the NCA are revealed, encouraging further interdisciplinary research.

Abstract (Français)

Les Alpes européennes ont connu plusieurs phases de colonisation humaine. Cependant, l'interaction entre climat et impacts humains sur l'environnement dans le passé n'est pas encore totalement comprise dans cette région de haute montagne. Il existe notamment un manque de connaissances sur la chronologie et l'ampleur des impacts humains dans les Alpes centrales du nord (ACN) pendant l'Holocène, que cette étude comble en utilisant des analyses géochimiques, de palynologiques et de datation radiocarbone comparées avec des données archéologiques et historiques régionales. Des tourbières dans trois secteurs des ACN ont été choisies comme sites d'étude: Petite Vallée de Walser (PVA, Autriche), Tourbière Piller (TP, Autriche), vallée de Fimba (VF, Suisse).

La géochimie de séquences de tourbe est une méthode bien établie pour détecter les apports minéraux, l'érosion ou les activités métallurgiques. L'application de l'analyse par fluorescence des rayons X portable (pXRF) sur les tourbières de montagne reste une approche peu courante, principalement en raison des limitations dues aux limites de détection, aux effets de matrice ou à l'absence de calibration. En étalonnant la pXRF à l'aide de mesures de spectrométrie de masse à plasma à couplage inductif (ICP-MS), cette étude montre que Ti, Pb, Sr, Zn, K, S, Fe, V, Zr et, dans une certaine mesure Rb, Ca et Mn, peuvent être étalonnés dans la tourbe.

À haute altitude, les processus périglaciaires influencent les processus de dépôt dans les tourbières. Vers 8200 et 6300 cal BP, les conditions climatiques sont plus froides et humides. La

première utilisation du sol a été enregistrée dans la PVA vers 5500 cal BP, avec de la déforestation, du pastoralisme et des signes d'une métallurgie régionale jusqu'alors non-détectée. Juste avant l'âge du bronze (environ 4300 cal BP), des siècles avant l'essor des régions minières des Alpes de l'Est, la métallurgie autour la TP est donc détectée. L'utilisation des sols par l'homme, probablement la plus forte de la préhistoire, affecte tous les sites d'études à l'âge du bronze (3500-3000 cal BP), comme le montrent l'érosion élevée et la modification significative du paysage - de la forêt aux systèmes agro-pastoraux. Les facteurs d'enrichissements en métaux (Pb EF) sont toutefois masqués par des apports élevés en minéraux. Cette période est suivie d'une phase d'utilisation plus faible des sols jusqu'à l'époque romaine. Un fort Pb EF dans la PVW est cependant enregistré autour de 2700 cal BP et l'impact humain augmente autour de la TP vers 2400 cal BP. L'exploitation minière romaine est indiquée par une augmentation du Pb EF dans toutes les tourbières. Les activités humaines intensives reprennent avec le déclin de la puissance romaine après 250 cal CE dans la PVW, mais sont interrompues par une détérioration du climat après 500 cal CE. Sur les sites situés en altitude plus hauts, l'intensification de l'utilisation des sols n'a pas lieu avant le haut Moyen Âge (1000 cal CE) et s'accompagne d'une augmentation du Pb EF. Alors que le Pb EF continue d'augmenter en raison de l'exploitation minière, de l'industrialisation et des essences plombées jusqu'en 1980, les fluctuations de l'impact humain (défrichements, pâturages, drainage) peuvent être liées à des facteurs climatiques, culturels et démographiques variables. Au cours du siècle dernier, la croissance du tourisme et la construction d'infrastructures ont augmenté l'érosion, mais le changement d'occupation des sols a entraîné une régénération des tourbières étudiées.

Les résultats de cette étude ajoutent une nouvelle dimension aux données archéologiques et historiques, en montrant l'étendue plus large de l'utilisation humaine des sols et les liens avec le climat. De plus, des périodes de métallurgie préhistoriques jusque-là inconnues, dans les ACN sont révélées, ce qui encourage la poursuite des recherches interdisciplinaires associant archéologie, paléobotanique et géochimie environnementale.

Abstract (German)

Seit dem Ende der letzten Eiszeit haben die europäischen Alpen mehrere Phasen der menschlichen Kolonisation erlebt. Allerdings sind für diese Gebirgsregion die Wechselwirkungen von Klima, menschlichem Einfluss und Umwelt noch nicht vollständig geklärt. Insbesondere das Wissen über die Zeitpunkte und Ausmaße der menschlichen Auswirkungen in den nördlichen Zentralalpen (NZA) während des Holozäns ist noch mangelhaft. Mit Hilfe von Geochemie-,

Pollen- und Radiokohlenstoffanalysen und deren Vergleich mit regionalen archäologischen und historischen Daten soll diese Arbeit zur Ausfüllung dieser Lücken beitragen. Dazu wurden Bergmoore in drei Untersuchungsgebieten der NZA ausgewählt: Kleinwalsertal (Vorarlberg, Österreich), Piller Moor (Tirol, Österreich) und oberes Fimbatal (Graubünden, Schweiz).

Aus diesen Mooren wurden Proben entnommen und untersucht. Die Verwendung geochemischer Proxys (lithogene Elemente, Spurenmetalle) in Torfen ist dabei eine etablierte Methode zum Nachweis von Mineraleintrag, Erosion oder metallurgischen Aktivitäten. Trotz der Vorteile einer schnellen Probenvorbereitung und Messung ist der Einsatz der tragbaren Röntgenfluoreszenzanalyse (pXRF) insbesondere für Moore selten: aufgrund von Einschränkungen durch niedrige Zählraten, Matrixeffekte oder fehlende Kalibrierungen für organische Materialien. Durch die Kalibrierung der pXRF mit Messungen der quantitativen „Induktiv gekoppelten Plasma-Massenspektrometrie“ (ICP-MS) konnte dieses Problem gelöst werden. Diese Studie zeigt, dass Ti, Pb, Sr, Zn, K, S, Fe, V, Zr und - zum Teil - Rb, Ca und Mn erfolgreich kalibriert werden und als paläoökologische Proxys in Torf verwendet werden können. Diese Proxys lassen folgende Schlüsse zu:

In hohen Lagen beeinflussen periglaziale Prozesse die Depositionsprozesse in den Mooren. Um 8200 und im späten 7. Jahrtausend cal BP herrschen feuchtere und kältere Klimabedingungen im Untersuchungsgebiet. Die früheste Landnutzung ist im Kleinwalsertal um 5500 cal BP zu verzeichnen, mit Brandrodungen, Viehzucht und Hinweisen auf bisher unentdeckte regionale Metallurgie. Kurz vor der Bronzezeit (ca. 4300 cal BP), Jahrhunderte vor dem Boom der Bergbaugebiete in den Ostalpen, sind metallurgische Spuren um das Piller Moor nachweisbar. Die möglicherweise umfassendste prähistorische menschliche Landnutzung betrifft alle Standorte von der mittleren bis zur späten Bronzezeit (3500-3000 cal BP) in Form erhöhter Erosion und erheblicher Landschaftsveränderungen – von Wald- zur Weidelandschaft. Mögliche Metallanreicherungen werden jedoch durch hohe Mineralstoffeinträge überdeckt. Dieser Zeit folgt eine Phase geringerer Landnutzung, die bis weit in die römische Zeit reicht (2800 cal BP bis 250 cal CE). Im Kleinwalsertal wird jedoch um 2700 cal BP eine erhöhte Bleianreicherung sichtbar, während in Nordwesttirol eine Zunahme des menschlichen Einflusses um 2400 cal BP registriert wird. Der weit verbreitete römische Bergbau wird durch einen erhöhten Bleianreicherungsfaktor (Pb EF) in allen untersuchten Mooren angezeigt. Eine kurze Zeit regionaler Bergbauaktivitäten scheint auch unmittelbar nach dem Zusammenbruch des Römischen Reiches stattgefunden zu haben. Intensivere menschliche Aktivitäten beginnen ab ca. 250 cal CE mit dem Verfall Römischer Macht im Kleinwalsertal, werden aber durch eine Klimaverschlechterung nach 500 cal CE unterbrochen. An den höher gelegenen Standorten findet die Intensivierung der Landnutzung erst im Hochmittelalter (ca. 1000 cal CE) statt. Ein

steigender Pb EF deutet außerdem auf stärker werdende Bergbauaktivitäten hin. Während der Pb EF aufgrund von Bergbau, Industrialisierung und verbleitem Brennstoff bis 1980 cal CE weiter ansteigt, können menschliche Eingriffe in die Landschaft (Rodungen, Weidemanagement, Entwässerung) mit unterschiedlichen Auswirkungen klimatischer, kultureller und demografischer Faktoren verbunden werden. Im Laufe des letzten Jahrhunderts verstärken wachsender Tourismus- und Infrastrukturbau die Erosion, doch eine veränderte Landnutzung führte schlussendlich zu einer Erholung der untersuchten Moore im Kleinwalsertal und in Tirol.

Die Ergebnisse der vorgelegten Studie verleihen den archäologischen und historischen Daten eine neue Dimension, indem sie das Ausmaß der menschlichen Landnutzung und dessen Verbindungen zum Klima zeigen. Darüber hinaus werden bisher unbekannte Perioden des prähistorischen Bergbaus oder der Metallurgie in den NZA aufgedeckt.

Acknowledgements

First of all, I would like to thank my three supervisors for supporting me in every situation, from the beginning to the end of the three years, and for giving me time and space but also for pushing me forward when I needed it. Ingmar Unkel for encouraging me to apply for this PhD-position in the first place. François De Vleeschouwer for making possible the cotutelle and especially for hosting me during my visits in Toulouse: with good food, drinks and SP-episodes. Also, Gaël Le Roux for advice in the lab, for involving me into fieldwork in the Pyrenees and for taking over François' position in the final phase. Particularly when hearing stories from other PhD-students, I can say that I have been really lucky and that I am very grateful to have had them as my supervisors.

During my stays at Ecolab in Toulouse, I met many very nice and kind people. Chuxian Li was not just a PhD-comrade and a helping hand for peat core slicing and in one of the field campaigns, but also became a dear friend to me. Besides being very kind, also Marie-Jo Tavella at Ecolab has always been there to help in the lab and Annick Corrège overcame any of my issues with the French bureaucracy. At Kiel University, I would like to thank Annika Lange for counting pollen, Britta Witt for managing organisational issues and paperwork, Marcus Schütz and Mathias Bahns for their support with technical issues and for rescuing a stuck corer, Alexander Suhm, Sandra Kiesow and the international Master students for joining field work in the Alps in 2016 and 2017, Joachim Schrautzer for the enthusiastic support in the Kleinwalser Valley and, of course, the proof-readers. Special thanks are also going out to Karl Keßler from the landscape conservation association of the Kleinwalser Valley for organising access to the mires, but also for a nice dinner with the best Käsknöpfle I ever had. I would also like to thank Dr. Ernst Partl of the Kaunergrat nature park in Tyrol. Besides life at universities, I would like to say thank you to my friends and family for understanding that my time has been limited lately. Finally, I do not want to forget to mention whomever I forgot to mention.

Funding

I would like to express my gratitude for several travel grants and financial support, which greatly contributed to the successful completion of this bi-national PhD-project:

- "*Soutien à la Mobilité Internationale (SMI) 2016*" from the *Institut National Polytechnique de Toulouse*.

- PPP (Nr 57316724)/PHC-PROCOPE Nr 37646SG from DAAD/Campus-France (partly funded by the BMBF – German Federal Ministry of Education and Research).

- Mobility grant from *Deutsch-Französische Hochschule/université franco-allemande* (DFH/UFA).

The PhD-project was co-funded by the Graduate School *"Human development in landscapes"* at Kiel University (DFG-Excellence Initiative, GSC-208).

1 Inhalt

List of figures

List of tables

List of abbreviations

a.s.l.: ..... Above sea level

(B)CE: ..... (Before) Common Era

BP: ..... Before Present

BWM: ..... Butterwiesen Mire

cal: ..... Calibrated

Cert.: ..... Certified

C:N:..... Carbon:Nitrogen Ratio

CRM: ..... Certified Reference Materials

DACP: ..... Dark Ages Cold Period

EF: ..... Enrichment factor

HFL: ..... Hoefle Mire

ICP-MS: ..... Inductively Coupled Plasma – Mass Spectrometry

ICP-OES: ..... Inductively Coupled Plasma – Optical Emission Spectrometry

LAD: ..... Ladstatt Mire

LALIA: ..... Late Antique Little Ice Age

LIA: ..... Little Ice Age

LLG: ..... Lower Las Gondas Mire

LOD: ..... Limit of Detection

MAR: ..... Mineral accumulation rate

MM: ..... Marmot Mire

Pi17: ..... Piller Mire core

n: ..... Number of measurements

pXRF: ..... Portable XRF

REE: ..... Rare earth element

sd: ..... Standard Deviation

UCC: ..... Upper continental crust

ULG: ..... Upper Las Gondas Mire

XRF: ..... X-Ray-Fluorescence analysis

1 Introduction

When the ice caps of the last glacial maximum disappeared, vegetation and game were returning. Humans began to repopulate and use a landscape that had previously been barren or inaccessible for thousands of years. Still today, high mountain areas like the Central Alps are harsh environments with extreme conditions for life. The onset of human activity on high Alpine passes, slopes, and valleys for travelling, trade, hunting (Leitner, 2015), agriculture, seasonal pastoralism (Oeggl, 2015) and dairy production (Reitmaier et al., 2018), or mining and metallurgy (e.g. Stöllner and Oeggl, 2015) is not yet fully understood. The impact radii of humans were limited by sensitive climate feedbacks and the heterogeneous landscape's morphology. Hence, periods of colonisation or occupation climaxes did not happen contemporaneously and originated from different regions and cultures (e.g. Carcaillet, 1998; Gulisano, 1995; Kutschera et al., 2014; Oeggl and Nicolussi, 2009; Reitmaier, 2012; Vorren et al., 1993). The regional climate conditions led to a half nomadic lifestyle or transhumance, which was and still is the basis for seasonal livestock management systems in the European Alps (Reitmaier, 2017; Reitmaier et al., 2018). Archaeological evidence for this ephemeral presence is, however, difficult to detect and one of the reasons why there is no consistent narrative for the European Alps so far. Moreover, strong erosive forces of ice and water are responsible for a general scarcity of suitable palaeoenvironmental archives and archaeological sites in high mountain areas. Single archaeological finds and historical documentation cannot provide continuous information and may bias interpretations towards separate findings. Any approach to reconstruct the history of land use has to be put together piece by piece, region by region and valley by valley from lowland to summit. In particular, the complex relationships between humans and the development of environmental and climatic conditions on local or regional scales still need detailed investigation. Gaps need to be closed by research on various continuous palaeoenvironmental archives, such as lakes, glaciers or mires.

Climate, environment and human impact in the Central Alps are variables in a complex system that can interact in intricate ways. Reconstructing their past and recent development is important to better understand such systems, also to prepare for future changes concerning disaster management, infrastructure, agriculture, forestry etc. Thus, getting a better understanding requires some background knowledge on the involved factors (the Alps, area, climate, land use) as well as on the archives (peat) and tools (methods) that are available to gather information about the past. Hence, they will be introduced in the following chapter after defining the main research questions of this work.

1.1 Aims and key questions of this study

Mires in the Central Alps are hardly used as a palaeoenvironmental archive when it comes to the application of geochemical methods. Compared to lowland mires, mountain peatlands are more heterogeneous and complex systems. They are dependent on geology, geomorphology, altitude, exposition and climate, all of which are controlling hydrology, trophic state, evapotranspiration and thus vegetation, peat growth and accumulation rates. Exploiting peat sediment cores from mountain mires as palaeoenvironmental archives therefore needs to consider many possible factors. As detailed geochemical studies have not been conducted so far on any mires in the region, it is yet unknown how human or climatic impact would be reflected in the samples. One of the aims of this work is, therefore, the detection of potential geochemical signals in peat cores that can be used as proxies for erosion, mining, metallurgy or environmental feedback. They can, thus, shed light on the interactions of climate, environment and human impact on a local and regional scale in heterogeneous, elevated landscapes like the Alps. To address this heterogeneity, this approach is applied on three different study areas at different elevations in the northern Central Alps (**Figure 1**): the Kleinwalser Valley (Vorarlberg, Austria – chapter **4**), the Piller Mire (Tyrol, Austria – chapter **5**) and the upper Fimba Valley (Canton of Grisons, Switzerland – chapter **6**).

The Kleinwalser Valley is both rural and touristic and a geographical gateway to the northern Alpine Foreland. By the presence of farms, roads and villages in the centre of the valley and by centuries of human activities, prehistoric traces were possibly overprinted. However, a few archaeological sites on the slopes outlived these transformations. The Piller Mire and the Fimba Valley are both located deeper within the Central Alps and further away from farms and settlements, however, prehistoric sites of particular importance exist there as well. Nonetheless, the histories of all the presented study areas are quite reduced to the last few centuries and little is known about the extent of human impact on the landscape before the Late Middle Ages: a research gap that this study is aiming to fill. It also aims at finding out if and how past human activity was recorded in local mires. Since and until when have humans been present and is there more information than archaeology and pollen could provide? What was the magnitude of their impact on environment and landscape, how was it triggered and what was the role of climate?

These research questions are related, but different when it comes to the local characteristics of the individual areas and sites and what is known about them already. One of the overarching main criteria for the selection of the studied mire sites was their vicinity to either existing archaeological sites or the availability of other complementing data. The three sites cover different levels of altitude to capture effects that could be dependent on elevation. Investigating

these spatially separated areas within a wider region allows, to some extent, to differentiate which of the recorded signals are local and independent of each other, and which could be linked by regional developments (e.g. climate) and impacts of e.g. population peaks. Furthermore, the proximity to former ore mines (**Figure 1**) helps to resolve questions on the existence of prehistoric mining or metallurgy in the region.

One of the basic requirements to be able to answer these questions is an efficient and reliable method to analyse the geochemistry in peat samples. Therefore, the rarely used application of a portable X-ray fluorescence (pXRF) on peat samples is critically assessed within this study. The semi-quantitative pXRF results are calibrated element by element using certified reference materials (CRM) and peat samples from the study areas, which are measured parallelly by Inductively Coupled Plasma – Mass Spectrometry or Optical Emission Spectrometry (ICP-MS/OES). This approach allows listing elements that are quantifiable in peat by pXRF and evaluating where the limitations of pXRF are within this study. Further analyses include direct XRF-core-scanning, Carbon (C) and Nitrogen (N) analyses as well as pollen analysis. A chronological framework is provided by Bayesian age-depth modelling of radiocarbon dates. This enables careful interpretation of the acquired data and comparison to other studies from connected disciplines like climatology, archaeology, palynology, dendrochronology and historical sources. Is the data from the mires, for example the geochemistry, showing signals contemporaneous with archaeological findings or pollen? What was behind these signals: human activities or climate? Ultimately, the results assess the significance of the geochemical data in these mountain mires and their potential use as palaeoenvironmental proxies to eventually draw conclusions about the development of climate, human impact and environmental conditions in these three study areas of the northern Central Alps.

2 Study area and background information

2.1 Geology and geography

The Alps are the highest and largest mountain range in Europe in terms of elevation, going up to 4800 m a.s.l., but also in terms of area, covering almost 191,000 km². Along the approximately 1000 km long alpine main ridge, they are often subdivided into Western and Eastern Alps. They are shared at least partly between eight countries: Austria, France, Germany, Italy, Liechtenstein, Monaco, Slovenia and Switzerland. The focus of this study is on the northern Central Alps, the area amidst the eastern and western part, from the Alpine Rhine Valley to the Zugspitze peak, until the Alpine Divide in the south, i.e. the main Alpine Ridge. All precipitation and meltwater are collected within four different watersheds and end up in either the Rhine (Northwest), Danube (Northeast), Rhône (Southwest) or Po (South).

In terms of geology, the orogenesis of the mountain range started at the end of the Cretaceous, due to the colliding plates of the African and European continent, although the main phase of uplift occurred around 30 million years ago. As a result of the complex collision tectonics, the geology of the Alps is very complex. The main geological units are the Helvetic, Penninic, Eastern and Southern Alpine Nappes (Fitzsimons and Veit, 2001). Going from north to south in the central part of the Alps, the Helvetic Nappes (Mesozoic to Tertiary sedimentary rock) are followed by Penninic Flysch, and then by the Eastern Alpine or Austroalpine Nappes (Geological Survey of Austria, 2013). The latter are divided into the prominent Northern Limestone Alps and, to the south of it, the Eastern Alpine Crystalline, consisting of metamorphic rock like Schist and Gneiss (Egger et al., 1999). Recurring large glaciations over the Quaternary period strongly shaped the Alps into their modern form (Fitzsimons and Veit, 2001).

The three study areas (**Figure 1**) are distributed over three consecutive altitudinal zones:

1. Kleinwalser Valley (Austria, 1200-1000 m a.s.l.) in the montane zone
2. Piller Mire (Austria, 1550 m a.s.l.) in the subalpine zone
3. upper Fimba Valley (Switzerland, 2400 m a.s.l.) in the alpine zone

They are all north of the Alpine main ridge, which is one of the few common features. The Kleinwalser Valley is the northernmost site and shares parts of the Northern Calcareous Alps (or Northern Limestone Alps), which belong to the Upper Eastern Alpine zone, but also to the Helveticum and to subzones of the Penninic Nappes. The Piller Mire is the easternmost site and separated from the limestone by the Inn Valley and already in the metamorphic eastern alpine crystalline zone. Also, the Fimba Valley, being the southernmost site, is within this zone, although the area around it belongs to the Penninic Nappes of the Engadine Window (Geological

Survey of Austria, 2013). A more detailed description of each study area and site is provided in each of the respective sub-chapters.

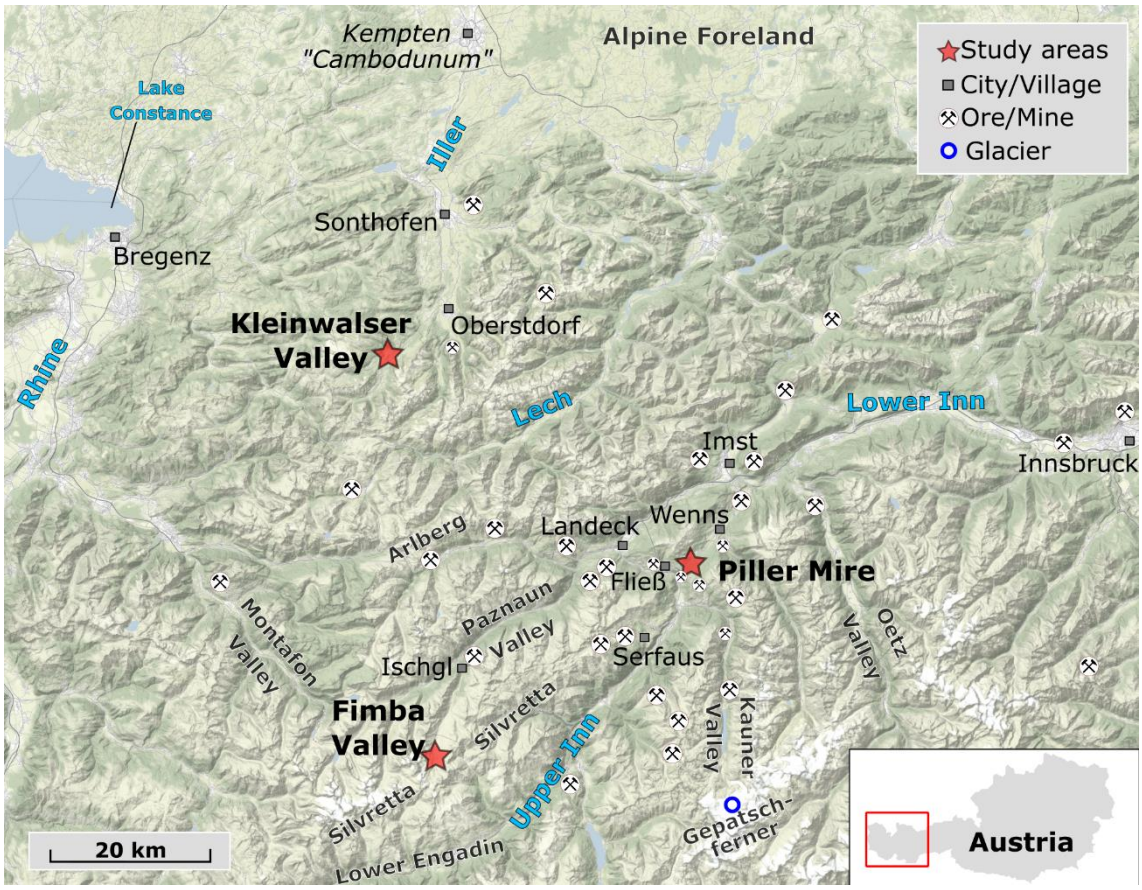

Figure 1: Overview of the northern Central Alps with study sites and documented ore deposits or ancient mines compiled from (Grutsch and Martinek, 2012; Vavtar, 1988; von Klebelsberg, 1939; von Srbik, 1929; Weber, 1997). *Edited from source: Stamen Design under CC-BY-3.0 and OpenStreetMap contributors under ODbl.*

2.2 Climate and environment in the Central Alps

The climate of the Alps is part of a complex system. Due to its heterogeneous topography and landscape, it can vary significantly on relatively small spatial scales. The differences are mainly the result of vertical and horizontal factors. Latitudinally and longitudinally, the Alps overlap with three climate zones. Two zones are within oceanic influence, the Atlantic in the North-western and the Mediterranean in the Southern Alps, whereas an increasing continental influence dominates the Eastern Alps. Furthermore, the Alps are right between the Icelandic Low and the Azores High and, therefore, influenced by the NAO, i.e. Northern Atlantic Oscillation (Beniston, 2005; Casty et al., 2005). One aspect of the horizontal climate pattern is expressed in the annual precipitation, which has two decreasing main gradients: from west to east and from the fringes to the inner Alpine valleys (e.g. Frei and Schär, 1998). Taking Austria as an example, the north-western regions can receive up to 4000 mm of precipitation, whereas years with less

than 700 mm are not unusual in parts of Eastern Austria (Frei and Schmidli, 2006). Moist air masses from the Atlantic and Mediterranean, are the main factor behind this distribution, as they precipitate after rising and cooling down at the slopes. Especially in the Northern and Central Alps, the highest precipitation occurs during summer (Frei and Schär, 1998).

Moving on from the spatial perspective, climate is strongly bound to altitude or elevation as well as exposure, which can be depicted with the Geiger-Köppen classification (Geiger, 1961). Based on this classification, Rubel et al. (2017) describe the modern climate zonation of the Alps with an alpine tundra climate prevailing above, and cool boreal climate below the theoretical (natural) timber line (10°C isotherm). An alpine frost or polar climate prevails only in the highest parts above the lower limit of the snow line (0°C isotherm).

However, these climate zones are not static. The current status is just a snapshot in time: The conditions will change in the future within decades and did so in the past (Rubel et al., 2017). Since the all-encompassing ice at the last glacial maximum melted away at the end of the Pleistocene, forests began to occupy the slopes and valleys, with a varying upper limit due to natural climate oscillation (e.g. Nicolussi, 2012; Nicolussi et al., 2005). Modern day's climate change will further change the environment, especially at higher elevations (Grabherr et al., 2010) and in interaction with human land use practices (Theurillat and Guisan, 2001).

2.3 Population dynamics and human land use

Only vague estimates can be made about the population in the Alps during prehistoric times. Supposing that most early communities were probably not bound to settlements and lived as hunters and gatherers or nomads, people might have travelled between high slopes and the lower Alpine Foreland in summer and winter. Estimated numbers for Switzerland of McEvedy and Jones (1978) were 30,000 by 5500 cal BP and a four times higher population by the Late Bronze Age around 3000 cal BP, which doubled again by 2000 cal BP. In Austria, their estimates show a steeper development since 5500 cal BP from 20,000 people to already half a million by 2000 cal BP. A severe decline was documented in both areas during the Early and Late Middle Ages. Austria lost almost 38 % of its population between 1300 and 1400 AD as a consequence of the Black Death. Around 1900 AD, both countries together counted approximately 11 Million inhabitants. By the year 2007, 14 Million people lived in the area of the Alps (Alpine-Convention, 2010), mainly in the lower areas and in touristic hot spots. Except for the south-eastern Slovenian part and the south-western part of Italy, the overall population increased over the last decades (Alpine-Convention, 2010). However, Bätzing et al. (1996) reported that, from 1870 to

1990, only lower-lying valleys attracted population and grew while an adverse trend was observed for higher elevated areas.

With increasing population, the use of land became an important factor in the development of the Alps. Under the term “land use” an endless list of human activities and their consequences concerning ecosystems worldwide was summarised by DeFries et al. (2004) and Foley et al. (2005). Basic needs for food, fibre, water and shelter need to be satisfied and consume space for crops, pasture, plantations, settlements. Concerning infrastructure, streets and railways for trade and transportation, dams and pipelines for water as well as power lines for electricity are necessary. Furthermore, all resources that are required to build and sustain the system need to be harvested or mined from natural sources and deposits: wood, coal, oil, metals, stone, salt, fertilisers, food (fish and game). It is undisputed that these human requirements threaten ecosystems worldwide and, as pointed out by Foley et al. (2005), even endanger the earth’s capacity of sustaining fundamental ecosystem services (Costanza et al., 1997). With the development of mass tourism, a new factor of land use heavily affects the environment (Shaw and Williams, 1994).

In the fragile landscape of the Alps, these types of land use and their consequences on nature can be observed. It can be seen everywhere that their impact does not stop at higher elevations. Nowadays, tourism is the most important economic pillar in otherwise weakly developed regions and the impact of mass tourism replaces ‘traditional’ alpine economy and landscapes (Barker, 1982). The economic transformation from pasture, animal husbandry and forestry, to industry all the way to tourism was rapid (Lichtenberger, 1965). It led to a decline of animal husbandry and reduced the number of mountain farms (in Austria partly by a decrease of 70 % between 1970 and 1999) after they had flourished during High Middle Ages (Bender, 2010). The types, distributions and intensities of land use are, of course, strongly associated to a population’s size and change with its individual culture, economy and technology. These anthropogenic activities are affecting the landscape and, thereby, vegetation cover and sediment fluxes and patterns.

2.4 Prehistoric mining and metallurgy

A special type of land use is open mining. The chronicle of prehistoric to historic mining is long and very complex as there are several factors which are complicating any attempts of reconstructing a continuous development. Until today, metals have gained more and more importance. Most ancient mining sites were probably destroyed by the demand of land of following generations and cultures, exploiting the same ores at the same spots. Pits or other

open sites are also prone to natural erosion, especially in the mountains, where processing structures like ovens or slags are destroyed and carried away easily by natural forces. In addition, metal artefacts found in an archaeological context may have been traded or re-casted and do not have to be related to in-situ smelting or mining. Only with the invention and acceptance of Pb-isotopic studies, these issues could be tackled (O'Brien, 2015).

Some very early indications for, partly even subterranean, mining activities date back as far as the Middle Palaeolithic or the Late Pleistocene at different spots in the world: in Australia (Bednarik, 1992), in South-Africa around 45,000 years ago (Dart, 1971) and in Egypt at least 50-60,000 years ago (Vermeersch and Paulissen, 1993). Most people think of gold, silver or other metals when hearing of mining. However, these early traces were related to chert or flint deposits, exploited to produce tools and weapons. In Europe, Meso- to Neolithic flint mines were reported for the Alps by Leitner et al. (2011). Besides flint and metal, the range of extractable resources also comprises coal, peat, clay, salt and any kinds of rock.

Metallic ores were used a long time before smelting technologies were discovered, but again differently than most people would think. Goethite (FeO(OH)) and Haematite (Fe_2O_3), forms of iron (hydr-)oxides, were exploited as pigments (ochre) on the African continent as early as 200,000 years ago (Barham, 2002). First hints at the existence of smelting technology as early as 7450 cal BP were suggested for lead objects in ancient Egypt. In the eastern Mediterranean, a metal hoard was dated to 5150 cal BP (Zwicker, 1989), slags in Israel at 5450 cal BP and copper artefacts on Cyprus at the same time. For the period from 4640 to 4130 cal BP, Véron et al. (2006) showed an immense Pb- pollution in bay sediments of ancient Alexandria.

One of the earliest direct evidence of copper smelting in Europe (Eastern Serbia) dates back to 7000 cal BP (Radivojević et al., 2010). The first copper objects spread from the Balkans through Central Europe in the 7th millennium BP as suggested by Höppner et al. (2005). In north Tyrol, near Brixlegg, a copper slag was dated back to a period between 6450-5590 cal BP by Bartelheim et al. (2002) but could not be connected to any local mining or deposits. The same applies to the lake-dwelling northern Alpine Pfyn- and Mondsee cultures, who produced copper tools in the 6th millennium BP (Höppner et al., 2005).

A continuous flow of new discoveries keeps the debate open, how the technology spread from the Eastern Mediterranean to Western and Central Europe or if it developed independently. As summarised by a review on prehistoric copper mining in Europe (O'Brien, 2015), copper metal was found in Italy as early as 6300 cal BP. Metalworking and mining activities started almost simultaneously around 5500 cal BP and were an established technology by 5250 cal BP in the region of modern Italy, but it might have taken almost 1000 years more to reach the Iberian

Peninsula via Southern France. However, this was lately challenged by a study by Martínez Cortizas et al. (2016), suggesting early metallurgy around 5000 cal BP in Northern Spain. The use of copper and the technology to mine and produce it could have spread from Southern France and the Pyrenées over Atlantic France into Ireland, where arsenical copper was produced between 2350-1850 cal BP, as hypothesised by O'Brien (2015). In Great Britain, Mighall et al. (2009) found early hints for local metallurgy in Wales in the early 4th millennium BP, however, widespread copper mining across the island was replaced by bronze metallurgy after 4150 cal BP.

Returning to the Alps, particularly the Eastern Alps (Austria) became a very important prehistoric district for copper extraction in Central Europe (Stöllner and Oeggl, 2015). First, it was mainly produced from fahlores (Cu-sulphides, often associated with As, Zn, Fe and Sb) in the Bronze Age (Goldenberg, 2015; Viehweider et al., 2013). Later, a purer type was produced from chalcopyrite ($CuFeS_2$), followed by an intensification of extraction from around 3500-3280 cal BP until 2750 cal BP (O'Brien, 2015; Stöllner, 2015a). The Bronze Age was a period of generally widespread metallurgic activities, not only across the Alps but also in adjacent areas, like South-West Germany (Krause, 1987). Metallurgy probably never ceased completely since then, and also salt became an important trade good and was mined by Celtic groups (Ebner et al., 1999).

Krause (1987) showed clusters of known exploited copper deposits and Early Bronze Age settlements in the Northern Alps. However, an almost empty spot was left right between the Eastern and Western Alps and this gap is still not closed (Stöllner, 2015b), despite a few indications. Also, considerable polymetallic ore resources, including Pb, exist in the northern Central Alps, of which some were being mined at least since the Late Middle Ages and partly until the 20th century AD (Grutsch and Martinek, 2012; Hammer, 1915a; Hanneberg et al., 2009a; Neuhauser, 2015; Vavtar, 1988; Weber et al., 1997). Nonetheless, clear evidence or indications for a prehistoric use of these ores are missing so far.

2.5 Peatlands: functions and implications for palaeoenvironmental-research

Peatlands cover approximately 3 % of the earth's landmass (Kivinen and Pakarinen, 1981). They are concentrated in temperate to cold regions of the Northern Hemisphere (North-America, Russia, Scandinavia), but also exist in (sub)tropical regions like South-East Asia (Limpens et al., 2008), Africa (Dargie et al., 2017), and at high latitudes or in mountain chains of the Southern Hemisphere (Cooper et al., 2010; Yu et al., 2010).

Besides serving as a supply for combustible material since at least 2000 years (Succow, 2012) or as an additive for agri- and horticulture, peatlands have rather been a nuisance to humanity and were drained over centuries, to gain new land for agriculture, pasture, settlements and other construction work. But over the last century, scientific efforts and discoveries have put peatlands into proper light and highlighted benefits and important ecological functions (Maltby and Proctor, 1996; Sjörs, 1980). Not only are wetlands and mires acting as a natural buffer for the hydrological balance of a region and sustaining unique ecosystems, peat can also retain and buffer or reduce the availability of anthropogenic pollutants like trace metals (Brown et al., 2000; Chaney and Hundemann, 1979; Couillard, 1994) or an excess of nutrients (Johnston, 1991; Kadlec, 1997). As climate change became part of scientific and public discourse, the role of peat as the most important terrestrial carbon storage, despite its tiny fraction of earth surface cover, became clear (Bragg and Lindsay, 2003; Page and Baird, 2016). However, human activities are still threatening wet- and peatlands by peat mining, groundwater extraction, drainage and cultivation for agricultural use. Pollution, droughts, induced fires, invasive species and eutrophication are raising the pressure put on these vulnerable ecosystems and their functions (Bragg and Lindsay, 2003; Brinson and Malvárez, 2002). For example, changing conditions like a decrease of the water table or higher temperatures can induce the release of CO_2 and dissolved organic carbon (Dise, 2009; Freeman et al., 2001) or the mobilisation of potentially toxic trace metals like As (Rothwell et al., 2009). Furthermore, the burning of tropical peatlands was held responsible for the highest rise in atmospheric CO_2 concentrations since the beginning of measurements (Page et al., 2002). The emissions of degrading peatland soils below expanding palm oil plantations are going to contribute steadily in the near future (Carlson et al., 2013).

To avoid any confusion in terminology, it is important to distinguish between peatlands, mires, peat bogs and fens. While a mire is a wet peatland that still accumulates peat, a (raised) peat bog is a special type of mire, which is – unlike a fen – very low in nutrients, acidic and only fed by atmospheric input. A fen receives nutrients from the mineral base and/or is constantly supplied with enriched surface or groundwater (Bragg and Lindsay, 2003; Dierßen and Dierßen, 2008). What all mires have in common is a mechanism that prevents or strongly limits the mineralisation and humification of organic material. As long as the combination of the overall decomposition process and compaction of buried material is slower than the biomass production in the living layers (acrotelm), a mire is still growing because peat can accumulate. The most important limiting mechanism on decomposition is the supply of oxygen. The replenishment of O_2 in the water-saturated lower part of the peat column (catotelm) is very slow. Furthermore, this tiny amount of oxygen is used up rapidly by the high abundance of decaying organic matter. Over time, most mires develop through different stages and rely on

certain conditions, like a constant supply of water or humidity, which often involves a sufficient amount of precipitation. Depending on the right conditions, e.g. water table and the water chemistry (nutrient supply), the resulting type of vegetation partly controls the accumulation of peat. The most important peat building species are mosses, which continuously grow on top of their dead stems, whereas higher plants that grow within such an environment (e.g. *Carex*) contribute mainly roots, since their superficial biomass decomposes before burial. Päivänen and Vasander (1994) demonstrated that only 2-16 % of the organic material produced is preserved by being buried in the catotelm.

At some point, fen type mires are theoretically making the transition from a minerotrophic fen over oligotrophic to an ombrotrophic mire (bog). While the lower part was and still is influenced by the basal sediment, the upper part has grown above the groundwater level and is out of influence of dissolved nutrient supply from deeper layers. The term 'raised mire' implies that it is elevated relatively to the surrounding area, often described as a convex surface form, while an exemplary fen's surface is concave. Hence, the convex bog incorporates only atmospheric inputs and, to some extent, takes up (i.e. recycles) nutrients from decomposing material. While minerotrophic fens range between 5 to 15 % of mineral matter (Shotyk, 1988), Tolonen (1984) characterised ombrotrophic peat with an ash content around or rather below 5 %.

The earliest stage of a mire typically begins in a morphological depression or lake (pond, pool, etc.), which is continuously filled by a mix of sediment and ingrowing and dying plant material until the water level is reached and the vegetation can cover and overgrow it. In another example setting, peat can start growing directly on an impermeable substrate, e.g. clay or even bare rock, but only if a constant supply of water is available – for instance, a close-by stream, a slope water runoff, precipitation etc. In this setting, a growing body of mosses builds up a sponge-like structure, which can buffer shortages in humidity by collecting and storing water. A feature that is induced by the capillary forces within such a peat moss body.

However, a classification where only minerotrophic, ombrotrophic and maybe a transitional oligotrophic state are distinguished would be a simplification. Dierßen and Dierßen (2008) suggested a characterisation based on the hydrology and development history, the chemistry of peat and soil water, stratigraphy and composition and the structure of current vegetation. For example, definitions strongly depend on the geomorphology below and around the mire. Nonetheless, mires are also dynamic systems and the classification can differ based on the criteria that are considered (Moore, 2013). Even within a single mire complex, mixed or transition types exist.

For this study, the exact classification does not play a major role apart from a differentiation into ombro- and minerotrophic. However, morphological, hydrological and vegetation features of a mire must be considered for the interpretation of geochemical proxies. In this context, a raised (ombrotrophic) bog is often dominated by *Sphagnum* (Huttunen and Tolonen, 2006) or by other mosses, which are adapted to low nutrient availability and therefore often used locally as an indicator plant for low pH and low nutrients. Due to this deficiency of mineral matter and unbuffered production of acids by decay and proton release from *Sphagnum* mosses into their environment, bogs are very acidic (Dierßen and Dierßen, 2008) and possess pronounced anoxic conditions in the water-logged catotelm (Gorham, 1995; Shotyk, 1988). Besides the already extreme conditions, the dominance of *Sphagnum* creates a microhabitat that most vascular plants do not tolerate (Van Breemen, 1995). As roots of these vascular plants are often pathways for oxygen transport into deeper layers, their growth inhibition limits further decomposition (Koppisch, 2012), i.e. promotes peat accumulation.

Over the last century and particularly over the last decades, peat bogs have proven to be excellent archives for a broad range of potential proxies for past climate, environmental conditions, trends and events in different parts of the world (e.g. Barber, 1993; Bindler, 2006; Chambers et al., 2012; Chambers and Charman, 2004; Rabassa et al., 2006). One of the great advances is the possibility to establish radiocarbon based age-depth models (e.g. Piotrowska et al., 2011). Nutrient-poor systems like bogs are decaying very slowly, because the biota's activity is inhibited by a lack of mineral nutrients and oxygen. Again, the dominance of *Sphagnum* in these systems is another factor, because it produces decay resistant components (Dierßen and Dierßen, 2008). The greatest advantage of this lies in a higher peat accumulation, which results in a higher resolution that undecomposed and thus less compacted mires can offer for palaeoenvironmental studies. These properties are also beneficial when the degree of preservation facilitates the selection of macrofossil samples for radiocarbon dating or for the determination of pollen or vegetation in a sample. Palaeoecology, including macrofossil, charcoal and pollen/spore studies (i.e. palynology) are one of the classic research techniques in peat (Erdtman, 1927; Firbas, 1923; Godwin, 1934; Van Geel, 1978). Methods to reconstruct past surface wetness and water table variations include the investigation of testate amoebae (Woodland et al., 1998), the ratio of Carbon (C) to Nitrogen (N) or other organic geochemical approaches (Biester et al., 2014; McClymont et al., 2010; Schellekens et al., 2015).

Aside from these approaches, inorganic proxies are used increasingly. The above-mentioned proton release of *Sphagnum* happens in exchange for metal- or other cations (of e.g. Na, Mg, Ca as nutrients or Pb, Ca, Zn, Cd etc. passively) and is very effective due to the large specific area of their leaves (Dierßen and Dierßen, 2008). Furthermore, humic and fulvic acids as decomposition

products of lignin and other organic material, are abundant in peat and partly responsible for complexation, adsorption and exchange of cations and molecules (Kerndorff and Schnitzer, 1980; Ma and Tobin, 2004).

Being fed almost solely by atmospheric input, the geochemical record retains traces of whatever settled or precipitated on the bog's surface. Immobile elements and their isotopes thus potentially serve as geochemical proxies for past conditions (Benoit et al., 1998; Damman, 1978; Nieminen et al., 2002; Shotyk, 1996a). The chemical signature of these inputs can be derived from aeolian dust (Shotyk et al., 2002), volcanic ash, also called tephra layers (Dugmore et al., 1995; Kilian et al., 2003; Swindles et al., 2010), sea spray or all kinds of anthropogenic pollution (De Vleeschouwer et al., 2007; Jones and Hao, 1993; Shotyk et al., 1998).

Among others, certain lithogenic elements are contained in their mineral matrix, and, therefore, conservative and immobile in ombrotrophic peat (Aubert et al., 2006; Krachler et al., 2003; Shotyk et al., 2001). Isotopes and elemental signatures were used for dust provenance tracing by comparing the peat samples to patterns from potential sediment source areas or rocks (Kylander et al., 2007; Vanneste et al., 2015). More specifically, in terms of anthropogenic traces, the ability for cation complexation and retention of metals and other pollutants (Cloy et al., 2009; Gao et al., 1999; Klavins et al., 2009; Ma and Tobin, 2004; Shotyk, 1996b, 1996a) opened new possibilities in interdisciplinary research. Among others, it merges archaeology, geochemistry and environmental studies by identifying and quantifying traces of ancient activities of mining and metallurgy (Mighall et al., 2009; Monna et al., 2004). It allows understanding of the natural and anthropogenic atmospheric fluxes and biogeochemical cycles of trace metals and toxic elements like Pb and Sb (Shotyk et al., 2004, 1996). In a similar way, total mineral accumulation rates, either of atmospheric input or of flushed in material, could be inferred from certain lithogenic elements (Chambers et al., 2012) and sometimes linked to human induced erosion (Hölzer and Hölzer, 1998; Lomas-Clarke and Barber, 2007; Schofield et al., 2010).

Part of these proxies can also be applied in the northern Central Alps, where a wet and humid climate, geological factors, but also human impact played a role in promoting mire development (Steiner, 2005), which hence provides appropriate palaeoenvironmental archives.

3 Methods

To provide quick information on what has been done, where and which techniques were applied in each of the three valleys and on the different peat cores, an overview is provided in **Table 1**. More detailed information is following in each of the sub-sections.

*Table 1: Summary of all coring sites, coordinates and analyses carried out. *Performed by A. Lange*

Mire Site, coordinates	Study Area	Sample (year)	Corer	Types of Analyses
HFL (Hoefle Mire), 47°21'52.5"N 10°10'37.2"E	Kleinwalser Valley	Peat Core(s) (2016, 2017)	Monolith, Russian (5cm)	Radiocarbon, pXRF, XRF-core-scanning, ICP-MS, ICP-OES, Pollen*, C:N
LAD (Ladstatt Mire), 47°21'28.1"N 10°09'26.9"E	Kleinwalser Valley	Peat Core (2016, 2017)	Monolith, Russian (5cm)	Radiocarbon, pXRF
HHA (Halden-Hochalpe), 47°20'19.5"N 10°03'48.7"E	Kleinwalser Valley	Basal sample (2017)	-	Radiocarbon
Pi17 (Piller Mire), 47°07'24.85"N, 10°39'45.45"E	Piller Saddle	Peat Core (2017)	Wardenaar, Usinger (8cm)	Radiocarbon, pXRF, XRF-core-scanning, ICP-MS
LLG (Lower Las Gondas), 46°54'3.51"N; 10°15'26.15"E	Fimba Valley	Peat/Sediment Core (2016)	Russian (5cm)	Radiocarbon, pXRF, ICP-MS, ICP-OES
ULG (Upper Las Gondas), 46°54'07.4"N 10°15'26.4"E	Fimba Valley	Peat/Sediment Core (2016)	Russian (5cm)	Radiocarbon
MM (Marmot Mire), 46°53'52.7"N 10°15'25.6"E	Fimba Valley	Peat/Sediment Core (2016)	Russian (5cm)	Radiocarbon, XRF-core-scanning,
LCM (Lower Coffin Mire), 46°53'49.9"N 10°15'46.5"E	Fimba Valley	Peat/Sediment Core (2016)	Russian (5cm)	Radiocarbon
BWM (Butterwiesen Mire), 46°54'27.30"N; 10°15'28.92"E	Fimba Valley	Peat/Sediment Core (2012)	Russian (5cm)	Radiocarbon, XRF-core-scanning,

3.1 Coring techniques

The coring of peatlands requires careful planning, which involves the selection of the coring system itself and related equipment. The decision can depend on the properties of the sampled peatland in terms of vegetation, wetness, decomposition and depth but also on the accessibility of the site, as the logistics are not negligible in mountainous environments. Furthermore, the types of planned analyses determine how much material is needed from a single core. In most cases, sampled mires seldomly go deeper than ten metres. The soft material means that peat-coring systems are constructed to be hand-driven. However, due to its softness, compression and other disturbances can occur during coring and need to be avoided. A detailed overview on coring techniques and a guide for a clean procedure from coring to subsampling was published by De Vleeschouwer et al. (2010) and Givelet et al. (2004). The systems and techniques that were used to obtain the peat (sediment) profiles for this study are shortly introduced here in the following:

With the acrotelm being still undecomposed, often with roots of *Ericaceae* or *Pinus mugo* embedded within a softer matrix of mosses, retrieving an undisturbed core is particularly

challenging. The simplest technique is the use of a serrated ceramic blade knife. Although the penetration depth is limited, any compaction is negligible.

A more sophisticated system to tackle the issue of coring the topmost metre is the Wardenaar corer (Wardenaar, 1987). The system has a rectangular 10x10x100 cm coring chamber, which is composed out of two connected, but independently moving stainless steel halves. Each side's lower end is reversely furnished with an inclined, sharpened edge. By pushing each side down stepwise and on a rotating basis, the corer can cut through the usually very fibrous acrotelm with minimum compression. A pillow of air can be created at the lower end of the core before pulling it out, which helps to disconnect the layers and to decrease suction at the lower end. Another advantage is the large quantity of sample material. However, the instrument is less suitable for dense (fen) peat or thick wood and root layers. It is easily damaged (bends, nicks) and, therefore, cannot be driven down with too much force.

For deeper layers, the use of a Russian peat corer is required. This type of corer was first introduced by Belokopytov and Beresnevich (1955) and further developed by Jowsey (1966). It is the most commonly used corer for soft sediments like peat, as it avoids vertical compression and is relatively easy to carry and to use. Theoretically, the maximum depth is limited only by the number of extension rods and the strength of the coring team. It has a semi-cylindrical coring chamber, which can be turned by a handle at the upper end by 180° around the attached blade to close the coring chamber. When retrieving a consecutive second core from the borehole, it is important to consider that the upper 10 cm could be disturbed by the metal tip of the Russian corer. Therefore, the upper 10 cm should be avoided, and a parallel core should be taken with a slight offset to obtain undisturbed material for this part.

The typical radius of the chamber can vary between 2.5 cm, 4 cm and 5 cm, with lengths of either 50 or 100 cm. Like the Wardenaar corer, it is pushed into the ground by hand or hammer blows, with the chamber at 0° position. When the targeted depth is reached, the sharpened edge of the chamber cuts horizontally through the peat. This design avoids vertical compaction, but horizontal compression or an incomplete filling of the chamber can occur in very soft peat. The Russian corer is, hence, most efficient for the catotelm.

Another method was deployed within this work: the Usinger coring system, which is a modified piston coring system (e.g. Livingstone, 1955) initially developed for lake sediments. It was developed further to be used for peat or other soft organic sediments and continuously refined to reach higher depths. The schematic and setup are described in detail by Mingram et al. (2007). It has an outer rod, which transmits the forces of pushing and pulling; and an inner rod, which controls the piston and depth of opening the barrel. The coring chamber is a cylindrical, walled

barrel of 1 mm thickness (available diametre: 10, 8, 5.5 and 4 cm) with sharpened edges at the lower end, which can cut through soft material like peat. The sediment (peat) is extruded from the barrel into an open half-cylinder tube with a stamp, which is connected to a lever. The Usinger system is the most complex method but has the advantages of a good depth control and plenty of sample material. As with the Russian corer, the topmost layers in a consecutive core segment could suffer from compaction and should not be used without having an independent parallel core to verify any conducted measurements. Optimally, the upper part is taken with a Wardenaar corer.

In this study, Russian Corers of 50 and 100 cm length with 5 and 8 cm chambers were used, while barrels of 8 cm were chosen for the Usinger corer. Regardless of the system used, the coring chambers were carefully cleaned and rinsed before retrieving the next core. After the extraction, every section was wrapped in plastic film, transferred into a rigid casing and enclosed in a plastic hose. This avoids loss of water, contamination and oxidation and provides protection during transport and storage. All cores were put into cold storage at 3°C.

3.2 Core slicing and subsampling

Prior to subsampling, each core segment was deep-frozen for several days and then cut into slices of approximately 1 cm thickness with a stainless-steel band saw. By carefully rinsing both sides of every slice with MilliQ-water and cutting away its outer fringes, any possible contamination has been removed. For cores from the Russian system, each slice was then chopped into two or three triangular subsamples: half of it for geochemistry, a quarter for macrofossils, pollen and dating and the last quarter as backup. Without a backup, the complete other half has been stored for palynology and dating. For the Wardenaar and Usinger cores, at least half of each slice has been used for geochemistry and the rest stored for palynology and dating (**Figure 2**). The dimensions (length x width x height) of every geochemistry subsample were measured with a Vernier calliper. To determine the dry bulk density of the peat, each geochemistry subsample was weighed first before freeze-drying over a minimum of 72 h and weighed again afterwards. Cores processed in this study resulted in a total number of 639 sample slices. All subsamples were transferred into pre-labelled plastic zip-bags before being stored in a freezer again.

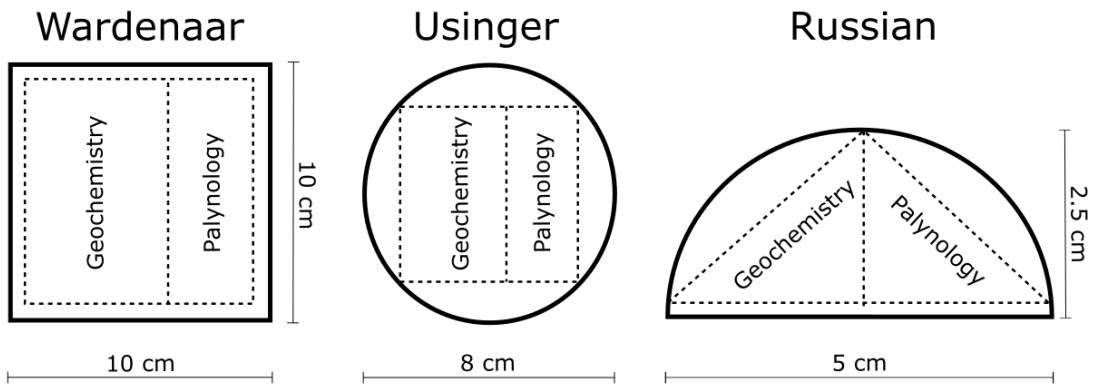

Figure 2: Schematic profiles of the three different core profiles of Wardenaar, Usinger and Russian system. Dimensions of geochemistry and palynology subsamples are marked with dashed lines.

3.3 Radiocarbon dating

The radiocarbon dating method and calibration to calendar ages renders numeric ages and is a crucial element of this study. It allows the direct comparison of the results of this work to already existing studies and relevant records. Piotrowska et al. (2011) summarised the basics of radiocarbon dating in peat. Macrofossil samples for radiocarbon dating were picked from fresh samples in MilliQ-water. If available, stems and leaves of *Sphagnum* or other mosses were preferably selected. Due to strong decomposition or the absence of *Sphagnum* in some parts (older, minerotrophic), other plant remains like *Eriophorum* spindles, seeds, *Ericaceae* leaves or wood were extracted. Only in case no identifiable remains could be found, bulk peat was dated. After drying the samples for 24 hours at 50°C, they were sent either to Poznan AMS Radiocarbon Laboratory (lab-code: Poz), Poland, or to the Gliwice Radiocarbon Laboratory (lab-code: GdA-code), Poland. The details of every sample are given in the respective chapters of each site. Calibrations of single radiocarbon ages were conducted with the clam-package (Blaauw, 2010) in the open source software R version 3.4.3. (R Core Team, 2017). Age-depth models (ADM) were produced with the rbacon package (Blaauw and Christen, 2011) version 2.3.3 in R version 3.4.3. as well. Both clam and rbacon are work based on the Northern Hemisphere IntCal13 radiocarbon calibration curve (Reimer et al., 2013). The model output yields ages in the 95 % confidence interval and includes maximum, minimum, mean and median ages. Only the median ages are used in this study and unless denoted otherwise, ages are reported as calibrated before present (cal BP) for prehistorical times. For a more convenient comparison to historical sources, interpretations for the period after 1950 cal BP are given in cal CE.

3.4 Geochemistry

The geochemistry of peat cores or peat samples can be analysed with different methods. A review and guideline of preparation techniques for different geochemical analyses was given by Le Roux and De Vleeschouwer (2010). In this study, only full core X-Ray Fluorescence-scanning would be completely non-destructive, whereas portable X-Ray Fluorescence Spectrometry (pXRF) needs a dried and homogenised sample powder (at least in this study). In contrast, Inductively Coupled Plasma Mass Spectrometry (ICP-MS) and Inductively Coupled Plasma Optical Emission Spectrometry (ICP-OES) need a complete chemical digestion to obtain a measuring solution.

A smaller number of samples for geochemical analysis with ICP-MS, ICP-OES and pXRF was initially selected to obtain a general elemental trend in each core. The sample selection was based on fluctuations in the density profile, which is giving a first idea about changes in the evolution of the peatland (e.g. mineral content). Depending on the first results and on the progressing quality of the age-depth models, more samples were picked to refine the data resolution.

Before the geochemical analysis, the selected dry samples were transferred into Falcon™ tubes of 15 or 50 cml and ground and homogenised with a FastPrep®-24. This was carried out by adding eight glass beads of 4 mm into each tube and running them for three times over 20 s at maximum speed ($6 m*s^{-1}$). Samples with wood were excluded or the wood was removed before homogenisation. This method is quite efficient in terms of time, costs and cleanliness. In comparison to other methods (e.g. mortar and pestle), it minimises the risks of cross-contamination and material loss because the sample does not have to be transferred back and forth into other containers, which also makes cleaning obsolete.

3.4.1 ICP-MS and ICP-OES

Both techniques have been used in palaeoenvironmental studies and yield quantitative results for a broad range of inorganic elements. Procedures for quadrupole ICP-MS were proposed by Krachler et al. (2002) and for ICP-OES by Sapkota et al. (2005). The main difference between the two is that ICP-MS has a much lower detection limit and can thus measure trace- and ultra-trace elements, resulting in a larger range of detectable elements. ICP-OES is therefore used for major, minor and some trace elements (Al, Ca, Fe, K, Mg, Mn, Na, P, S, Sr, Ti, Zn, Pb, Cu) and can also serve to determine the dilution factors for ICP-MS.

140 samples from the selected main sites (**Suppl. Table 1**) were processed in a class 100 clean room at *EcoLab* (Toulouse, France), following the protocol in Vanneste et al. (2015): Using a disposable plastic spatula, 100 ± 5 mg of the powdered peat were weighed into Savillex™ 30 mL Standard Teflon® vials. A smaller amount was taken for samples with a visibly higher sediment content or with high density (e.g. 90 mg for basal sediment). The basic goal of the complete wet chemical digestion was to achieve a complete solution of carbonate and silicate minerals and the removal of all organic compounds, because they would produce matrix effects, which can affect the measured signals (e.g. Kralj and Veber, 2003).

The first step involved the addition of 2 ml of Suprapur® 65% nitric acid and 15 minutes of the beakers in an ultrasonic bath. Afterwards, the samples were left to react at room temperature over a minimum of 10 hours. The high degree of organic material provoked a strong exothermal reaction, making it necessary to let the vials degas for a few minutes before adding 0.5 ml of HF (Suprapur®) to every beaker. The vials were then put on a hotplate at 110°C to react for two days. After evaporation at 50°C, 1 ml of H_2O_2 (Suprapur®) was added to oxidise the still organic rich solution for a minimum of six hours until they were put into the ultrasonic bath for 15 minutes and evaporated slowly at 30°C. After adding 1 ml of 65% nitric acid, a 15-minute ultrasonic bath and heating at 90°C for 48 hours, the samples were visually controlled for particles and finally evaporated. Due to an incomplete digestion of a few samples, all were treated with 1 ml of aqua regia for one day at 90°C and evaporated again. The residues were dissolved again in 35 % HNO3 and diluted with Milli-Q-water to a 3 % measuring solution.

For ICP-MS, 50 µl of an In/Re spike (ratio of 0.403) were added to every sample. Furthermore, an internal calibration with a multi-element standard in five different dilutions was run every 10^{th} sample to correct for internal drift of the mass spectrometer during the measurement. For ICP-OES, a multi element standard of four different dilutions was used and run at the end of analysis. To verify the quality, precision and accuracy of the ICP-MS and ICP-OES results, five different certified reference materials (CRM) with an organic matrix were processed with each series of 21 samples. They were measured in regular intervals on both instruments (**Suppl. Table 1**). These CRMs were: GBW-07603 (bush branches and leaves), NIST-1515 (apple leaves), NIST-1547a (peach leaves), NJV-941 (*Carex*/sedge peat) and NJV-942 (*Sphagnum* peat). Procedural blanks were additionally processed throughout the digestion and measured to monitor possible contamination or systematic errors during the digestion process. A total number of 168 solutions (140 samples, 24 CRMs and 4 blanks) were measured on a Quadrupole-ICP-MS Agilent 7500 CE (Q-ICP-MS) at *Observatoire Midi-Pyrénées*, Toulouse, France. Before that, 72 of them (60 samples, 9 CRMs, 3 blanks) were measured on an IRIS Intrepid II (Thermo Electron Corporation™) ICP-OES at EcoLab, Toulouse, France.

The ICP-OES measurements allowed an estimate of the sample concentrations, which gave an indication for the dilutions that had to be prepared for ICP-MS. Apart from Sulphur, all elements that were measured with ICP-OES were covered by ICP-MS as well. Therefore, S is the only element taken into account from ICP-OES. The spectroscopically measured concentrations in the CRMs and their respective deviations from the certified values as well as the blanks are given in **Suppl. Table 1**. None of the blanks showed any significantly elevated concentrations, which demonstrates that no systematic contamination occurred during the sample preparation in the clean laboratory or measurements.

Except for a few outliers, the measurements of Al, Ca, Ti, Pb, Zn, Rb, K, S, Sb, Sr (outlier of 48 % in Nist1515 c), V (outlier -26.5 % in NIST1515 b) and Al (outlier of 81 % in NJV-941 d) deviated less than 20 % from the certified values. Cu was systematically lower by -10 to -30 %, with larger negative deviations at concentrations < 2 $mg*kg^{-1}$. The lanthanides i.e. rare earth elements (REE) Nd and Sm deviated less than -25 % from the certified values. The errors for As, Cr, Ni, Sc but also Mn and Fe were higher but not systematically, so they should be considered with caution. For the potential reference element Sc, Prohaska et al. (1999) observed spectral interferences on ICP-MS. Stetzenbach et al. (1994) attributed possible interferences, which could affect the measurement of Sc, to organic components. Although organic matter should have been removed by the complete wet geochemical digestion, such an effect cannot be excluded.

A general observation is that most of the deviations are negative. A possible explanation could be a dilution effect, caused by the uptake of air humidity of the powdered CRMs during longer storage time and frequent use (opening and closing). However, this effect most likely did not affect the peat samples, as they were processed shortly after freeze-drying.

3.4.2 Portable XRF scanning

Portable or handheld X-ray fluorescence scanners (pXRF) are common instruments for the quick chemical analysis of all kinds of material. They were applied for archaeological artefacts (Liritzis and Zacharias, 2011), in food safety (Palmer et al., 2009) and for the detection of pollution in environmental samples, including soils and other sediments (Kalnicky and Singhvi, 2001). For these purposes, the instrument uses internal calibrations that yield quantitative values.

The use of portable/handheld XRF to obtain geochemical data from peat or other highly organic sediments is still rather scarce and only a handful of studies have evaluated the instrument's potential on samples with such a matrix (Kalnicky and Singhvi, 2001; Mejía-Piña et al., 2016; Shand and Wendler, 2014; Shuttleworth et al., 2014). However, studies using pXRF on peat with

a palaeoenvironmental background are rare (e.g. Gałka et al., 2017; Kapustová et al., 2018). Despite being a relatively quick and simple method, it is semi-quantitative for peat and still bears many uncertainties. Elemental concentrations are usually very low, which leads to low counts. The water and organic contents are affecting XRF-spectroscopy even more (Böning et al., 2007; Ravansari and Lemke, 2018; Sahraoui and Hachicha, 2017; Tjallingii et al., 2007). Hence, parallel measurements by quantitative methods and CRMs are needed to calibrate the pXRF's output.

Figure 3: The pXRF with connected sampling chamber.

A pXRF Thermo-Fisher Niton XL3t was used in this study. It is equipped with an Au-anode and a 50 kV X-ray tube. The limit of detection (LOD) is defined by the 3-sigma value. As this is influenced by factors like measurement time and sample matrix, the LOD may vary slightly between samples for each element. All 406 dried and homogenised peat samples from the three main cores (**Table 1**) were filled into 12.5 ml PP-vials and closed with Fluxana TF-240-255 film and rubber band. Using dry samples can already remove potential effects related to moisture. The sample powder was neither compressed nor weighed before scanning. Among the 406 samples, 140 samples were analysed by ICP-MS. In addition, nine organic and two mineral CRMs were prepared in the same manner. Besides the five organic CRMs that were measured by ICP-MS, the following materials were scanned: BCER-060 (aquatic plants), IAEA-336 (lichen), IPE-176 (reed/*Phragmites*) and NIST-1575a (pine needles) and the two mineral CRMs GBW-07411 (polluted soil) and LKSD-3 (lake sediment). The pre-defined "soil mode" was used with a minimum of 180 s measurement time for both the main- and low-filter, which is 60 seconds above the minimum duration recommended by Shuttleworth et al. (2014).

The CRMs as well as the 140 ICP-MS peat samples were scanned for at least three times. Every time a sample was measured more than once, the container was shaken before the next scan, to control the reproducibility (precision). Repeated measurements were the first step to develop a calibration for pXRF via independent values and to obtain quantitative values by a solid regression analysis. The corresponding squared Pearson correlation coefficient, or coefficient of determination, is expressed in this work as R^2. In this chapter, elements are briefly discussed and pre-selected, based on the comparison to CRMs; either for further calibration with the ICP-MS results or to be discarded from further consideration.

*Table 2: Mean values of CRMs measured with pXRF, number of measurements (n), percental sample standard deviation of pXRF-scans of certified reference (sd in %) and certified concentration (mg*kg^{-1}). Values in yellow are informative or indicative values. Red columns mark mineral sediment CRM.*

	Unit	BCR 060	GBW 07411	GBW 07603	IAEA 336	IPE 176	LKSD 3	NIST 1515	NIST 1547a	NIST 1575a	NJV 941	NJV 942
As	[-]	23.8	202.6	14.4	1.6	5.4	27.3	NA	NA	NA	6.9	3.0
n	[-]	8	11	5	4	5	5	NA	NA	NA	8	6
sd	[%]	12.6	4.1	7.7	16.3	11.0	6.2	NA	NA	NA	7.7	18.3
Cert	[mg*kg^{-1}]	NA	205	1.25	0.63	2.63	27	0.038	0.06	NA	NA	NA
Ca	[-]	54012	36232	42760	8262	8736	16772	44634	41795	8882	33936	4024
n	[-]	8	11	5	4	5	5	3	3	3	8	6
sd	[%]	2.0	2.7	0.4	5.2	6.1	0.9	1.9	0.1	0.3	4.4	2.5
Cert	[mg*kg^{-1}]	NA	NA	16800	NA	4160	16438	15260	15600	2500	10200	1200
Cr	[-]	29.57	64.61	NA	46.06	32.80	95.55	117.67	100.88	115.71	57.98	13.7
n	[-]	7	11	NA	4	5	5	3	3	3	8	2
sd	[%]	58.9	5.1	NA	52.2	53.7	7.0	35.0	40.8	35.2	31.1	18.9
Cert	[mg*kg^{-1}]	26	59.6	NA	NA	11.3	87	NA	NA	NA	NA	NA
Cu	[-]	119.36	70.31	42.40	50.98	47.55	45.14	92.81	82.58	74.56	50.05	39.1
n	[-]	8	11	5	4	5	5	3	3	3	8	6
sd	[%]	14.3	5.3	11.8	16.6	19.4	11.4	24.8	29.9	21.4	12.7	13.0
Cert	[mg*kg^{-1}]	51.2	65.4	6.6	3.6	9.97	35	5.64	3.7	2.8	2	1.7
Fe	[-]	4468	61815	2368	1233	14293	48299	347	813	190	11959	3252
n	[-]	8	11	5	4	5	5	3	3	3	8	6
sd	[%]	13.7	0.6	6.3	10.1	13.7	10.2	19.9	17.9	19.2	5.4	6.7
Cert	[mg*kg^{-1}]	NA	55790	1070	430	6410	40000	80	218	46	NA	NA
K	[-]	46709	19285	25248	5395	37925	19986	54636	80449	14183	137	126
n	[-]	8	11	5	4	5	5	3	3	3	8	6
sd	[%]	1.0	2.6	0.5	4.6	4.4	1.6	1.5	0.4	0.8	31.7	36.7
Cert	[mg*kg^{-1}]	NA	13982	9200	1840	13000	18262	16100	24300	4170	3900	1300
Mn	[-]	3136.4	10010.5	57.8	83.5	164.6	1524.6	139.1	265.8	1575.0	23.6	NA
n	[-]	8	11	5	4	5	5	3	3	3	5	NA
sd	[%]	13.5	0.8	13.3	24.2	22.4	10.7	28.2	25.2	13.6	24.7	NA
Cert	[mg*kg^{-1}]	1760	9700	61	63	113	1440	54	98	NA	36	8
Ni	[-]	25.2	97.4	NA	NA	NA	35.7	16.6	NA	NA	NA	NA
n	[-]	7	11	NA	NA	NA	5	1	NA	NA	NA	NA
sd	[%]	58.8	8.2	NA	NA	NA	27.5	NA	NA	NA	NA	NA
Cert	[mg*kg^{-1}]	NA	24.2	1.7	NA	7.86	47	NA	0.69	1.47	NA	NA

	Unit	BCR 060	GBW 07411	GBW 07603	IAEA 336	IPE 176	LKSD 3	NIST 1515	NIST 1547a	NIST 1575a	NJV 941	NJV 942
Pb	[-]	92.55	2617.25	73.68	6.18	13.40	35.16	NA	NA	NA	2.33	14.3
n	[-]	8	11	5	4	5	5	NA	NA	NA	8	6
sd	[%]	4.3	0.8	3.0	10.1	8.7	7.4	NA	NA	NA	10.8	3.4
Cert	[mg*kg^{-1}]	64	2700	47	4.9	8.24	29	0.47	0.87	NA	2.4	10.1
Rb	[-]	25.6	106.4	7.2	5.2	39.1	81.5	14.4	28.9	23.7	4.3	11,2
n	[-]	8	11	5	4	5	5	3	3	3	8	6
sd	[%]	3.2	0.9	4.1	3.1	4.3	5.3	1.3	2.4	0.5	3.6	2.9
Cert	[mg*kg^{-1}]	NA	111	4.5	1.76	NA	78	NA	19.7	16.5	NA	NA
S	[-]	6204	1418	8924	702	2687	840	2182	1873	986	3530	2365
n	[-]	8	11	5	4	5	5	3	3	3	8	6
sd	[%]	1.2	6.8	1.7	4.9	4.3	5.8	1.4	4.2	6.8	4.4	2.0
Cert	[mg*kg^{-1}]	NA	NA	7300	NA	2360	1400	NA	NA	NA	2900	2170
Sc	[-]	51.88	21.79	36.49	8.29	4.85	13.35	42.90	41.10	8.40	35.12	5.46
n	[-]	8	11	5	4	5	5	3	3	3	8	6
sd	[%]	3.6	12.0	3.8	7.0	14.6	7.7	9.5	8.2	1.5	5.6	9.2
Cert	[mg*kg^{-1}]	0.5	11	0.32	0.17	NA	13	NA	NA	NA	NA	NA
Sr	[-]	238.4	129.3	319.9	16.3	46.2	276.4	37.6	77.1	14.6	50.7	27.2
n	[-]	8	11	5	4	5	5	3	3	3	8	6
sd	[%]	2.5	1.0	1.0	3.0	4.7	4.7	2.7	2.4	2.4	1.8	2.1
Cert	[mg*kg^{-1}]	NA	131	246	9.3	NA	240	25.1	53	NA	NA	NA
Ti	[-]	280.5	4544.4	214.4	219.6	1172.5	3211.9	15.9	18.7	15.3	64.1	262.
n	[-]	8	11	5	4	5	5	1	2	2	8	6
sd	[%]	11.6	2.0	4.1	6.0	6.8	0.6	NA	0.1	12.4	18.8	2.9
Cert	[mg*kg^{-1}]	NA	4100	95	NA	707	3330	NA	NA	NA	NA	NA
V	[-]	10.85	116.64	5.13	13.82	32.50	108.50	25.58	19.39	15.67	16.22	9.17
n	[-]	6	11	1	4	5	5	3	3	3	8	2
sd	[%]	25.0	8.5	NA	36.2	12.0	4.4	22.6	27.8	36.1	21.8	4.5
Cert	[mg*kg^{-1}]	NA	88.5	2.4	1.47	11.6	82	0.26	0.367	NA	NA	NA
Zn	[-]	665.22	3623.95	129.91	78.72	77.65	158.96	33.78	51.41	113.70	16.50	13.9
n	[-]	8	11	5	4	5	5	3	3	3	8	6
sd	[%]	10.2	0.8	4.9	5.6	10.4	9.4	9.4	15.3	6.9	36.7	10.3
Cert	[mg*kg^{-1}]	313	3800	NA	30.4	40.2	152	12.45	17.9	38	NA	NA
Zr	[-]	21.5	189.0	15.4	14.4	67.8	194.1	12.9	15.5	13.7	14.5	15.1
n	[-]	8	11	5	4	5	5	3	3	3	8	6
sd	[%]	41.3	1.9	15.8	3.6	14.0	8.8	1.1	3.6	0.7	9.3	4.8
Cert	[mg*kg^{-1}]	NA	192	NA	NA	NA	178	NA	NA	NA	NA	NA

As a first step, elements with a percental standard deviation > 40 from n measurements of organic CRMs were exempted from further consideration in the site-specific calibrations of pXRF. The value of 40 is arbitrary. However, too many elements would have had to be removed, due to a limited number of certified values, if a more restrictive limit was chosen. Moreover, most of the CRMs consist of almost pure organic from all kinds of plant material, which might not be fully representative for a matrix that is typically found in peat. A more detailed regression

analysis is going to be conducted later in the site-specific chapters, when ICP-MS- and pXRF measurements of peat samples are compared.

A high sd of 30 to 50 % was observed, for example, for Cr and Ni (**Table 2**). Contrastingly, Cr was well measured in the mineral CRMs with a sd below 10 %. Beside these two elements, Cu, V, Mn, Zn and K showed a relatively high sd of up to 30 % in some of the organic CRMs. However, for Zn and K, this high sd was limited to the scans of NJV-941.

Most values that were acquired via pXRF from the organic CRMs were significantly elevated compared to the certified concentrations. In contrast, the values for the mineral CRMs GBW-07411 and LKSD-3 systematically were not too high and relatively much closer to their certified values than the organic CRMs. Direct comparisons are shown in **Figure 4** as cross-plots of pXRF-values versus certified values of organic CRMs. Linear regression curves were plotted and preliminary coefficients of determination (R^2) are given. These are based only on very few data points and the regression curves are therefore not likely to represent a stressable function.

Ti had one certified reference value in GBW-07603 (95 $mg*kg^{-1}$). Only with an indicative concentration (of IPE-176) a linear relationship could be established. These high concentrations are, however, not representative for typical peat. After removing the mineral CRMs from the regression, Pb, Ca, Rb, S, Zn, Sr, Fe, K and Mn had a promising R^2 of over 0.95. Also, Sc seemed promising for organic materials with a R^2=0.9. However, the unsatisfactory ICP-MS results for Sc are obstructing a decent calibration of the element, despite its use as a conservative reference element in peat (Shotyk et al., 2002). Measurements of As, V and Cu had a relatively high sd, at least in the range of lower concentrations, which would be expected in peat samples. The same is true for Cr, for which the regression analysis suggested that it could be used for sediments with elevated Cr concentrations (> 25 $mg*kg^{-1}$).

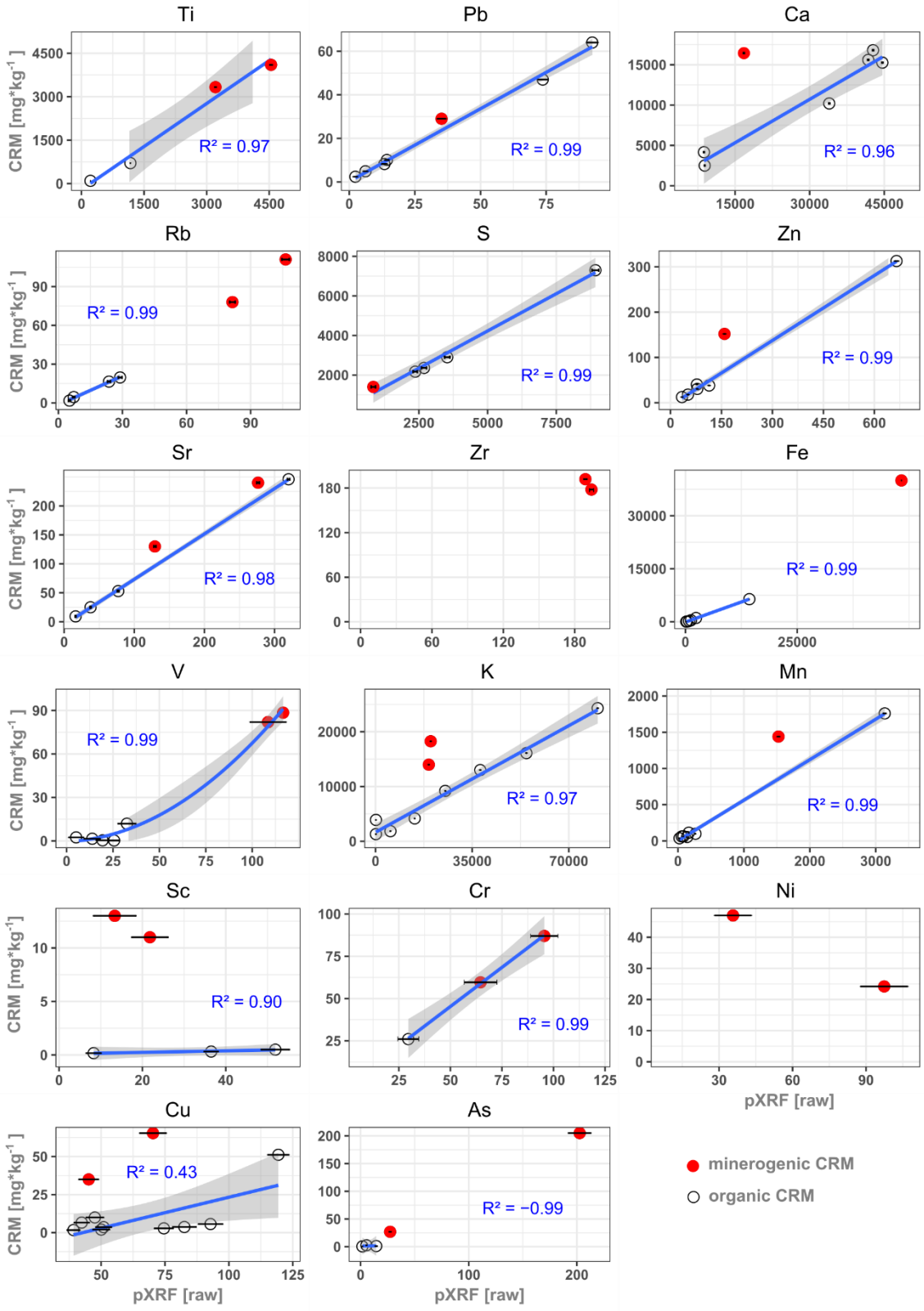

Figure 4: Regression analysis of CRMs vs pXRF measurements and coefficients of determination (R^2) if applicable. Mineral CRMs in red. Except for Ti, Pb, V and Cr, mineral CRMs (red) were mostly excluded from the regression analysis, except for Ti, V and Cr.

When factoring in the two non-organic CRMs, the individual plots in **Figure 4** illustrate that some elements change their correlation between organic and mineral matrix. These elements comprise for example As and V, which both correlate linearly at higher concentrations (or in

mineral sediments). Copper, on the other hand, shows a strong deviation between pXRF and certified concentration in both organic and mineral material. For the elements Ca, K, Fe, Mn and K, the mineral CRMs are outside of a possibly linear regression. The discrepancy between the fit of organic and mineral materials is least pronounced for Pb, S and Sr and it can be suggested that these elements are less affected by matrix effects. In particular, Ti, Rb, Fe and perhaps V would need more samples (CRMs) in an intermediate range between maximum and minimum concentrations so that the type of regression can be described. The regression curves of some elements (potentially Ti, Rb, V) in **Figure 4** leave the possibility of establishing a non-linear function (polynomial of 2nd order). For Mn, Zn and Pb, intermediate concentrations are under-represented in the CRMs as well.

Due to the issue of a limited concentration range in the available and investigated CRMs and because site specific effects may appear from different factors, like the local geology or peat type, the outcome of pXRF vs. ICP-MS/OES is addressed separately in each of the three study-area chapters. Based on these individual regression analyses, it is possible to produce non-site-specific transfer functions for certain elements, which could allow their quantification by pXRF-measurements, even in peat samples of any source. A global evaluation with ICP-MS versus pXRF of all peat samples is presented later in this thesis (Chapter **7.1**).

3.4.3 XRF core scanning

XRF (core-)scanning is an established method used on marine- or lake sediment cores (Boyle, 2000), which is currently run on two different systems: the ITRAX-scanner (Bloemsma et al., 2018; Croudace et al., 2006) and the Avaatech-scanner (Richter et al., 2006). It allows very efficient geochemical analyses of sediment core profiles in high resolution (up to sub-mm). Nevertheless, it has the disadvantage of being only semi-quantitative, measuring intensities, translated to counts per second, instead of concentrations. Several attempts of cross calibrating XRF-counts to quantitative methods have been carried out. But issues of varying organic content (Chawchai et al., 2016; Löwemark et al., 2011), surface and particle inhomogeneity, pore water content and matrix effects (Weltje and Tjallingii, 2008) are high obstacles that cannot be overcome easily (Weltje et al., 2015). In peat cores, very low amounts of mineral matter lead to low counts, while high water and organic matter content are producing noise. Therefore, the scanning of peat cores is not very common and only few studies used it, either directly on the wet core (Chawchai et al., 2016; Unkel et al., 2010) or on resin impregnated slices (De Vleeschouwer et al., 2008). However, Poto et al. (2015) directly compared XRF-core (Avaatech-system) with ICP-MS measurements on a split core of ombrotrophic peat and demonstrated high

correlation estimates of R^2 up to 1 for Pb, Cd, Cr, Sr, Ti and Zn, while Cu, Fe, Y, Ga and Ca were still good or acceptable with $R^2>0.5$. Another methodological study of Longman et al. (2018) compared a core scanned with an ITRAX-system to ICP-OES measurements on the same material and came to a similarly positive general conclusion, suggesting that results are best for Fe and Ti. Despite their results, the quality still depends strongly on the condition of the core and the available means to prepare it for scanning (e.g. clean and plain surface). As peat can be very heterogeneous, already the presence of a wood particle or other larger macrofossils could heavily influence the output.

For this study, four cores (**Table 1**) were scanned on an Avaatech XRF core scanner at the Institute of Geosciences at Kiel University, Germany. The instrument is equipped with a Rh-anode and a helium—flushed pillow between the beam-emitting chamber and the core. Scans were performed on the core segments in a 10 mm resolution in two different settings. The instrument was set to an excitation time of 10 s at 10 kV and 750 µA without filter, covering the lighter elements Al, Si, S, K, Ca, Ti, Mn and to 20 s at 30 kV and 2000 µA with the Pd-Thick filter setting for the heavier elements Fe, Ni, Cu, Zn, Se, Br, Rb, Sr, Zr and Pb. The filter cancels out excitations from the light elements. Four powdered mineral standards were measured before and after every scanning session (morning/evening) to monitor internal drift.

Unlike the ITRAX-, the Avaatech core-scanner is not designed to work on round surfaces. This is of great importance for the 5-cm Russian cores. The flat side of these cores is most susceptible to vertical cross-contamination, gets easily disturbed during transfer from corer to the storage tube and is usually not plain. Any modification to get a levelled surface would lead to the loss of more, already scarce, sample material. This is even more complicated in undecomposed peat or when wood or roots are present. For the full Usinger core, it would require a lengthwise cut of the full core (plus proper equipment), which would risk disturbing, breaking or contamination of the core. The latter is also relevant for the full Usinger cores. As a consequence, the cores were scanned as they were. Because peat is usually soft enough, the head of the scanner can move onto the core without leaving an empty -air filled- space in between. Even if the peat surface is slightly compressed, it allows scanning of the round core surfaces with the Avaatech. The results are partly interpreted in form of ratios. For single element profiles, the signal should be normalised to account for effects of matrix changes, for example, a changing proportion of organic matter, which could dilute the signal (Löwemark et al., 2011). Aluminium (Al), which is an often-used element for normalisation (e.g. Löwemark et al., 2011), needs long exposure times and has a low detection limit, which is problematic for peat sediments and is therefore not suitable in this study. Therefore, a normalisation to the total counts per second (tcps) was chosen, as suggested for sediment cores by some studies (Chagué-Goff et al., 2016; Haenssler

et al., 2013; Ohlendorf et al., 2015). This method reduced otherwise prominent effects of surface irregularities or smaller ruptures in the core, especially for the lighter element range.

3.4.4 Carbon/Nitrogen ratio

C and N analyses can provide information about the degree of decomposition and therefore about wetter or drier episodes (Biester et al., 2014). The C:N ratio is strongly connected to the type of peat, i.e. the vegetation (Koster and Favier, 2005), and age of the peat (Wang et al., 2015). Its significance for palaeoclimatic interpretations is therefore debated and can be ambiguous (Hansson et al., 2013), implying that C:N-data should not be interpreted on its own.

Here, 63 C:N-samples were selected from the already homogenised geochemistry peat sample powder. Around 5 mg of each sample were weighed in for the final analysis on a EuroVector Elemental Analyser 3000.

3.4.5 Enrichment factors and mineral accumulation rates

Enrichment factors (EF) are a way to illustrate either enrichment or depletion of a certain elemental ratio in the respective layer of peat relative to the natural ratio in the local geology or pre-anthropogenic sediment. Hence, they are a proxy to detect, interpret and discuss the possible mechanisms behind fluctuations in this signal.

An EF is generally calculated by taking the ratio of the element A to a conservative reference element B and divide it by the ratio of A to B that represents the Upper Continental Crust (UCC) or the regional or local natural background. The elemental composition of the UCC was taken from McLennan (2001).

$$A\ EF = \frac{(A/\mathrm{B})_{\mathrm{Sample}}}{(A/B)_{\mathrm{UCC\ or\ background}}}$$

Concentrations of A and B in sample and UCC or background in $mg*kg^{-1}$

To give an example, the enrichment factors of Pb (Pb EF), Sb (Sb EF), Cu (Cu EF) and Zn (Zn EF) can be taken as indicators for anthropogenic pollution by mining, metallurgy or in some cases for coal and leaded gasoline combustion (Nieminen et al., 2002; Shotyk, 1996a, 1996b; Weiss et al., 1999). However, an EF_A should only be calculated under the condition that element A is immobile in the investigated peat section, if conclusions on the timing and time of deposition are drawn. In ombrotrophic peat this requirement is fulfilled for the above-mentioned elements (Novak et al., 2011). Otherwise, a different behaviour (dissolution and transport) in the

minerotrophic part of a core could lead to false interpretations (Shotyk, 1996a). A lower binding capacity or less effective complexation of metals can be induced by the much higher presence of competing binding partners, like Fe^{2+}, Mg^{2+}, Ca^{2+}, for fulvic- or humic acids (Benedetti et al., 1995; Iglesias et al., 2003; Zhou et al., 2005).

Table 3: UCC values of relevant elements from McLennan (2001)

Element	**Ti**	**Pb**	**Zn**	**Cu**	**Sb**
UCC-value [$mg*kg^{-1}$]	4100	17	71	25	0.2

Moreover, the reference element B has to meet a number of requirements. It needs to be conservative and immobile in the peat column: It should not be affected by physicochemical (e.g. dissolution and diffusion) or biological processes (e.g. plant cycling of nutrients) under changing conditions of pH, water saturation, etc. Further, it must be equally distributed in mineral source material without significant partitioning during (chemical) weathering, entrainment, transport and sedimentation or in biological processes. Finally, precise and accurate measuring of the element of choice must be ensured. Studies of i.a. Aubert et al. (2006), Boës et al. (2011), Cloy et al. (2011), Krachler et al. (2003), Shotyk et al. (2001, 1992), Shotyk (1988) and Zaccone et al. (2008) discussed the behaviour of several lithogenic elements in terms of enrichment and mobility. As a quintessence of their results, Ti, Sc, Al, Pb, Y and REE, Rb and V could be judged as immobile and conservative, at least in ombrotrophic peat, although some results contrasted each other.

Yet, Weiss et al. (1997) underlined the importance of choosing the conservative element individually in every study or location, since conditions may vary. Shotyk et al. (2001) reviewed and predestined Sc as the most suitable lithogenic reference element for atmospheric deposition, as it is not bound to any crustal rock or mineral in particular. It is, furthermore, only used since recent times, e.g. in aerospace techniques (Røyset and Ryum, 2005), and is only enriched in bauxite deposits (Binnemans et al., 2015). After Henderson (1982), it does not get residually enriched or depleted in the crystallization of magma and in contrast to other elements, chemical weathering affects the Sc inventory the least (Nesbitt and Markovics, 1997). Krachler et al. (2003) proposed Al as the best reference after Sc and studies of Muller et al. (2008) and Shotyk et al. (2001) backed this finding. Bennett et al. (1991) and Damman (1978) reported some Al mobility in parts of the peat column. Furthermore Nesbitt and Markovics (1997) observed an enrichment of Al in aerosols. The behaviour of REE in peat was discussed in several studies (Aubert et al., 2006; Krachler et al., 2003; Kylander et al., 2007) and all agreed on their immobility in peat. Unfortunately, the analytical quality of Sc in both ICP-MS and pXRF

analyses hampers its use in this study and neither Al nor REE or Y are covered by the pXRF soil-mode spectrum. Therefore, Ti, Zr and V remain as possible choices.

Ti and Zr are not susceptible to dissolution (i.e. to leaching from minerals within the peat) but can be subject to physical fractionation processes. They are most abundant in heavy accessory minerals like rutile, ilmenite, titanite and zircon (Goldschmidt, 1954), which are resistant to chemical weathering (Jackson and Sherman, 1953). The density of these minerals can lead to sorting effects during weathering and transport, making them generally less abundant in small and light particles (Schütz and Rahn, 1982). At the same time, Zr can be depleted relative to Ti in clays and aerosols derived from weathering (Krachler et al. 2003), which would infer that Ti is less affected. Furthermore, Zr gets more easily fractioned during transport and sedimentation processes, due to its abundant occurrence in heavy minerals (Fralick and Kronberg, 1997). In contrast, Ti has been widely used to quantify mineral inputs into peatlands (Sapkota et al., 2007) and is, in contrast to Pb and V (Cloy et al., 2011), not enriched by anthropogenic pollution. It was also used by Le Roux et al. (2004) as a reference element to calculate Pb EF in peat. In addition, V has higher measurement errors and a lower correlation between ICP-MS and pXRF measurements and the CRMs. As Zr is not covered by the organic CRMs and lacks an independent control, Ti is used as the conservative reference element in this study. Now, to finally calculate an EF, some of the relevant UCC-values can be found in **Table 3**. However, as already suggested by Kempter et al. (1997), the combination of Ti and Pb is a powerful set of proxies to detect metal emissions and changes in land use history.

Accordingly, Ti is chosen as a tracer for soil erosion. Knowing the element's proportion in the UCC, it allows quantifying the annual deposition of mineral matter on the mire's surface. It can be addressed as Mineral Accumulation Rate (MAR) or Atmospheric Soil Dust (ASD) in an ombrotrophic mire. MAR is accounting for the total amount of mineral matter deposited on the mires surface, whereas ASD is, as the name implies, a measure for material deposited solely by the atmosphere. Even if the UCC may not be completely representative everywhere, Shotyk et al. (2002) used the Ti_{UCC} value to quantify the annual atmospheric mineral input on a Swiss mire. Thus, the same approach is used here to calculate the mineral accumulation rate (MAR in $g*m^{-2}*a^{-1}$) with the following formula:

$$MAR = {}^{100}/_{0.41} * Ti * \rho * pa$$

Ti concentration in sample (Ti in $mg*kg^{-1}$); dry bulk density (ρ in $g*cm^{-3}$); peat accumulation rate (pa in $cm*a^{-1}$)

As this calculation of deposition rates includes the factor of time (in the form of accumulation rates drawn from the age-depth model), it overcomes the issues of looking at concentration

profiles versus depth or time only, because it normalises effects of decomposition, compaction or lower peat accumulation.

3.4.6 Principal Component Analysis

Principal Component Analysis (PCA) is a statistical method allowing to handle big and complex datasets with numerous variables and to reveal patterns and relations within it (Shlens 2014). In brief, PCA filters out a component by rotating the coordinate axes of a multi-dimensional dataset and aligning it along the vector with the highest variance of variables. The PCA approach is used in all kinds of research fields. It has already been applied in palaeoclimatic and -environmental studies in peat by i.a. Mauquoy et al. (2004), Muller et al. (2008) and Hansson et al. (2013). Here, it is used to analyse relations within the available data, e.g. geochemical elemental concentrations or ratios, but also depth, density and accumulation rate. The analysis was computed with the open source software R version 3.4.2 (R Core Team, 2017) and the internal "prcomp" package. For each run, the package centres and scales (i.e. normalises) the variables to get a mean of zero and to account for large variations within the dataset.

3.5 Core descriptions and macrofossil analysis

Visual core descriptions were carried out on the fresh cores, aided by the high-resolution line scan photos of the Avaatech core-scanner, which provides an adequate and uniform light source to still detect colour changes. Besides, observations from macrofossil analysis (see below) is considered in the description. In this way, it is possible to distinguish between certain peat layers and to identify changes (e.g. of the vegetation) that are invisible for the eye on the core's surface. This is important because the quickly oxidising surface of the peat core blurs changes in colour to a large extent. Furthermore, interchanging illumination in the field or other relative factors (e.g. subjective vision) have to be considered as well.

A coarse macrofossil analysis was carried out on a minimum sample volume of 1-2 ml in a petri-dish with bi-distilled water under a binocular microscope, partly in parallel to the picking of samples for radiocarbon dating. Although it is a rather subjective approach, the content of suspended organic matter and the state of preservation of plant remains (e.g. *Sphagnum* leaves) gave an idea about the degree of decomposition and humification. Furthermore, the frequent occurrence of charcoal and mineral grains yields information about local fires and increased sediment content. The presence or absence and type of macrofossils (like wood particles, leaves,

needles, moss, *Oribatidia*, macro-charcoal, etc.) also add valuable information on past vegetation and trophic status.

3.6 Pollen

A volume of 2 ml was taken from 14 samples of cores HFL-B and HFL-C in the overlapping section. These samples were selected at depths were trends or events were visible in the preliminary geochemical profiles. The samples were prepared for pollen analysis by following the method described by Moore et al. (1991). The raw material was pre-treated in separate steps in 10 % KOH and 10 % HCl to get rid of humic substances and carbonates. Macro remains were sieved out with a 200-µm mesh. Afterwards, the samples were cooked for 4 minutes in a 9:1 solution of acetic anhydride and concentrated sulphuric acid and then centrifuged. With ultrasonic sieving, particles smaller than 6 µm were removed. Coarser siliciclastic sediment layers did not occur in the analysed samples, so that the application of HF was not necessary. Pollen were counted until a sum of 200 tree pollen grains was reached. Although this relatively low counting rate might miss especially rare pollen, the general trends and higher signals should appear clearly in the samples. In addition, *Corylus* pollen were not considered as tree pollen for the definition of the point where to end pollen counting because they potentially bias the result due to their high abundance when they were present in the area. Fern spores without perine were counted as indeterminate pteridophytes.

3.7 Terminology of chronological classification

In the scientific disciplines of archaeology and history, temporal classification into cultural periods is based on technological and cultural transitions. These terms are not globally convertible to calendar ages but must be defined in the context of the investigated region and the cultural level of the palaeo-communities. It means that a certain region already transitioned from period A to B, while another region remained in period A. The transformation from Mesolithic cultures – sustaining themselves by hunting and gathering – to the Neolithic is supposed to be the point when humans started to alter their environment through agro-pastoral activities. This is also the point when human presence should have started to leave (geochemical) traces in palaeoenvironmental archives, which is important for the scope of this study. Following a compilation published by Roepke and Krause (2013), the Neolithic began around 7450 cal BP in the northern Central Alps. Their studied site in the northern Central Alps (Montafon) region is south of the Kleinwalser Valley in the state of Vorarlberg in Austria and

thus not far from the other studied areas as well. Their classification is thus adopted in the scope of this study. As an orientation, the ages of cultural periods in the northern Central Alps were additionally transformed to absolute ages (**Table 4**).

Table 4: Chronological classification of cultural periods, based on Roepke and Krause (2013)

Cultural period	Age
Modern Times	< 450 BP (>1500 CE)
Late Middle Ages	750 - 450 BP (1200 - 1500 CE)
High Middle Ages	1050 - 750 BP (900 - 1200 CE)
Early Middle Ages	1450 - 1150 BP (500 - 800 CE)
Roman period	1965 - 1500 BP (15 BCE - 450 CE)
Late Iron Age	2400 - 1965 BP (450 - 15 BCE)
Early Iron Age	2750 - 2400 BP (800 - 450 BCE)
Late Bronze Age	3250 - 2750 BP (1300 - 800 BCE)
Middle Bronze Age	3500 - 3250 BP (1550 - 1300 BCE)
Early Bronze Age	4150 - 3500 BP (2200 - 1550 BCE)
Neolithic	7450 - 4150 BP (7500 - 2200 BCE)

4 Kleinwalser Valley

4.1 Introduction (Kleinwalser Valley)

The first out of three study areas is the Kleinwalser Valley, which is located at the northern boundary of the northern Central Alps. Its name is derived from the Walser people, migrating from the Swiss Wallis region to this part of the Allgäu Alps in the Late Middle Ages (1200–1500 CE). Wagner (1950) spoke of five Walser families, who entered the valley from the south in 1310 CE and built up permanent housing and settlements. The connection towards the foothills of the southern Allgäu region and Swabia remained thin and ran across a bridle path until the construction of a proper road to Oberstdorf (**Figure 5**) in 1572 CE (Fritz, 1981) as the main trade connection. Until tourism became the most important economic sector during the 20th century, the landscape was shaped by forestry and animal husbandry for dairy production (Wagner, 1950). Many localities still bear names that provide information about their past use. For example, “Schwende” (English: swidden) is derived from a technique to keep an area free of trees, shrubs and weeds by girdling and burning, also referred to as “slash and burn”. A historical compilation about life and economy of the valley is given by Fink and Klenze (1891). The holders of local land and farms (called alp) documented their activities in so called “alp books”. Some of these single copies were partly transcribed by Willand & Amann (2013) and provide valuable knowledge about the extent of Walser people’s activity in the valley.

However, from the time before the arrival of the Walser people, there is no proof of any permanent prehistoric settlements in the Kleinwalser Valley. Gulisano (1994, 1995) was among the first to work on the question of earlier human occupation of the Kleinwalser Valley in more detail. Until today and only in the last decade of the 20th century, three major archaeological sites have been discovered, revealing a so far unknown human presence, dating back to the Mesolithic, about 9000 years ago. The most famous evidence is related to the discovery of one of the oldest and most elevated flint mines in Europe, located at the southern end of the valley (Leitner, 2007; Gemstel Valley, **Figure 1**, site c). The latest mining of this radiolarite stone resource has been radiocarbon dated to around 4200 cal BP by Bachnetzer (2017). Another archaeological site called Egg (see **Figure 5**, site a) has first been mentioned by Gulisano (1995). It is located on a gentle rise between the rivers Schwarzwasser and Breitach, west of the village of Riezlern, and has been interpreted as a Mesolithic open campground by Bachnetzer (2017). Radiocarbon dates from a third site are covering time windows in a period from 9000 to 2000 cal BP (Leitner, 2003) and evidence the recurring presence of hunters or herdsmen at a rock shelter on the western slopes of the valley (Schneiderkürenalpe, **Figure 5**, site b). Palaeovegetation studies from mires in the valley (Dieffenbach-Fries, 1981; Grosse-Brauckmann, 2002) gave indications for vegetation changes, possibly induced by prehistoric

pastoral and agricultural activity, but they are lacking a more defined age-depth model. An important piece on the Holocene climate development in the valley is given by the speleothem record of the Hölloch cave by Wurth et al. (2004).

Going further south towards the inner alpine valleys, the studies of lake sediments in the neighbouring Tannberg area (**Figure 5**) by Walde and Oeggl (2004, 2003), or pollen records around the Montafon region in western Austria and eastern Switzerland (Bringemeier et al., 2015; Roepke et al., 2011; Roepke and Krause, 2013) give valuable information about the regional vegetation and land use history at higher elevations, south of the Kleinwalser Valley. Other studies covering the Alpine Foreland (e.g. Clark et al., 1989; Herbig, 2009; Liese-Kleiber, 1993; Rösch, 1992, 1993; Stojakowits, 2014) need to be considered when investigating the history of the Kleinwalser Valley because it is connected to the foreland and a possible pathway into the mountains.

Interestingly, no evidence for direct Roman influence in form of structures or documentation exists for the Kleinwalser Valley. The Roman Empire had conquered the region of the Raetia province, of which the valley was a part of, around 0 BCE/AD or 1950 cal BP (Weber, 1995) and fortified its northern borders against Germanic tribes. The former Celtic settlement of *Cambodunum* (Kempten) became an important provincial city in the Alpine Foreland. Just north of the valley, an east-west trading route ran from *Brigantium* (Bregenz) at eastern Lake Constance through Sonthofen to Innsbruck (Heuberger, 1955; Schönberger, 1969). More and more civilian settlements were established (Weber 1995) in the province of Raetia, but although human impact in the Alpine Foreland rose coevally under Roman authority, recurring raids by Alemannic tribes are believed to have discouraged widespread and extensive cultivation of crops in this part of the province (Clark et al., 1989; Stojakowits, 2014). The last Romans left with the empire's demise after 400 CE (Mackensen, 1995) and it took until the Middle Ages for human impact to become stronger again with the foundation of new settlements and increased land cultivation. The rising population and its need for space to live, fuelwood, arable land, roads and resources, particularly for glass and metal production in this region, led to regional, heavy deforestation (Kata, 1995; Merbeler, 1995).

Despite this, little is known about this transition zone in the Kleinwalser Valley, between lowlands and high mountains. Especially the archaeological evidence is spotty and can only act as evidence to say that humans were present and maybe even why they came (flint, pastoralism). But this information does not allow to draw conclusions on the impact of human presence on the landscape of the valley. If at all, how did they shape it? Also, the lack of continuity of archaeological traces is not sufficiently covered by the existing pollen studies

(Dieffenbach-Fries, 1981; Grosse-Brauckmann, 2002), as their age-depth models are not well constrained by radiocarbon dating, and they are not yielding information about erosion or the extent of human impact.

This study aims at answering the following research questions: What did the landscape look like in prehistoric times? When, how and to what extent was it impacted and changed by human activities and climate factors compared to its previous state? Were the Walser people really the first occupants, which not only used but also altered and shaped the valley's landscape?

These questions seek to be answered by investigating peat cores from mires in the Kleinwalser Valley, using a combination of geochemical proxies and pollen analysis, coupled with radiocarbon dating to compare the acquired data to relevant studies.

4.1.1 Geographical and geological setting (Kleinwalser Valley)

Although it is part of the federal state of Vorarlberg in north-western Austria, the Kleinwalser Valley is not directly connected to the rest of the country by a road (**Figure 5**). Most of its area is situated in the lower montane zone but connects the higher altitudes with the Alpine Foreland in the north. The valley is located at the junction of the geological units of Northern Limestone Alps, Flysch and Helvetikum (Völk, 2001). While the valley floor is located between 1086 and 1215 m a.s.l., it is framed by mountains rising well over 2000 m a.s.l.: At its southern end, the Great Widderstein (2533 m a.s.l.) is the highest peak, which belongs to the main dolomite of the Upper Triassic, while the eastern slopes with the Fellhorn (2083 m a.s.l.) belong to the Flysch Nappes of mainly the Upper Cretaceous (Völk, 2001). The latter are striking north-east to south-west and their northern boundary to the Helvetic Nappes is roughly drawn by the river Schwarzwasser before it joins the river Breitach close to the village of Riezlern. The Breitach is then continuing this geological line before it enters the river Iller at Oberstdorf (see **Figure 5** for orientation). Flysch is a rather soft rock formation, which is composed of interchanging layers of sandstone and marl. The silicate rich products of weathering and erosion are probably the major natural source of lithogenic elements like Ti, Zr, Rb, Fe, Mn, and Pb in local sediments. However, silicate rich layers with a higher proportion of sand, silt and clay can be found within the Helvetic Nappes as well, of which the sub-formation Schrattenkalk is part of as well. This competent lower Cretaceous limestone formation is responsible for the prominent morphology of Hoher Ifen (2230 m a.s.l.) and forms the highly karstified Gottesacker plateau to its north. As a consequence, several karstic cave systems exist in the study area on the north-western flank of the valley, resulting in a complex hydrology (Goldscheider, 1998).

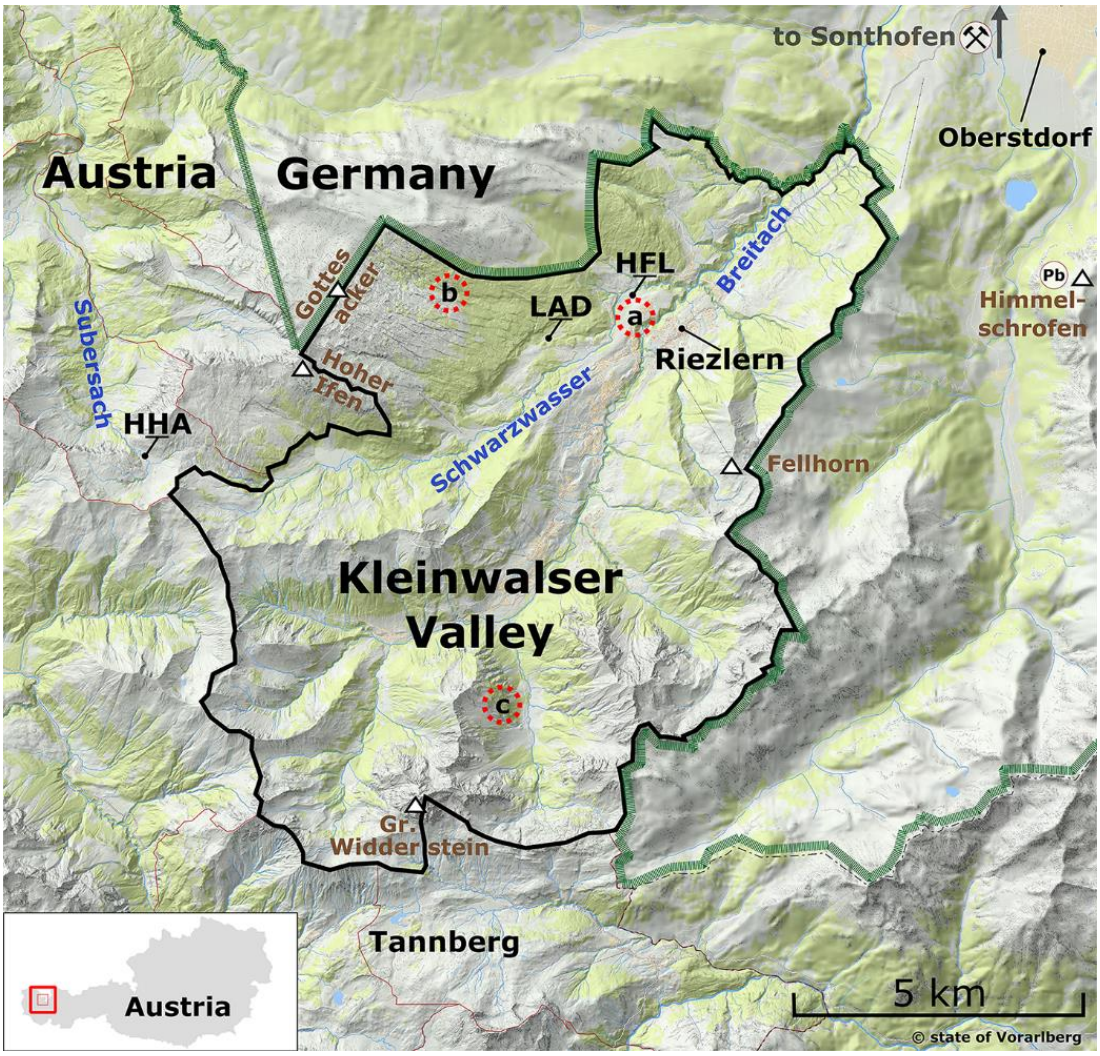

Figure 5: Map of the Kleinwalser Valley and surrounding areas. Archaeological sites (red dotted circles): Egg (a), Schneiderkürenalpe (b), Neolithic flint mine (c). Sampled mire sites: Hoefle Mire (HFL), Ladstatt Mire (LAD), Halden-Hochalpe (HHA). Mountains (white triangles). Modified from source: state of Vorarlberg – http://data.vorarlberg.gv.at

The valley itself was shaped by glaciers, which advanced from the south and covered the whole valley during the last glacial maximum. After the "Gschnitz" stadial around 15400 BP (Ivy-Ochs et al., 2006) at the latest, the valley bottom at elevations below 1200 m was free of ice (Völk, 2001). The receding glaciers left several side moraines parallel to the rivers Schwarzwasser and Breitach and glacial till on parts of the valley floor. In the aftermath of the glacier regression, lake clays formed in the area of the upper Schwarzwasser river (Völk, 2001), just before it joins the Breitach.

Although the Kleinwalser Valley is not known for any metallic ores, several deposits exist in adjacent areas within 35 km distance (cf. **Figure 1**):

- Oolithic Iron ore deposits at the Grünten in Sonthofen, known and exploited at least since 1471 CE (Merbeler, 1995; Oblinger, 2002).

- Pb-ores at the mouth of the neighbouring valley in the east, south of Oberstdorf at Himmelsschrofen (von Gümbel, 1861).
- Triassic sedimentary heavy metal sulphide ores with Pb- and Zn contents of 1.5 to 7 % at Roßkopf in the upper Ostrach Valley, east of Oberstdorf, known already in 1620 CE (Oblinger, 1996).
- Polymetallic copper ores in the south at Bartholomäberg (Tropper et al., 2011).
- Pb-Zn-ores in the Arlberg area, south of the valley: at Zug/Gstüat Alp (Niedermayr et al., 2014), at Zürs, St. Christoph and St. Anton (Cerny, 1989; Vavtar, 1988)
- Permian copper ores in the south-east at Flirsch and Gand (Grutsch and Martinek, 2012).

4.1.2 Climate (Kleinwalser Valley)

The climate is temperate with an annual mean temperature of 5.7°C and a precipitation total of 1863 mm in a period from 1961 to 1990 (Hydrographischer Dienst Österreich (HDÖ), 1994) with a monthly mean of over 200 mm from June to August. These higher proportions, falling as rain during the vegetation period from May to October, provide optimal conditions for peat growth and accumulation. In combination with clayey impermeable sediments of glacial or post-glacial lacustrine or fluvial origin at the bottom, several mires could develop across the valley (Balti et al., 2017; Schrautzer et al., in press 2019; Völk, 2001).

4.1.3 Coring sites description (Kleinwalser Valley)

The first study site, the Hoefle Mire (HFL, GPS: 47°21'52.5"N 10°10'37.1"E), lies in the direct vicinity of Egg (archaeological site a, **Figure 5**) at 1020 m a.s.l., on the western side of a small rise in between the valley's north-western and south-eastern slopes. This rise is almost in the middle of the valley bottom, just between the rivers Breitach and its tributary Schwarzwasser. The small mire covers an area of about 50×100 m (**Figure 5**). It is situated well above the riverbed of the Schwarzwasser. The underlying sediment consists of glacial ground moraine material and localised lake clays (Zacher, 1990), which are both rather impermeable and allow mire development. Due to its sheltered position, the mire is protected from both river erosion and surface sediment input from the south-eastern- and north-western slopes of the valley. This characteristical setting is making the mire a suitable archive to potentially record atmospheric signals, which should be undisturbed by small scale processes.

Figure 6: Photo of Hoefle Mire (centre), northward view toward river Schwarzwasser. Footpath with small ditches left and right to it.

The current vegetation in the centre of the mire is dominated by the ombrotrophic species *Sphagnum*, *Eriophorum, Ericaceae* and *Vaccinium*. The surroundings mainly consist of meadows with goats and cattle, several groves and stands of spruce. Several buildings (houses, hotels and farm buildings) are clustered east of the mire, upon the top of the rise. Anthropogenic factors, affecting the mire nowadays, are regular mowing and ditches, which are draining off the mire along its eastern edge to the river Schwarzwasser. Along this ditch, a gravelled hiking road (**Figure 6**), leads down to the river and separates the mire from a gentle slope. The local name for the area around the mire is “Schwende”, indicating its historical use (see above).

Figure 7: Surface vegetation and boreholes of HFL (left) and LAD (right).

Only 1.7 km to the southwest of Hoefle Mire lies the Ladstatt Mire (LAD, GPS: 47°21'28.1"N 10°09'26.9"E, **Figure 5**) at 1140 m a.s.l. This second study site is situated just at the foot of the forested slope of the Gottesacker karst plateau, 400 m below the important archaeological site "Schneiderkürenalpe" (**Figure 5, site b**). This dry slope, called Küren Valley, is characterised by the lack of surface runoff, as most of the precipitation is disappearing into the karstic underground (Goldscheider, 1998). In terms of size and vegetation, Ladstatt Mire is more or less similar to Hoefle Mire, although the bog vegetation is more pronounced here in the form of dominating *Sphagnum* moss (**Figure 7**). In contrast to Hoefle, it is almost surrounded by forest. A gravelled forest road, accompanied by ditches, runs in between the mire and the northern upper slope to the Gottesacker. Just at the mire's fringes, several overgrown doline structures act as natural gullies and are probably related to a nearby karst cave (Goldscheider, 1998). Furthermore, a cross-country ski route is running across the peatland.

Both HFL and LAD are in the vicinity of or interconnected by the above-mentioned archaeological sites (Schneiderküren and Egg, **Figure 5, sites a + b**).

Figure 8: Photo of HHA, taken from a westward view from the Gehrachsattel, showing the stream meandering through the mire and cattle (left centre).

A third peat profile was surveyed and briefly investigated in the subalpine zone at Halden-Hochalpe (HHA, GPS: 47°20'19.5"N 10°03'48.7"E, **Figure 5**). It does not belong to the Kleinwalser Valley anymore but is only a few hundred metres west off the municipal boundary. The HHA-mire developed on an elevation of 1660 m a.s.l. in a sediment-filled kar or glacial cirque form (de Graaff et al., 2003), slightly west of Gehrachsattel between the crests of Steinmandl and Hählekopf. Compared to HFL and LAD, it covers a much larger area. The peat profile was about 130 cm deep and is readily incised by the meandering uppermost part of the river Subersach, which is, however, no tributary to the river Breitach. The Subersach drains to Lake Constance

through a bottleneck at the northern end of the kar, which naturally gets blocked from time to time and floods the mire. The surface vegetation indicates a fen mire type, although small patches of *Sphagnum* were found. Although the mire site is below the forest line, the surrounding area is almost bare of trees. From spring to fall, cattle are grazing in the area.

4.1.4 Coring and subsampling (Kleinwalser Valley)

Field sampling in the Kleinwalser valley was performed in early August 2016 on the highest point of Hoefle Mire. A peat sequence of 241 cm was recovered in three parallel, overlapping cores (HFL -B, -C, -D) using a Russian peat corer (5x50 and 5x100 cm). A 10x10x30-cm monolith of the topmost part was additionally sampled with a serrated ceramic blade. Another core (HFL17) was taken in HFL with the Wardenaar one year later. Similar to HFL, an 83 cm-long uninterrupted sediment core and an additional 28 cm-long monolith were recovered at the centre of LAD in 2016. At HHA, only a single radiocarbon sample was collected from a charred wood debris layer at the bottom of the open peat profile (c. 145 cm depth) to date the approximate onset of peat accumulation. Tree rings of the charred piece were counted to approx. 60 years (**Figure 9**).

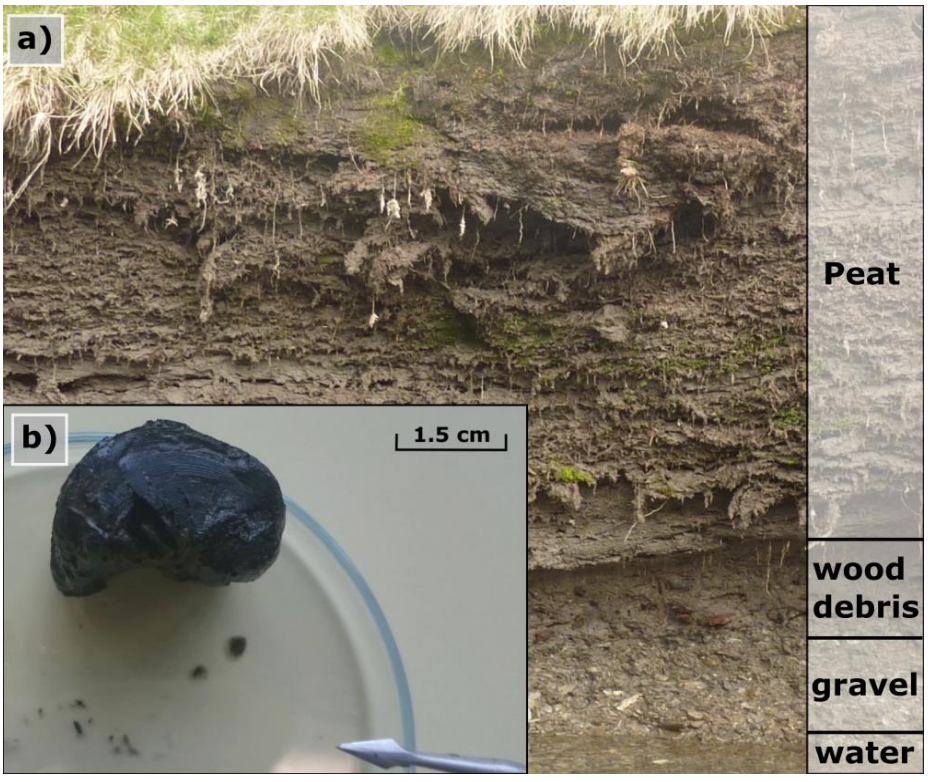

Figure 9: Open profile of HHA and charred wood radiocarbon sample. Tree rings counted to approx. 60 years.

Slicing and subsampling were conducted on core sections B and C by following the procedure described in the methods section (chapter **3.2**). Both LAD sections yielded 86 samples while HFL yielded a total of 232 samples.

To cover the disturbed part between the first two core sections in HFL, an overlapping part of core (C) was fitted to the main core (B) by comparing the dry bulk density profiles. This first estimation was later confirmed by bringing the geochemical profiles of both sections into phase. The same was done to synchronise the core and monolith recovered in LAD.

4.2 Results & discussion (Kleinwalser Valley)

4.2.1 Core descriptions (Kleinwalser Valley)

Hoefle Mire (HFL composite)

Table 5: Core description of the composite HFL peat sequence.

Depth (cm)	Description of HFL
241-237	fine, grey organic rich mineral sediment
236-232	wood
232-227	dark, highly humified peat with few small wood pieces
228-214	lower decomposition, wood at 222 cm, tree (*Picea*) needles
213-203	dark, decomposed peat, very high wood content
192-180	very dark decomposed peat, highly humified peat with rhizomes and few small wood pieces
179-125	dark brown decomposed peat, wood at 152 cm
125-115	very dark peat, higher humification and decomposition, sediment grains, appears in cores B and C, few *Sphagnum* leaves, *Oribatida*
114-101	dark fibrous peat, less decomposed but humified, *Eriophorum* and *Sphagnum*
100-90	dark brown peat, very porous, 4 cm with little material, less fibrous, *Eriophorum* and *Sphagnum*
89-60	dark peat, lower humification, well preserved *Eriophorum* and *Sphagnum*
59-51	dark peat, higher humification, *Eriophorum*, decomposed *Sphagnum*, *Oribatida*
50-47	lower humification, *Eriophorum* and *Sphagnum*
46-40	higher humification, *Eriophorum*, few *Sphagnum*
39-38	dark peat, lower humification
37-33	brown peat, higher decomposition and humification, *Eriophorum* with sparse *Sphagnum*, charcoal at 36 cm

32-27	medium-light fibrous brown peat, lower decomposition, *Eriophorum* spindles and *Sphagnum*, charcoal zone (1-6mm), Quartz and whitish mineral grains
27-21	medium-light brown fibrous peat, *Eriophorum* and *Sphagnum*
21-0	light brown peat, *Sphagnum* dominance, slightly higher humification around 21 cm

A line scan of HFL can be found in **Suppl. Figure 1**. The second parallel core (D) showed a similar development, which could be inferred from the darker marker layer that appears around 115-125 cm. Although it hasn't been analysed in detail, a horizontally lying tree trunk of around 20 cm thickness with a strongly charred upper side was buried in a depth of 215-195 cm.

Ladstatt Mire (LAD)

Table 6: Core description of the composite LAD sequence.

Depth (cm)	Description of LAD
103-101	grey, slightly yellowish fine/clayey mineral sediment with org. material
100-86	highly humified dark peat/gyttja with high mineral content, wood from 89-96 cm
85-77	dark, highly humified peat with few small wood pieces
76-71	pure wood
71-66	dark humified peat, few *Eriophorum* spindles
65-56	humified peat, greyish sediment at 60-61 cm
55-40	dark humified peat, sparse *Eriophorum* spindles
39-33	transition from dark brown to brown peat, still highly decomposed, charcoal and mineral grains at 33 cm
32-25	brown peat, lower humification and decomposition, *Eriophorum* spindles, *Oribatida*
25-0	light brown peat with *Sphagnum* dominance, low decomposition, darker layer around 22 cm

A line scan of LAD can be found in **Suppl. Figure 1**.

4.2.2 Radiocarbon dates and age-depth models (Kleinwalser Valley)

Table 7: List of radiocarbon samples from Kleinwalser Valley, including information about site origin, depth, dated material, uncalibrated ^{14}C-ages and additional information.

Lab. No.	Site	Depth (cm)	Material	^{14}C-age (BP)	Comment
Poz-101727	HFL1B	21.3	*Sphagnum* stems and leaves, few *Eriophorum* spindles	127 ± 0.35 pMC	
Poz-104865	HFL1B	29.9	*Eriophorum* spindles, *Sphagnum* stems and leaves	65 ± 30	0.5 mg C
Poz-92252	HFL1B	36.0	*Eriophorum* spindles	1110 ± 30	0.7 mg C (Figure 10)
Poz-101728	HFL1B	48.3	*Sphagnum* stems and leaves, *Eriophorum* spindles	1525 ± 30	
Poz-92255	HFL1C	80.0	*Sphagnum* leaves	2410 ± 30	
Poz-92251	HFL1B	120.3	*Sphagnum* stem, *Eriophorum* remains	3065 ± 35	
Poz-86728	HFL1B	152.0	Bulk peat	4105 ± 35	
Poz-96113	HFL1B	176.7	Wood and *Eriophorum* remains,	4710 ± 40	
Poz-92253	HFL1B	202.0	Ligneous material, wood	2730 ± 35	Excluded outlier, 0.2 mg C
Poz-86726	HFL1B	235.0	Wood	5330 ± 40	
Poz-86729	HFL1D	175.0	Bulk peat	4400 ± 35	
Poz-95963	HHA	~145.0	Charred wood, outer age ring, min. tree age 60 years	3195 ± 35	(Figure 9)
Poz-99319	LAD Monolith	24.8	*Sphagnum* stems and leaves	127.74 ± 0.37 pMC	0.7 mg C
Poz-103202	LAD1A	31.2	*Eriophorum* spindles	40 ± 30	0.8 mg C
Poz-99198	LAD1A	63.5	*Eriophorum* spindles	3185 ± 35	
Poz-86730	LAD1A	102.5	Bulk peat/gyttja	5320 ± 40	

The age-depth models for HFL and LAD were run with the radiocarbon dates summarised in **Table 7**. As only a single date exists for the basal layer, no model was created for the HHA profile. The settings that differed from the default settings in rbacon (Blaauw and Christen, 2011) and influence the behaviour of both models are given in **Table 8**.

Due to a high degree of decomposition in the lower parts of the cores, not all radiocarbon samples consisted of identified plant remains (**Table 7**). Poz-92253 in HFL1B turned out to be too young. In addition, because of the very low carbon content, it was treated as an outlier and excluded from the age-depth model. Both models are presented in **Figure 11**.

Figure 10: Eriophorum vaginatum spindles and Sphagnum leaf. Part of radiocarbon sample material in Poz-92252.

The outer ring of charred wood of HHA was dated to 3360-3480 cal BP, implying that peat accumulation cannot have started earlier. A minimum tree age of more than 50 years was determined by counting the year rings of the sampled piece of charred wood. In HFL, most samples in the upper part consisted of *Sphagnum* and *Eriophorum* spindles (**Figure 10**). The basal radiocarbon sample was dated to a period around 6000 to 6200 cal BP. This date is setting the onset of mire development shortly afterwards, as a slightly older age should be taken into consideration because of the type of sample material (wood). Over the deepest part, HFL had a peat accumulation rate (AR) of almost 0.9 mm*a^{-1} until around 5500 cal BP, after which it decreased to rates around 0.03 mm*a^{-1} until 3500 cal BP. A slow increase was calculated for the next 700 years, reaching 0.06 mm*a^{-1}, before the AR returned to a rate around 30-40 mm*a^{-1} between 2350 and 1100 cal BP. The following period of around 900 years saw a very low AR between 0.02 and 0.006 mm*a^{-1} over just 10 cm. Only in the uppermost layers, or 28 cm (100 cal BP to the surface), the AR in HFL accelerated significantly and reached over 8 mm*a^{-1} in the upper 8 cm. However, as this layer had been part of the living layers, the term peat accumulation rate should be replaced by “peat growth rate”.

Table 8: Settings in rbacon for the age-depth models of HFL and LAD

Site	thick	acc.shape	mem.strength	mem.mean	acc.mean
HFL	2,0	0,5	9,2	0,25	20
LAD	1,2	0,5	9,0	0,7	50

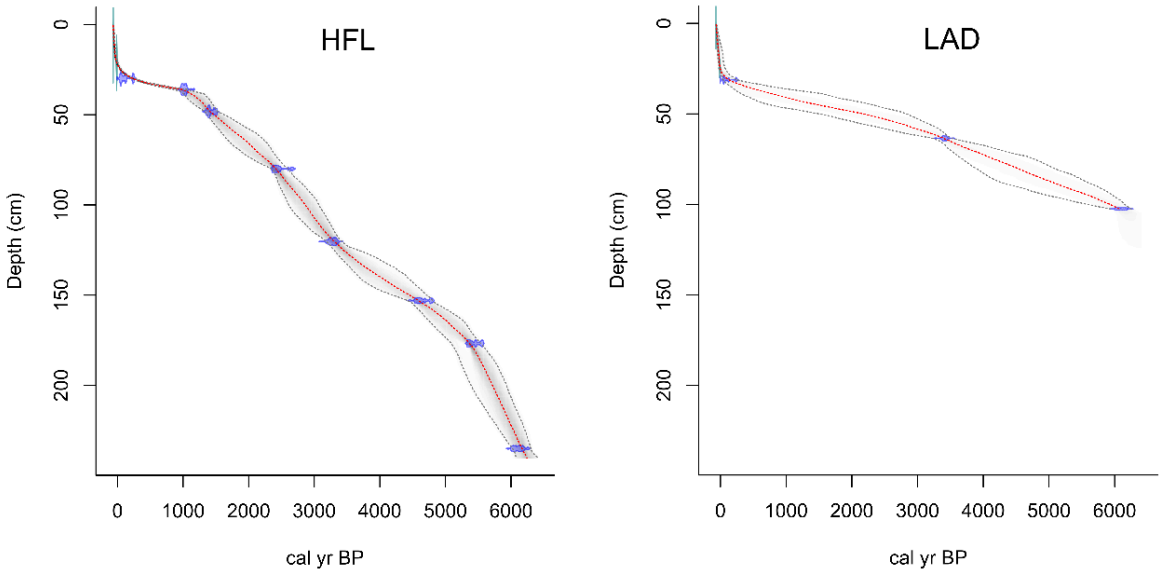

Figure 11: Age-depth models of HFL (left) and LAD (right). The red dotted line denotes the median age and the grey shaded area the 95% confidence interval.

In LAD, the age-depth model in **Figure 11** is pointing to an almost simultaneous date for the onset of peat accumulation (see **Table 7** for comparison of ^{14}C-age). The AR was generally lower than in HFL and did not exceed 0.02 mm*a^{-1} over the lower 65 cm (around 6100 to 500 cal BP). Yet again, similar to the development in HFL, the AR (or peat growth) strongly increased to values of up to 10 mm*a^{-1} in the upper/surface layers.

Both cores were dated using radiocarbon only. This is generally problematic for dates younger than 350 years (Hua, 2009), which is partly due to the Suess effect (Revelle and Suess, 1957). These issues add a higher relative uncertainty to the description and interpretation of recent centuries. However, both models included a radiocarbon date of the bomb-pulse (Goodsite et al., 2001; Piotrowska et al., 2010), which could confine the uncertainty of the high AR in the upper sections. Furthermore, it turned out that characteristic atmospheric Pb pollution by leaded gasoline and coal (Pacyna and Pacyna, 2001) and resulting Pb EF profiles for European peat bogs (Shotyk et al., 1998; Weiss et al., 1999) were consistent with the Pb EF profiles of this study (see e.g. chapters **4.3** and **5.3.5** or **7.2.4**). The decline of Pb EF, after the ban of leaded gasoline, around 1980 CE was therefore used as a chronological marker for both models.

Consequently, both bomb-pulse radiocarbon dates could be set to the rise of the bomb-pulse, as they otherwise would have intersected with the point of Pb EF decline.

4.2.3 Geochemistry (Kleinwalser Valley)

For geochemical analysis of the HFL-core, 172 samples were selected for pXRF of which 51 were measured with ICP-MS and 40 out of these 51 with ICP-OES. For the analysis of the LAD sequence, 63 samples were selected for pXRF. The measurements of HFL samples were used to perform a regression analysis.

4.2.3.1 Regression analysis (HFL)

After having pre-investigated the performance of pXRF on organic CRMs, this section treats the correlation of pXRF- and ICP-MS/OES measurements in the 51 peat samples of HFL by a site-specific regression analysis. The elements Sc, Ni, and Cr were already excluded because of their unsatisfactory measurements (see chapter **3.4.2**). The cross-plots of the comparison for the HFL samples are illustrated in **Figure 12**, with the two lowermost samples at or close to the mineral sediment bottom coloured in red.

While the regression curve of Ti in the CRMs (chapter **3.4.2**) suggests almost quantitative values for high concentrations, i.e. in a minerogenic sediment matrix, the HFL peat samples draw a different picture. In fact, values in the peat samples were generally strongly overestimated by pXRF. Nevertheless, a high fit (R^2=0.97) is observed for concentrations up to 500 mg*kg^{-1}, corresponding to a signal of about 1600 in pXRF. A polynomial (2nd degree) regression model could be assumed if the mineral sediment samples were included. However, two samples with a higher mineral content are barely enough to cover the transition between a linear and a polynomial regression. The results illustrate that concentrations of Ti in samples with a higher mineral sediment load would be underestimated when using the linear regression function for peat (see **Figure 12**).

The regression analysis of Pb measurements resulted in an almost perfect linear fit (R^2=0.99), without a visible matrix effect, as also the mineral samples lined up on the linear regression function. In contrast to Ti, the pXRF-values are also below ICP-MS-concentrations, but to a lesser extent. As already expected from the CRM measurements, **Figure 12** shows that the fit for Cu is low (R^2=0.19), indicating that it is not quantifiable in peat by pXRF, at least not at concentrations below 20 mg*kg^{-1}. In contrast, the measured values of S, Sr and Zn behave coherently, with fitting linear regression models (R^2_S=0.98, R^2_{Sr}=0.98, R^2_{Zn}=0.99), and without major differences between peat and mineral samples. The mineral samples range only slightly above the

regression curve. However, transfer functions are individual for each element, with the highest slope (a) for S (a=0.83) and the lowest for Zn (a=0.24). Calcium and Fe (both R^2=0.95) as well as Zr (R^2=0.87) and Mn (R^2=0.95) had an almost linear regression for the peat samples. The two mineral samples were off the line, most pronounced for Fe and Ca (**Figure 12**). For Zr, a large proportion of the samples ranged around a minimum of 1.5 mg*kg^{-1}, which translated to a pXRF signal minimum of 14-18, suggesting that the LOD is reached. Furthermore, concentrations higher than 7 mg*kg^{-1} exhibited a larger offset from the linear regression function. A special behaviour can be observed for the two elements As and Rb in **Figure 12**. Although high deviations occurred for As at certified concentrations <0.01 mg*kg^{-1}, a use for contaminated sites could still be possible. While Rb measurements in the upper core-half (above 125 cm, where *Sphagnum* was detected first) had a linear fit with R^2=0.84, the lower part (mineral sediment excluded) did not show any recognisable trend or relation. In contrast to Rb, the measurements of As in the deeper section had a very good fit of the regression model (R^2=0.97). To a limited extent, this is true for the upper half as well, but with a significantly lower slope and two outliers. These outliers turned out to be the two shallowest correlated samples.

Obvious matrix effects between peat and sediment samples appear in the regression analysis for the HFL samples. As a first interpretation, this depth dependent behaviour could be related to the trophic status of the layers, as they were probably loaded with elements leached from the sediment and influenced by enriched groundwater from lateral sources (cf. chapter **4.2.3.2**). Furthermore, partly mobile elements were possibly transported from the top layers downward. This generally higher element load could have affected the matrix of the samples. Yet, it demonstrates that pXRF can be used for geochemical analysis of mire samples from the Kleinwalser Valley. At least for Ti, Pb, Ca, S, Zn, Sr, Fe, K, Mn, and V, the regression analysis suggests a reliable calibration or quantifiability of peat measurements, which allows the potential use of these elements for interpretation. For As and Rb, there were serious matrix effects influencing the measurements.

For K, V and maybe Ti, the fit between both measurements could be described by a polynomial of 2nd degree instead of a linear transfer function, specifically when mineral samples are involved. However, more samples in an intermediate concentration range (or transition matrix between peat and mineral sediment) would be needed to prove this, because the presence of a non-continuous function could also be possible.

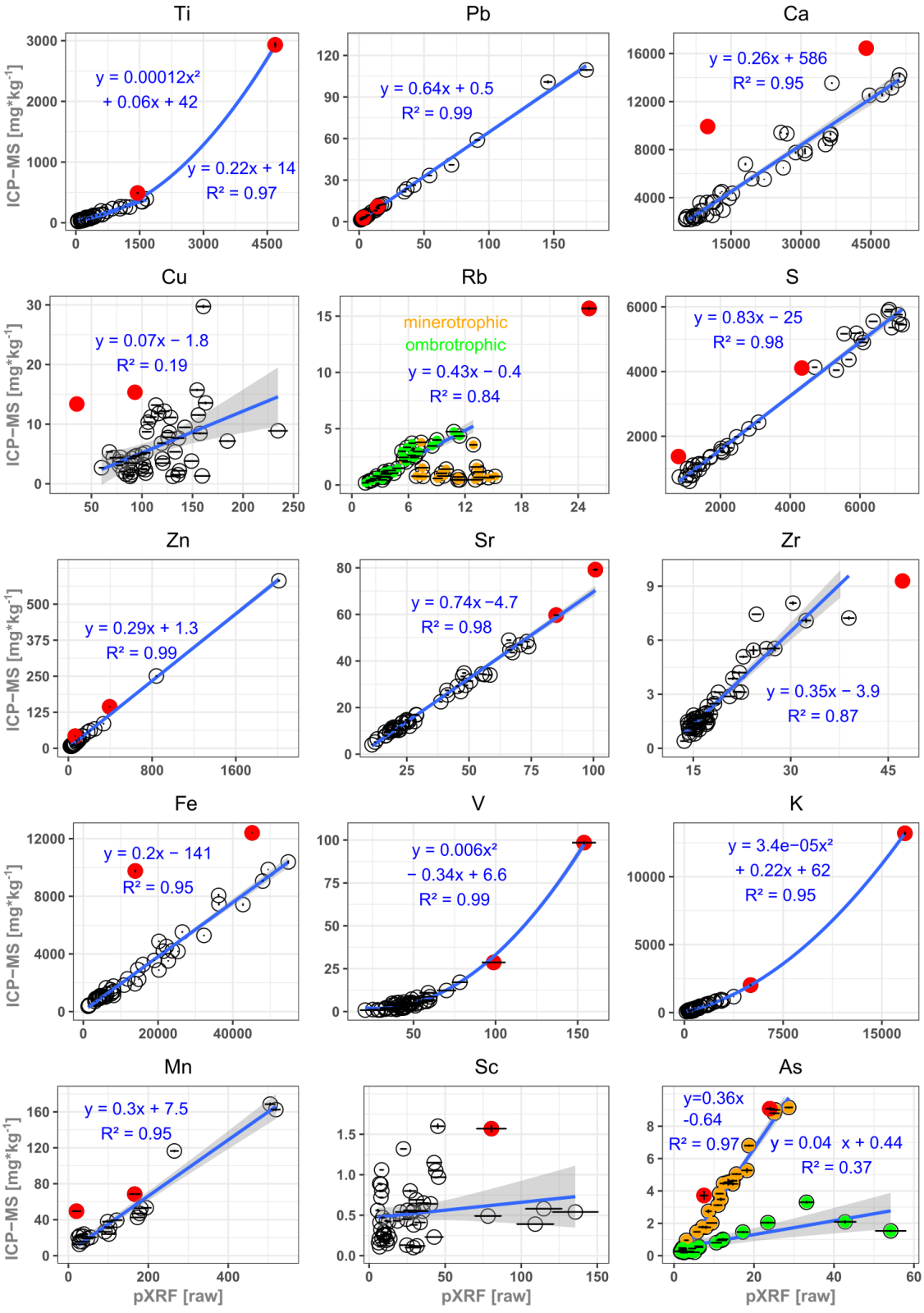

Figure 12: Regression analysis with cross-plots of ICP-MS/OES vs pXRF measurements in HFL peat samples. Transfer functions of the regression analysis and their respective coefficients of determinations (R^2) in blue text. Red = mineral rich, green = ombrotrophic, orange = minerotrophic. Error bars depict the standard deviation of the instrument.

4.2.3.2 Elemental profiles in HFL

Before interpreting the elemental concentration profiles versus age regarding climate and human impact in the valley, this chapter describes element concentration profiles versus depth in **Figure 13**. First, in order to get an idea about the behaviour of each element with depth and second, because data points in the uppermost part would be indistinguishable due to their characteristical age-depth relations. If not indicated otherwise, all profiles are based on the pXRF measurements which were transformed into concentrations by their respective transfer functions (**Figure 12**). The errors of all pXRF measurements were transformed in the same way.

At first, the matrix effect is illustrated by Ca (**Figure 13**) where the bottom sediment concentrations could not be calibrated with the transfer function given in **Figure 12**. The true concentration (from ICP-MS) for the bottom sample is 10,000 (red-curve) instead of the estimated 3000 $mg*kg^{-1}$ (blue-curve). To a lesser extent, this underestimation also affects the following three samples (cf. outliers of Ca in **Figure 12**). A similar behaviour can be observed in the Fe-profile. Also, for Ti, Mn and Zr, the lowermost four samples are biased by an insufficient depiction of mineral samples by the linear transfer functions.

Ca: Concentrations in the deeper peat samples (>175 cm) are still higher than in the mineral sediment base. They decrease continuously from >14000 $mg*kg^{-1}$ at 225 cm to below 6000 $mg*kg^{-1}$ at around 122 cm. Above, the concentrations go below 4000 $mg*kg^{-1}$ and to around 2500 $mg*kg^{-1}$ in the upper 65 cm. The fact that the surface sample differentiates from the others can be explained by its function as a biologically cycled macronutrient in vegetation. Taking all of these observations into account, or can be stated that they suggest a post-depositional leaching, which leads to an enrichment of Ca in the deeper peat layers (e.g. Shotyk, 1988).

Fe: Iron shows the same trends as Ca. It declines from over 10000 $mg*kg^{-1}$ and keeps a level of around 1000 $mg*kg^{-1}$, interrupted only by a short increase to 3000 $mg*kg^{-1}$ around 16 cm.

Sr: Not being affected by the matrix effect, Sr behaves similarly to Ca and Fe, with 70 $mg*kg^{-1}$ at the bottom, decreasing towards 122 cm and keeping a level of 10 to 20 $mg*kg^{-1}$ above.

S: Sulphur is very low in the mineral sample (500 $mg*kg^{-1}$) but high in the peat layers up to 122 cm (4000 to 6000 $mg*kg^{-1}$). An abrupt drop to less than 2000 $mg*kg^{-1}$ was recorded until a temporary rising trend at 50 cm and a climax at 25 cm (3000 $mg*kg^{-1}$). Despite its generally mobile character in peat (Novák et al., 2005), the comparison to the core-description shows that a higher decomposition and humification could be related to a higher S content. This would be in line with Lowe and Bustin (1985), who observed a positive correlation between decomposition and S-content in peat.

Mn: The profile of Mn is below the LOD (around 12 mg*kg^{-1}) between 140 and 21 cm. As a micronutrient, it strongly increases again in the living vegetation layers.

Cu: The ICP-MS derived concentrations of Cu illustrate its distribution in HFL. They are generally elevated in the lower part (10-30 mg*kg^{-1}) and decrease to concentrations mostly around the range of 2 to 5 mg*kg^{-1} after 130 cm. A stable period of a still low signal from 100 to 50 cm is followed by a rising trend with a maximum of 10 mg*kg^{-1} around 24 cm. As the concentrations are generally above 2 mg*kg^{-1}, larger deviations from the reference (see chapter **3.4.1**) should not be of great significance.

Zn: The concentrations in the deepest layers fluctuate strongly, from 35 to 484 mg*kg^{-1} and back to values around 20 mg*kg^{-1} at 200 cm. Another peak (>100 mg*kg^{-}1) appears from 184 to 181 cm. Afterwards, a slow decline down to 5 to 10 mg*kg^{-1} continues until 150 cm depth. This level is kept until 47 cm, with short periods of elevated concentrations over 20 mg*kg^{-1} at 144 cm and around 93 cm. Between 47 and 14 cm, a rising trend climaxes with 96 mg*kg^{-1} but decreases to 29 mg*kg^{-1} again at the surface.

All the above described elements (Ca, Sr, S, Fe, Mn, Cu and Zn) are elevated in the lower half of the core, with a generally decreasing trend ending at approximately 122 cm. It is difficult to distinguish between an element load that is distributed by downwash from the upper layers and elements that are transported upward by richer groundwater or originate from dissolution from peat-mineral interfaces. It can, however, be stated that a post depositional redistribution by diagenetic processes is likely for these seven considered elements. As the decreasing trend of these elements stops at 122 cm, it can be assumed that the influence of groundwater ends at this point as well. Particularly the markedly decrease of S suggests a change in the geo-hydro-chemical regime. Already, Brown (1985) and Vitt and Chee (1990) observed elevated S-concentrations in peat layers with a richer trophic status. The stabilisation on a lower level above 122 cm points to the transition of HFL from fen to bog, i.e. from minerotrophic to ombrotrophic or oligotrophic conditions, between 120 and 125 cm. This interpretation of the Sr-profile was used in other studies as well (Le Roux et al., 2005; Shotyk and Krachler, 2004), and is supported by the subsequent first appearance of *Sphagnum* in the macrofossils (chapter **4.2.1**) and pollen record (chapter **4.2.4**) of HFL.

Having identified the transition point of mire development, the recorded signals of most elements should reflect atmospheric input at the time of growth/deposition above 122 cm, whereas concentrations in the lower part should be considered with caution. Although Cu and Zn are both micronutrients, they can – like Pb – be used as proxies for past mining and metallurgic activities in peat records (Martínez Cortizas et al., 2016; Mighall et al., 2002;

Nieminen et al., 2002). However, Pb can be immobile, even under conditions of a fluctuating water table (Rothwell et al., 2010), and original deposition signals can be conserved in minerotrophic peat (Baron et al., 2005; Shotyk, 2002, 1996b). In contrast, Cu and Zn get more easily mobilised from i.a. adsorption to *Sphagnum* and *Carex* peat under certain conditions (Ringqvist and Öborn, 2002) and could thus be affected by post-depositional redistribution (Dumontet et al., 1990). This would be even stronger in layers with a higher decomposition or peat mineralisation (Biester et al., 2012), where they would be released from their bonds to humic and fulvic substances and thus be available for biological cycling again. The effect of a much higher competition for binding sites in organic matter of the minerotrophic peat probably plays a major role as well (Benedetti et al., 1995; Impellitteri et al., 2002; Kinniburgh et al., 1999; Ma and Tobin, 2003).

Rb: In the second row of **Figure 13**, both the pXRF and ICP-MS profiles of **Rb** are shown. Due to the described issues of pXRF in the deeper part (chapter **4.2.3.1**), the red curve (ICP-MS) shows the real concentrations. The blue curve (pXRF) demonstrates, what the profile would look like if the linear regression was applied on the whole core. Elevated concentrations (114 $mg*kg^{-1}$) were recorded in the mineral sediment, followed by a relatively stable profile until around 45 cm. Only one noteworthy peak (6 $mg*kg^{-1}$) appears around the fen to bog transition. Concentrations up to 4.5 $mg*kg^{-1}$ show from 60 to 25 cm. Except for lower concentrations around 23 cm and from 14 to 4 cm, the concentrations stay on an elevated level above 10 $mg*kg^{-1}$.

Ti: The profile of Ti starts with almost 1000 $mg*kg^{-1}$ in the basal sample, continues on a low level (20 to 60 $mg*kg^{-1}$) from 225 to 125 cm and ends with a major peak of 380 $mg*kg^{-1}$ around 122 cm. Thereafter, moderately low Ti concentrations continue until 60 cm before a rise to 360 $mg*kg^{-1}$ at 32 cm. This trend is interrupted briefly around 48 cm. After 31 cm, concentrations decrease stepwise, to < 30 $mg*kg^{-1}$ at the surface.

Zr: It shares the same trends and peaks with Ti, with maximum concentrations of 50 $mg*kg^{-1}$ at the bottom and 7.5 and 10 $mg*kg^{-1}$ in the upper two peaks, pointing at similar input sources.

V: An ongoing decrease from the bottom to 200 cm suggests a slight mobility of V close to the mineral base. The rest of the profile resembles the Ti and Zr profiles.

K: Despite its function as a macronutrient and an associated solubility and mobility, the concentration profile of K does not suggest a significant upward migration from the mineral base (13200 $mg*kg^{-1}$). It rather resembles the course of Ti until 30 cm. The increase in the top layers could be explained by a rising influence of living vegetation.

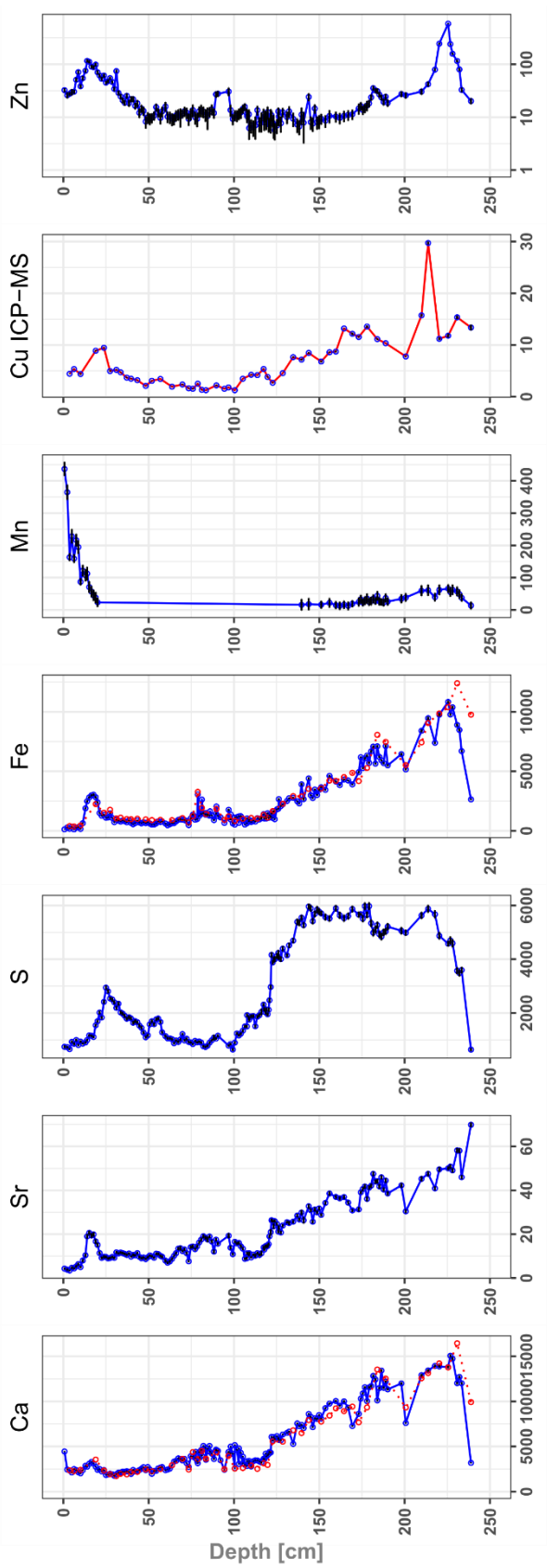

Figure 13: Concentration profiles of HFL peat samples, derived from calibrated pXRF (with calibrated errors) and ICP-MS (in red). Mineral sample removed for Rb, Ti, Zr, V and K. Zn-profile is plotted on a log-scale.

Pb: Lead was well measured by pXRF and is of great importance for this study in order to detect enrichment and trace human activity and pollution. The bottom sample has only 11 $mg*kg^{-1}$. Until 190 cm, concentrations are below the detection limit of pXRF (1.5 $mg*kg^{-1}$). Also due to the strongly elevated concentrations in the upper quarter, more subtle signals around 178 and 144 cm are less visible in the deeper sections. A significant rise to over 25 $mg*kg^{-1}$ was measured around 96 to 90 cm. Although concentrations are generally higher than in the lower half of the core, an accelerating trend of increasing Pb-content sets in after 50 cm, rising from around 12 $mg*kg^{-1}$ and exceeding 110 $mg*kg^{-1}$ at 20 cm. However, a steep decline follows this peak. At a depth of 6 cm, Pb-concentrations arrive at concentrations around or below LOD again.

Sb: Antimony was only measured successfully by ICP-MS, but is considered here nonetheless, because it is an anthropogenically enriched (toxic) element that can be retained in ombrotrophic peat, although not as strongly as Pb or Cu (Rothwell et al., 2010). The profile is almost flat in the lower half, except for the deepest part. A fluctuating profile shows above 122 cm. A first more distinct rise to 3 $mg*kg^{-1}$ at 43 cm transforms into a sharp increase to 11 $mg*kg^{-1}$ at 31 cm. This maximum value decreases again below 1 $mg*kg^{-1}$ in the uppermost peat layers.

Another aspect concerns the discussion of potential reference elements. Taking Nd (or Sm) as representative for the REE, they were more concentrated in the deeper, minerotrophic part of HFL. This is illustrated by the ratios of the two REEs to Ti in **Figure 14**, staying almost completely flat from 122 cm to the top layer. Interestingly, the local sediment (bottom sample) has a very low Nd/Ti ratio of less than 0.01 (magnified by 6 in **Figure 14**), while a maximum of 0.125 appears between 225 and 200 cm. A direct comparison with the ratio of Cu/Ti shows a striking analogy to the Nd/Ti ratio, which suggests a relation between Cu and REE. At the same time, it indicates mobility in minerotrophic peat and competition with other cations as potential binding partners to humic and fulvic substances in these layers. While mobility of Cu under certain conditions is not surprising (see above), other studies described a conservative behaviour of REEs in peat (Aubert et al., 2006; Kylander et al., 2007), which can be confirmed here only for the ombrotrophic part.

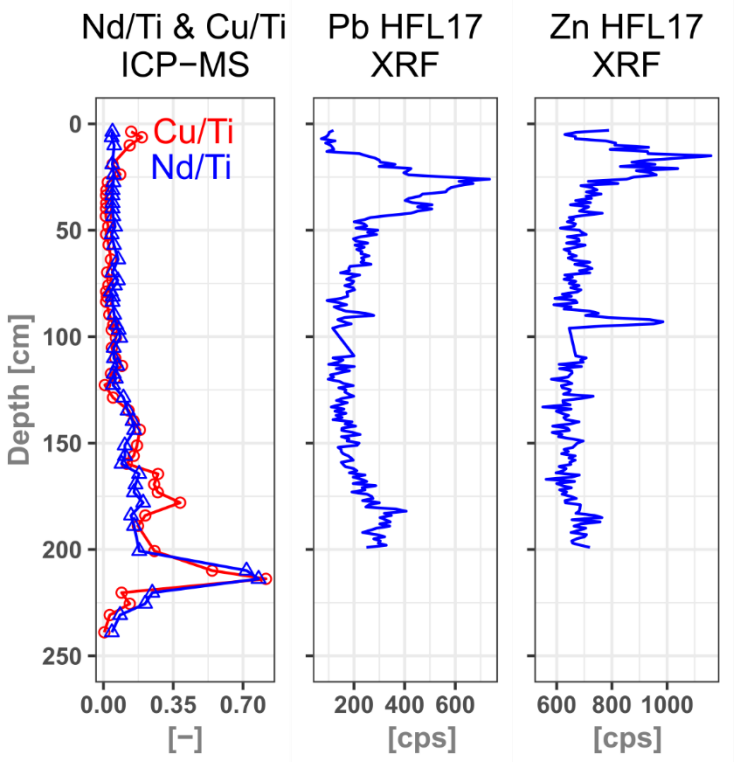

Figure 14: HFL depth-profiles for Nd/Ti in HFL (left) and for Pb and Zn (both XRF-core-scanner) in parallel core HFL17. Profile of Nd/Ti is magnified by the factor of 6 for illustrational purposes.

Besides testing the potential of XRF core-scanning when comparing it to ICP-MS and pXRF results of the Kleinwalser Valley, another purpose of it is to have an independent measurement (or record) to confirm signals, in either the master core or a parallel one. Scanning data for Pb and Zn from the parallel core of HFL (**Figure 14**) shows significantly increased signals, almost parallel to the Pb- or Zn signal in the HFL main core. This is at least the case for the signals around 178 cm, from 96 to 90 cm and for the large peak around 25 cm. As in the pXRF-profiles of these two elements, the Zn-signal seems to be slightly off phase with the Pb-signal (e.g. in the peaks around 93 cm), which can be explained by its higher mobility and a displacement of the element in the peat column. Furthermore, differences between the depths of the observed peaks in both cores can be related to the fact that the presented parallel core was taken one year later and in about 1 to 2 m distance from the master core location. Hence, a slightly differing stratification is possible.

Figure 15 demonstrates that the XRF-core-scanner signal for Ti resembles the calibrated pXRF profile of Ti, although the core-scan was conducted on a parallel core. The signal for Si shows a profile that follows the pXRF profile of Ti even more. This result suggests that Si is the better choice to detect layers with higher mineral content in peat cores with the Avaatech system. These concurrent but independently measured signals of two separate cores illustrate, like Pb

and Zn in **Figure 14**, that the signals are representative for the mire. Moreover, significant contamination, errors or malfunctions during preparation or measurement are unlikely.

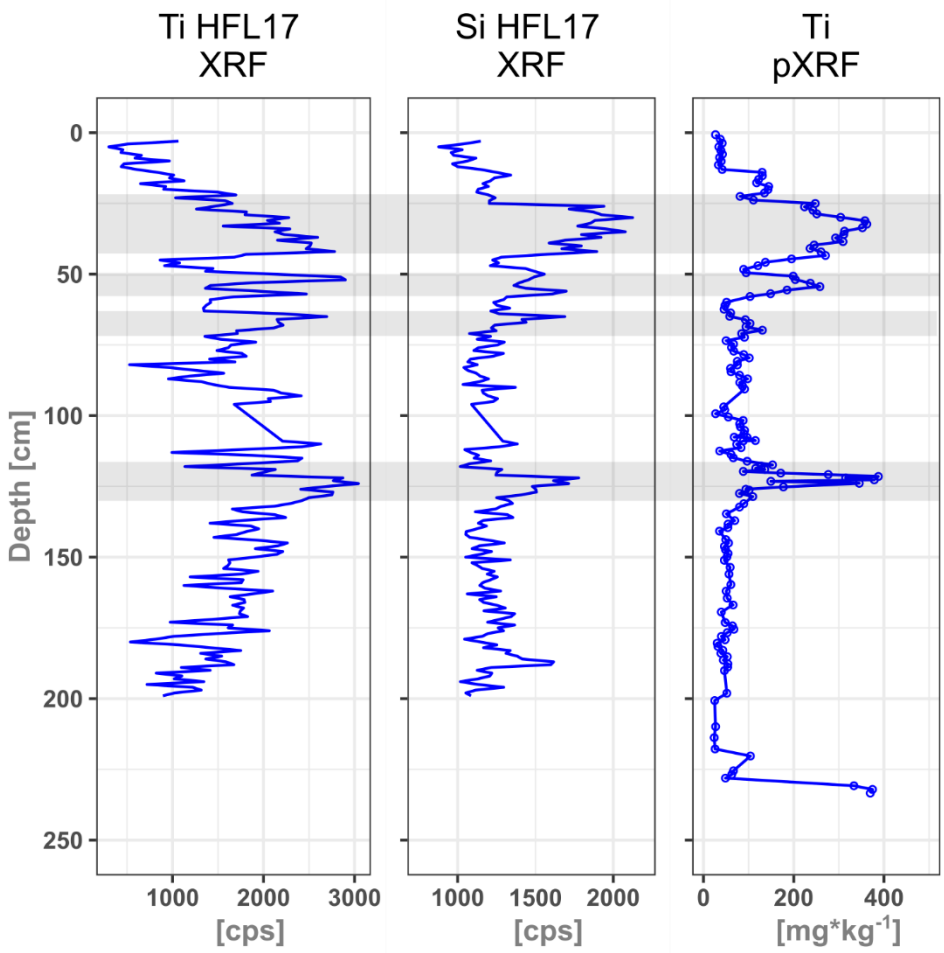

Figure 15: Profile of quantitative Ti (pXRF) in HFL in comparison with qualitative Ti and Si (XRF) of a parallel core HFL17. Grey shaded areas denote similarly elevated phases.

4.2.3.3 Elemental profiles in LAD

Although the regression analysis (chapter **4.2.3.1**) was conducted on the HFL peat samples, the element specific transfer functions were applied on the pXRF—measurements of the LAD-samples as well. It shares both the watershed and the geology with HFL. However, the visibly higher sediment content could have affected the measurements (matrix effect).

Ca, Fe: Because of matrix effects, the regression function (**Figure 12**) would strongly underestimate the true content of Ca in the mineral rich layers of LAD. Consequently, Ca and Fe were relinquished from further discussion in this core.

Sr: In contrast, Sr probably mirrors the true trends of Ca in HFL, because the two elements are closely associated due to similar size. Moreover, none of the pXRF-measurements of Sr had a significant offset from the regression function. It declines from around 50 $mg*kg^{-1}$ in the bottom

mineral sediment to 12.5 mg*kg^{-1} at 78 cm. Except for an increase to over 25 mg*kg^{-1} at 61 cm and lower concentrations in the acrotelm, the profile stays around 12.5 mg*kg^{-1}.

S: The profile of S shows a partly contrasting behaviour, starting with less than 400 mg*kg^{-1} and rising to a maximum of 3000 mg*kg^{-1} around 30 cm before decreasing again. In HFL, S was associated to the deeper peat layers that were geochemically influenced by mineral rich groundwater, but it also coincided with higher decomposition. Here in LAD, a high decomposition of the layers around 30 cm was also observed during the core description (chapter **4.2.1**) which supports the suggestions made earlier for S. The high content of conservative mineral matter (see e.g. Ti-profile) in the deeper layers explains the low S-concentration, despite a supposedly minerotrophic character.

Mn: The element was below LOD in the core, except for the living vegetation.

Zn: The course of Zn in LAD is different than in HFL and does not show an increase with depth. Instead, the concentrations range between 10 to 20 mg*kg^{-1} until 35 cm, after which an increasing trend starts, reaching a maximum of >70 mg*kg^{-1} at 19 cm. Over the following 10 cm, the profile decreases to 20 mg*kg^{-1} before rising again in the living surface layers.

Ti: Titanium needs to be discussed carefully, because of its importance in this study and due to possible matrix effects. Because of much higher Ti-concentrations than in HFL, the polynomial regression function was used for calibration instead of the linear one (**Figure 12**). While the application of either one or the other function would not have made a significant difference in HFL, **Figure 16** shows the significance in LAD: The linear function (blue-curve) would strongly underestimate the Ti signal in more mineral layers, so that the polynomial function had to be applied (red-dashed curve). The mineral bottom sediments reach almost 5000 mg*kg^{-1} but concentrations decline to < 1000 mg*kg^{-1} around 80 cm. Above, a level around 1000 mg*kg^{-1} is kept between 75 and 31 cm, before the concentrations continuously decrease towards the surface. There is, however, a short but distinct peak (3000 mg*kg^{-1}) at 61 cm.

Zr, V, Rb and K: The profiles of these elements are similar to Ti and differ mainly in their relative peak-height (e.g. Zr higher at 61 cm). Only K and Rb increase at the surface. The regression analysis of Rb (chapter **4.2.3.1**) suggested that pXRF measurements could be problematic in minerotrophic peat. Nevertheless, in contrast to HFL, Rb shows a high accordance to the Ti-profile, indicating that it was measured correctly in LAD samples.

Pb: The concentrations of Pb in the mineral samples range around 25 mg*kg^{-1} and below or around 15 mg*kg^{-1} between 75 and 50 cm. Shortly afterwards, an accelerating increase ends

with a maximum of over 180 mg*kg^{-1} at 25 cm. Similar as in HFL, Pb declines sharply afterwards to values below the LOD in the upper 10 cm.

In general, and mostly expressed for the lithogenic elements, the concentration peak around 61 cm is the most distinct feature in LAD. In addition, the peaks in the profiles of Pb and Zn just above 25 cm are remarkable and very much resemble profiles in HFL.

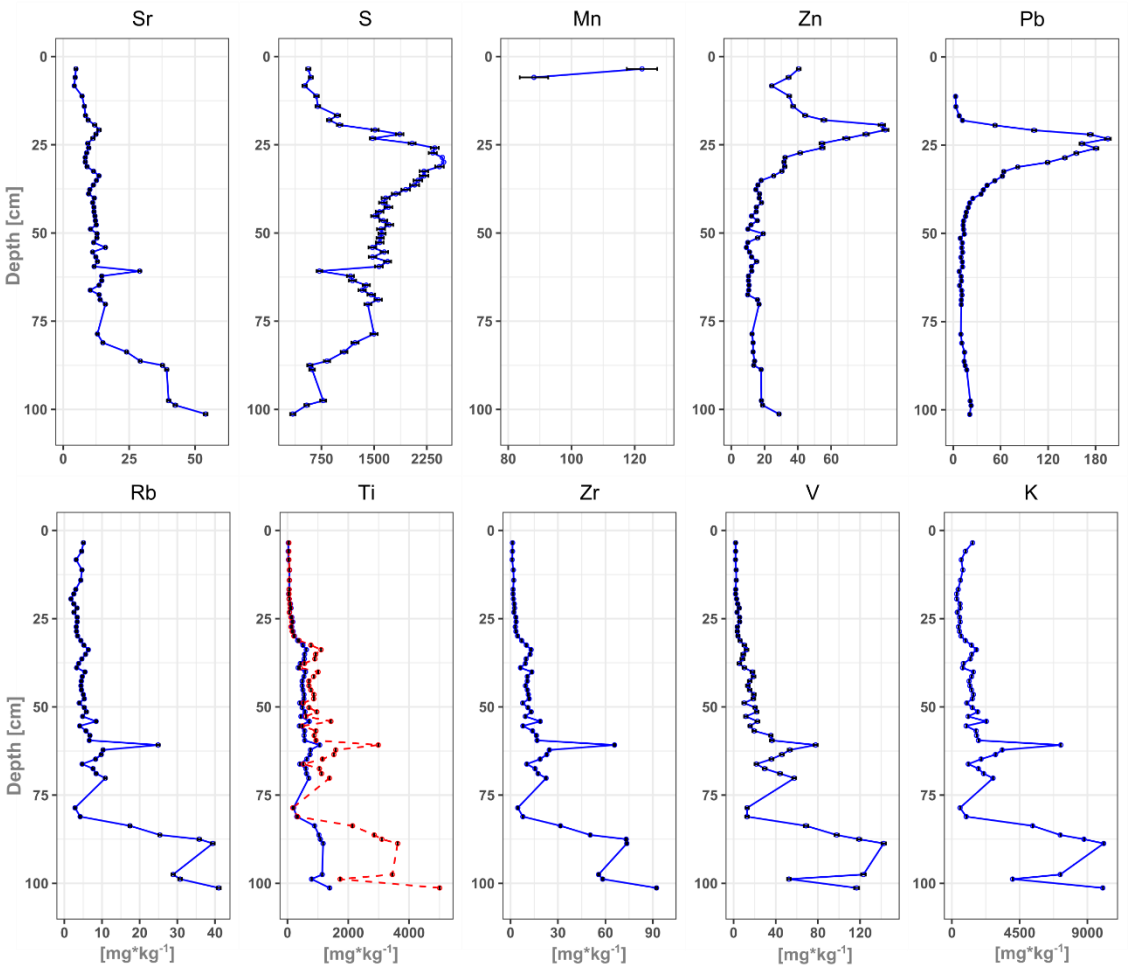

Figure 16: Elemental concentration vs. depth profiles of calibrated pXRF (with calibrated errors) in LAD. Ti results calibrated with polynomial transfer function plotted as dashed line.

4.2.3.4 Reference values (Kleinwalser Valley)

In order to use Ti, Pb (and Cu, Sb, Zn) to calculate EFs and MAR in HFL and LAD, it is assumed that the ratio within the mineral bottom sediment reflects the local background. Despite the successful calibration of the pXRF for Ti and Pb, the concentrations of these elements in the mineral layer of HFL were taken from the ICP-MS measurements for calculation. In this way, the uncertainty was kept as low as possible, especially since the linear transfer function of Ti did not work in mineral sediment and the polynomial could be further elaborated. With Pb at 10.9 mg*kg^{-1} and Ti at 2932 mg*kg^{-1}, the resulting ratio of 0.0037 is close to the ratio in the UCC

(0.004). It indicates that the signature of local sediment is not very different from diffuse atmospheric input. The ratios of Cu, Zn, and Sb to Ti were 0.0046, 0.012 and 0.001 respectively.

4.2.3.5 PCA (HFL)

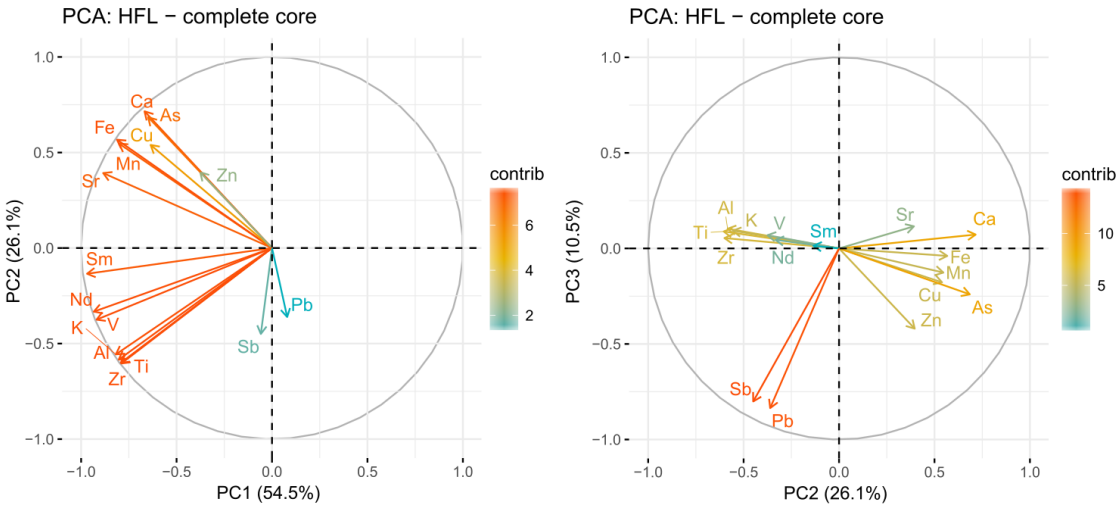

Figure 17: PCA of the ICP-MS results of the complete core of HFL.

The PCA was conducted on the ICP-MS results only. Samples from the uppermost 15 cm were excluded as they would be largely influenced by the living vegetation. The criteria behind the selected range of elements were the quality of measurements and their quantifiability by pXRF. The outcome (**Figure 17**) illustrates and statistically supports some of the patterns and findings that were inferred from the geochemical profiles in the previous chapters. Three components could explain over 90 % of the total variance.

1. Ti, Zr, Al, V, K, Sm, Nd
2. Ca, Fe, Cu, Mn, Zn, Sr, As
3. Pb, Sb

The elements of group 1 are mostly classified as conservative in peat, lithogenic and possibly derived from mineral soil dust, whereas group 2 comprises partly micronutrients. The close connection of mobile elements (e.g. Ca, Fe, Mn) to Cu, As and Zn, implies that the latter could be mobile as well. Group 3 consists of only Pb and Sb which can be distinguished as anthropogenic pollution. They have no biological function and are toxic to organisms (Shotyk et al., 2004). At the same time, they are coexisting in many minerals (Nriagu, 1983). When looking at Nd and Sm in **Figure 17**, their association to group 1 is less strong and they tend a bit towards the clustering of group 2, which supports the previous assumption of REE mobility.

As the HFL core is divided into a minerotrophic and an ombrotrophic half, measurements of the upper half were treated with a separate PCA to look for differences in the element behaviour. As expected, the results in **Figure 18** show group patterns that are slightly different to **Figure 17**, even though three components are again responsible for 90 % of the total variance in the considered data. Here, the group of mobile elements (Mn, Fe, Sr and Ca) clusters without As, Cu, and Zn, which are now associated with the anthropogenic group of Pb and Sb. This points to a conservative behaviour or reduced mobility of these metals and metalloids and a potential preservation of their initial deposition pattern in the ombrotrophic section of HFL.

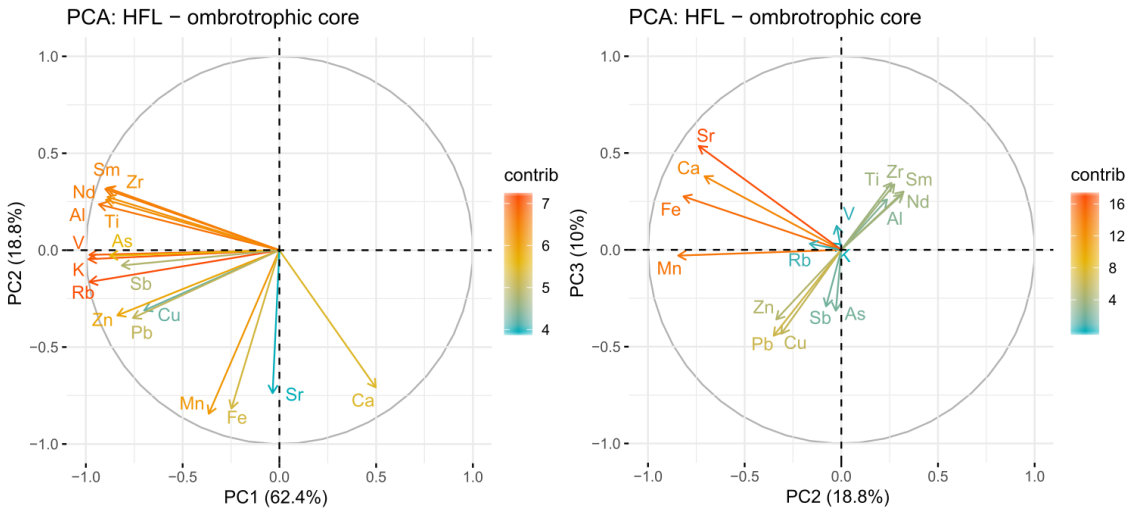

Figure 18: PCA of ICP-MS measurements in the ombrotrophic upper section of HFL.

4.2.3.6 C:N-analysis (HFL)

Aside from looking at elements and their patterns of original deposition, C:N can provide indications for post-depositional processes in the peat. The profile of C:N was measured down to a depth of 140 cm in HFL. The profile in **Figure 19** increases above 120 cm, from a ratio below 20 to partly over 60 between 100 and 80 cm depth. The positive trend turns around afterwards and coming to 20 again between 60 and 50 cm. A short-lived increase to 40 is observed around 48 cm, but again, the ratio drops to about 15 in a depth around 30 cm. The following steep increase towards a ratio of 60 at the surface is probably linked to the high content of *Sphagnum,* paired with a low degree of decomposition (Koster and Favier, 2005). Furthermore, the profiles of S and C:N in **Figure 19** show completely opposing fluctuations. The C:N-ratio can be ambiguous, as it depends on the decomposition but also on vegetation and mineral sediment content (Biester et al., 2014; Hansson et al., 2013). In this case, however, the observations support the previously made assumption that elevated S-contents could be related to higher decomposition and hence to a lower C:N.

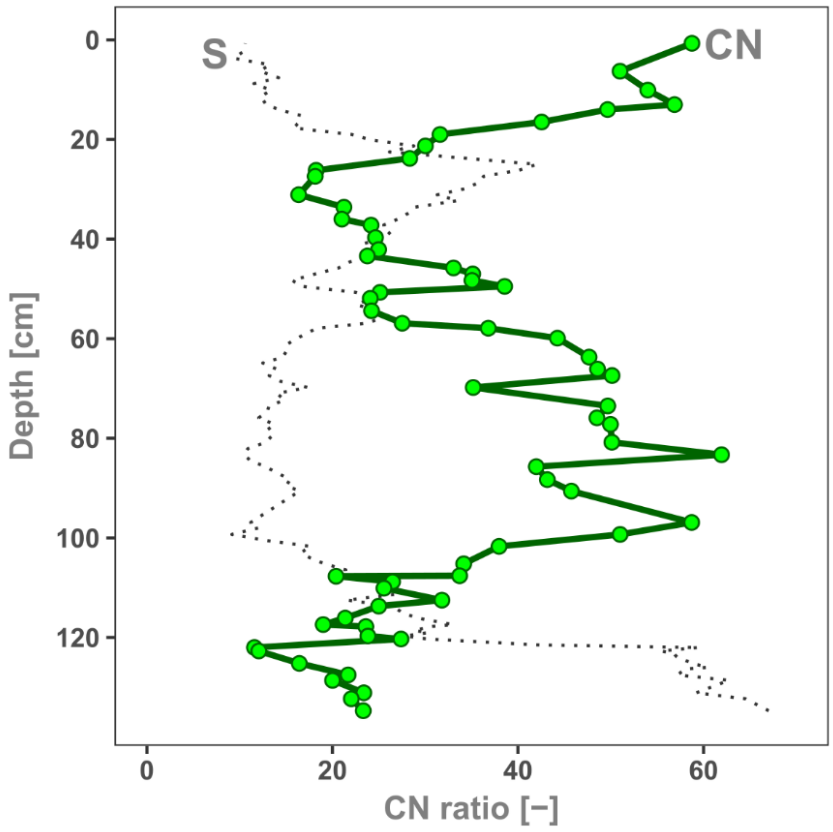

Figure 19: Profiles of C:N (green) and S (black dotted line) in HFL (S is downscaled by factor of 70).

4.2.4 Pollen (HFL)

Pollen from *Cannabaceae* or *Cerealia* like *Secale* and *Triticum/Hordeum* but also from *Plantago* and *Rumex* are indicators of human activity in general, either agriculture or pastoralism. In particular pollen of *Poaceae* and *Cyperaceae* as well as most entomophilic plants, but also ferns like *Thelypteris palustris* and light demanding shrubs like *Corylus,* indicate a more open landscape. Bracken fern (*Pteridium aq.)* can indicate forest pasture or at least a higher grazing pressure (Fritz, 2000; Rösch, 1996). Moreover, *Pteridium* and *Calluna* are more tolerant to fire and their assertiveness can be promoted by recurring burning (Goldammer et al., 1997).

For further interpretation, pollen from certain plants were thus divided into six groups (see **Figure 20**), representing indicators for a more or less strong human impact from a very local up to a regional scale:

Cultural and pastoral (1): *Triticum/Hordeum*, *Secale, Humulus/Cannabis, Rumex acetosa, Plantago lanceolata/major, Artemisia, Ranunculus acris, Cirsium, Chenopodium, Pteridium aquilinum, Juglans*

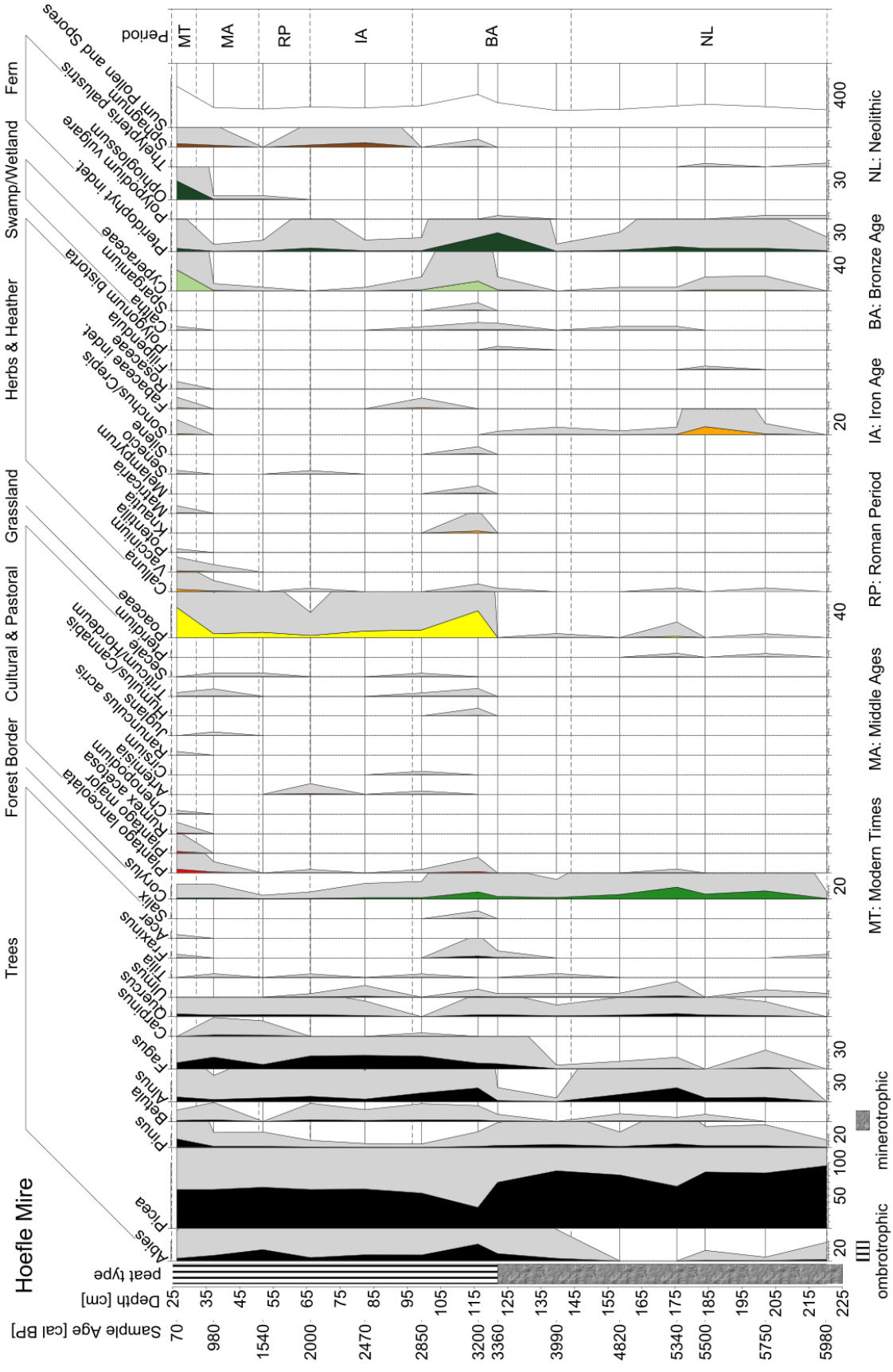

Figure 20: Pollen diagram of HFL Mire. Fully coloured profiles represent pollen percentages, shaded areas enhanced by factor 12. Black=trees, green=forest border (Corylus), yellow=open grassland (Poaceae), red=cultural and pastoral indicators, orange=herbs and heather, light green=swamp/wetland, dark green=fern, brown=Sphagnum, white=total spores and pollen. Dashed vertical lines=cultural periods. Vertical full lines depict cal. sample ages.

Open grassland (2): *Poaceae*

Herbs and heather (3): entomophilic herbs, *Calluna vulgaris*, *Vaccinium*

Forest border or patchy forest clearings (4): *Corylus*

Swamp/Wetland (5): local wetland vegetation with *Cyperaceae* and few entomophilic swamp species

Ferns (6): All ferns except for *Pteridium aquilinum*

As shown in **Figure 20,** except for Modern Times and briefly during the late Middle Bronze Age, tree pollen make up more than 50 % of the total pollen sum. Three periods of a generally more open- and partly more cultivated landscape could be identified from 5800 to 5000 cal BP (Late Neolithic), from 3400 to 2800 cal BP (Middle to Late Bronze Age) and from 1000 cal BP until present (High Middle Ages until industrial era).

4.3 Chronological discussion (Kleinwalser Valley)

Figure 21 (see further below) shows the chronological profiles of proxies that are used in the following discussion on mire development, climate and human impact in mires of the Kleinwalser Valley.

4.3.1 Mire formation

The fine clayey sediments of probably glacial till followed by gyttja at the bottom of both HFL and LAD indicate standing water conditions, which favoured the onset of peat formation. Already Völk (2001) suspected lake clays in the area of the mires. However, angular stones below the gyttja could also be interpreted as a mass movement with silting up or simply as moraine material.

As indicated by the age-depth model, peat formation in HFL and LAD began around or shortly after 6200 cal BP. Pollen proportions and the occurrence of tree needles in the following layers suggest a *Picea* swamp in a densely forested valley at 6000 cal BP, fitting well to the findings of Dieffenbach-Fries (1981). During approximately the same period, other studies report a wetter and colder climate in the Central Alps (Haas et al., 1998; Van der Knaap et al., 2004; Wurth et al., 2004). This phase could be addressed as the Rotmoos I cold phase, which was reflected in glacier advances and forest line decreases (Ivy-Ochs et al., 2009).

Wyllie (2014) showed that the risk of land- or rockslides is elevated during wet and cold periods. Ancient structures of rockfalls in the watershed exist mainly along the upper Schwarzwasser

river around the Hoher Ifen (Schmidt-Thomé, 1960; Völk, 2001) and may have reorganised the complex valley's hydrology (Goldscheider, 1998). This could have further promoted mire formation in certain places, as suggested by Grosse-Brauckmann (2002). But as of today, Völk (2001) argued for an age of these rock-slides dating to an age between LGM and Holocene. A connection between climate, rockfalls and mire formation in the Kleinwalser Valley would therefore need more detailed investigations.

4.3.2 5800 to 3500 cal BP: early human occupation

Only little archaeological evidence suggests early human occupation in the area (Bachnetzer, 2017; Leitner, 2003). Similarly, little palaeoecological evidence exists on early local land use. Regional studies show fire practices (Clark et al., 1989) and crop cultivation around Lake Constance (Jacomet, 2009; Rösch, 1992) and at Oberstdorf, north of the valley (**Figure 5**) (Dieffenbach-Fries, 1981). In HFL, a significant decrease of tree pollen, increasing *Poaceae* pollen and the presence of *Plantago* as well as the emergence of *Corylus* suggest anthropogenic landscape opening around 5550 cal BP. As *Corylus* prefers forest borders, a rather patchy forest clearance is suggested. This interpretation is further strengthened by a significantly elevated erosion signal (MAR) in HFL. Prehistoric fire practices in the valley can be inferred from the presence of *Pteridium* and *Calluna*: species that are tolerant to and promoted by recurring fire (Fritz, 2000; Goldammer et al., 1997; Rösch, 1996). While not dendrochronologically dated, a charred tree trunk was pierced (horizontally) by the corer at parallel depth in the parallel HFL D core (not analysed in detail). Although the cause of fire (anthropogenic or natural) cannot be deciphered, it supports the other indicators, suggesting prehistoric patchy land clearances by the use of fire, probably for livestock grazing. The main core (HFL-B) also showed a high content of wood debris during that time. Moreover, a single date from an archaeological site coincides with the early phase of the observed anthropogenic signals in HFL (Leitner, 2003). Many regional studies from lower elevations to the north confirm an increased human impact around this period with evidences for slash and burn as well as *Cerealia* cultivation (Clark et al., 1989; Dieffenbach-Fries, 1981; Herbig, 2009; Jacomet, 2009; Rösch, 1992; Stojakowits, 2014). Moreover, increased human impact was suggested at higher elevations of the Central Alps (Oetz Valley) by Vorren et al. (1993).

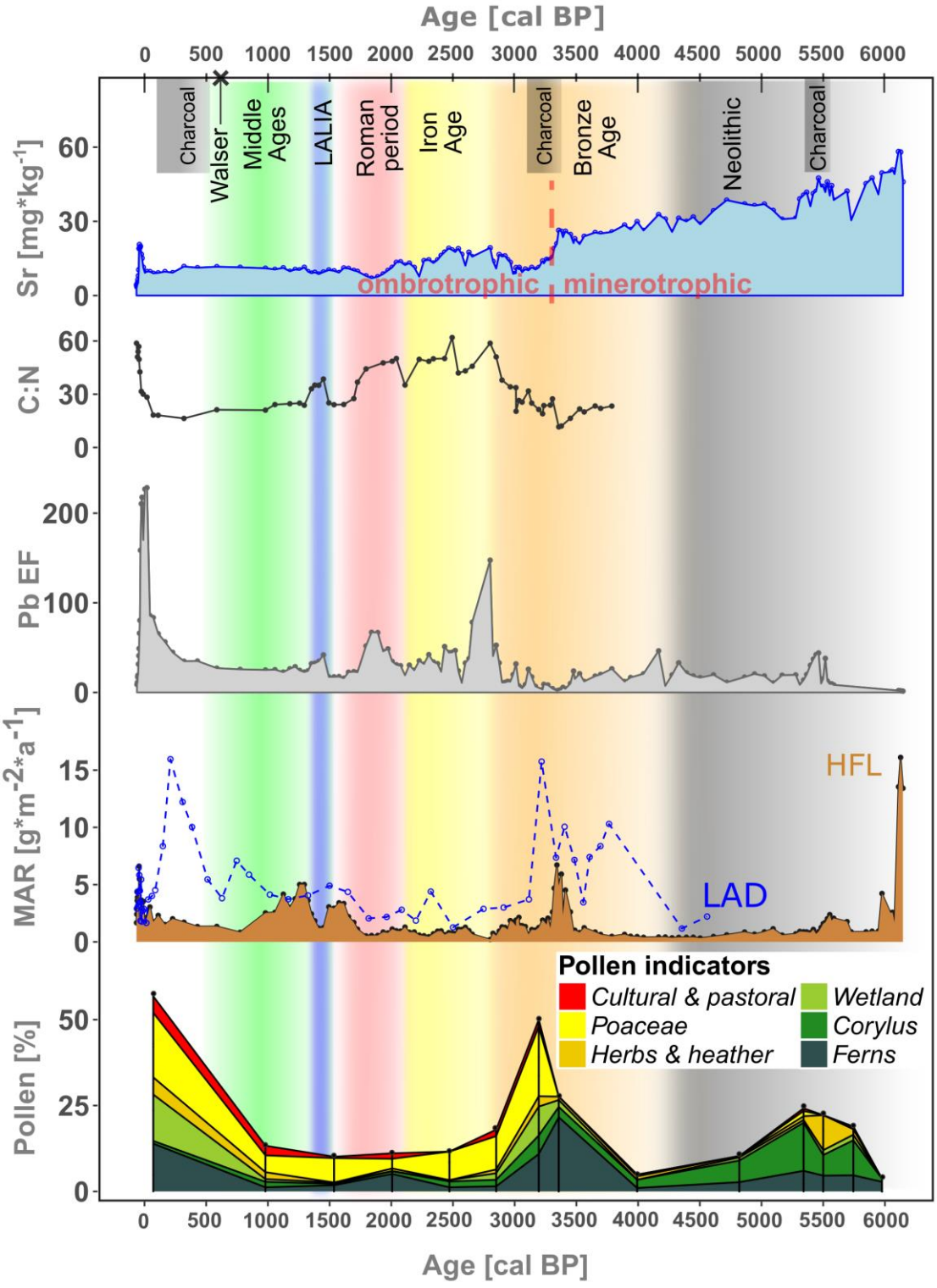

*Figure 21: Chronological profile of Sr-concentrations [mg*kg^{-1}], C:N and Pb EF in HFL, Mineral Accumulation Rates [g*m^{-2}*a^{-1}] in HFL and LAD and Pollen groups as percentage of total pollen [%] in HFL. Colours of shaded areas represent cultural periods in the northern Central Alps: grey=Neolithic, orange=Bronze Age, yellow=Iron Age, red=Roman period, green=Middle Ages.*

Almost simultaneously to the elevated MAR, Pb EF rose significantly (to 50) at 5450 cal BP and remained around an average value of 22 until 3500 cal BP. Only around 4200 cal BP, the profile shows another short rise. Although they are more difficult to interpret in minerotrophic peat, also Cu EF, Zn EF and Sb EF show less confined increases relative to their surrounding layers around the same age (**Figure 22**). While these first episodes of elevated Pb EF were in the minerotrophic stage of the mire, several authors showed that Pb can be used as an anthropogenic indicator in minerotrophic peat (Baron et al., 2005; Shotyk, 2002; Shotyk et al., 2001). This makes the possibility of a signal that is derived from a post-depositional displacement from the mineral sediment or another natural process less likely.

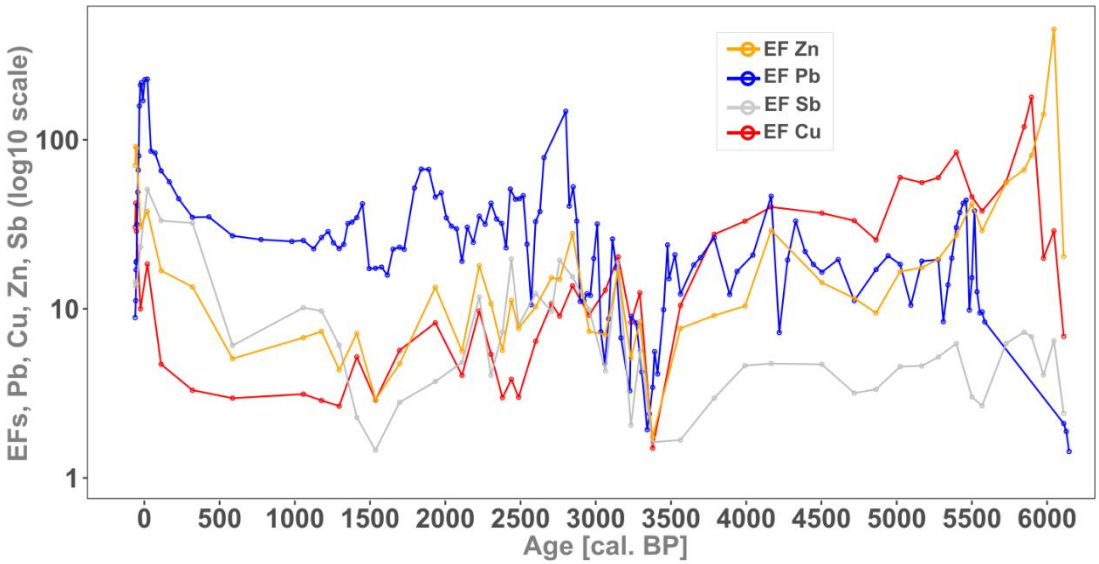

Figure 22: Enrichment factors in HFL of Pb, Cu, Zn and Sb (in log10 scale) vs. time.

The studies of Leitner (2003) and Bachnetzer (2017) presented direct evidence for human presence in the valley for the timing of the second Pb EF rise around 4200 cal BP. The latter was even contemporary with mining in the valley, but only for local silex/flint deposits. However, archaeological evidence showed that metal tools were circulating in the Central Alps as early as around 5500 cal BP (e.g. Artioli et al., 2017; Pernicka and Frank, 2015). Metallurgy at that time was dominated by Cu, which unfortunately cannot be used indiscriminately in HFL, as its mobility in the minerotrophic part indicated earlier (chapter **4.2.3.2**). However, Pb is often present as an impurity within poly-metallic ores (Höppner et al., 2005; Lutz and Pernicka, 2013; Lutz and Schwab, 2015) and could therefore have been detected in HFL. Despite the regional ore deposits, the closest and earliest copper mining, was suggested for the Early Bronze Age (Krause, 2007) but could not be evidenced so far. Also in the Eastern Alps, along the (lower) Inn Valley, earliest archaeological evidence only indicates significant metallurgical and mining activities for the Early Bronze Age (Breitenlechner et al., 2013; Stöllner, 2015b; Töchterle, 2015; Tomedi et al., 2013).

The record of HFL strongly suggests that metallurgical activities in the area could already have taken place around 5500 cal BP, which would be more than 1500 years earlier. These findings are in agreement with other studies, which show that Alpine metallurgy had started well before 5000 cal BP (Bartelheim et al., 2002; Frank and Pernicka, 2012; Höppner et al., 2005).

Altogether, the combined data leads to the conclusion that humans were present in the Kleinwalser Valley and had a significant impact on the landscape in the form of increased erosion during the Neolithic period. As already hypothesised by Leitner (2007), people could have been attracted by the flint/silex resources at the southern end of the valley, following fieldstones upstream in the riverbed of the Breitach, eventually arriving at the flint mine. However, access could have emanated from the south, as archaeological finds by Gulisano (1995, 1994) suggest. Besides flint mining, the data of this study indicates so far unknown metal related activities around 5450 cal BP, which would predate any existing evidence in this region.

4.3.3 3500 cal BP to 2800 cal BP: Bronze Age

The start of this period experienced the evolution from minerotrophic to ombrotrophic conditions in HFL, characterised by the occurrence of *Sphagnum,* a stabilisation of Sr- and a sudden drop of S-concentrations, suggesting an independence from bottom sediment influence. The landscape opened, as shown by the emergence of *Poaceae, Cyperaceae* and *Corylus*, while tree pollen sank below 50 %. Moreover, *Calluna*, *Plantago* and cultural pollen *(Triticum/Hordeum, Humulus/Cannabis)* support the interpretation of an anthropogenic landscape opening and human presence. A very distinct MAR peak in HFL and LAD between 3500 and 3200 cal BP suggests that deforestation and openness promoted soil and slope erosion. Afterwards, another short period of an increased, but less strong erosion was recorded around 3050 cal BP. In line with the first larger peak, the partly charred wood debris layer below the onset of peat growth below HHA was dated to an age between 3360 and 3480 cal BP. When looking at the spatial distribution of the three investigated mires, this strongly points at a widespread deforestation by fire and further supports the interpretation of an opened landscape. For HHA, it even implies that the debris layers had blocked the kar's outlet and initiated the formation of the mire in the first place. Archaeological evidence, consisting of a series of radiocarbon dates from charcoal and ovine bones from Schneiderkürenalpe (**Figure 5**), also suggest more intensive pastoral activities in the valley (Leitner, 2003) from around 3500 to 3200 cal BP. This would have promoted soil erosion on the karstic western slopes above LAD (**Figure 5**). On the same slopes, the speleothem record from the Hölloch Cave (Wurth et al., 2004) registered a contemporaneous negative $\delta^{13}C$ excursion, which could have been caused by

an enhanced input of soil-derived carbon. Cultural indicators and pastoral weeds were observed locally around this time by Dieffenbach-Fries (1981) while Walde and Oeggl (2004) documented fire clearings in the Tannberg area (**Figure 5**) between 3600 and 3300 cal BP. A highly increased sedimentation rate was observed in western Lake Constance by Rösch (1993) at that time. Other lakes and mires also recorded an increasing human impact on the Central Alps' landscape during the period around Middle to Late Bronze Age (Festi et al., 2014; Schmidl and Oeggl, 2005a; Vorren et al., 1993; Wick and Tinner, 1997). In line with the findings in this study, results of Dietre et al. (2017) show that fire management reappeared in North-East Switzerland (Engadin). Only at the end of this period, pastoral impact decreased again, as some studies show (Roepke and Krause, 2013). Contemporaneously, settlement patterns changed after 3500 cal BP as a result of climatic deteriorations and new sites appeared at higher elevations in the Central Alps (Della Casa, 2013). The same author saw technical and agricultural innovations as a driver of higher human impact during the Middle to Late Bronze Age. In terms of climate, a trend to wetter and colder conditions began after approximately 3300 cal BP (Hormes et al., 2001; Ivy-Ochs et al., 2009; Magny et al., 2009), which could have promoted such erosive events by both descending the timberline and bringing more precipitation on an already heavily open and disturbed landscape. While some studies suggested that warmer conditions can promote human activities (Tinner et al., 2003; Vorren et al., 1993), the HFL pollen record does not allow drawing conclusions about warmer or colder conditions.

Having arrived in the ombrotrophic part of the HFL-core, the metal record could now be used for more profound interpretations, as also Cu and Zn should be less mobile. Potentially higher EFs during this period were, however, masked by higher MAR, i.e. input from soils not enriched in metals. Only in the aftermath, they rose again steadily towards the end of the Bronze Age.

It can, however, be argued that the large erosive event observed in the Kleinwalser Valley between 3500 and 3200 cal BP and the specific cultural pollen assemblage were a direct consequence of a strong and deliberate human land use rather than being the direct result of climate factors. It also appears that this drastic deforestation and increase of erosion on the slopes and sedimentation rates in the catchments had a formative influence on the landscape and that they were of a larger regional extent. Despite intensive human activities, no clear indications for metallurgy could be detected.

4.3.4 2800 cal BP to 600 cal CE: Iron Age and Roman period

The pressure of agro-pastoralism progressively disappeared from 2800 to 2500 cal BP as shown by the disappearance of *Artemisia, Fabacea, Cirsium* and *Plantago*. Cerealia pollen

(*Hordeum/Triticum* and *Secale)* also went missing around 2500 cal BP. Forests progressively recovered in a stable landscape with minimum erosion, as also shown in the low MAR. The decreasing human impact in the Kleinwalser Valley may have been triggered by a cold phase (Haas et al., 1998; Ivy-Ochs et al., 2009; Joerin et al., 2006; Nicolussi, 2012; Nicolussi and Patzelt, 2000; Patzelt and Bortenschlager, 1973), making harsh mountain environments less attractive. Declining cultural indicators were also documented at the same period in the Central Alps (Vorren et al., 1993). In the Central and Eastern Alps lower human impact and a re-expansion of forests was described by Oeggl (2015). Yet, this decline contrasts with continuous human impact in the neighbouring Tannberg area (Walde and Oeggl, 2004, 2003) and charcoal layers not much further south (Roepke et al., 2011). A more holistic or less climate deterministic approach to resolve the reasons behind generally lower human activities during this period was also suggested by several studies (Armit et al., 2014; Roepke et al., 2011; Tinner et al., 2003). Why the human impact in the Kleinwalser Valley decreased remains therefore unclear at this stage. It can, however, be hypothesised that humans have never abandoned the valley completely, as the favourable warm and dry period, starting around 2000 cal BP (Büntgen et al., 2011), could have attracted people again for hunting and pastoralism. This is suggested by pollen (*Artemisia, Plantago)* and by archaeological evidence dating to the beginning of this period (Leitner, 2003).

While anthropogenic impact in the Kleinwalser Valley declined from 2800 to 2000 cal BP, Pb EF suggests that metallurgical activities continued in the area. A Pb EF of up to 175 hints at intensive mining or metallurgical activities not far from HFL between 2800 and 2600 cal BP. Synchronously increased EFs of Zn and Sb around this period are supporting this interpretation (**Figure 22**). The exact locations of these activities remain unclear, but they could be either local or regional, as metallurgy from autochthonous ores became widespread in the Eastern Alps around 3500 cal BP (Höppner et al., 2005; Lutz and Pernicka, 2013). At that time, copper was the most importamt metal. However, a study of Tomedi et al. (2013) suggested that the technology advanced during this period to produce alloys with Pb in the lower Inn Valley and Eastern Austria. However, the only works made of pure Pb during that time were found in the south-eastern Alps (Gleirscher, 2015a). Afterwards (2600-2300 cal BP), short episodes of moderate Pb EF indicate ongoing metallurgy in the region. While the earlier signals, starting with the transition from Bronze- to Iron Age around 2800 cal BP, would be related to the Hallstatt culture, the signals in the second half of the Iron Age would belong to the Celtic La Tène culture, as metal artefacts and metallurgy evidences were found in the northern Central Alps (Bächtiger, 1982; Mansel, 1989). During early Roman times (c. 2000 cal BP in this region) HFL and LAD recorded a low MAR, indicating little erosion and therefore decreased land use, as already suggested by Walde and Oeggl (2004, 2003). This is in contrast with increased land use in the Alpine Foreland (Friedmann and

Stojakowits, 2017). Later on, the study of Büntgen et al. (2011) suggested warm summers with moderately low precipitation from 200 to 300 cal CE. Simultaneously, rising mineral input (MAR) in HFL indicates increased land use in the Kleinwalser Valley. Such an early regional human activity and connectivity of the valley can only be inferred from vague historical sources: Raetia's renown for cheese and wood and the renewal of Raetian mountain passages and roads under Emperor Severus' reign (Weber, 1995) could have generated an increased demand and production in the region and promoted the development of an extensive local animal husbandry and a more intense cutting of wood. Higher local land use is implied by the completion of the Roman trade route Via Decia around 250 CE, which connected Brigantium (Bregenz at eastern Lake Constance) with Veldidena (Innsbruck) and ran over Sonthofen, just north of the Kleinwalser Valley (**Figure 1**). A possible Roman pathway from Sonthofen through the Kleinwalser Valley to the region south of it was discussed by von Raiser (1830), with small local outposts, whose stones were re-used later by the valley's inhabitants. In addition, Dertsch (1974) mentioned the Fideri Pass, on the south-eastern slopes, as the "oldest" connection to Oberstdorf, and Fink and von Klenze (1891) described it as a "too well" constructed switchback mountain path, deliberately suggesting Roman origin. Another lead is a Roman coin of the first half of the 3rd century CE, found on the Gottesacker (Gulisano, 1995). However, no modern studies could substantiate Roman presence in the valley so far, as more recent occupation overprinted or reworked potential evidence. But alternative trading routes to the south were needed, especially because the years from 200 to 300 CE were particularly violent, so that most of the Roman territories north of the Alps and west to the river Iller (**Figure 1**) had to be given up by 260 CE and any kind of agriculture was abandoned (Mackensen, 1995). These events may have pushed trade, production and hence rural communities further up into the less populated mountain valleys. It is therefore suggested here that people used the valley's slopes, which led to the observed MAR peak in both HFL and LAD around the 3rd century CE. If it was a direct management by the Romans or not, cannot be corroborated. An elevated Pb EF around 100 cal CE can, in contrast to a suggestion of Mackensen (1995), not be attributed to local Roman mining around Sonthofen. As strong Pb-emissions of Roman origin were recorded in lakes and mires across Europe (Allan et al., 2018; Brännvall et al., 2001; De Vleeschouwer et al., 2010b), the enrichment of Pb in HFL is rather ascribed to diffuse distal sources.

After 400 cal CE, increased *Abies alba* pollen indicate forest expansion in cool and humid conditions. The absence of herbs (e.g. *Plantago)* and *Corylus* suggests a low human influence in the Kleinwalser Valley or at least no fresh cuttings and occupation of the adjacent area around HFL. In parallel to the forest expansion and decreased anthropogenic pollen indicators, the MAR dropped significantly in the first half of the 6th century CE, which is pointing to decreased

landscape and soil disturbances. In addition, the C:N in HFL is showing a significant contemporaneous increase. This hints at a higher effective humidity or water level in the bog, which would have reduced decomposition. Furthermore, less intensive land use (e.g. by livestock grazing) would have decreased disturbance and resulting decomposition of the mire's surface. Although not very pronounced, but in line with the observations in HFL, corresponding pollen patterns were observed in the Kleinwalser Valley (Grosse-Brauckmann, 2002) as well as north of it (Rösch, 1992; Stojakowits, 2014). Palaeoclimate studies showed, that a wetter climate around 400 cal CE was directly followed by approximately 3°C colder summer temperatures from 536 to 660 cal CE (Büntgen et al., 2016, 2011), being called the Late Antique Little Ice Age (LALIA). The LALIA itself falls within the period that was termed "Dark Ages Cold Period" (DACP) by Helama et al. (2017). Furthermore, Winckler (2012) outlined the general scarcity of settlements in the mountain valleys but also the lack of written sources. Around the time frames of these periods, Holzhauser et al. (2005) observed glacier advances in the Swiss Alps. The studies of Büntgen et al. (2016) and Sigl et al. (2015) indicate that an Icelandic eruption (Loveluck et al., 2018) at 536 CE was most likely among the triggers for this exceptionally cold climate episode. The severe consequences on human population in the Alps can also be inferred from a population decline in Austria by approx. 30 % (McEvedy and Jones, 1978).

The comparison of our data with the above cited palaeoclimate records suggests that, due to a climatic deterioration between 500 and 600 cal CE, human activities in the Kleinwalser Valley and its surroundings collapsed. Mineral input (i.e. erosion) temporarily decreased as a combined result of forest expansion and soil stabilisation after it had been trending upwards at around 250 cal CE. Furthermore, the Pb EF in the HFL core recorded a metallurgical signal of Roman- but rather not of local origin.

4.3.5 600 cal CE to 2016 CE: from Early Middle Ages to Modern Times

This period partly saw the expansion of the Frankish empire (Kaiser, 2010) to higher elevations, but little is known about it in this part of the northern Central Alps, as neither Roman nor Middle Age historical sources exist (Babucke, 1995). Only Alemannic line graves at the village of Fischen (between Sonthofen and Oberstdorf, **Figure 1**) are among the rare evidence for human presence before 700 to 800 CE, until the same village (and region) was referred to in 860 CE for the first time by the Abbey of Saint Gall (Dertsch, 1974). Nevertheless, a growing human impact can be observed in the HFL record in **Figure 21**, reflected in the MAR, which increased sharply after the LALIA to peak around 700 cal CE, which is in accordance with observations in the Alps of Tinner et al. (2003) and also with deforestation and settlement expansion in the Alpine Foreland

(Friedmann and Stojakowits, 2017). However, a short lived but sharp drop was recorded at 770 cal CE, followed by a decreasing trend along the Medieval climatic optimum (900 to 1300 CE) (Mann, 2002) until the onset of the Little Ice Age glacier progressions (1300 to 1950 CE) (Matthews and Briffa, 2005).

Concerning the increase of MAR after LALIA, the study of Cheyette (2008) summarised the setback of landscapes from arable to pastureland as a pan-European phenomenon, partly as a result of a cooler climate after the Roman period. It could therefore be hypothesised that, except for the special case of LALIA, the re-establishment of pastoralism in the Kleinwalser Valley promoted erosion again, while previously recovered forests on the slopes were destroyed again to generate larger pasture area.

Despite a decreasing MAR, increasing proportions of cultural pollen (*Juglans,* Cerealia, *Plantago)* at 970 cal CE suggest human presence in the proximity of HFL. At first, these two proxies seem to be contradicting each other. However, it can be argued that stronger human interventions were already disturbing the soils and environment of the valley around the Early to High Middle Ages and that the landscape stabilised in a pasture system, under ongoing but, at the same time, less severe interventions and management of the area.

The MAR decrease together with cultural indicators suggest a landscape stabilisation. Historical sources indeed suggest that the Kleinwalser Valley has been managed for hunting since the 11th century CE. This information can be inferred from the first ever mentioning of the Kleinwalser Valley in historical sources by a deed of Heinrich IV in 1059 CE, which had delegated a hunting privilege to the bishop of Augsburg, putting the Widderstein and the Breitach river (**Figure 5**) as a boundary (Amann, 2013a). Hunting would suggest that other land use, like forestry or animal husbandry, were limited or forbidden in this area. However, the same deed also mentioned a specific name (“gemeinbengunt”) of a cooperative alp (alpine pasture/farm) at the southern end of the valley, which still exists under a similar name today (“Bärgunt”). Therefore, agro-pastoral use must have existed already before 1059 CE. A direct proof for cattle drive from the southern Allgaeu region into the valley was, however, documented at 1200 CE (Amann, 2013a) for the first time.

The Walser arrived in the early 14th century CE (Wagner, 1950) and should have been responsible for most of the changes since then. The presence of macro-charcoal (> 1 mm) in HFL after 1350 cal CE is in line with the onset of Walser settlements and indicates an intensive use of fire across the valley. The uppermost pollen sample in HFL had the highest proportion of cultural and open landscape indicators. However, the palynological resolution is coarse and the age-depth model is limited for that period, placing this sample at the industrialisation period (ca 1880 cal CE). It is

therefore assumed that the Walser intensified deforestation until the mid-19th century, as illustrated on a land cover map from 1857 CE (VoGIS, State of Vorarlberg, 2018a). The MAR progressively increased from the 13th century CE toward the Industrial period, reflecting ongoing clearances by the Walser, growing population and increased agricultural activities (cheese and meat production). This accelerating openness trend could, however, have been buffered by early land (forest) management regulations (Amann, 2014; Fink and von Klenze, 1891), mitigating further destabilisation of land cover.

In contrast to HFL, the MAR in LAD seems to have taken another development between Middle Ages and industrialisation. Even if the accumulation rates in this part need to be considered with caution, MAR appears to have risen quite strongly after around 1400 cal CE. Particularly this western side of the valley started to be increasingly used for cattle grazing after 1450 CE (Amann, 2013b). Consequently, the vulnerable slopes suffered from erosion, induced by timber cutting and cattle trampling. An important driver behind a high MAR (LAD), was most likely also the road construction at 1572 CE, which was connected to extensive clearings (Fritz, 1981) and promoted the development of the valley.

Pb EF and also the EFs of Cu, Zn and Sb increased after around 1400 cal CE. Part of this increase may be attributed to the Sonthofen mining district, where exploitation was first documented for 1471 CE (Merbeler, 1995). Also elsewhere in the northern Central Alps, mining for silver, copper, salt and other resources intensified (Brandstätter, 2015; Hanneberg et al., 2009b; Hofmann and Wolkersdorfer, 2013). However, the emergence of widespread European mining activities in the Middle Ages (e.g. Forel et al., 2010; Le Roux et al., 2005) did most likely contribute to the observed signal in HFL. The interpretation of the Late Middle Ages in the Ladstatt record is however limited by the age constrain. A more detailed discussion would therefore be speculative. It is however observed that the trends that were described above for the Pb EF, the MAR, and pollen in Hoefle, continued towards the 19th century. Moreover, several interpretations from the geochemical data for the late 19th and 20th century are suggested: As a result of heavy industry and the introduction of leaded gasoline in Europe, the Pb EF in HFL strongly increased continuously from around 50 at 1850 cal CE to a maximum of 250 in the 1980s, which is perfectly fitting to the maximum use of Pb fuel and its subsequent ban (Pacyna and Pacyna, 2001). The radiocarbon chronology of the last centuries is not well constrained when compared to historical documentation. This could have partly been caused by drainage of Hoefle Mire, by temporarily reducing peat accumulation and enhancing decomposition in intermediate depths. However, the Pb EF and Pb concentration profiles of HFL and also LAD are strikingly similar to the well-dated Pb EF and Pb concentration profiles of several Swiss mires (Shotyk et al., 1998; Weiss et al., 1999). It therefore provides a chronological constraint for the

topmost part of the HFL- and LAD core. Hence, it can be said that, during the first half of the 20th century, the MAR remained low in both mires. An intensification of tourism in the valley (Fritz, 1981) and the construction of related infrastructure most likely promoted a MAR increase in both mires again after 1950 cal CE over several decades. In the Swiss part of the northern Central Alps, Schneeberger et al. (2007a) concluded that mainly increased road- and house construction as well as a technological evolution towards the use of heavy machines in agriculture/forestry induced a high rate of transformation for landscape changes during exactly this period. A deceleration was, however, observed for the late 20th century (Schneeberger et al., 2007b). Similar processes behind the observed signals in HFL and LAD should therefore be transferable to the Kleinwalser Valley.

Another aspect that is concerning the mire development since the Late Middle Ages is observed in the upper 35 cm of HFL and LAD. Either, there had been a serious decline in peat growth or or post-growth decomposition took place, which affected or still affects the layers between Middle Ages and Modern Times. Drainage that has most likely been installed along with a path already before 1857 (VoGIS, State of Vorarlberg, 2018a), could have changed the established conditions in the growing layer significantly. This change could have temporarily reduced peat growth and, even more importantly, enhanced decomposition in intermediate near-surface layers by aeration. Satellite imagery from 1980 (VoGIS, State of Vorarlberg, 2018b) even shows that new ditches were opened at HFL and elsewhere in the valley. The theory of higher decomposition would be supported by the recorded decrease to uncommonly low C:N after 1200-1300 cal CE. It strongly suggests that there is a connection to human impact (e.g. drainage) by the Walser people. The contemporaneous onset of the Little Ice Age as a climatic driver behind this observation is less likely, as colder conditions would have rather resulted in lower decomposition (higher effective humidity) and consequently higher C:N. As another aspect of human impact, the appearance of macro-charcoal in this part of the HFL core (1400-1800 cal CE) could also indicate burning of the mire's surface. So far, little is known about this phenomenon of decreased peat accumulation during this time window, which is well known for mires across Europe but was addressed in detail only by Sjögren et al. (2007) for several mires along an east-west profile of the Alps. Their results are pointing to a mix of livestock trampling and drainage as the driver, which could be valid for the Kleinwalser Valley too.

However, a *Sphagnum* moss growth boost of over 8 mm*a^{-1} was initiated in HFL and in LAD in the late 20th century, which is rather unexpected in drained mires. Of course, the growth rate of the living part of the acrotelm is not the same as the overall peat accumulation rate, because it is not yet affected by decomposition and compaction by peat layers growing on top of it (Stivrins et al., 2017). But even growth rates in this range are still very high for the montane setting.

Longer growing seasons after the Little Ice Age could have played part of the role. Another, additional, possibility is that an artificial lowering of the groundwater does not inhibit *Sphagnum* peat growth here, because precipitation is high enough to retain a sufficient amount of water in the upper layers and compensate the effect of drainage. Instead, an artificially lowered water level could even keep away richer waters from below and might be one reason for a higher productivity and assertiveness of peat forming vegetation like *Sphagnum* mosses (ombrotrophication). The drainage channels accompanying the pathways along HFL and LAD effectively inhibit any possibility of enriched ground- or soilwater inflow from the slope behind, possibly leading to an anthropogenic ombrotrophication. The existence of such a mechanism has been proven for example by Tahvanainen (2011). The use of the bog for grazing or hay production would even further promote this effect, because the usually more competitive, higher growing plants (e.g. reeds, shrubs, trees) are taken out and suppressed efficiently. In addition, mowing or hay production removes nutrients from the system and promotes the oligotrophication of rewetted fens (Zerbe et al., 2013). Hence, growth rates in natural bog- or fen systems may be lower without management like mowing or grazing, especially nowadays, when eutrophication via atmospheric input is ubiquitous (Bergström and Jansson, 2006), also in the Alps (Rogora et al., 2006).

The last 1500 years are showing an increasing impact of human activities, either recorded as changes in vegetation, as increased erosion during the High Middle Ages and again towards present times. A very strong increase of Pb EF also happened during recent centuries. Besides, a direct influence on the hydrology and ecology on HFL and LAD is reflected in a horizon of highly increased compaction or decomposition, which is followed by a boost in *Sphagnum* growth starting after 1950 cal CE.

4.4 Conclusions on the Kleinwalser Valley

This chapter presents two peat records of the Central Alps, which are covering the last 6200 years. By combining geochemical, palynological and chronological tools, it was possible to understand the occupation and high human impact on the landscape in a valley of the northern Central Alps and beyond. Calibrating a portable geochemical tool with ICP-MS also allowed the quantification of geochemical elements in different peat types, from minerotrophic to ombrotrophic. The geochemistry suggests that REE (Sm, Nd) are not fully conservative/immobile in the minerotrophic part of the peat column and show - like Cu, Sr or other mobile elements - an increasing ratio to Ti with depth. The data is furthermore pointing at the possible use of S as a decomposition proxy as a marker to define the transition from minero- to ombrotrophic.

A cooler and wetter climate around 6200 cal BP promoted mire formation in the Kleinwalser Valley. Pollen spectra and erosion suggest human presence in the valley as early as around 5700 cal BP, lasting over several centuries, which is in line with studies on regional occupation. Increased Pb EF values around the same time suggest metallurgical activities in the area, which predates regional archaeological evidences by 1500 years. Large-scale deforestation and land use (agro-pastoralism) took place between 3500 and 2800 cal BP causing a drastic landscape opening and high erosion rates both at low and high elevation. At the end of this period, a prominent Pb EF points to strong metallurgical activities in the area. However, landscape stabilised and forests could recover thereafter until the early Roman period. A second period of increased erosion and land use started after 230 cal CE and climaxed at around 700 cal CE. This increased land use period was, however, interrupted by climatic deteriorations around 500 to 600 cal CE. Pb EF also saw an increase during the Roman period. It is yet challenging to pinpoint its origin as Roman Pb pollution had been widespread. The Middle Ages saw progressive land management and the arrival of the Walser people. While historical data point to a strong Walser influence on the area, our data only allow us to suggest that deforestation, agriculture and pastoralism continued during that period. Yet, the extent of those activities remains unclear. A marked decline in the peat accumulation rate paired with low C:N after 1200 cal CE hints at a direct disturbance of HFL by either drainage, cattle trampling or burning.

The Pb EF increased during Late Middle Ages. It then rose faster during the industrial revolution and peaked before leaded gasoline was banned, allowing its use as a chronological marker to constrain the last century, which experienced increasing tourism and its consequences taking place in the Kleinwalser Valley.

Sveral archaeological findings and sites give evidence for three prehistoric hot-spots of human activity. Our pollen and geochemical data allow us to detail the evolution of local and regional landscape and its use in the northern Central Alps. The combination of historical sources with erosion- and pollen indicators points to local land use and human presence in the valley thousands of years before the Walser people’s arrival. A landscape that had been shaped strongly by humans before is probably the reason why the impact of the Walser was ultimately less conspicuous than expected.

5 Piller Mire

5.1 Introduction (Piller Mire)

The second study site is the Piller Mire, which is located in the Piller Valley in northern Tirol (Austria) and belongs to the municipal of Fließ (**Figure 23**). The surroundings are often referred to as Piller Saddle (Piller Sattel or Pillerhöhe). It acts as a pass, which connects the Upper Inn Valley with the Pitz Valley, but the main roads are still running along the lower Inn Valley. It is neither densely populated nor very frequented by tourists, except for people that are heading for the more popular Pitz- and Oetz Valley. It, however, belongs to the Kaunergrat nature conservation park and is known for a network of bogs and fens.

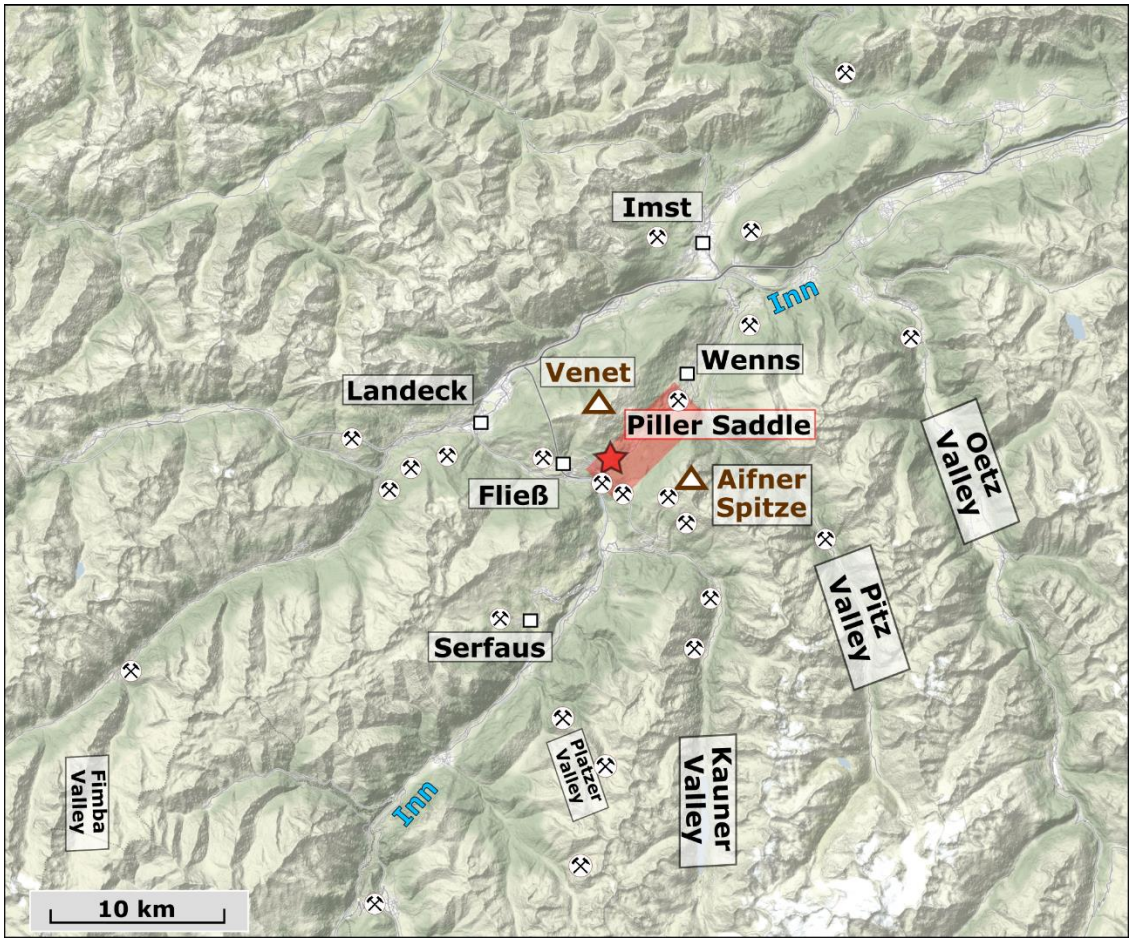

Figure 23: Overview map of the region around the Piller Mire (red star) with relevant ore deposits/ancient mines indicated, compiled from (Grutsch and Martinek, 2012; Vavtar, 1988; von Klebelsberg, 1939; von Srbik, 1929; Weber, 1997). *Edited from source: Stamen Design under CC-BY-3.0 and OpenStreetMap contributors under ODbl.*

The nearest city is Landeck, down in the Inn Valley and north-west of the study area. First direct evidence of prehistoric human presence in the surroundings of Landeck are dating back to the Neolithic period and metallic finds date back to around 3700 cal BP (e.g. Pöll, 1998). Depot finds of bronze objects of an age around 2600 cal BP were found in Fließ, which is on the slopes between the Inn River and the Piller Saddle. Among the most relevant archaeological sites for this study is a prehistoric ritual fire place in the direct vicinity (**Figure 23**) of the studied mire

(e.g. Heiss, 2008; Tschurtschenthaler and Wein, 1998). This ritual sacrificial site was in use already between 3500 and 3300 cal BP and a continuous occupation of the site has been suggested until around 2000 cal BP (Tschurtschenthaler and Wein, 1998, 1996). Furthermore, a hoard find of 360 copper artefacts on the Piller Saddle was probably deposited during the Mid Bronze Age between 3500 and 3200 cal BP (Tomedi, 2012, 2002a).

Several pollen studies on palaeo-vegetation along the Holocene have been carried out in the area: In a fen peat sequence from Fließ at 1365 m a.s.l., Walde (2006) reported the first human fire clearances starting already around 5800 cal BP. In a site about 10 km southeast of Piller (at c. 1900 m a.s.l., Komperdellalm, Serfaus, **Figure 23**) Wahlmüller (2002) observed earliest human impact with the onset of the Early Bronze Age around 4200 cal BP. A similar age for human activity was documented by Hubmann (1994) also in the Piller Mire. All three studies indicate increased land use periods during the Bronze and Iron Age and in early Roman times, before an intensification starts again in the Early Middle Ages in all three sites. In a larger perspective, the studies of e.g. Festi et al. (2014) in the Oetz Valley and Dietre et al. (2014) in the Silvretta region show the Holocene development of climate and human impact east and west of the Piller Saddle.

Beside archaeological findings and pollen studies, the reconstructions of glacier activity and tree line changes in the nearby Kauner Valley (Nicolussi et al., 2005; Nicolussi and Patzelt, 2000) provide valuable information about regional changing climate conditions in the past.

In spite of the existing studies on glaciers, local vegetation changes, and many archaeological finds, there are no palaeoenvironmental studies based on geochemical analyses. Therefore, no information is available on episodes of increased mineral input, as a signal of erosion that was either derived from anthropogenic land use or climatic disturbances. The comparison to existing pollen studies helps in distinguishing between these two possible driving factors and, at the same time, in assessing the scale of impact. Furthermore, the specific focus on the metal record could give, for example, clues on the question if the Bronze Age hoard find correlates with increased metal EFs. While archaeological excavations often give only isolated information, the analysis of EFs could reveal episodes of local or regional impact of metallurgy.

Hence, this work presents the first palaeoenvironmental study of the region based on geochemical analysis of a peat core from the Piller Mire is presented. In contrast to the record of the Hoefle Mire in the Kleinwalser Valley, pollen were not analysed in parallel. The earlier palynological- and archaeological studies, in particular the one of Hubmann (1994) are therefore used as an independent basis for the discussion and comparison of the geochemical results with respect to regional climate, human activities and their possible interactions.

5.1.1 Geographical and geological setting (Piller Mire)

North of the Piller Saddle, the slopes rise from around 1550 m a.s.l. to the Venet at 2512 m a.s.l. and the next mountain to the southeast, the Aifner Spitze, rises to 2780 m a.s.l. (map, see **Figure 23**), Both the Venet and the Piller Saddle are delineated by the Upper Inn Valley to the west and the north. The Piller Valley runs in a SW-NW direction, with the Inn- and Kauner Valley at its SW-end. The NE-end passes into the lower Pitz Valley, which then enters the Inn Valley again at its northern tip. A small stream (Pillerbach) drains all surface waters towards the Lower Pitz Valley.

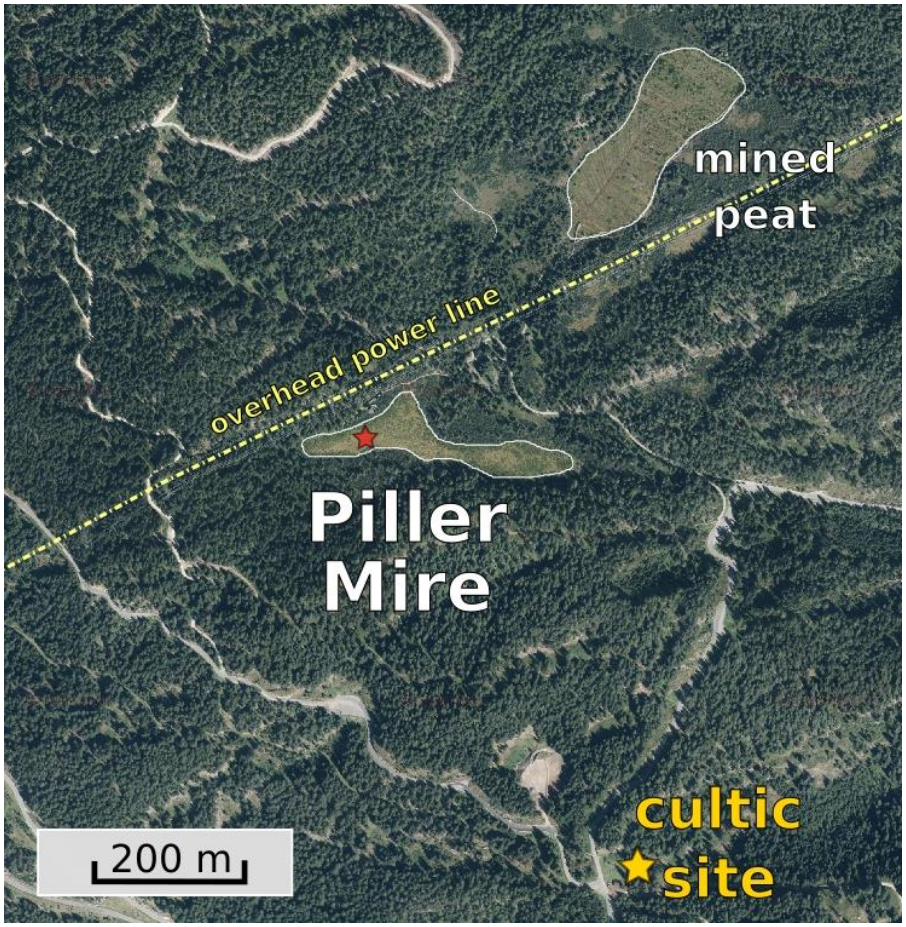

Figure 24: Detailed view of the direct surroundings of the Piller Mire. Coring spot marked with red star. ©State of Tyrol, edited from source: State of Tyrol - http://data.tirol.gv.at, see also (State of Tyrol, 2019a).

Geologically, the area is still part of the northern tip of the Silvretta formation, but with a relatively low metamorphic degree. The Inn Valley marks the line between the metamorphic zone to the south of it and the calcareous Alps north of it. The bedrock is composed of quartzites, quartz phyllite, phyllite gneiss and muscovite schists, which are bearing minerals like garnet, feldspar, chloritoids and staurolite (Nowotny et al., 1993).

In a larger radius, the rock formations bear numerous metal ore deposits (Hammer, 1915a, 1915b; Schach and Minsinger, 1849; Vavtar, 1988; von Srbik, 1929; Weber et al., 1997). To the north, mainly lead (Pb) and silver (Ag) in form of sulphides (galena, calamine, smithosonite and

hemimorphite) were exploited around Imst and the Fernpass area together with secondary elements such as molybdenum (Mo), iron (Fe) and copper (Cu) (Hanneberg et al., 2009b; Wolkersdorfer, 1991). Other ore deposits around the study area saw non-modern mining activities (Grutsch and Martinek, 2012) and complement this knowledge about ore deposits and indications for potential historic to prehistoric mining in the area.

5.1.2 Climate (Piller Mire)

The climate in the area is already influenced by its position behind the first northern Alpine chains, which are shielding part of the precipitation arriving with moist air masses from the north-west (rain shadow effect). It can therefore be classified as belonging to the inner alpine/continental climate with annual precipitation between 600 and 1000 mm. The climate data considered here covers the period from 1971 to 2000 CE (Central Institution for Meteorology and Geodynamics of Austria, (ZAMG, 2018)). In Landeck (785 m a.s.l.), mean annual precipitation from 1971-2000 CE was at 753 mm with maxima during the vegetation period from June to August. A similar pattern, with a lower precipitation of only 633 $mm*a^{-1}$ was recorded for Prutz, which is about 5 km south of the Piller Saddle. The mean annual temperatures in Landeck and Prutz during that period were 8°C and 6.8°C respectively, so that it should be around 4 to 5°C lower on the Piller Saddle due to the higher altitude. When considering four of the closest climate stations around the site (Landeck, Imst, Prutz and Obergurgl), the predominant wind directions were SW and NE.

5.1.3 Coring site description (Piller Mire)

We carried out a first survey of the supposedly undisturbed part of the Piller Mire complex in late July 2016 (**Figure 23**). The mire stretches about 380 m in length from west to east and between 30 to 100 m in width from north to south. The mire's surface is at an elevation of about 1540 m a.s.l. and thus within the lower subalpine vegetation zone. It is within a topographical depression, which is not surrounded by steep slopes but is probably up to 15 m deep (Naturpark Kaunergrat, 2000).

There is no channelled surface inflow, but a tiny stream leaves at the mire's eastern end ("*rechter Kohlplatzbach"*). Although it was neither visible by eye in the field nor on satellite imagery, the digital terrain model (State of Tyrol, 2019b) indicates a tiny channel structure in the mire's centre, which leads toward this outlet.

Figure 25: Piller Mire borehole, showing the high water level. Vegetation includes Sphagnum, Eriophorum and Andromeda polifolata.

During three consecutive visits to the mire in 2016 and 2017 (July, August, September), the observed water table was just a few centimetre below surface (see **Figure 25**), even during hot and dry periods, which is hinting at permanently water-logged conditions.

The mire vegetation consists primarily of bog species like *Sphagnum*, *Andromeda polifolata, Drosera* and *Cyperaceae* in the centred areas. Towards the margins, stands of *Pinus mugo rotundata* (a mire subspecies) are dominating. All around the mire, the dryer slopes are dominated by a dense *Picea* forest, mixed with *Pinus* and *Larix* (Heiss, 2008), which surrounds the mire into all directions by almost one km the least.

Being part of a complex of several smaller mires, a nature path is leading along the northern flank of the mire, which is declared a national “natural monument” of Austria since 1971. A wooden watch tower was constructed recently between the path and the north-western side of the Piller Mire. Parallel to the footpath and less than 50 m from the wooden tower, an overhead power line was constructed some decades ago. No traces of peat extraction could be observed at the coring site, even if it is only around 100 m south of a former peat mining facility to the north-east (**Figure 24**). At least nowadays, agriculture or livestock grazing do not exist in the direct vicinity. Their impact increases behind the dense forests on cleared areas, for example upslope to the Venet or downslope towards Fließ or the villages in the lower Pitz and Kauner Valley.

5.1.4 Coring and subsampling (Piller Mire)

During the 2016 survey, the peatland was probed with a Pürckhauer rod and the Russian corer. It was difficult nonetheless to retrieve material in the upper 3 metres using the 5-cm Russian system because of the very soft and well-preserved structure of the peat.

Coring of the Piller Mire took place in early August 2017. The coring spot was selected west of the mire's centre, in front (south) of the watch tower (**Figure 24** and **Figure 26**). This part was judged to be suitable, because it was as far away from *Pinus mugo* stands as possible, which reduced the probability of hitting roots. In addition, it was further away from the outlet and thus probably less influenced by both water level changes and any surface runoff from the northern- and southern slopes. Due to the special conditions of this mire, a Wardenaar corer was used for the uppermost metre. The deeper sections were then taken with the 8-cm barrel Usinger piston corer system (Mingram et al., 2007). Two overlapping peat sequences were retrieved: the main sequence Pi17 (47°07'24.85"N, 10°39'45.45"E) and Pi17-B at 2-3 m SE of the main core.

Figure 26: View to the south down from the tower on the open Piller Mire, framed by Pinus mugo and Picea. Coring spot in the centre of the mire (centre of photo).

The main sequence reached a maximum depth of around 280 cm in three separate sections without problems. The consecutive fourth piston got stuck and returned empty. Section B started at a depth of 80 cm and went down to almost 360 cm. Again, the fourth coring got stuck at a depth of around 400 cm and returned with an inward bend of the sharpened barrel's edge.

Subsampling was conducted at Ecolab in Toulouse and followed the procedure described in chapter **3.2**. As the cores had shrunk due to a considerable water loss and vertical compaction during transport from Kiel to Toulouse, the core lengths before and after transport were used to calculate a separate correction factor for the sample slices of each segment. Otherwise, the

calculated mid-point depths of the slices would not be true to their respective original depth in the mire. By doing so, also the dry bulk density and depending calculations were corrected.

5.2 Results & discussion (Piller Mire)

5.2.1 Core description (Pi17, Piller Mire)

Due to the absence of any distinct layers below the first metre, a systematic detailed description of the Piller Mire core was difficult and did not prove to be helpful. Furthermore, ongoing colour changing during the process of oxidation of the core surface was not fully completed at the time of core-scanning and complicated the visual examination. A line scan of the Pi17 core can be found in **Suppl. Figure 2**.

Except for the topmost part, the different core sections of Pi17 were very similar in their brown colour and structure. They all had in common that the peat was very soft and wet. The degree of decomposition was relatively low over the whole profile, which allowed the determination of macro remains. The mire was dominated by *Sphagnum* and other bog species, which is suggesting that ombrotrophic conditions prevailed permanently. Furthermore, light and fine but very few muscovite flakes of mm-scale were found evenly dispersed along the whole profile's outside without being concentrated in any part of it. Mineral layers were neither observed in the main nor in the parallel core B.

In the lower part, darker peat layers with an obviously lower humification were found at depths of 338-339 cm, 328-329 cm, 301-302 cm, 253-257 cm and at 206 cm. A higher decomposition was observed around 185 cm. In the upper part, darker layers showed up again at 160-162 cm and at 100-101 cm. A generally darker and less soft or light peat with a higher decomposition was observed at a depth between 92-87 cm, which got lesser until 68 cm. The layers above were showing a decreasing humification up to 28 cm depth, with peat that was strongly dominated by *Sphagnum* and *Eriophorum.* Along this gradient, the colour changed from dark brown to an almost reddish/yellowish light brown. The upper 19 cm consisted almost solely of *Sphagnum* without any visible humification.

5.2.2 Radiocarbon dates and age-depth models (Piller Mire)

Table 9: List of radiocarbon samples including information about origin, depth, dated material and reported uncalibrated ^{14}C-ages. Lab codes: GdA=Gliwice, Poz=Poznan.

Lab. No.	Site	Depth (cm)	Material	^{14}C-age (BP)	Comment
GdA-5492	Pi17A	43.2	*Sphagnum* stems and leaves	1.4250 ± 0.0022	F14C Bomb pulse
Poz-99320	Pi17A	80.3	*Sphagnum* stems and leaves	725 ± 30 BP	0.5 mgC
GdA-5494	Pi17A	106.0	*Sphagnum* stems and leaves	1505 ± 35	
Poz-101724	Pi17A	184.6	*Sphagnum* stems and leaves	2150 ± 30	
GdA-5495	Pi17A	209.5	*Sphagnum* stems and leaves	2455 ± 40	
GdA-5496	Pi17A	267.3	*Sphagnum* stems and leaves	3255 ± 25	
Poz-101726	Pi17B	268.7 (cor.)	*Sphagnum* stems and leaves, *Ericaceae* leave	3260 ± 30	
GdA-5493	Pi17B	340.0 (cor.)	*Sphagnum* stems and leaves	4150 ± 30	See **Figure 27**

Out of all three study areas, the Piller Mire was the only one without the need to date any bulk radiocarbon samples. All eight samples consisted of plant remains that were identified to a family level, ascertaining good quality and lower uncertainty of the age-depth model.

Table 10: Settings in rbacon for Pi17

Site	thick	acc.shape	mem.strength	mem.mean	acc.mean
Pi17	2,5	0,5	9,0	0,6	10

To extend the depth of the analysed core, the three upper core sections of Pi17-A were linked to the lowest section of Pi17-B by the radiocarbon dates from their lower/upper end. Both samples were coincidentally dated to almost the same age (**Table 9**), which facilitated the synchronisation. The parameters used in rbacon for the model are given in **Table 10**.

Figure 27: Photo of Sphagnum stem with leaves from 340 cm corrected depth (part of ^{14}C sample GdA-5493).

The mean total AR in the catotelm of Pi17-A was at 0.8 mm*a^{-1}. The lower end of the core was predicted by the model to have an age of around 4750 cal BP. Until 2150 cal BP (185 cm) the AR stayed almost constantly around 0.7 mm*a^{-1} but rose to values around 1.1-1.4 mm*a^{-1} until 1480 cal BP (115 cm). A period of a decreased AR around 0.3 mm*a^{-1} stretched from around 1200 cal BP (100 cm) to around 140 cal BP (84 cm). From this point on towards the surface layers, the AR steadily increased, from around 2.4 mm*a^{-1} at approximately 1950 CE (50 cm) to an AR of over 10 mm*a^{-1} between 1990 and 2017 cal CE.

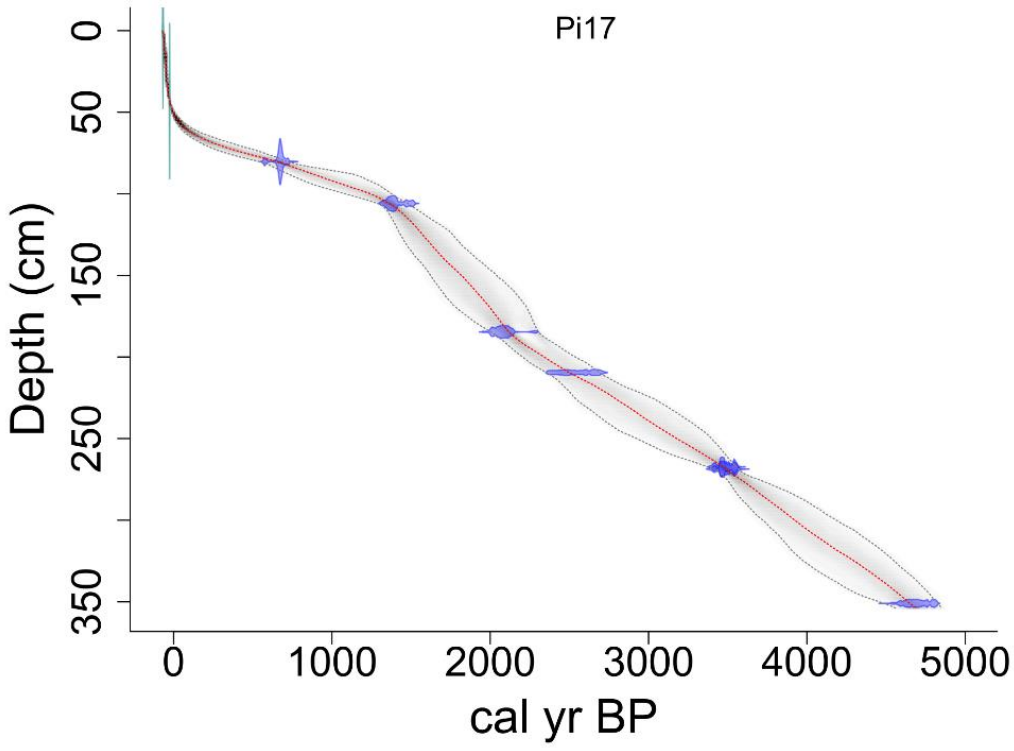

Figure 28: Age-depth model of Pi17. Red dotted line=median age, grey shaded area=95% confidence interval.

Similarly as for the Kleinwalser Valley cores, the age-depth model in the upmost part was built upon a single bomb-pulse radiocarbon date for the upper part, but the Pb EF profile (cf. **Figure 36**) helped again to confine this age: this time to the declining slope of the pulse (ca. -23 cal BP).

5.2.3 Geochemistry (Piller Mire)

Out of a total of 238 subsamples of the Pi17-sequence, 143 sub-samples were selected for geochemical analysis by pXRF. Of these, 63 were measured with ICP-MS. All measurements were carried out by following the procedures described in the methods chapter (**3.4.1** to **3.4.3**).

5.2.3.1 Regression Analysis (Piller Mire)

Mire site specific conditions (e.g. surrounding geology, vegetation) could have unknown effects on the behaviour of the pXRF analysis. Therefore, an individual regression analysis in the 63 samples of the Pi17-profile was conducted and is presented and briefly discussed in this chapter for the elements that are potentially measurable by pXRF (**Figure 29**) and of which some can act as potential proxies.

The cross-plots in **Figure 29** show that the maximum concentrations are lower than in HFL. The regression function between ICP-MS and pXRF measurements of **Ti** is linear and has a very good fit of the regression model with a R^2=0.98. The values from pXRF are, however, systematically higher than the ICP-MS results. Unlike HFL or the CRMs, the Piller Mire core did not contain mineral sediment layers, but the linear regression is obviously valid for concentrations up to 630 $mg*kg^{-1}$ of Ti. By removing the sample with the highest Ti concentration, the fit would increase to an R^2 of almost 1. A similarly linear behaviour can be observed for **Pb**, although with a lower overestimation and an R^2 of 0.99. The linear correlation of **Ca** works only for 75 % of the dataset, whereas the other 25 % from samples of two separate parts in the core (100 to 160 and 190 to 230 cm) are far off the potential regression model. Without these sections, a fit of R^2=0.75 would be reached. With all samples included, the fit would decrease to a R^2 of 0.13. There were no obvious differences in the material and also the other elements do not show irregularities in samples of this part, which complicates the identification of a reason behind this behaviour of **Ca**. Linear regressions with R^2 >0.96 are reported for **Rb**, **Sr**, and **K** while the fit for **Zn** is at R^2=0.93. With almost quantitative pXRF measurements, **Sr** is least influenced by the peat matrix.

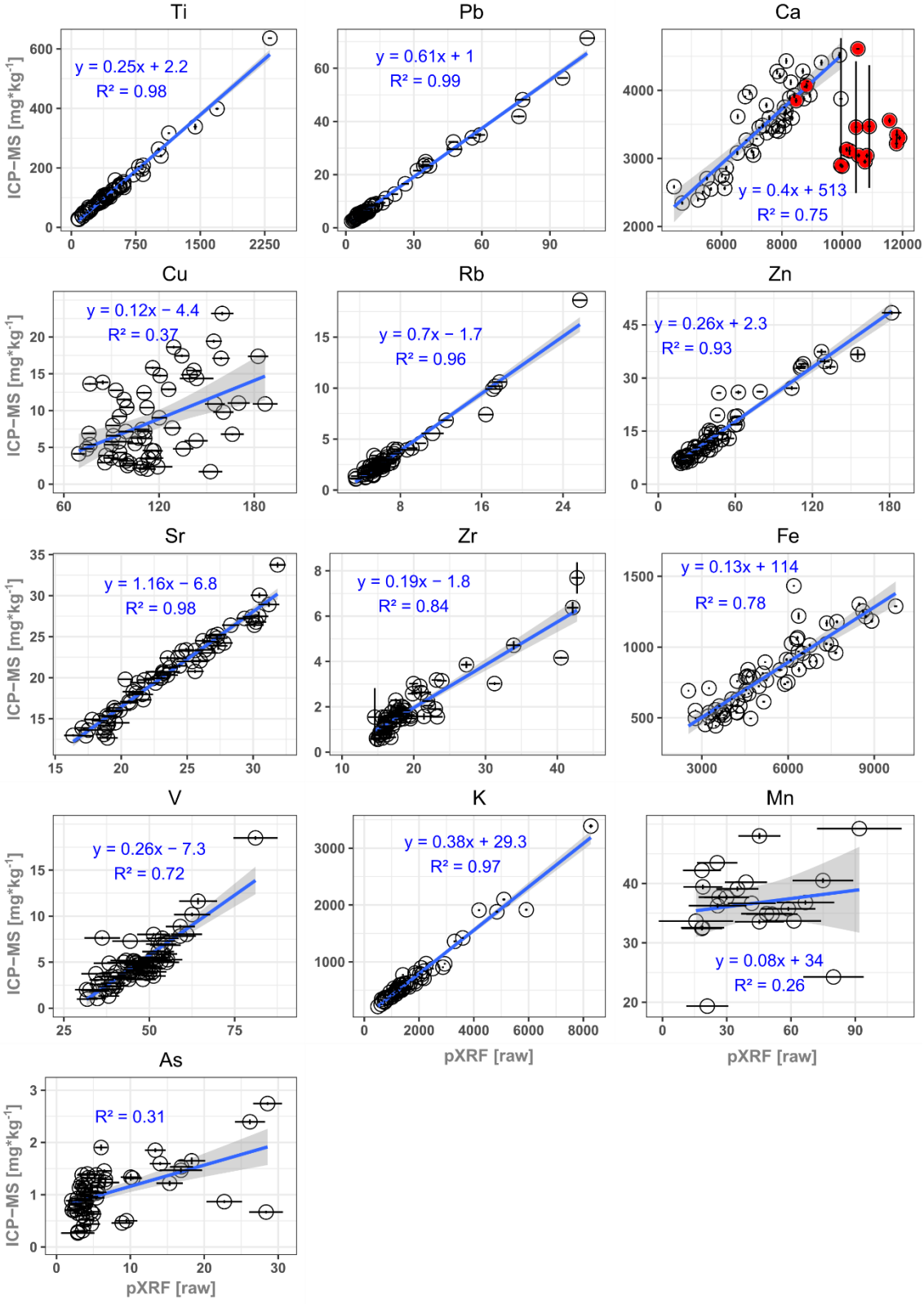

Figure 29: Cross-plots with regression analysis of ICP-MS and pXRF measurements of peat samples from the Pi17-sequence. Error bars depict the standard deviation of the instrument. Samples in red are not considered in regression analysis.

Although they are still linear, the fit of the regression models of **Zr** (R^2=0.84), **Fe** (R^2=0.78) and **V** (R^2=0.72) are not as good as for the previously described elements. This is most likely due to the generally low concentrations in the Piller Mire. For Zr, more than half of the samples cluster between 15 and 23 for the pXRF and from 0 to 2 mg*kg^{-1} for ICP-MS, indicating that the LOD is reached within this range. Based on similar observations, the pXRF-LOD for **Mn** appears to range around 30 mg*kg^{-1}. The fit (R^2=0.26) is low, but only about a 25 % of the samples have concentrations above this limit and just five samples are above 50 mg*kg^{-1}.

If at all, **Cu** and **As** have an only weak fit, with R^2_{Cu}=0.37 and R^2_{As}=0.32. It can therefore be stated that Cu, As and Mn are not satisfactorily measured in samples from the Pi17 peat sequence. The same applies for Ca, which shows an undefined uncertainty in two separate parts of the core. However, the regression analyses suggest that Ti, Pb, Rb, Zn, Sr and K can be measured in peat samples by the Niton Xl3t pXRF. The analysis clearly shows that the non-quantitative values can be transformed into concentrations by their respective transfer functions given in **Figure 29**. The scatter in pXRF-measurements of Fe, Zr and V is higher in these low concentration samples, but linear function would still allow a quantification estimate. All analyses have in common that they overestimate the ICP-MS concentrations, but each one follows its individual regression function.

5.2.3.2 Elemental profiles (Piller Mire)

This section covers the elemental profiles of the Piller Mire, calibrated with the transfer functions obtained in the previous chapter. All described profiles are plotted in **Figure 30**, with calibrated pXRF derived concentrations in blue and ICP-MS derived concentrations in red.

Ca: The regression analysis revealed issues for the calibration of Ca. Furthermore, three ICP-MS measurements exhibited relatively high uncertainties. In any case, clear trends or events are missing in the profile (**Figure 30**, ICP-MS, red).

Sr: The Sr profile increases continuously from 10 mg*kg^{-1} at 350 cm to the profile's maximum of 30 mg*kg^{-1} at 200 cm. A declining trend shows from 155 cm up to the surface. In between the two trends, the concentrations sink to a temporary minimum (12 mg*kg^{-1}).

S: Sulphur was measured in Pi17 by pXRF only, because the samples did not go through ICP-OES. Due to the very good linear fit of the regression analyses of S in both HFL and LLG (chapters **4.2.3.1** and **6.2.3.1**), the transfer function of HFL was applied to the pXRF measurements of the Pi17-samples as well. Compared to HFL, the concentrations range on a relatively low level, between 200 mg*kg^{-1} in the surface layers and a maximum of 2000 mg*kg^{-1} around a depth of 49 cm. From 350 cm upward, a level of more than 1500 mg*kg^{-1} is observed until a sharp

decrease to around 1000 mg*kg^{-1} at 250 cm. Afterwards, a range between 1000 and 1500 mg*kg^{-1} is maintained before a rising trend climaxes at the above-mentioned depth of 49 cm.

Fe: The usually mobile Fe increases stepwise from the lower core's end (600 mg*kg^{-1}) and doubles until 100 cm, just to decline by half again at the surface.

V: Vanadium stays between roughly 4 to 7 mg*kg^{-1} with only few outliers. A bold peak of 15 mg*kg^{-1} appears at about 200 cm, followed by a sharp decline to concentrations around 2 to 6 mg*kg^{-1} from 185 to 90 cm. Then, a period of concentrations of approx. 8 mg*kg^{-1} appears until 62 cm. Concentrations in the upmost 60 cm range around 2 mg*kg^{-1}.

K: Potassium fluctuates between 300 to 700 mg*kg^{-1} in the lowermost 40 cm. A sharp peak of >3000 mg*kg^{-1} is observed at 312.5 cm and a few layers with over 750 mg*kg^{-1} from 262 to 256 cm and around 228 cm. Then, a maximum of >3300 mg*kg^{-1} is reached around 200 cm. Two smaller increases over 750 mg*kg^{-1} appear at 176 and 143 cm, before a stronger increase to >2300 follows around 88 cm. The profile decreases again to less than 750 mg*kg^{-1} at 70 cm and sharply rises again to over 1500 mg*kg^{-1} at 62 cm. Just afterwards, the concentrations stay around 750 mg*kg^{-1} until 25 cm and increase towards the surface.

Rb: It behaves just like K with only slightly different levels of the peaks and maxima. The two deeper peaks reach around 17 mg*kg^{-1} and the upper around 11 mg*kg^{-1} while otherwise, the profile has < 5 mg*kg^{-1}, with only minor exceptions around 259 and 143 cm and at the surface.

Ti: Titanium ranges mostly around 125 mg*kg^{-1}. Considerably lower concentrations show at 340, 317, 251 and 171 cm as well as in the upper 50 cm. The peaks at 312.5 and around 200 cm reach over 380 mg*kg^{-1} and over 600 mg*kg^{-1} respectively. Three smaller increases show around 330, 261 and at 143 cm. More than 400 mg*kg^{-1} are observed at 88 cm and at 62cm more than 260 mg*kg^{-1}. For Zr, the highest peak is the one at 312.5 cm, with 12 mg*kg^{-1}, while the next one at 200 cm shows only 9 mg*kg^{-1}. The double peaks (88 and 62 cm) go up to 8 and to 4 mg*kg^{-1}, whereas the upmost 50 cm range around 1 mg*kg^{-1}.

Pb: Lead is mostly on a level between 3 and 10 mg*kg^{-1} (**Figure 30**). A short phase with almost 20 mg*kg^{-1} shows around 328 cm, while smaller increases around 253, 200 and 143 cm are subtle. Unlike the lithogenic elements, the Pb shows a triple- instead of a double peak in the upper metre. Furthermore, the first peak is the smallest and the last peak has the strongest Pb-concentration, illustrating that it cannot be bound to mineral input or soil dust. The first significant increase from 5 to 35 mg*kg^{-1} is observed after 90 cm. The mid peak reaches 60 mg*kg^{-1} at 67 cm and the maximum elevation of almost 70 mg*kg^{-1} is at about 39 cm depth.

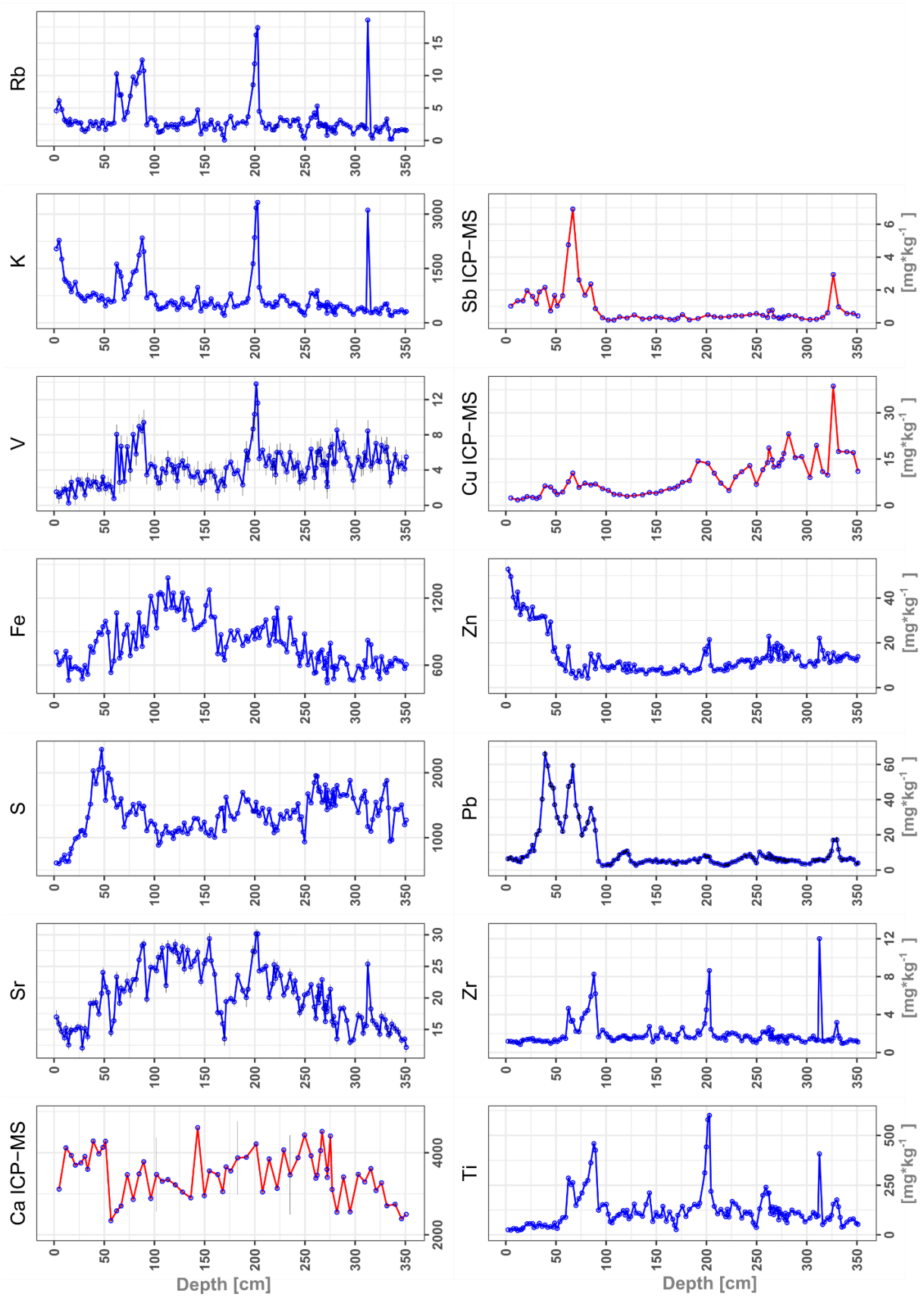

Figure 30: Elemental profiles measured in the Pi17 composite core by pXRF (blue) and ICP-MS (red).

Zn: Except for the upper 50 cm, Zn maintains a level around 10 mg*kg^{-1} with only minor elevations between 15 to 20 mg*kg^{-1} in the lower 300 cm of the core: at 312.5, around 10 , 270, 200 and at 62 cm. Probably due to biological cycling and accumulation of living plants, the concentrations exceed 20 mg*kg^{-1} at 45 cm and more than 40 in the top sample.

Cu: Copper decreases from the bottom to top. However, peaks show at depths of 326 cm (39 mg*kg^{-1}) and 282 cm (23 mg*kg^{-1}). Smaller rises to less than 20 mg*kg^{-1} appear at 310, 262 and around 200 cm. After a stable course of the profile with a minimum of 2.9 mg*kg^{-1} at 121 cm, a slight increase starts above 100 cm with a small relative peak of 10 mg*kg^{-1} at 67 cm depth.

Sb: Synchronously to Pb and Cu, **Sb** rises to 3 mg*kg^{-1} at approx. 326 cm but stays below 1 mg*kg^{-1} until 90 cm, after which a maximum of 7 mg*kg^{-1} shows at 67 cm (synchronous to 2nd large Pb peak). Above, the concentrations are constantly higher (over 1 mg*kg^{-1}) than in the deeper part.

The rather low concentration levels of mobile elements and *Sphagnum* dominance indicate that ombrotrophic conditions prevailed throughout the whole profile of Pi17. This suggests that, besides Pb, also the signals of Zn, Cu and Sb should be almost unaffected by post-depositional mobility and could therefore be used as proxies for past metallurgical activities. However, the suspiciously higher concentrations of Cu in deeper layers indicate mobility. In addition, the Zn-profile is most likely influenced by nutrient cycling in the uppermost layers.

The four lithogenic elements K, Rb, Ti, Zr and V share certain features in their profiles, like the marked peaks. The sharpness of their swings suggests insignificant mobility or a preservation of the original signal. The rise of K and Rb in the surface layers is, however, in contrast to that.

Due to the lack of mineral layers of local origin within the core, no natural or geological background ratio was calculated for Pb or other metals and the reference element Ti. Therefore, the values to calculate the ratios were taken from the UCC (McLennan, 2001) (see **Table 3**).

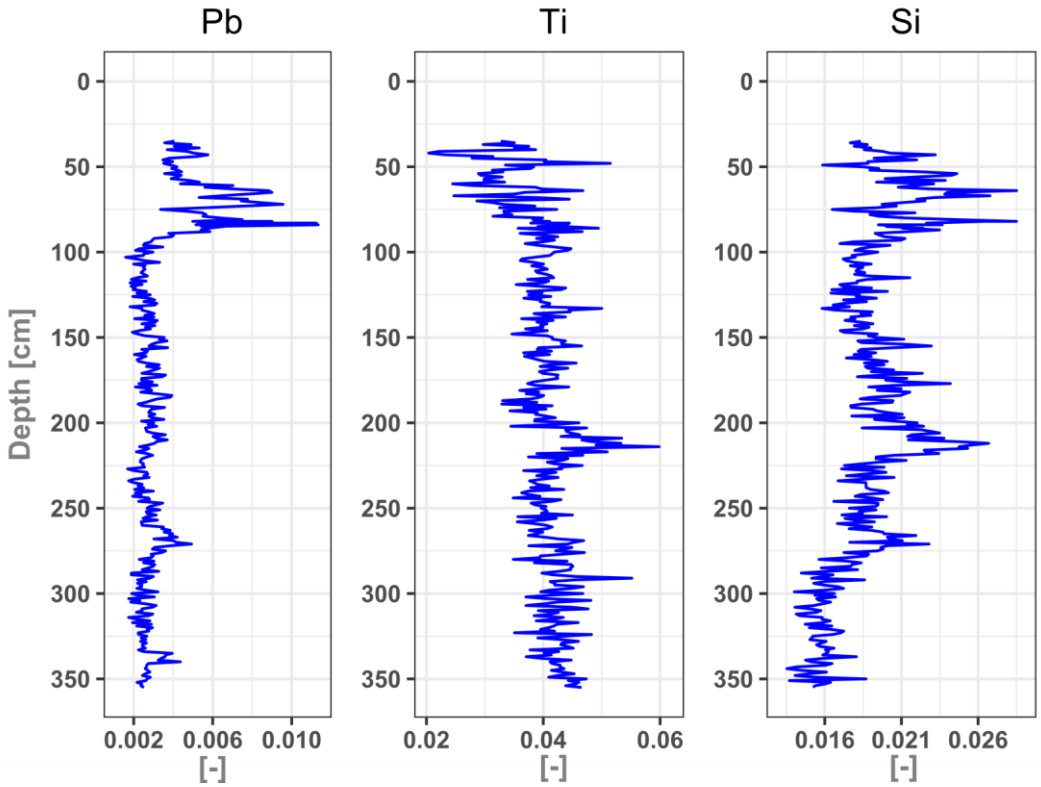

Figure 31: Normalised (tcps) elemental profiles of Pb, Ti and Si, derived from XRF-core-scanning of parallel core Pi17B (90 to 352 cm) plus Pi17A (upper 90 cm).

The XRF-scan was performed on the Wardenaar section of Pi17A (0 to 91 cm) and on the Usinger sections of parallel core Pi17B (80 to 353 cm; corrected depth for deepest section), to validate the overlaps between the separate sections of the main Pi17 sequence (**Figure 31**). For example, segment 3 of Pi17A began at 196 cm and the pXRF results revealed a distinct peak of e.g. Ti around 202 cm (**Figure 30**): The question now was, if this signal could be disturbed (e.g. allochthonous from further above). In the deepest section, core-scanning acted as an independent measurement to substantiate the quantitative results (pXRF). The upper 35 cm are missing because the material was too soft for the head of the core-scanner to automatically detect and scan the core's surface.

The core-scan profile of **Pb** in Pi17B (**Figure 31**) exhibits an increase in a depth of 337 cm, which was also registered by pXRF in the main sequence of Pi17. Another rise was measured around 260 to 270 cm, corresponding to a slightly upward shifted pXRF-signal (see **Figure 30**). The profile of Pb illustrates that the sharp increase around 90 cm is not the relict of a missing piece in the Pi17A-core. In line with the pXRF-scans, the core-scanner detected the same Pb peaks in the Wardenaar section.

Neither the normalised core-scan profiles of **Ti** nor of **Si** show the first large peak around 312 cm. As it was only a single sample in pXRF, it might be possible that the XRF-scanner did not

catch this very thin signal due to the 1 cm resolution. Above 275 cm, the first significant increase corresponds well to an elevated signal of lithogenic elements in the pXRF—measurements of the main sequence. The peak of Ti below 200 cm in Pi17A (top of core segment) was also detected in Pi17B, although shifted about 10 cm deeper (as for Pb). It confirms that this signal was not the result of disturbances (e.g. spread material). While the pXRF signal of Ti went up significantly between 100 and 50 cm, the detected Ti in the core-scan decreased to a lower base level in this part. Just as in HFL, the XRF-scaning data of Si seems to reflect the true Ti-signal better than Ti (see **Figure 31**). Such very light peat with generally very low concentrations (counts) probably hampers the correct measurement by the Avaatech-scanner.

5.2.3.3 PCA (Piller Mire)

A PCA for the Piller Mire profile was performed, based on ICP-MS, similarly to the PCA in HFL. Here, the uppermost 25 cm were excluded to reduce influence of the living vegetation. Ca, Mn and As were excluded, either due to issues in the analysis or an unsuccessful calibration. Three components explain about 90 % of the total variance, but grouping the elements is not trivial (**Figure 32**). Mainly Ti, Zr, V, Al and, in decreasing order, Nd, Sm, Rb, K, Sr, Fe and Cu determine the largest and probably lithogenic component (PC1). The conformity of Sr and Fe is probably due to their mobility in the peat column, whereas Pb and Sb group together as rather recent anthropogenic pollutants. It appears that the trace metals Cu, Zn, Sb and Pb are responsible for a large part of the total variance of PC3. However, no explanation can be presented for the relation between Sm, Nd, Al and Cu.

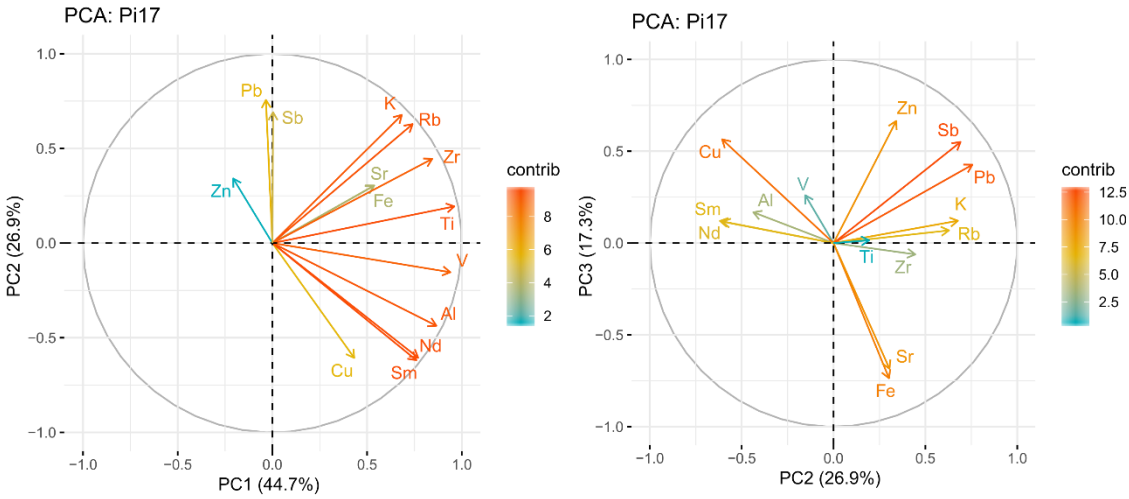

Figure 32: PCA of ICP-MS measurements in the Pi17 core. Upper 25 cm (living vegetation) excluded.

The Pi17 sequence is not divided into an ombro- and minerotrophic section. However, two considerations led to performing a second PCA. Firstly, the acrotelm is less compact and much thicker in the Piller Mire, so the living section should reach deeper (insinuated by the Zn-profile in **Figure 30**). Secondly, prehistoric signals of metallurgy or mining could have been very different from modern pollution signals (leaded gasoline, coal, industry). Hence, both factors were ruled out by performing another PCA with samples older than 1000 cal BP (deeper than 90 cm), to test if, or how, the grouping of elements changes.

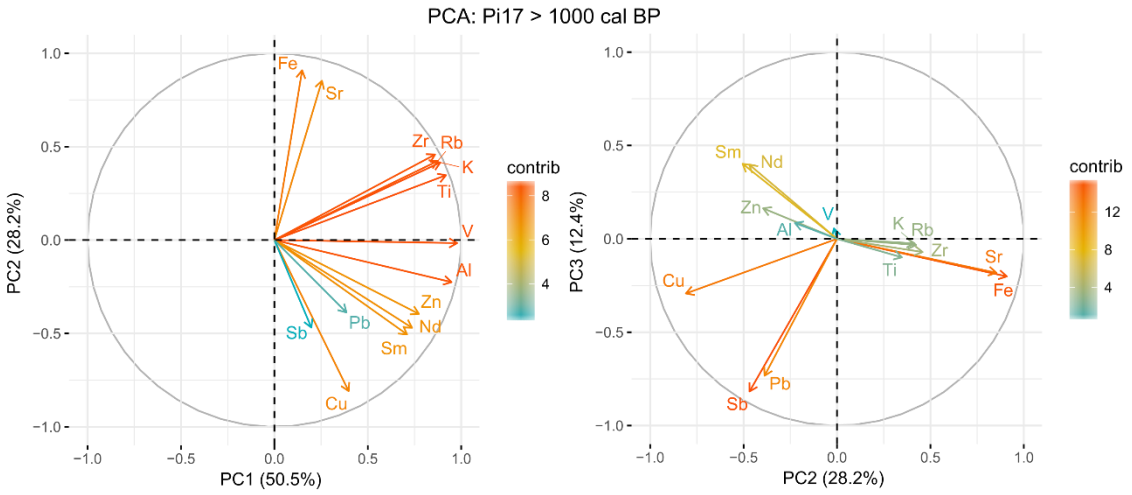

Figure 33: PCA of ICP-MS measurements in Pi17-samples older than 1000 cal BP.

Indeed, the results in **Figure 33** are different to the first PCA. The grouping is now more articulated, especially for the anthropogenic tracers Pb, Sb and Cu, whereas Zn, being highly concentrated in the excluded upper 80 cm, became slightly disconnected from them. This can for example indicate that Zn had been less important in prehistoric metallurgy. The content of Pb, Sb and Cu seems to be controlled by all three components. But while Cu is more strongly represented in PC2, Pb and Sb are influenced stronger by PC3.

An interesting aspect is the separation between the lithogenic mineral elements Nd, Sm, Al and Ti, Rb, Zr, K in PC2, which is difficult to explain. Additionally, the two REEs and Al are closer to Zn, Cu, Sb and Pb in PC2. However, it cannot be resolved here, if maybe a second mineral component, richer in REE and these metals, or post-depositional processes within the peat column could be responsible.

5.3 Chronological discussion (Piller Mire)

Because of its maximum depth, the retrieved core did not allow drawing conclusions about the early stage of the Piller Mire. Despite a supposed depth of 15 m and a maximum age of the

archive that reaches probably into the Late Pleistocene (Naturpark Kaunergrat, 2000), the record of this study covers only the last 4800 years. Two parallel cores came to a halt at an approximate similar depth about not more than 30 to 50 cm deeper than the end of the final core section (approx. 4 m). The sound and type of impact, but also the resulting bend of the coring tube suggests wood rather than stones as a barrier.

The abundance of *Sphagnum* as well as the distribution of mobile elements with depth strongly suggested ombrotrophic conditions throughout the whole core. Therefore, the mire should have been fed solely by atmospheric input, and effects of very small-scale processes, like e.g. small landslides or flooding after heavy rainfall events, should not have been of influence in the Pi17 record. It implies that mineral input (MAR, calculated with Ti) and anthropogenic/metallurgy tracers like Pb, Cu, Sb and Zn, should originate from the atmosphere and not from dissolution of the basal rock or sediment. As mentioned earlier, ombrotrophic conditions reduce the mobility of metals in peat, which allows using chemical proxies besides Pb. However, due to the discussed concentration profiles in HFL and Pi17, Cu is used with caution.

5.3.1 4800 to 4000 cal BP: transition to the Bronze Age

The deposition of mineral matter (i.e. MAR), started with very low values, below or around 1 $g*m^{-2}*a^{-1}$ (**Figure 34**), comparable to values that were observed in the HFL record (see chapter **4.3**). At 4500 cal BP, a first minimum was documented. Then, a small increase to > 2 $g*m^{-2}*a^{-1}$ appeared at about 4450 cal BP and another sharper peak of 5 $g*m^{-2}*a^{-1}$ at 4150 cal BP.

Both the earlier and the later peak correlate well with an increasing human impact with an opened landscape by forest clearings, charcoal and pastoral indicators at Fließ (Walde, 2006). Similar evidence was also observed by Wahlmüller (2002), who suggested first human impact at Serfaus around 4250 cal BP. Moreover, the sharp MAR peak of Piller Mire is in good agreement with charcoal peaks, emergence of *Poaceae* and pastoral weeds observed by Hubmann (1994), during the same time window (around 4600 to 4400 cal BP). To the southwest, in the areas of lower Engadine, agricultural field terraces existed (Zoller et al., 1996). In the Urschai Valley (Silvretta, **Figure 37**), a rock shelter was used in time windows around 4700 and again around 4350 cal BP, when alpine pastures appeared in the Silvretta (Reitmaier, 2012). Nicolussi and Patzelt (2000) reported glacier low stands before and after 4500 cal BP, with a glacier progression in between, which would fit to the temporally decreased MAR but also to the occupation-gap of the Urschai Valley rock shelter. Furthermore, Dietre et al. (2014) showed a rise of charcoal and cultural indicators (e.g. Cerealia) around 4400 to 4200 cal BP in the Fimba Valley. To the southeast, Bortenschlager (2010) documented landscape openness paired with

cultural indicators around 4400 cal BP and Dietre et al. (2017) suggested an almost continuous fire management in the lower Engadine Valley (Ardez, East Switzerland) in this period. As Tinner and Ammann (2001) reported generally warmer conditions for the Swiss Alps between 5000 and 4000 cal BP, these could have promoted human activities and erosion. At the end of this period, Nicolussi et al. (2005) observed a permanent decline of the tree line in the Kauner Valley (southeast**, Figure 23**) after around 4200 cal BP. It is unclear if this can be attributed to climate alone or if human impact played a major role as well, because the short but distinct MAR peak in the Piller Mire at that time coincides with locally increased charcoal occurrence and an opening of the landscape, as suggested by rising grass and pastoral pollen (Hubmann, 1994).

Very little evidence exists about prehistoric metallurgy and almost nothing is known about prehistoric mining activities in this area of western North Tyrol or elsewhere in the Alps as early as this. Although the objects are unpublished yet, prehistoric mining stone tools were found at a mining site at Serfaus, as communicated by Grutsch and Martinek (2012). Moreover, the oldest evidence for mining activities in the famous mining districts of the eastern part of North Tyrol (e.g. Schwaz/Brixlegg) and Central Austria, were not older than the Early Bronze Age around 3750 cal BP (O'Brien, 2015). **Figure** 34 illustrates that the first significant enrichments of Pb, Zn and Cu in the Piller Mire appeared as early as around 4550 cal BP and again just posterior to 4400 cal BP (Pb, Cu, Sb). The phase of increased metal EFs (Pb, Zn) ended after a small peak by the age of 4200 cal BP, coinciding with the onset of the Bronze Age (see definition in chapter **3.7**). The abrupt decline of metal enrichment around 4200 cal BP directly followed on a MAR peak. Establishing a link between these two signals is therefore possible. But especially as the pollen in the study of Hubmann (1994) indicated continuing human land use, questions on what was responsible for ending or stifling a regional culture that had the technology for metallurgy or mining in the region remain unanswered. In any case, even without any archaeological proof of Neolithic local mining or metallurgy around the Piller Saddle, the region is rich in a variety of smaller and partly polymetallic ores within a radius of mostly less than 15 km (Hammer, 1915a, 1915b; Schach and Minsinger, 1849; von Srbik, 1929). Among other traces, these deposits contain Pb, Cu, Sb, Ag and As and might have been exploited by Late Neolithic communities in the area.

This study's combined evidence of shorter episodes of an elevated MAR with the metal EFs suggests early human land use and metallurgy around the mire. The latter would be earlier than any direct evidence. Even if no location can be pinned down for these activities, it becomes clear that human impact was widespread in the transition from Late Neolithic to Early Bronze Age. Furthermore, the synchronicity of these signals with changes in timber line and glacier extent around 4500 cal BP indicate a relation between climate and human activity.

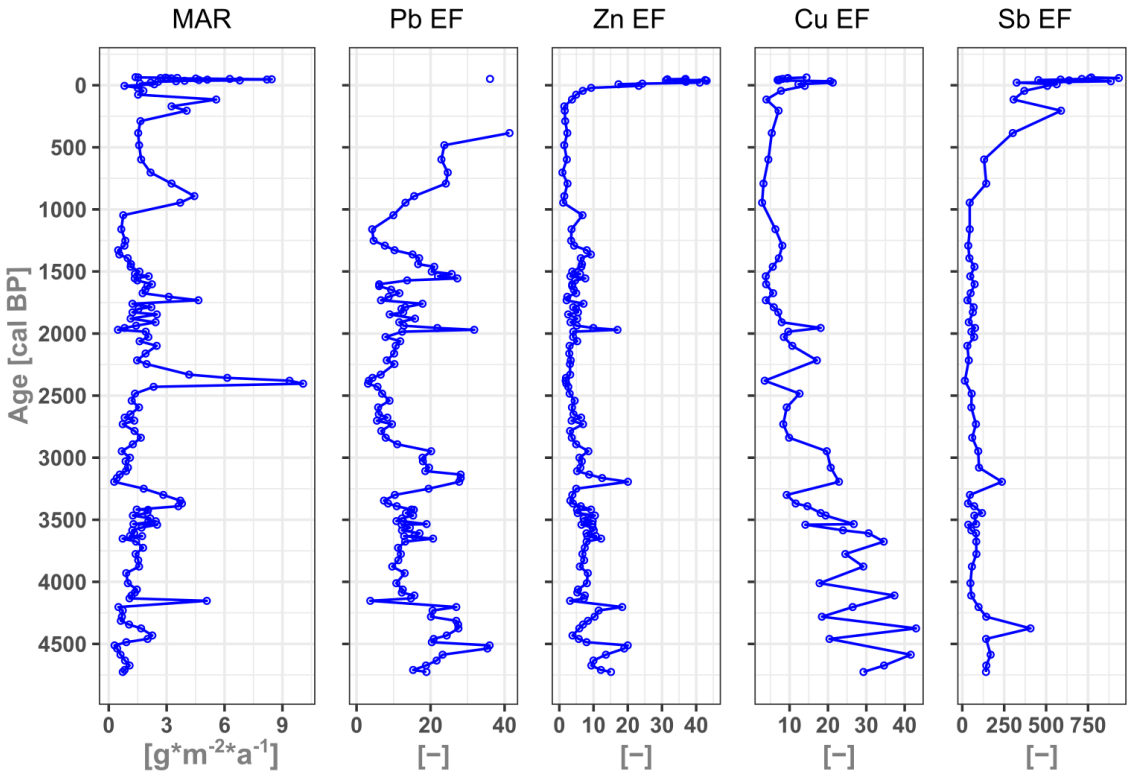

Figure 34: Chronological profiles of MAR, EF Pb (clipped at 10 % of max. EF), EF Zn, EF Cu and EF Sb in Pi17.

5.3.2 3900 to 2800 cal BP: Bronze Age

During the Early Bronze Age, the MAR had been stable on a low level around 1.5 g*m^{-2}*a^{-1} until a small increase was recorded directly prior to 3500 cal BP (**Figure 34**). A significant increase to about 4 g*m^{-2}*a^{-1} followed at 3400 cal BP but mineral input declined again, sinking to a minimum of 0.3 g*m^{-2}*a^{-1} at 3200 cal BP. Thereafter, it stayed relatively low around 1 g*m^{-2}*a^{-1} with only a slight increase towards 2800 cal BP.

Glacier progressions were documented in the Kauner Valley around 3600 cal BP (Nicolussi et al., 2005) and the colder conditions could have hampered an earlier rise of human impact. In contrast, receding glaciers in the Alps and a probably warming climate in a phase around 3640 to 3350 cal BP provided a better conditions and accessibility to the mountainous areas. Around the age of 3450 cal BP, Hubmann (1994) found the first *Cerealia* pollen. Increasing human activities in adjacent areas were also suggested by Wahlmüller (2002), Walde (2006) and Hubmann (1994), who recorded rising pollen of grasses, herbs and pastoral indicators. The latter also recorded a frequent use of fire by the presence of elevated charcoal values, which is in accordance with generally increased fires in the Alps over the Bronze Age (Valese et al., 2014). Direct archaeological evidence of a Bronze Age building in Fließ (Tomedi et al., 2009) and a Late

Bronze Age settlement at Kaunerberg (Staudt and Tomedi, 2015), about 5 km south of Piller Mire, further support the theory of local human activity.

To a certain level, the observations on palaeovegetation are in line with this study's results (MAR) and with the conclusions from the Kleinwalser Valley in the northwest, where the strongest impact occurred between 3500 and 3200 cal BP (chapter **4.3**). In the Eastern Alps, Viehweider et al. (2013) observed more forest clearings, probably to fuel intensifying copper mining operations (Stöllner, 2015b). But also in the Swiss Central Alps, strong human presence was widespread as the result of technological and cultural factors (Della Casa, 2013), which illustrates the strong pulse of human impact across the mountain chain.

A probably less severe or less erosive human influence followed towards 3000 cal BP, as suggested by MAR and the results of Hubmann (1994) and Walde (2006). Again, a coinciding climate cooling (e.g. Ivy-Ochs et al., 2009) could have been partly responsible for this decline.

Slightly elevated Pb EF, Zn EF and Cu EF show from 3650 to 3450 cal BP (**Figure 34**). Another, more pronounced, episode of Pb EF was recorded from 3250 to 2950 cal BP, with a maximum of 30 around 3150 cal BP. A synchronously elevated signal is visible for Zn EF, Cu EF and Sb EF. For the beginning of the Iron Age at approximately 2800 cal BP, no more enrichments were detected. The first period of enrichment is in line with metal artefacts found in Landeck (Pöll, 1998). Moreover, the second period of more strongly elevated EFs coincides perfectly with the first phase of activities at the ritual sacrificial burning site on the Piller Saddle (Tschurtschenthaler and Wein, 1998, 1996). This is evidenced by two radiocarbon ages given in Heiss (2008), which could be calibrated to 3330-3450 and 3230-3390 cal BP. An equally important evidence is the bronze hoard find, in a distance of about 2 km northeast from the bog (Moosbruckschrofen), which was dated to this period of the Middle to Late Bronze Age around 3500 to 3200 cal BP (Tomedi, 2012, 2002a). It partly consisted of cast but not completely processed copper (Tomedi, 2002b), suggesting that it belonged to a workshop. Only a few kilometre to the northeast, local ore deposits (malachite) as well as archaeological finds of a casting mould and copper slag mixed with Bronze Age pottery are strongly insinuating local copper mining and metallurgy (Tomedi, 2002b). Furthermore, unprocessed copper was found at a Bronze Age archaeological site in Fließ (Nicolussi Castellan et al., 2008). So far, mining operations in the Bronze Age were only evidenced for the Eastern Alps (O'Brien, 2015) and not in the northern Central Alps.

At least for the Middle to Late Bronze Age, the results of this study are indicating a connection of the ritual burning site and the Bronze hoard find with a locally and regionally increased land use and human impact on the environment and landscape. It substantiates earlier theories of

early mining or metallurgy not far from the Piller Mire (Tomedi, 2002b) but the results of this study would be one of the strongest evidence for now.

5.3.3 2800 to 1950 cal BP: Iron Age to Roman Expansion

The low MAR during the Late Bronze Age continued along the Early Iron Age and until approximately 2500 cal BP, on a level that was only slightly higher than before, with values around 1.5 $g*m^{-2}*a^{-1}$. Thereafter, the largest peak MAR of the whole profile was recorded between 2450 and 2350 cal BP with a maximum of 10 $g*m^{-2}*a^{-1}$ at 2400 cal BP. The erosion proxy declined back to values between 1.5 and 3 $g*m^{-2}*a^{-1}$ and even to another minimum with < 0.4 $g*m^{-2}*a^{-1}$ at the end of this period.

Within this timeframe of high erosion around 2500 cal BP, Walde (2006) documented an increasing anthropogenic influence on the vegetation around Fließ, in the form of forest clearances, pastoralism and the cultivation of cereals in the vicinity. The pollen profile of this study reveals that the timing of a maximum of *Poaceae* and low *Pinus* and *Picea* is perfectly fitting the timing of the distinct MAR peak in Pi17 around 2400 cal BP. This is also in line with the pollen profile of Wahlmüller (2002) and even more so with the study of Hubmann (1994), which observed highly elevated charcoal and *Plantago* as well as *Poaceaea* and *Cyperaceae* as indicators for burning and for an opened landscape in the direct surroundings of the mire. Furthermore, the latter also shows the presence of *Cerealia* for the second time. In the Silvretta region (**Figure 1**), Reitmaier (2012) and Reitmaier et al. (2013) found archaeological evidence of permanent structures for livestock management in an Alpine environment above 2000 m a.s.l. during this episode of the Iron Age. In the area between Inn and Pitz Valley, several metal Iron Age artefacts of La-Tène and Hallstatt cultures were found (Lutz and Schwab, 2015; Zemmer-Plank, 1992) and archaeological excavations discovered structures and buildings from this time, e.g. at the villages of Wenns, in the lower Pitz Valley (Staudt, 2011) or in Fließ (Sydow, 1995). Most likely, human presence and its observed impact directly around the Piller Mire were related to the cultic site, which had been in use at until the Roman period (Tschurtschenthaler and Wein, 1998, 1996) at least, and made this area a hotspot of anthropogenic activities.

Besides cultural changes, a reduced anthropogenic activity at the beginning of this period could have been related to a general cooling trend in the Alps after 3300 cal BP and marked advances of greater Alpine glaciers from 3000 cal BP to maximum extensions at 2600 cal BP (Ivy-Ochs et al., 2009). In the aftermath of it, warming or at least stable conditions could have favoured a higher human activity in the region around 2400 cal BP. Thereafter, a lower level of MAR and the minimum at 1950 cal BP are in good agreement with higher tree coverage and reduced

pastoral indicators (Bortenschlager, 2010; Hubmann, 1994; Wahlmüller, 2002; Walde, 2006). As an explanation, Walde (2006) suggested that the newly constructed *Via Claudia Augusta* (Grabherr, 2006), down in the Inn Valley, attracted people to settle closer to it and to give up their dwellings on the elevated slopes. This development can be assumed to be responsible for less or only moderate anthropogenic signals in the Piller Mire despite Roman influence. The beginning of Roman influence around 2000 cal BP is clearly reflected by the appearance of newly introduced cultural trees like *Juglans* (Hubmann, 1994).

Evidence for metallurgical activities was not detected, as none of the EFs is exhibiting significantly increased values during the Iron Age (**Figure 34**). Only the other way around, significant decreases of Pb and Cu EF show at the same time as the MAR peak around 2400 cal BP. This can, however, be explained by a dilution through local mineral soil dust, which is closer to the UCC reference. An increase to around 10 followed towards the beginning of the Roman expansion to the region. Altogether, local metallurgical activities seem to have been low during this period.

Despite missing indicators for mining or metallurgy, it can still be concluded that the region underwent serious landscape changes with anthropogenically enhanced erosion during the Middle Iron Age. These were most likely induced by activities like deforestation and widespread agro-pastoralism. As suggested by archaeological studies, the ritual burning site was still in use during that time and a relation to the observed MAR is likely.

5.3.4 1950 cal BP to 700 cal CE: Roman period and Early Middle Ages

The beginning of this period started with a very low MAR, which rose and fluctuated around 2 $g*m^{-2}*a^{-1}$ until 200 cal CE. Around 230 cal CE, a short peak of 4.6 $g*m^{-2}*a^{-1}$ marks the highest atmospheric mineral input into the mire during the described period. After staying around 2 $g*m^{-2}*a^{-1}$ from around 280 to 400 cal CE, the MAR decreased to values below 1 $g*m^{-2}*a^{-1}$.

Human activity on the higher slopes above 1000 m a.s.l. probably lessened, either forced or pulled by Roman influence (see previous chapter), although pastoral and settlement indicators never ceased completely (Walde, 2006). The peak around 230 cal CE coincides only with a slight increase of *Poaceae* and charcoal particles in Fließ (Walde, 2006). There was, however, a period of highly increased micro-charcoal in the record of Hubmann (1994) around 150 cal CE, which directly preceded the MAR peak in this study and suggests a link between these signals. Afterwards, the Piller Mire profile of Hubmann (1994) shows a short presence of *Juglans* and *Castanea sativa* around 300 cal CE. However, the increased erosion signal also coincides with a

crisis of the Roman Empire in the 3rd century CE. Aside from this, there was only a single sample with *Cerealia* within this period (450 cal CE) and very few pastoral indicators. Moreover, another minimum of *Poaceae* was recorded around 600 cal CE. The profile of Walde (2006) exhibits a gap for most cultural indicators until around 600 cal CE and a significantly increasing forest cover of mainly *Pinus* around 500 cal CE. Considering the uncertainty range of radiocarbon age depth models, this decline of MAR and pollen indicators (around 500 cal CE) could be the equivalent signal to the changes observed in the Kleinwalser Valley around that time.

Many studies from the Alps suggest a prolonged period of a warmer climate, with reduced glacier stands, prevailing along with the Roman Empire (Holzhauser et al., 2005; Holzhauser and Zumbühl, 1996; Ivy-Ochs et al., 2009; Nicolussi and Patzelt, 2000; Suter et al., 2005). It is likely that these conditions favoured the initial Roman northward expansion. In the transition from Roman Times to Early Middle Ages, wetter and colder conditions superseded the previously warmer climate (Büntgen et al., 2011; Helama et al., 2017; Ivy-Ochs et al., 2009). As proposed for the Kleinwalser Valley earlier, these climate disturbance could be referred to either as the *Late Antique Little Ice Age* (LALIA) (Büntgen et al., 2016) or as part of the *Dark Ages Cold Period* (DACP) (Helama et al., 2017). This change probably suppressed a re-expansion of humans to higher elevations – even at or after the decline of the Roman Empire around 400 to 500 cal CE.

After having risen already in the Iron Age, the Pb EF rose to a peak of over 30 around 1950 cal BP, in parallel to Zn EF (17) and Cu EF (18) (see **Figure 34**), while Sb EF did not increase significantly. Only Pb EF stayed on an elevated level between 10 and 20, but went below 10 from 200 to 350 cal CE. A sharp, but more prolonged increase than before is then observed for Pb EF at around 380 cal CE, climaxing right after 400 cal CE with an EF of 28 and slowly declining to less than 5 at 700 cal CE (**Figure 34**). During this decline of Pb EF, the profiles of Zn and Cu EF also show minor increases.

Mining activities at this time are still not evidenced in the area for this period, probably because intensive mining during the Late Middle Ages and Modern Times (Grutsch and Martinek, 2012) destroyed or overprinted older traces (O'Brien, 2015). As suggested by the elevated metal EFs and archaeological evidence found around the Piller Mire, some of the ore deposits in the region were already known to prehistoric local communities. It is therefore unlikely that the Romans did not know of these valuable resources, especially in the direct vicinity of the important trade route (*Via Claudia Augusta*). However, the Roman Empire was already in decline around another

peak of Pb EF after 400 cal CE, so it is speculative to relate increased mining or metallurgy to any group or place amidst this period of upheaval.

In this period, either Roman influence did not have a disturbing impact on the landscape, or land use practices and settlement preferences were changed. Later, climatic factors could have also reduced both anthropogenic pollen indicators and the erosion signal. Enrichment factors are pointing to two episodes of regional mining at the beginning and at the end of the Roman period.

5.3.5 700 cal CE to 2017 cal CE: Middle Ages and Modern Era

Around the Early Middle Ages, MAR stayed on a low level, below 1 $g*m^{-2}*a^{-1}$, until 950 cal CE. A significant rise to values between 3 and 4.5 $g*m^{-2}*a^{-1}$ started at 1050 cal CE. The mineral input declined to values below 2 $g*m^{-2}*a^{-1}$ between 1240 and 1650 cal CE, just to temporarily rise again between 1700 cal CE and 1850 cal CE to almost 6 $g*m^{-2}*a^{-1}$. Another increase was recorded after 1950 cal CE, which culminated at a MAR of about 8 $g*m^{-2}*a^{-1}$, shortly before the end of the 2nd millennium. Twenty years later, MAR returned to values around 1.5 $g*m^{-2}*a^{-1}$, which is a level that is equivalent to the median MAR along the whole core.

For the comparison of the geochemical proxies from this study, it has to be stressed that the most important (local) reference studies (Hubmann, 1994; Walde, 2006) have their youngest radiocarbon ages between roughly 1300 and 900 BP, which brings a growing uncertainty into the interpretations, starting from around 1000 years ago. In contrast, the age-depth model of the Pi17-core is better constrained by anchoring points for the 20th century and another date around 650 cal CE, which can refine interpretations on the last millennium. This also means that a better comparison of the data to the increasing number of exact historical dates is possible. This effect is promoted by the decline in peat accumulation rates. Whereas the uncertainty of the age-depth model in Pi17 is around ±200 years at 1000 cal CE, it decreases towards ±10 around 1950 cal CE. However, the uncertainties in Hubmann's model are unknown.

Nonetheless, both Hubmann (1994) and Walde (2006) reported rising pastoral and cultural indicators (e.g. *Plantago* and *Cerealia*) and also grasses were rising again since around 700 cal CE, suggesting an opening of the landscape. This timing can be confirmed for the period after 750 cal CE (Wahlmüller, 2002) at higher elevations (approx. 2000 m a.s.l.). The increased erosion at 1050 cal CE coincides with a higher occurrence of grasses, *Plantago*, charcoal and with low *Picea* values in the Piller Mire (Hubmann, 1994). Furthermore, *Cannabaceae*, *Humulus lupulus* and *Juglans* suggest local agriculture. By the beginning of the Late Middle Ages around 1300 cal CE, grasses decreased slightly again, while *Picea* recovered. Another temporary decrease of land

use, this time more reflected by cultural indicators, appeared around 1600 cal CE. The implied reduced human impacts are coinciding with a decreased MAR and with the first and second cooling pulses of the Little Ice Age (Matthews and Briffa, 2005), which are also reflected in regional glacier progressions in the Kauner Valley (Nicolussi and Patzelt, 2000). A possible reason for the generally low MAR at the beginning of the Modern Era could hence be the continuous decline of mountain farming in the Alps after the High Middle Ages (Lichtenberger, 1965), which Bender (2010) already attributed specifically to aggravating climate conditions. Connecting the MAR peak around 1800 cal CE to any of the references becomes increasingly difficult, but an increase around the same time also occurred in the Kleinwalser Valley (HFL and LAD) and a similar mechanism behind this phenomenon is likely. Local historical data on the agricultural economy is delivering a possible clue about the cause of this peak. From 1774 cal CE to 1880 CE, the forest at Kaunerberg (about 5.5 km south of the mire) lost about 140 ha (Fromme, 1957). Thereafter, numbers from the same area for the years of 1850 and 1951 cal CE can explain the subsequently shrinking MAR: Agricultural yield declined by almost 50 % and also the livestock lost about 40 % of its former size during these 100 years (Fromme, 1957). Several km further south (Radurschl Valley), the same study described a decline of forested areas to only 15 % of their former size between 1774 and 1880 CE. Similar trends of dramatic forest destruction after 1774 CE, and a decline of livestock and agriculture between 1850 and 1950 CE, were also documented east and west of the mire in the Pitz, Oetz and Paznaun Valleys (Fromme, 1957). This documentation suggests that it was a regional phenomenon and that it is therefore also valid for the direct surroundings of the Piller Mire.

From 1949 until 1971 CE, peat was mined in the bog to the northeast of the studied mire (Naturpark Kaunergrat, 2000). However, the site was recommended as a potential natural resource before (von Klebelsberg, 1939), which indicates earlier small-scale peat mining earlier than 1949 CE. A hydrological connection between the two peatlands might have affected the “pristine” analysed mire as well. After 2000 CE, an educational nature trail and a watch tower were constructed along both the exploited and the “natural” mire. Not much earlier, power poles for a high voltage line were erected in a minimum distance of 100 m from the coring spot of Pi17 as well as new roads in the area. The strong MAR increase after 1950 cal CE could therefore be explained by a mix of these different impacts. First, the commercial mining of peat certainly played a role in the initial increase. Not much later, the construction of the overhead power line as well as of the touristic infrastructure (path and tower) could have been responsible for the MAR increase prior to 2000 cal CE. The very recent decline of MAR towards 2017 cal CE can probably be explained by the recovery of forests in the area but also by the end of peat mining and the effort of putting the area under nature conservation, shortly after the peat

mining facility (see **Figure 35**) burned down and was not rebuilt. The comparison to recent aerial photos (**Figure 24**) illustrates that the mire's surface was less covered with shrubs or trees only 40 years ago.

Figure 35: Aerial photo from 1974 CE of the Piller Mire and the peat mining facility. Source: State of Tyrol - http://data.tirol.gv.at, accessible also at (State of Tyrol, 2019c)

Like the MAR profile, the EFs of Pb, Cu and Sb (**Figure 34**) were quite variable, with marked peaks, since the beginning of the Middle Ages. An increasing trend of Pb EF commenced at 900 cal CE, starting at 5 and reaching a plateau around 25 that stretched from about 1200 to 1450 cal CE. The next, stronger rise to 60 appeared between 1500 and 1650 cal BP. But a temporary decline to values below 40 followed, running until the mid—19th century before an accelerating positive trend set in around 1850 cal CE. A maximum Pb EF was reached at about 1980 cal CE with almost 400, followed by a steep decline (see complete Pb EF in **Figure 36**). In line with Pb EF, Cu EF trended upward from around 900 onward, with a similarly sharp increase starting around 1850 cal CE. This trend peaked around 1980 cal CE (EF=20) and declined subsequently. Like Pb EF, the EF of Sb started to increase rather stepwise since 900 cal CE, with a plateau before 1500 cal CE, but got to a first peak around 1750 cal CE and a second one around 2000 cal CE.

The EF profiles in Pi17 are suggesting rising input of metals related to mining and metallurgy (Pb, Cu and Sb), starting around 1000 cal BP. As summarised by Wolkersdorfer (1991) and Hanneberg et al. (2009), historical sources suggest mining of Pb, Ag and Zn north of Imst (around 30 km north of Piller Mire) in the 12th century and at 1483 CE. Furthermore, mining rights were given away at 1352 CE (von Srbik, 1929) for a site close to Landeck (8 km from the mire). An intensification of silver mining around Imst started around the late 15th century CE (Hanneberg

et al., 2009b), which is fitting very well to more strongly rising EFs of Pb and Sb. As an example, Pb ores were mined and smelted at high elevations (~2500 m a.s.l.) about 20 km to the south in the Platzer Valley since around 1538 CE (Vavtar, 1988). The mine was still active around 1900 CE, however, a temporary abandonment was reported for the time between 1610 and 1888 CE, due to progressing glaciers (Vavtar, 1988). This interruption is mostly in line with a decreasing trend in Pb EF for more than 100 years.

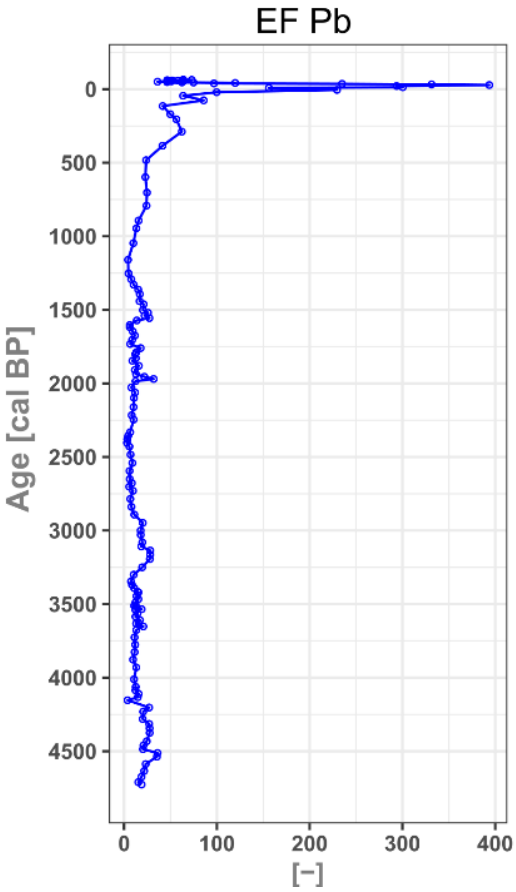

Figure 36: Full profile of Pb EF in the Piller Mire.

Altogether, the intensified exploitation of metals since the beginning of Modern Times was probably not restricted to the districts north of the mire and rather happened on a regional scale. Moreover, the EF trends from 1000 cal BP onward indicate an earlier onset of mining and/or smelting in the area than suggested by the little existing evidence. After around 1700 cal CE, a climatic cause could be deduced as a possible reason behind stagnating or sinking metal EFs in Pi17 (see above). However, a decreasing mining activity was also the consequence of rising unprofitability (Wolkersdorfer, 1991).

The accelerating EFs after 1850 and especially after 1950 cal CE can be assigned to the introduction of leaded gasoline and the resulting strongly increased atmospheric deposition (Pacyna and Pacyna, 2001). The sharp decrease after the 1980's is the response to the ban of

leaded fuel. With reference to the age-depth model of the Kleinwalser Valley, this time marker is confirming the approximate validity of the age-depth model of the Pi17 core.

Just like in the Kleinwalser Valley, a period of stronger decomposition and/or decreased accumulation rate (see **Figure 28**) is also observed in Pi17 within the upper metre. Again, this could be related to the effects of human disturbances, namely livestock trampling and drainage, suggested by Sjögren et al. (2007). Very likely, drainage of the exploited peatland probably affected the water table in the studied mire as well and triggered decay in the surface layers. Although no C:N-data was acquired for Pi17, the elevated S-content, starting at 1050 and peaking around 1950 cal CE, is in line with the higher degree of decomposition observed in the macrofossil samples (cf core description Pi17, chapter **5.2.1**). This horizon of highest decomposition is therefore too young for the time frame reported by Sjögren et al. (2007), which illustrates that some signals can be very local. The same conclusion can be drawn from the proposed causes for the very recent MAR peak in the late 20th century. Although the growing of peat building vegetation could have been disturbed by the assumed effects of drainage during peat extraction, the extraordinary high growth rates, exceeding 11 mm*a^{-1} over recent decades, were probably favoured by modern conservation measures (e.g. drainage removal).

To summarise this period, an increase of cultural and pastoral pollen indicators in reference studies after 700 cal CE was only reflected by a higher MAR during shorter episodes around 1050 and 1800 cal CE. To a certain degree, lower land use could have been induced by the Little Ice Age. In the the 20th century, peat mining and the construction of infrastructure led to another increase of mineral input and disturbance of the mire. The more recent elevations of metal EFs fit well to historical sources on mining and metallurgy in the region as well as to modern pollution. Nonetheless, there are traces for an onset of these activities already during the High Middle Ages at c. 1000 cal CE, predating the first historical evidence.

5.4 Conclusions on the Piller Mire

The chronology of the Piller Mire core spans approximately 4800 years, from Late Neolithic to Modern Times. It reveals episodes of increased land use and mining or metallurgy in the surroundings of the mire. Although some of these findings have already been suggested by palynological studies or archaeological evidence, independent proxies, like this geochemical study, were lacking so far to substantiate the findings. A regression analysis supports the potential of pXRF to measure low concentration samples derived from ombrotrophic peat and allows the linear calibration of proxy elements to detect and reconstruct erosion (Ti) and metallurgy, mining or industry (Pb, Zn). Moreover, the distribution of mobile elements (Sr, S, Fe)

and the concentration profiles of other elements (K, Rb, V, Zr) can be measured. But the results also demonstrate the limits of pXRF for some elements (e.g. Ca, Cu, Mn) in this type of peat.

As suggested by the registered data, the area or region around the mire saw episodes of mining or metallurgy between 4700 and 4200 cal BP, which would predate the earliest evidence in the Eastern Alps (e.g. in the lower Inn Valley). Human activities can also be inferred from erosion signals and the comparison to vegetation proxies from other studies. By the Mid to Late Bronze Age (3500 to 3000 cal BP), a higher land use and metallurgical activities are evident by both increased erosion and elevated EFs of Pb, Cu and Zn, which is in line with archaeological and palynological findings. This episode and as well as a distinct erosion peak around 2400 cal BP can be connected to important archaeological sites in the direct vicinity of the mire.

Despite proven influence of the Roman Empire in the region, their impact on the landscape was relatively low and may have even decreased land use of local communities. Only a short peak of MAR is observed in the 3rd century cal CE. However, metallurgical or mining activities are recorded around 1950 cal BP and again around 450 cal CE. Towards the Early Middle Ages, all available proxies indicate a generally decreasing human impact until both erosion and metal EFs show renewed impact on the region after 1000 cal CE. While mining and metallurgy did almost continuously increase, land use was low again until around 1750 cal BP. These low impact phases concurred with a colder climate. Another episode of strong land use (deforestation, agriculture and livestock) is suggested until 1850 cal CE again. The late 19th and the 20th century experienced a drastically rising Pb EF until 1980 cal CE. Peat mining and the installation of touristic and power infrastructure probably affected the mire's hydrology and mineral input temporarily before 2000 cal CE. The good accordance of MAR and EFs to well documented developments and events can minimise doubts about the proposed age-depth model and therefore supports the quality of the conclusions drawn from the used proxies.

6 Fimba Valley

6.1 Introduction (Fimba Valley)

The Fimba Valley (also Fimber Valley or Val Fenga) is located partly in the western area of the state of Tyrol (Austria) and partly in eastern Switzerland, belonging to the Silvretta mountain range. Certain local names in the valley are of pre-Roman origin and are referring to pastoralism, which indicates a pre-historic land use in the area (Kathrein, 2012). The study of Pott et al. (1995) gave valuable information on timber line fluctuations while Bauerochse and Katenhusen (1997) investigated Holocene vegetation changes and patterns. Hertl (2001) investigated the Late Pleistocene-Holocene transition glacier advances. Over the past decade, the valley, which is belonging to the Silvretta region, was intensively studied with an archaeological and palynological focus. Within the project "*Silvretta historica, alpine archaeology in the Silvretta",* different disciplines started to systematically excavate and investigate sites and collect data from different archives in different valleys of the Silvretta mountains (Reitmaier, 2012). As part of these efforts in the Fimba Valley, Walser and Lambers (2012) analysed the regional interrelation of climate and human activity during the Holocene based on archaeological and palaeoecological data from the contributing disciplines. Other studies focused son tree mega-fossils (Nicolussi, 2012), on soils (Kothieringer et al., 2015), on NPPs (non-pollen-palynomorphs) and on pollen in Alpine mires (Dietre et al., 2014). Reitmaier (2017) reviewed the development of prehistoric mountain farming in the region, whereas Carrer et al. (2016) presented evidence for early dairy production in the Iron-Bronze Age transition.

The Silvretta region and especially the Fimba Valley have been frequented repeatedly over the last 11000 years (Reitmaier, 2012): Evidence of Mesolithic (ca 10,500 cal BP) hunters and gatherers was found in a neighbouring valley, close to the upper end of the Fimba Valley, at 2800 m a.s.l. However, these archaeological findings for human presence are chronologically fragmented and can often only be complemented or supported by continuous records from mires or lakes, which are rare at high elevations. Due to the topography of alpine environments (2000-3000 m) like the Fimba Valley, mires are often very small, but at the same time very complex and heterogeneous. Palaeoenvironmental studies were carried out (Bauerochse and Katenhusen, 1997; Dietre et al., 2014; Pott et al., 1995). However, geochemical and sedimentological studies on micro mires have not been performed so far in such an environment of the Alps. And certainly not with the aim of investigating the links between the valley, climate, human occupation and the intensity and development of land use.

The methods used here evaluate the potential of pXRF in this type of micro mires first, as these peatlans usually have higher fluctuations in mineral content and thus can be subject to heavy

matrix effects. Thereafter, the results allow an assessment of the general suitability of using these mountain peat archives as geochemical records of past climate and land use changes. Geochemical traces (e.g. erosion or metal enrichments) of either human activity or climatic developments in peat cores of several high Alpine small-scale mires (close to archaeological and palynological study sites cited above), act as a complementing source for new findings and ways of interpretation. By comparing the acquired data to the existing local studies from other disciplines, but also to regional palaeoclimate studies, it will be possible to detail both the timing and extent of the recorded signals. Eventually, getting closer to the overarching aim of gaining a better understanding of the consequences of climate or anthropogenic impact on this fragile alpine landscape will be possible.

6.1.1 Geographical and geological setting (Fimba Valley)

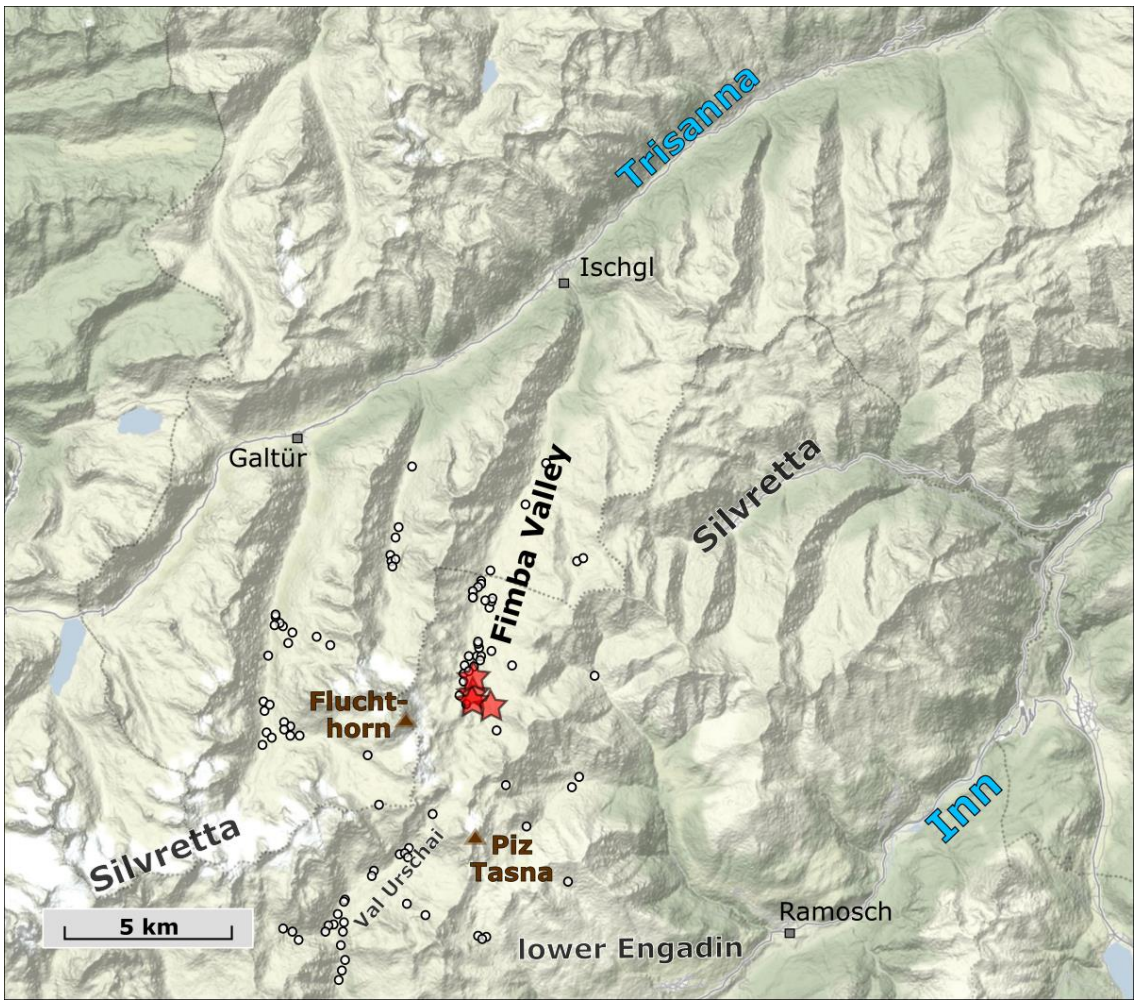

Figure 37: Overview on the Fimba Valley and its direct surroundings. Approx. compilation of selected archaeological sites (empty circles) from Dietre et al. (2014). *Cored mire sites (red stars). Map edited from source: Stamen Design under CC-BY-3.0 and OpenStreetMap contributors under ODbl.*

The Silvretta Massif is located roughly between the upper Inn Valley to the south and the Paznaun Valley to the north. The Fimba Valleys lower end starts at an elevation of 1400 m a.s.l. at the town of Ischgl and several of the highest peaks are reaching above 3000 m a.s.l. (e.g. Piz Tasna) at the upper end. It is accessible only by passing the small town of Ischgl at the valley's lower end. While this part still belongs to Austria (state of Tyrol), the other above 2000 m a.s.l. belongs to Switzerland (Canton of Grisons).

All active glaciers have disappeared, but bare and relatively fresh morphological features as well as some smaller residual snow fields are bearing witness of their recent existence. The valley is drained by the Aua Naira (upper valley), which becomes the Aua da Fenga river as the main water body. It then enters the Trisanna River in the Paznaun Valley at Ischgl as a tributary to the Inn River in the east. The U-shape of the upper part of the valley is characteristic of formerly glaciated mountain valleys. Its wide bottom is reducing the risk of rock and stone avalanches (Fromme, 1957) and is making it generally favourable for human activities (Bätzing, 2015).

A large part of the valley belongs to a so-called geological window, the Engadin Window, as it is showing the Penninic amidst the Austroalpine Nappes (Springhorn, 2007; swisstopo, 2018a), which are two main units of the European Alps. Although the surface is mainly covered by mixed Quaternary moraine sediments and rubble, the bedrock is highly heterogeneous with varying degrees of metamorphism. The eastern side of the valley is characterised by more gentle slopes, which is a consequence of the composition of mainly Penninic Flysch (Roz-Champatsch formation) consisting of sandy marls, shale and sandstones, formed during the Cretaceous. The western side is similarly covered mostly in Quaternary moraines but also has outcrops of Tasna-Flysch, which is consisting of clay shale, calcareous schist, sandstone, phyllite, quartzite and mica. Furthermore, the Arosa Nappe outcrops on the western higher slopes as well. It consists of a mix of dolomites radiolarites, pelagic limestones and black shales, formed during the Permian to Cretaceous. Higher above, the Fluchthorn Peak consists of Palaeozoic amphibolite.

6.1.2 Climate, vegetation and recent land use (Fimba Valley)

The Austrian climate station Obervermunt at 2040 m a.s.l. in the western Silvretta mountains recorded an annual precipitation of about 1109 mm and an annual mean temperature of 1.1°C (period 1971–2000). East of the Fimba Valley, the station at Obergurgl (1940 m a.s.l.) recorded 940 mm*a^{-1} and an annual mean temperature of 2.2°C (ZAMG, 2018). For the upper part of the Fimba Valley, where the study sites are located, a mean temperature of slightly above -1°C with an annual precipitation of around 1000 mm can be assumed. Almost 50 % of the precipitation are falling from June to August. Another good part falls in form of snow during wintertime. At

the elevation of the investigated mires, the prevailing climate limits the vegetation growth period to only 80 days or less (Bauerochse and Katenhusen, 1997). The highest stands of trees are well below 2200 m a.s.l., although the natural tree-line would currently reach higher than that (Remy, 2012).

The Fimba Valley is nowadays used to graze cattle, whose impact is visibly imprinted on the treeless slopes in form of typical stair-like structures on the soil. These structures cover the valley up to 2600 m a.s.l., where the highest occurrence of larger grass patches is found. Furthermore, the touristic activities (skiing, hiking, mountain biking) and a chalet for over 150 people (Heidelberger Hütte) at 2264 m a.s.l. constructed in 1889 CE, represent the heavy human impact in the valley in recent years.

6.1.3 Coring site descriptions (Fimba Valley)

The most important mire site of this study is the Las Gondas Mire (**Figure 39**). It is located at an elevation of about 2360 m a.s.l. and sits right on a side moraine (**Figure 40**) on the western slope of the Fimba Valley in a distance of about 1 km south of the chalet. A lower part of the mire (Lower Las Gondas – LLG) is located slightly southeast of the Upper Las Gondas (ULG) at 2354 m a.s.l. (**Figure 38**), which had been subject of earlier studies (Bauerochse and Katenhusen, 1997; Dietre et al., 2014; Pott et al., 1995).

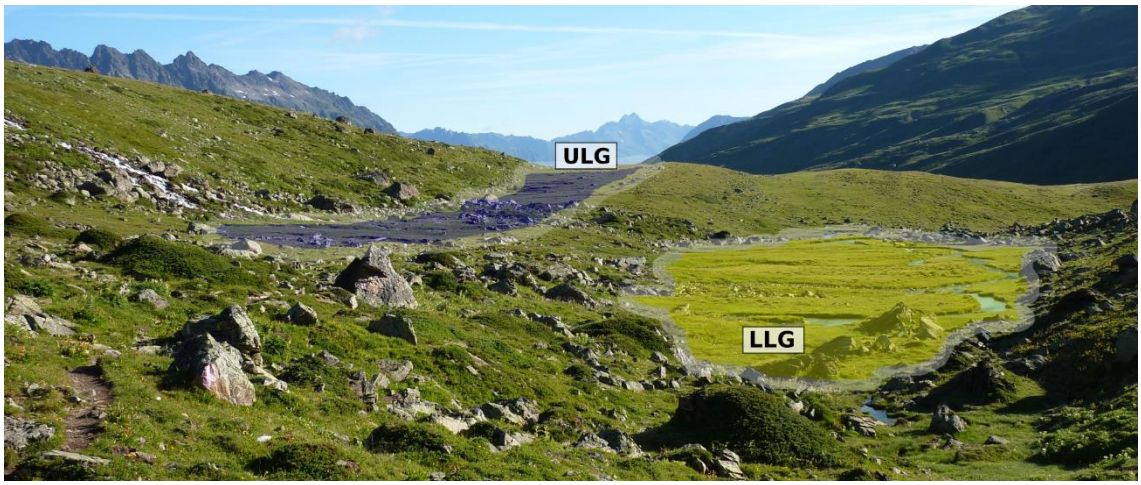

Figure 38: Upper and Lower Las Gondas (ULG and LLG). ULG left (blue), LLG right (yellow).

The small brook Aua da Gondas flows by at the southern end of both mire parts and drains into the Aua Naira. It comes from a former glacial field (>2500 m a.s.l.) on the slope to the Fluchthorn/Piz Fenga (Vadret da Fenga Nord), which is southwest of the mire and has a potentially strong current. This brook is also accompanied by a former debris flow between the glacier field and the Aua Naira in the valley's centre. The glacier field was still ice covered in the

late 19th century (Jacot-Guillarmod et al., 1896). Moraines in front of the glacier and around the Las Gondas Mire were classified as Late Pleistocene-Holocene transition (Hertl, 2001).

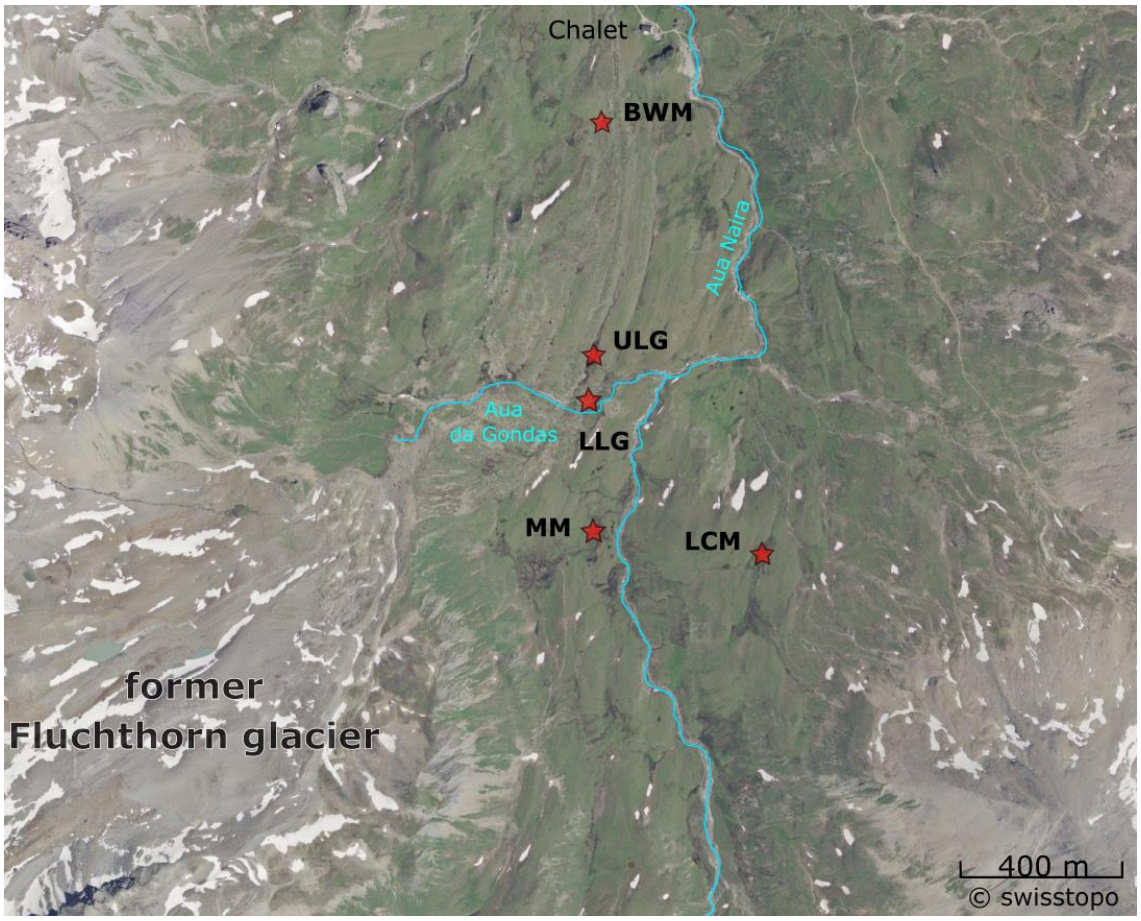

Figure 39: Satellite image of the upper Fimba Valley. Cored sites (red stars) and the former ice glacier field in front of the Fluchthorn. Side moraine stretches from Butterwiesen Mire (BWM) to Lower Las Gondas (LLG). (swisstopo, 2018b)

The Marmot Mire (MM) is about 340 m south of LLG and a smaller stream is flowing through at its eastern boundary. This brook is coming from the slope just below the ice field in front of the Fluchthorn and traverses through another mire, about 150 m upstream (west) of MM.

A third spot on the eastern side of the valley was cored and given the name Lower Coffin Mire, with reference to a coffin-shaped glacial boulder deposited next to it (LCM; at 2410 m a.s.l.). Compared to ULG, LLG and MM, the LCM mire appears more waterlogged. This is due to a tiny brook, coming from the southeastern slope, which is not channelled through the peatland but rather seeps through. Finally, there is the Butterwiesen Mire (BWM) (Kappelmeyer, 2014), at an elevation of 2300 m a.s.l., which is a few hundred metres north of the three other sites and closest to the chalet. It is fed by a more diffuse and rather low energy slope runoff. It is also the smallest of all mires investigated here.

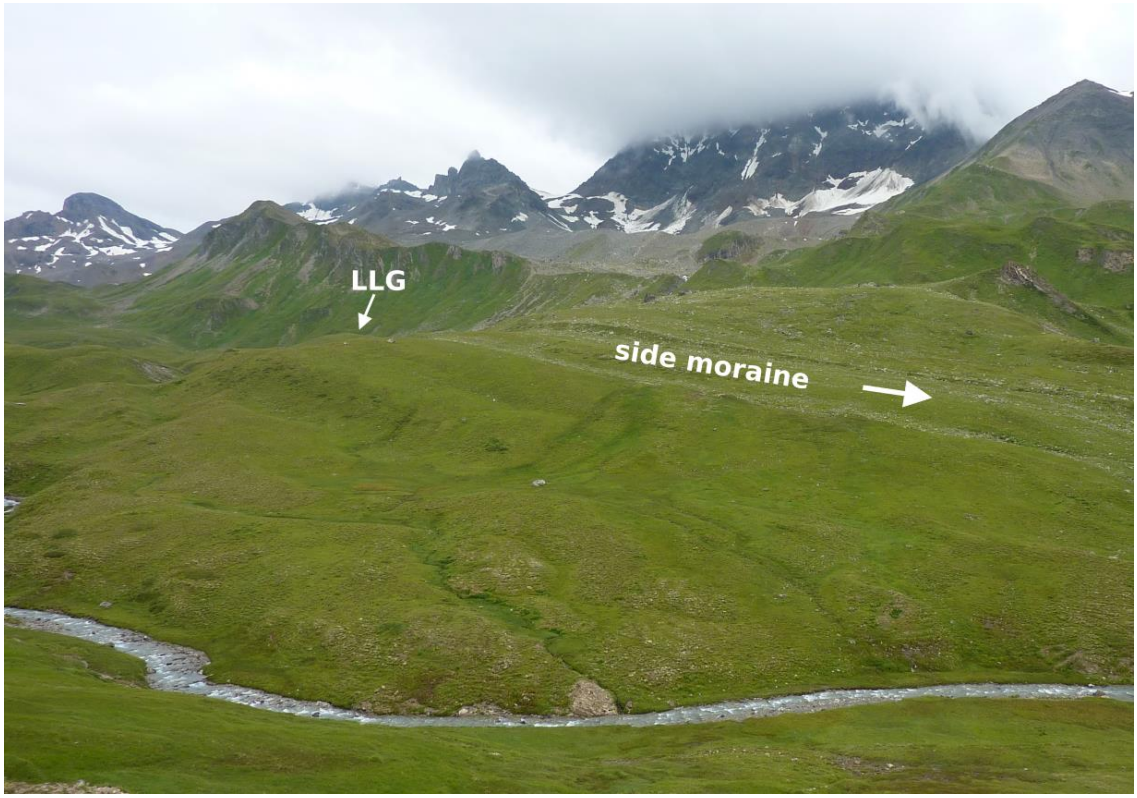

Figure 40: View to the southwest from the eastern side of the Fimba Valley and the Aua Naira Stream. The side moraine can be seen in the centre. The summit of the Fluchthorn (upper centre) is covered by clouds. Its former glacial field can be seen at its foot. The coring site LLG is behind the left side's end of the side moraine.

All four mires show a vegetation dominated by *Cyperaceae* and herbs. The upper part of the Las Gondas Mire (ULG) is showing typical degradation features, probably from cryoturbation and cattle trampling (Remy, 2012). The selection of these mires at an elevation around 2400 m a.s.l. is based partly on the assumption that it is or was the approximate zone of the natural timber line (Nicolussi, 2012) and because it is a strategically favourable position for humans to occupy (hunting and livestock grazing), as archaeological findings in close proximity suggest (see **Figure 39**). Hence, it enhances the probability of capturing signals of both climate and human impact.

6.1.4 Coring and subsampling (Fimba Valley)

Coring in the Fimba Valley was conducted in early August 2016 with the Russian coring system (Jowsey, 1966). Prior to coring, the deepest and most suitable spots were identified by sounding the underground with a Pürckhauer rod. The soundings demonstrated that maximum depths and layering are heterogeneous and, in some mires, can differ within a few metres. It is not clear if this is due to shifting water courses or because of the heterogeneous topography or buried boulders. To answer that, geophysical analyses would be necessary. To minimise the risk of possible effects of erosion or mineral layers from the nearby brooks, each coring spot was

selected at a distance of at least 10 m from the closest (present day) water channel. The very dense mix of peat and mineral layers strongly increased traction and therefore the force needed to drive down the corer and pull it out. Due to these circumstances, a barrel of 5 cm diameter and 50 cm length was used.

In the lower part of the Las Gondas Mire (LLG; at 46°54'3.51"N; 10°15'26.15"E), two overlapping cores were retrieved. The first (LLG-A) reached a depth of approx. 250 cm. A parallel core (LLG-B) was taken less than 2 m away, covering 30 to 230 cm depth. As the surficial peat was very dense compared to a regular moss peatland, compaction was negligible. Driving a Wardenaar system in such dense peat is moreover practically impossible. No monolith was therefore retrieved.

In the Marmot Mire, the first core (MM; 46°53'52.39"N; 10°15'25.53"E) was driven down to a depth of 112 cm until hitting coarse impenetrable sediment. The second section taken from a depth of 60 cm, to directly skip the potentially disturbed upper 10 cm of the Russian corer. The parallel core MM-B was only taken from 30 to 80 cm depth, after clearing the upper 30 cm of the borehole.

Three more cores were taken: one at the upper Las Gondas Mire (ULG; 46°54'07.4"N 10°15'26.4"E) and another one at Lower Coffin Mire (LCM; 46°53'49.9"N 10°15'46.5"E) on the eastern side of the valley. They were used only for dating the bottom layers to gain information about the onset of peat growth. An additional core of 92 cm length was retrieved with the Usinger system (8 cm barrel) already in 2012 in the “Butterwiesen Mire” (BWM; at 46°54'27.30"N; 10°15'28.92"E).

The upper metre of LLG-A was sliced and subsampled for geochemistry, density and radiocarbon dating. The lower 150 cm were described and sampled for macrofossils (dating) only, as it mainly consisted of mineral sediment, making it unsuitable for geochemical analysis. The cores of MM and BWM were used for line- and XRF-core-scanning.

6.2 Results & discussion (Fimba Valley)

6.2.1 Core descriptions (Fimba Valley)

Las Gondas

Table 11: Core description of LLG(A).

Depth (cm)	Description of LLG
251-190	mineral; fine grained light grey clay with very few black organic material

188	mineral layer of coarser sediment (mm-sized grains)
187-174	mineral; gradually more organic, macro-charcoal (187, 184 cm), charred wood chunks (180-183 cm), coarser layer at 183 cm, sediment-peat matrix in upper part with brown moss
174-172	mineral; fine grey clay/silt
171-164	brownish-grey mix of peat and mineral sediment, wood at 167 cm
163-158	interchanging layers of grey clay with organic content and dark blackish peat with brown moss, few wood
157-146	coarse angular mineral sediment, unsorted gravel (mm to cm scale)
145-128	interchanging layers of grey clay and organic rich sediment/peat, wood at 139 cm
125-127	transition to dark, blackish peat
124-110	dark/blackish brown, humified, decomposed peat, roots and rhizomes, mineral layer at 119 cm
109-98	dark humified peat, decomposed
97-93	light grey sediment, clay/silt, Muscovite, with organic content (roots)
93-91	mineral sediment rich dark brown peat, decomposed
90-43	dark brown humified peat, decomposed, roots and rhizomes, blackish and less humified at 78 cm, *Eriophorum* spindles and lower decomposition at 65-67 cm, higher sediment content at 63 and 54 cm
41-42	decomposed peat with high mineral content, grey clay
40-19	dark brown decomposed peat, roots and rhizomes, lower humification around 20 cm
18-10	brown decomposed peat, less humified, darker around 10 cm, wood at 11 cm
10-3	brown decomposed peat, slightly reddish, roots and rhizomes, *Eriophorum spindles*, charcoal at 8 cm
4-1.5	fine yellowish mineral sediment with rootlets

A line scan of LLG(A) can be found in **Suppl. Figure 3**. The LLG-core generally consisted of highly decomposed sedge peat, without any moss or other easily identifiable plant remains in the upper 150 cm. *Eriophorum* spindles were only found in a few layers. With only a few cm of varying offset, core LLG-B exhibits the same mineral layers as A. These layers were used as a marker horizon to synchronise cores A and B.

Marmot Mire (MM)

Table 12: Core description of MM.

Depth (cm)	Description
112-107	coarse yellowish-grey sediment, gravel (mm to cm scale)
107-101	fine dark blueish grey sediment
101-93	transition to dark peat, wood 99/100 cm, fine grey sediment layer at 93.5 cm
93-83	dark brown humified peat
83-62	brown humified peat
52-34	lighter brown humified peat, some yellowish sediment in lower part, darker peat 39/40 cm
33-24	dark brown peat, lower humification after 29 cm
23-12	lighter brown peat, roots, relatively low humification around 20 cm, brown moss stems and leaves
11-2	lighter brown peat, higher decomposition, higher humification

A line scan of MM can be found in **Suppl. Figure 3**. In contrast to LLG, MM shows a continuous peat accumulation and mosses were found in the upper part. Similar to LLG, the MM sequence consits of dense and compacted peat.

Butterwiesen Mire (BWM)

Table 13: Core description of BWM.

Depth (cm)	Description
92-68	dark, black/brown humified and decomposed peat, silt band at 81/82 cm
67-42	greyish sandy/silty mineral layers with little organic content
42-35	dark brownish peat, sediment around 40 cm
34-15	dark grey clayey/silty sediment, more brownish until 27 cm; yellowish brown/grey from 27 to 14 cm
13-6	gradually layered transition to dark brown peat, decreasing mineral sediment
6-0	dark brown fibrous peat with lower decomposition

Figure 41: BWM core (92 cm length) image from the Avaatech line scanner camera.

Additional cores (ULG, LCM)

The ULG core can be briefly described as a complete sequence of dense, decomposed sedge peat over a length of 145 cm and a highly decomposed, soft and wet gyttja down to 160 cm. However, it was not analysed in detail because of empty or thin parts in the coring chamber.

Figure 42: A section from the heterogeneous LCM core showing alternating peat and sediment layers.

The LCM core on the other hand was a very complex profile of interlayering peat and sediment, which were also heterogeneous in themselves. Because very complex age-depth models were expected and half of the core consisted of mineral sediment, this sequence was not selected for geochemical analysis either.

6.2.2 Radiocarbon dates and age-depth models (Fimba Valley)

Table 14: List of radiocarbon samples from Fimba Valley, including information about origin, depth, dated material and uncalibrated ^{14}C-ages.

Lab. No.	Site	Depth (cm)	Material	^{14}C-age (BP)	Comment
Poz-96231	LLG1A	9.0	Ligneous material *Eriophorum* spindles	1660 ± 40	0.14 mgC
Poz-91981	LLG1A	20.1	Ligneous material	2500 ± 30	
Poz-86683	LLG1B	46 (43 cor.)	Unident. plant remains	3395 ± 30	
Poz-91983	LLG1A	67.0	Ligneous material round seeds	4630 ± 35	
Poz-86682	LLG1B	92.5 (cor. 98)	Humified bulk peat	5660 ± 40	
Poz-86681	LLG1B	120 (126 cor.)	Humified bulk peat	6710 ± 50	
Poz-91984	LLG1A	161.5	Brown moss	7500 ± 40	**Figure 43**

Poz-86698	LLG1B	226.0	Plant remains in clayey sediment	9240 ± 50	
Poz-104864	MM1A	17.0	Brown moss	1600 ± 30	0.5 mgC
Poz-86685	MM1A	36.5	Humified bulk peat	2400 ± 35	
Poz-86684	MM1A	93.0	Humified bulk peat	5910 ± 50	
Poz-86688	LCM2B	122.5	Humified bulk peat with sediment	5560 ± 40	
Poz-86687	ULG1A	46.0	Humified bulk peat	2180 ± 30	
Poz-86686	ULG1B	134.0	Humified bulk peat	8080 ± 50	
Poz-79595	BWM3A	42.0	Humified bulk peat	1520 ± 30	
Poz-79597	BWM3A	68.0	Humified bulk peat	2015 ± 30	

A compilation of all radiocarbon samples from the Fimba Valley is given in **Table 14**. Four of the radiocarbon samples in the LLG-sequence were picked directly from the fresh parallel core B, directly adjacent to the synchronous marker horizons (parallel mineral layers). Due to the high degree of decomposition, most of the sample material picked for radiocarbon dating was unidentified plant debris or bulk peat, except for a few brown moss samples in LLG (below the massive rock debris layers at 161.5 cm) and in MM (**Figure 43** and **Table 14**).

Figure 43: Brown moss from LLG, depth of 162-163 cm, selected for dating (Poz-91984), with grey mineral particles.

The radiocarbon dates could be integrated into consistent age-depth models of LLG and MM as the main mire profiles for interpretation. The models for BWM and ULG were simulated as well, although the cores are not discussed in greater detail. The settings that were applied in rbacon (Blaauw and Christen, 2011) are summarised in **Table 15**.

Table 15: Settings in rbacon for LLG, MM and BWM

Site	thick	acc.shape	mem.strength	mem.mean	acc.mean
LLG	1.5	0.5	7.0	0.6	30
MM	1.5	0.5	9.0	0.3	50
BWM	1.5	0.5	9.0	0.3	20
ULG	1.5	0.5	9.0	0.3	50

The complete LLG profile accumulated with a mean rate of 0.29 mm*a^{-1} (**Figure 44**). The sedimentation of silty grey material in LLG started before 10,500 cal BP. The sediment accumulation rate until 8400 cal BP was predicted by the model to be around 0.3 mm*a^{-1}, followed by a higher accumulation rate of up to 0.5 mm*a^{-1} for the next 700 years. Afterwards, it did not return to rates higher than 0.3 mm*a^{-1}. By then, peat accumulation had taken over from 5300 to 3500 cal BP with an AR of < 0.2 mm*a^{-1}. It stayed above this value for the following 1000 years. The uppermost 20 cm took over 2500 years to accumulate, which illustrates a very low peat AR that fell below 0.1 mm*a^{-1} after 1500 cal BP.

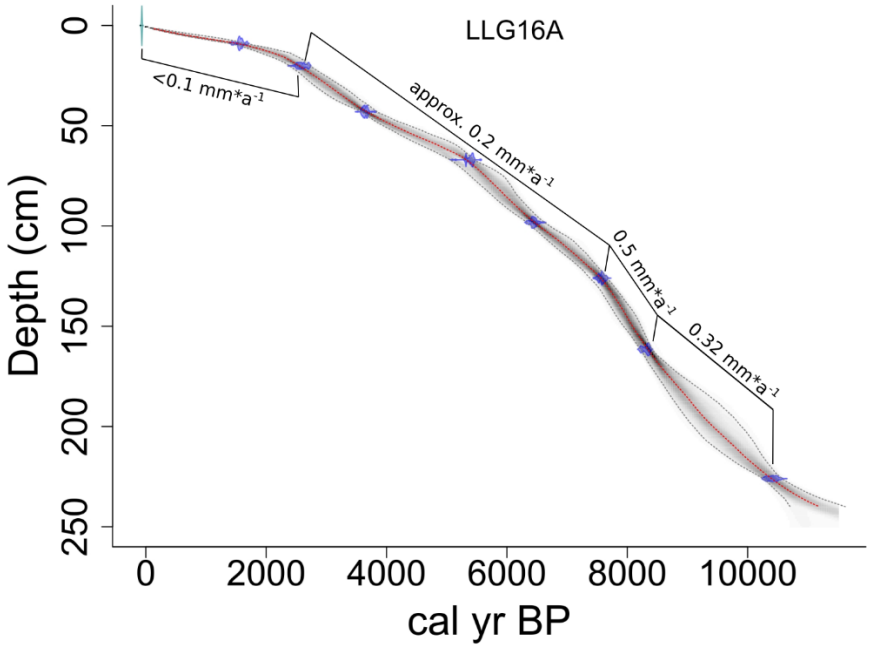

Figure 44: Age-depth model of LLG-A. Red dotted line=median age, grey shaded area=95% confidence interval.

In MM, the age of the lower end was modelled to a median age of about 7600 cal BP (**Figure 45**). Due to the absence of reliably datable material in the lowermost coarse mineral sediment, the age-depth model's output for this part was only a possible scenario. This means that the bottom layer could as well be around or older than 8000 cal BP, whereas a younger age seems less probable. The AR in MM ranged around 0.3 mm*a^{-1}, similar to LLG. Slightly higher AR's (>

0.3 mm*a^{-1}) were observed from 2400 to 1500 cal BP. Same as in LLG, the upmost 20 cm of the profile saw a decreasing AR to values below 0.2 mm*a^{-1} (after 1200 cal BP).

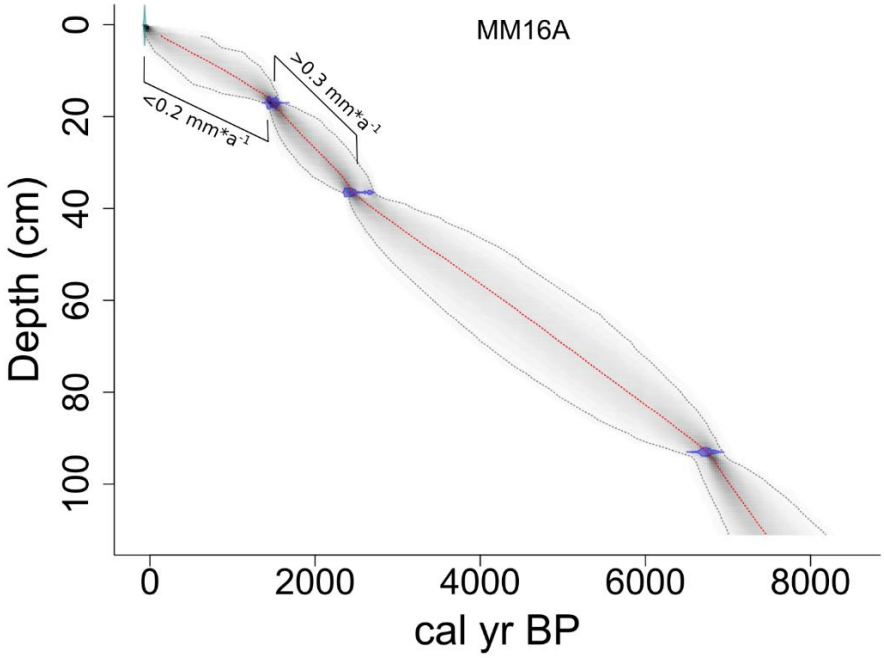

Figure 45: Age-depth-model of MM-A. Red dotted line=median age, grey shaded area=95% confidence interval.

Although there were only two radiocarbon dates for the BWM core, the sampling resolution was better than for LLG or MM. The lower end started around 2500 cal BP, although the range of uncertainty is between 2800 and 2150 cal BP for that part. The overall sediment accumulation rate (0.5 mm*a^{-1}) was almost two times higher than MM or LLG.

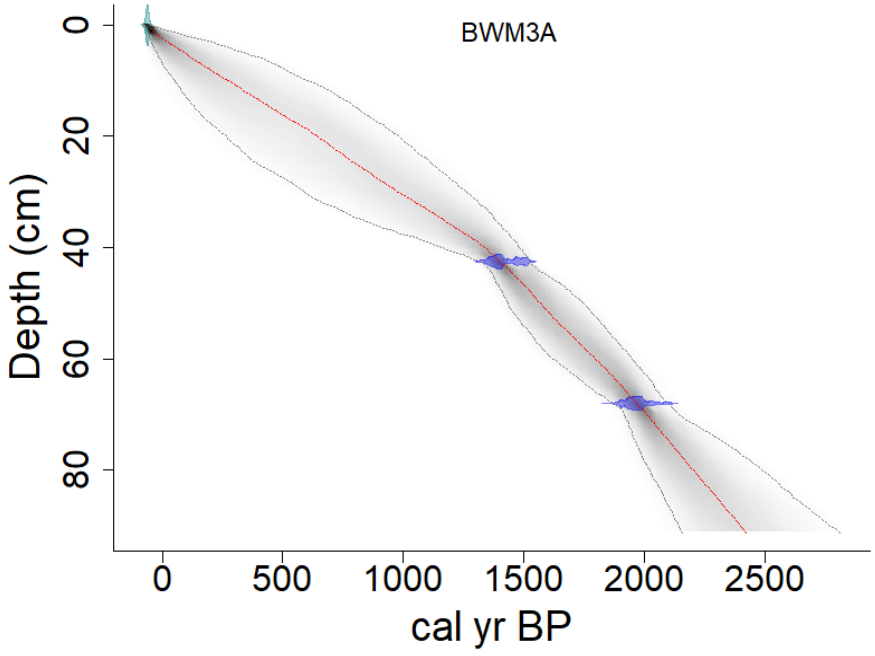

Figure 46: Age-depth model of BWM core. Red dotted line=median age, grey shaded area=95% confidence interval.

In contrast to MM and LLG, peat accumulation in the ULG already started around 8800–9100 cal BP and had a higher AR than LLG in the upper 50 cm. The basal date of the LCM mire suggests an onset of peat accumulation around 6300 to 6400 cal BP.

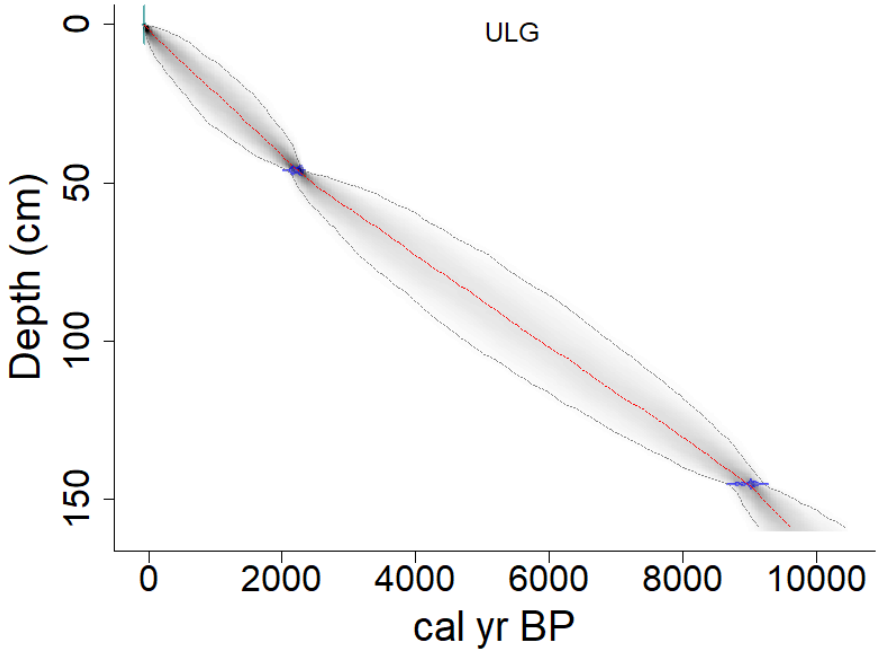

Figure 47: Age-depth model of ULG. Red dotted line=median age, grey shaded area=95% confidence interval.

6.2.3 Geochemistry (Fimba Valley)

Out of a total of 82 subsamples of the LLG-A-sequence, 75 were selected for geochemical analysis by pXRF and a share of 26 samples was measured by ICP-MS. As the LLG-sequence consisted largely of mineral sediment below 100 cm depth, only the upper 100 cm were sliced and subsampled to analyse the geochemistry. The MM- and the BWM-profile were only scanned with the XRF core scanner.

6.2.3.1 Regression Analysis (LLG)

The regression plots of LLG-Mire (**Figure 48**) illustrate that the concentrations of most elements are generally much higher than in HFL and Pi17 (chapters **4.2.3.1** and **5.2.3.1**). For **Ti**, two different regressions are possible: a linear regression for the peat samples and a polynomial one for all samples including the sediment layers. When looking at the linear regression first, the three samples with a concentration around 1000 mg*kg^{-1} start following a non-linear trend. At least for this pXRF-instrument, these three samples mark the transition range between peat and mineral sediment matrix. Either way, the R^2 of both regressions is above or equals 0.95. If the transition samples were removed, the linear transfer function would be close to the one for Ti in HFL.

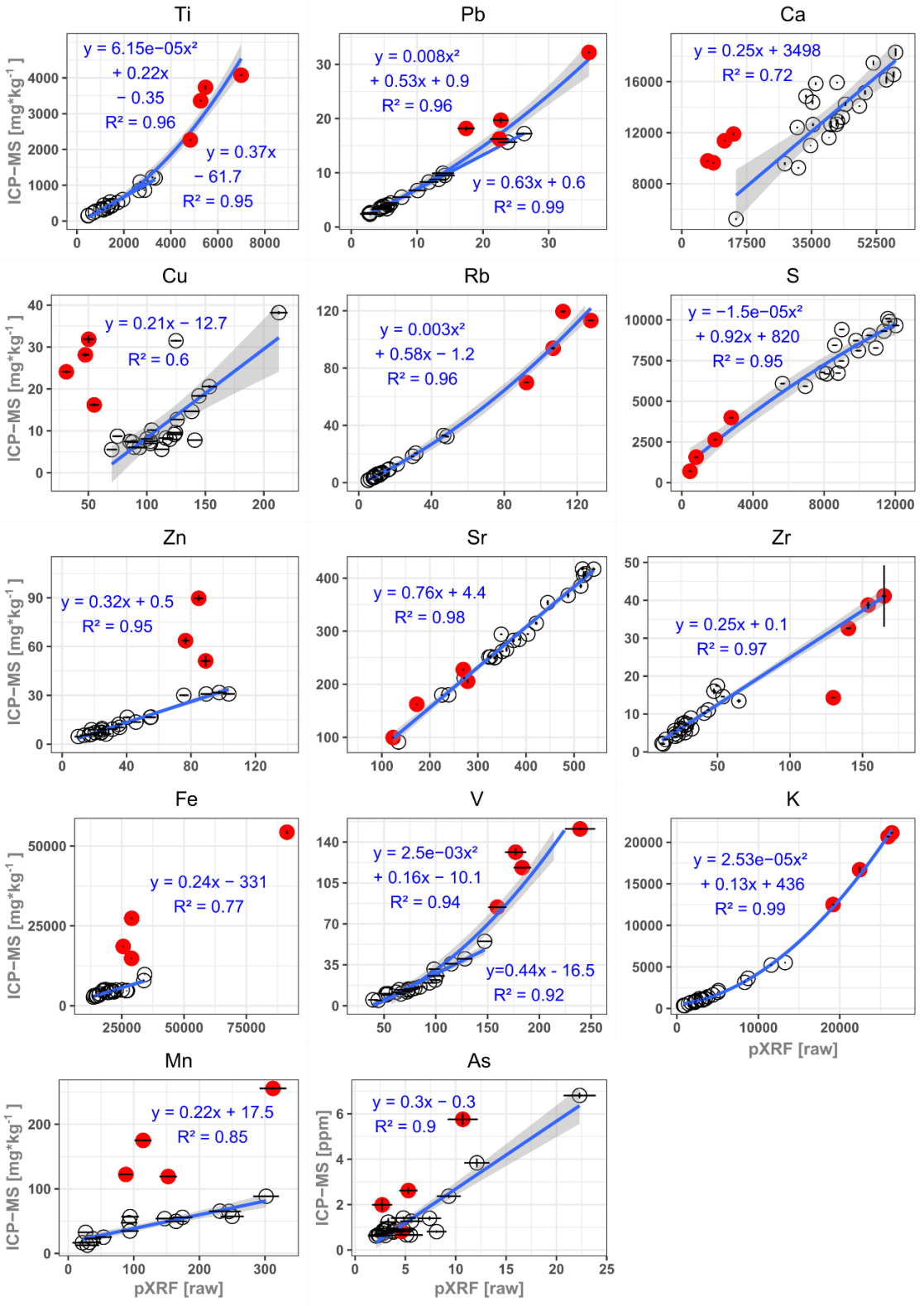

Figure 48: Regression analysis cross-plots of measured concentrations by ICP-MS versus scanned values by pXRF in LLG. Empty circles = peat, red full circles = mineral sediment.

The same applies for the **Pb**-measurements. However, the linear regression of Pb in LLG would shift slightly, if mineral sediment samples were considered. In any case, the linear regression model without mineral sediment samples had an excellent R^2 of 0.99.

The measurements of **Ca** resulted in a linear regression, although the fit R^2 was only at 0.72 with the mineral samples excluded. For Ca, the three peat-mineral-transitional samples plot above the regression line (at 35,000 pXRF raw).

The transfer function of **Rb** in LLG is described by a linear function for concentrations up to 40 $mg*kg^{-1}$ by using a 2^{nd} degree polynomial with the mineral samples included (R^2=0.96). Lower concentrations were still overestimated by pXRF, but Rb was measured closer to quantitative values the higher the mineral content in the sample was.

Compared to the mineral samples, the peat in LLG is high in **S**, but both measurements were linearly correlated with an R^2 of 0.94 and a relatively low overestimation by pXRF. Very similar to S is the behaviour of **Sr**, with a coefficient of determination (R^2=0.98). The regression of **Zn** was linear (R^2=0.95) when excluding the mineral samples.

Probably attributable to the high concentrations of **Zr,** the regression analysis yielded an R^2 of 0.97 for the whole range of samples, although one outlier (mineral sample) had to be excluded (see **Figure 48**). The **Fe** values show a linear regression, but only for the peat samples and with a relatively low fit (R^2=0.77). Despite higher errors, **V** shows a linear regression in peat (R^2=0.92) or a polynomial of 2^{nd} order (R^2=0.94) with including mineral samples. However, the transition range between peat and minerogenic samples poses a problem here as well.

The regression analysis for **K** is depicted perfectly (R^2=0.99) by a polynomial of 2^{nd} degree with a decreasing overestimation of pXRF with increasing concentration. With a fit of R^2=0.85, **Mn** appears to be quantifiable in peat samples as well. In contrast, **Cu** shows a weak fit again. Most samples (5 to 10 $mg*kg^{-1}$) scattered largely, indicating that the LOD was reached. Finally, **As** shows a linear regression with a good fit of R^2=0.9, but only without the mineral samples. Furthermore, a large scatter shows in the median range of concentrations (0.5 to 1.5 $mg*kg^{-1}$).

The generally elevated concentrations illustrate the matrix effect, which affects the pXRF measurements relative to the mineral content in the sample. Similar to the regression analysis of the HFL samples (chapter **4.2.3.1**), the pXRF instrument overestimates most elements, but with rising mineral content, the measurements are getting closer to their true concentrations.

This regression analysis demonstrates that pXRF measurements of Ti, Pb, Rb, S, Sr, Zn, K, V, Zr and – with some limitations – of Fe, Mn and Ca in peat can be transferred into absolute concentrations by transfer functions. For the elements Ti, Rb, S, Sr, Zr, and K, even the mineral (rich) samples can be integrated into a single transfer function, which allows their quantification in samples of these kinds of mires.

6.2.3.2 Elemental profiles (Lower Las Gondas, LLG)

Ca, Sr, S: As the regression analysis of **Ca** in LLG was strongly affected by changes between mineral and peat matrix on the pXRF measurements, the ICP-MS results of Ca are presented in **Figure 49**. The concentrations are mostly higher than in HFL, with a maximum of around 18,000 $mg*kg^{-1}$ in the lower third. Afterwards, a declining trend can be observed, reaching concentrations below 10,000 $mg*kg^{-1}$ in the upper 25 cm. Another minimum occurs in the mineral layers from 98 to 92 cm. The **Sr**-profile shows a similar trend, with concentrations of up to 400 $mg*kg^{-1}$ between 83 and 65 cm and minimum concentrations of 100 to 120 $mg*kg^{-1}$ in the top 6 cm and in the mineral layer around 95 cm. This suggests that LLG is strongly influenced by rich groundwater or dissolution of Ca from the recurring mineral particles and layers in the mire, which also points to a relatively high Ca-content in the local geology. Also **S** had high concentrations of over 9000 $mg*kg^{-1}$ in the peat and around 2000 $mg*kg^{-1}$ in the mineral layers.

Fe, Zn, V: In contrast to Sr and S, these elements are elevated in the mineral rich layers, which is an almost inverse pattern. The calibrated pXRF results (blue lines, **Figure 20**) were significantly underestimated in mineral layers because of the matrix effects in the calibration, illustrated in comparison to the ICP-MS results in **Figure 20** (red curves).

K, Rb, Ti, Zr: Showing main trends similar to the three elements above, K, Rb, Ti and Zr pXRF-measurements could be calibrated. Their concentrations share a sharp maximum from around 97 to 93 cm and a decrease thereafter. Phases of relatively low content were recurringly interrupted by sharp peaks at 62 and at 56 cm, from 44 to 40 and two smaller peaks at 38 and 33 cm, corresponding to visible sediment layers in the core. Variations within the peat layers without visible mineral content (e.g. 82—63 cm and 32—6 cm) were small, relative to peaks in the mineral layers around 95 cm or at the surface. The profiles of Ti and Zr also revealed smaller periods of elevated mineral content or input, at 68.5, at 21 and around 16.5 cm. All these elements share a sharp increase in the upper 6 cm.

Inferred from the profiles, it can be assumed that Fe, Zn, V, K, Rb, Ti and Zr represent mineral input into LLG. Less distinct smaller peaks for Fe and Zn and a smoother profile in the peat layers for K and Rb, however, indicates that these elements were affected by redistribution. Especially for Fe and Zn, biological cycling by the vegetation is obvious in the upper layers. A general observation is that the concentrations of the lithogenic components in this mire are generally very high, when compared to the other study areas. Despite the continuous decline of Ca and Sr in the upper 25 cm, the geochemistry is far from ombrotrophic conditions.

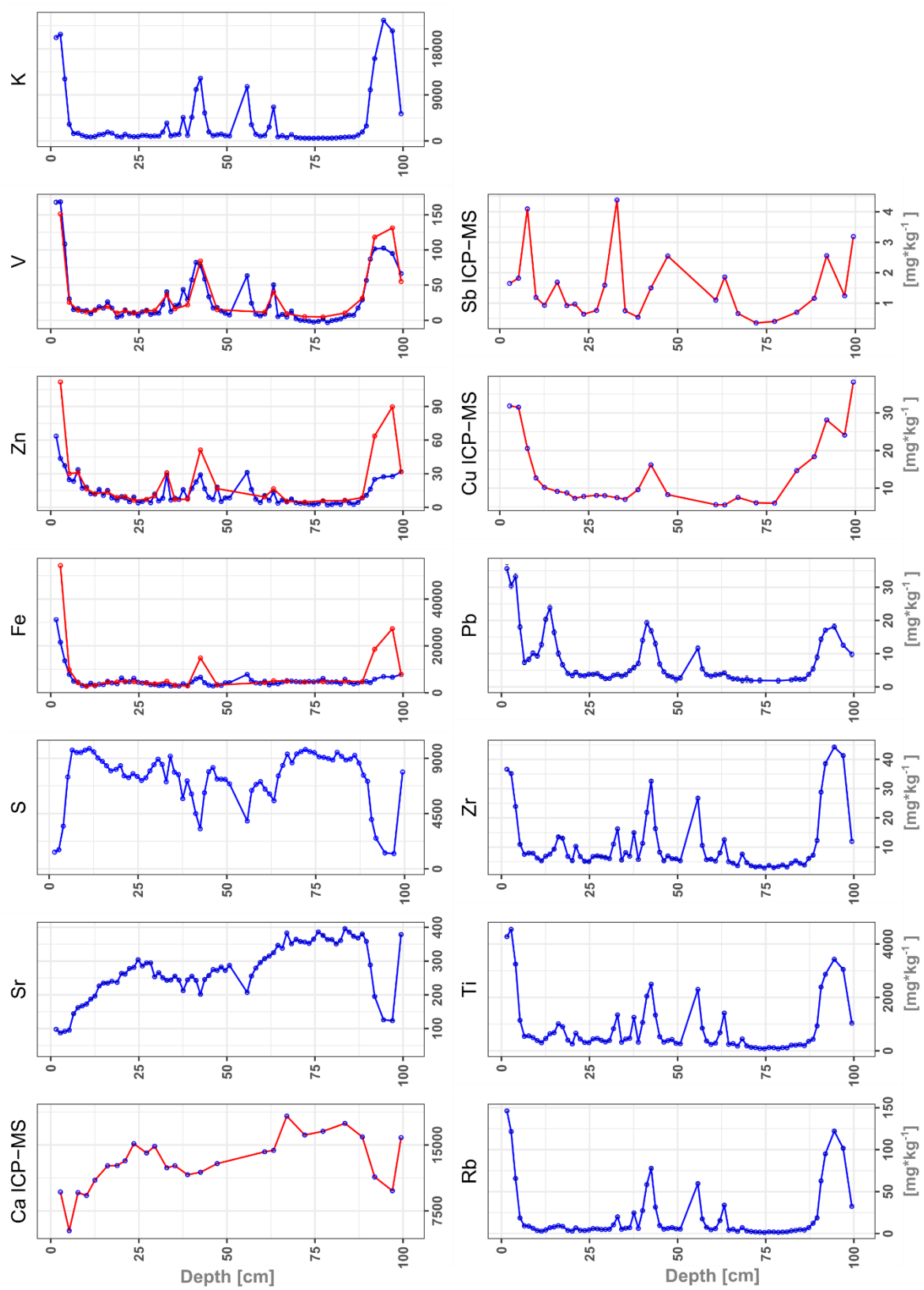

Figure 49: Elemental profiles in LLG derived from ICP-MS and pXRF. ICP-MS for Fe, Zn, V, Cu, and Sb in red.

Pb: Lead peaks were measured in the mineral layers as well, although less pronounced than the lithogenic elements described above. The almost pure minerogenic sediment around 95 cm is at a concentration of almost 20 mg*kg^{-1} but the following peat sequence is partly below LOD (1-2 mg*kg^{-1}). Significant peaks in the generally low profile appear around 56 and 42 cm (12-20 mg*kg^{-1}), which is contemporaneous to high lithogenic loads (e.g. Ti). A rise to 25 mg*kg^{-1} at about 13 cm is not connected to mineral content, while the increase in the top 6 cm is again.

Sb, Cu: Their concentrations were derived from ICP-MS only (similar to HFL and Pi17). The deepest peat sample starts at a Cu content of 27 mg*kg^{-1}, which is lower than the content in the minerogenic sediment directly above. Even in the next period of peat growth above, the sample at 80 cm is still higher in Cu (15 mg*kg^{-1}) than the peat samples further upward (< 10 mg*kg^{-1}). These elevated concentrations around the mineral layer suggest a release of Cu to the peat layers. A slow but accelerating rising trend sets in around 15 cm, ending with > 30 mg*kg^{-1} at the surface. Antimony has a more dynamic profile, with distinctly elevated concentrations at 100, 92, 63, 47, 33 and at 8 cm. However, these elevated concentrations neither correspond to elevated Pb nor to Cu and only have a slight contemporaneity with mineral layers.

6.2.3.3 Elemental profiles (Marmot Mire, MM)

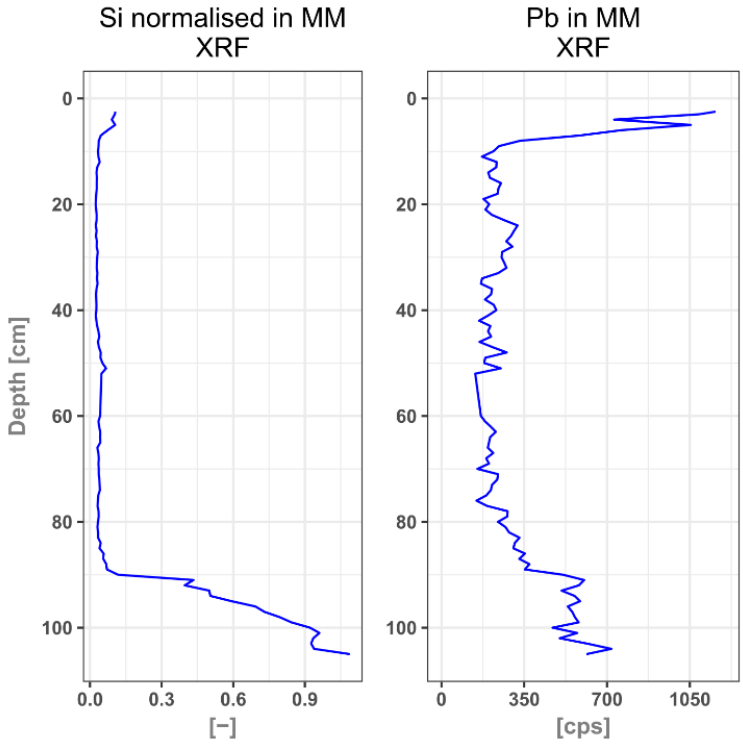

Figure 50: XRF core scanning profiles of Si (normalised to tcps) and Pb in the MM core.

In MM, only XRF core scanning data is available, of which Si (normalised by total counts) and Pb are shown in **Figure 50**. In line with the coarse mineral sediment layers, which are documented in the core description for the lowest 15 cm of the core, the normalised Si profile was highly elevated (1) until peat started accumulating above 90 cm and the signal falls below 0.05. A positive trend sets in toward the surface layers at 10 cm depth, reaching a maximum signal around 0.1. In between, only a tiny peak appears at 51 cm.

The profile of Pb decreases from the bottom until 80 cm and remains relatively constant around 180 cps. Smaller elevations appear around 50 cm and from 32 to 24 cm. A strong increase starting at 10 cm reaches the fivefold value just below the surface. Although this near-surface increase looks similar to the Pb-profile in LLG, it is less related to mineral input, as the concomitant rise of Ti in MM is less pronounced.

6.2.3.4 Definition of the geochemical background (LLG, Fimba Valley)

By looking at the high concentrations in the Fimba Valley, it is obvious that the mires are not ombrotrophic. Like in the Kleinwalser Valley (HFL mire), the elemental ratios (e.g. Pb/Ti) within the fine mineral sediment in LLG around 95 cm (i.e. 6400 cal BP) should be representative for the local natural (geological) background. The ICP-MS measurements of this sample are used as the background ratio, which is applied to calculate Pb EF. With Pb at 18.2 $mg*kg^{-1}$ and Ti at 3732 $mg*kg^{-1}$, the resulting ratio of 0.0049 is higher than the one in the Kleinwalser Valley (0.0037) but still not far off the UCC (~ 0.0042). Similarly, the local ratios for Cu (0.0064), Zn (0.02) and Sb (0.00033) are used to calculate the EFs of these elements.

6.2.3.5 PCA (Lower Las Gondas, LLG)

A PCA was conducted on the ICP-MS measurements of the LLG samples. Because LLG does not have the typical acrotelm and catotelm structure, only the topmost samples in the upper 5 cm were excluded. **Figure 51** illustrates that more than 90 % of the total variance can be explained by three components, whereas PC1 makes up for 73.5 % and PC3 only 7.6 %. The considered elements are mostly concentrated on PC1, except for Sb and the mobile Ca and Sr. There is no clear clustering of the mining/metallurgy indicators (Pb, Sb, Cu and Zn), probably because of a diluting effect of the general dominance of high mineral matter content in the sampling material. Moreover, the minerotrophic character of LLG increases the probability of a post-depositional mobilisation of e.g. Cu, Zn and Sb. Antimony plays a prominent role only in the smallest of all three components (PC3). The PCA demonstrates that LLG is dominated by the geological

background, confirming the observations in the concentration profiles. The outcome of the PCA was strongly influenced by the mineral layers within the profile, reducing its explanatory power for the behaviour of elements in the peat samples.

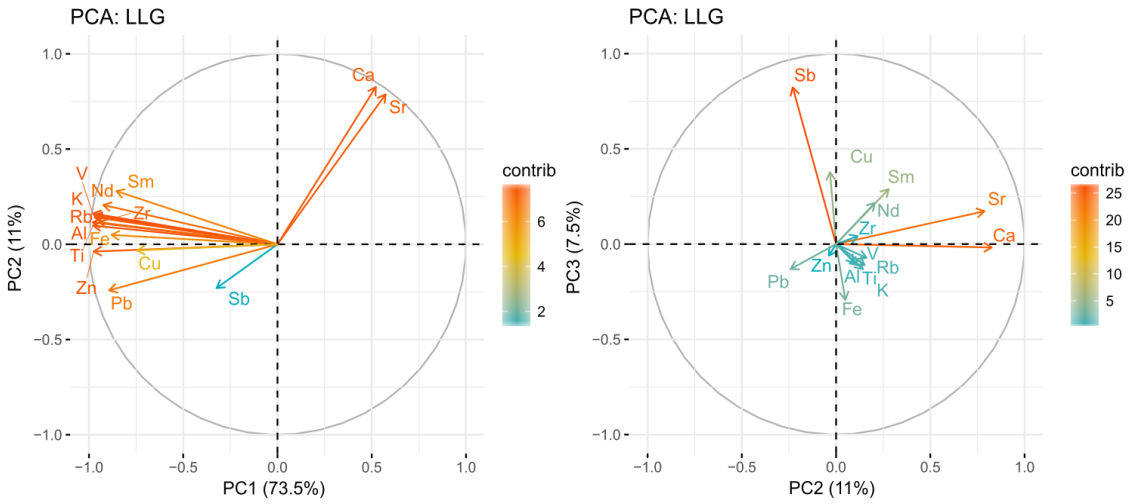

Figure 51: PCA of ICP-MS measurements in LLG.

As for the chapters on the Kleinwalser Valley and Piller Mire, Ti represents the lithogenic mineral component. Strong changes in the sample matrix and the minerotrophic character of LLG, however, complicate the interpretation of metals, as their signals were quite weak and not strongly associated to a separate PC.

6.3 Chronological discussion (Fimba Valley)

Which mechanisms are controlling an increased sediment input or peat development in the Fimba Valley? These mechanisms can be anthropogenic, mainly changes in land use and land-cover, or climatic, mainly variations in temperature or precipitation. During the Early Holocene, the most important cause of erosion at this altitude was a changing climate without any human interference. Hence, this chapter first compares the timing of changes in sedimentation with known climate variations or events during this “undisturbed” period. In general, stable and relatively warm conditions foster peat accumulation, whereas variable and rather cool conditions could limit mire growth. Several studies used glacio-fluvial stream-bank mires to reconstruct glacial activities by identifying and dating sediment layers from increased meltwater input (e.g. Matthews et al., 2005; Shakesby et al., 2007).

6.3.1 Early to Mid-Holocene (10,500 to 6300 cal BP)

The earliest onset of minerogenic sedimentation and peat accumulation in the mires of the upper Fimba Valley remains unclear and suggests a heterogeneous development between and within the different sites. Starting with the (Upper) Las Gondas Mire, the study of Dietre et al. (2014) suggested that peat started accumulating at 10,450 cal BP and that trees were present around the Las Gondas site at that time. Bauerochse and Katenhusen (1997) dated the basal peat of the mire to a range between 8050 and 7621 cal BP. In this study, the oldest radiocarbon sample in Lower Las Gondas (LLG) taken in the basal clay deposits (pro-glacial lake or fluvial deposits) at a depth around 225 cm provides an age of 10,260 to 10,520 cal BP, but no peat was accumulated then. The first phase of peat growth dates to around 8750 cal BP, although the peat (partly moss) was completely flushed and filled with sediment. The first phase of undisturbed peat started around 7500 cal BP. In contrast, the Upper Las Gondas (ULG) core, which was not analysed in detail, shows that peat accumulation had already started between 9150 and 8750 cal BP. This is, however, significantly younger than the 10,450 cal BP of Dietre et al. (2014). For MM, a basal age range between 8600 to 7100 cal BP was modelled, although peat accumulation did not start earlier than 7000 cal BP. The different dates for the onset of peat accumulation in the mires demonstrate the heterogeneity of the mire.

A review on Alpine glaciers and timber line studies by Ivy-Ochs et al. (2009) puts the beginning of a warmer period to around 10,500 cal BP, which would be in line with the earliest dates of beginning sedimentation or peat growth in Las Gondas. Favourable conditions are also inferable from human presence in the neighbouring valley at that time (Cornelissen and Reitmaier, 2016).

Coarse grained sediment (very fine gravel) amidst of the otherwise fine and clayey material at about 9200 cal BP coincides with the 9.2 ka cold event (Fleitmann et al., 2008). A cooling just prior to this age was suggested in the Western Alps by Tinner and Kaltenrieder (2005). It is, therefore, suggested that the coarse layer itself is related to the culmination of a cold event or to the beginning of glacier retreat in Eastern Switzerland (Joerin et al., 2008), which could have temporarily increased sediment transport by glacial activity. Consequently, warmer and probably more stable conditions are in line with wood pieces and a continuously increasing organic content (peat/silt mix) after this event until around 8700 cal BP. At this point, a short phase of glacier regression (Nicolussi and Patzelt, 2000) coincides with a layer of sediment with less plant remains in LLG. Thereafter, wood pieces and the first small peat layers indicate a stable and warm period again between 8500 and 8300 cal BP. This is in line with the presence of *Pinus cembra* trees at the mire (Nicolussi, 2012) and also Tinner and Ammann (2001) are arguing for a continuous warm period in the Alps from 9000 to 8200 cal BP.

The layer of angular gravel (157 to 146 cm) in LLG is calibrated to a period from 8240 to 8000 cal BP and has a relatively good age constraint because of the dated brown moss just below this sedimentation event (**Figure 52**). Since such a layer is likely to accumulate during a much shorter time (years to decades), its upper end is probably closer to 8200 than to 8000 cal BP. In any case, it points to strong erosive forces upstream of the Aua da Gondas (glacier, **Figure 39**) around 8200 cal BP. The basal gravel layer in MM dates within the same age range. Prior to 8300 cal BP, Dietre et al. (2014) suggested a beginning descent of the tree line. Bauerochse and Katenhusen (1997) documented a retreat of *Pinus* around 8200 cal BP, and Nicolussi (2012) reported the absence of dated trees after 8400 cal BP. Moreover, the ultimate decline of *Corylus* around Las Gondas between 8200 and 8000 cal BP was attributed to significantly lower temperatures (Dietre et al., 2012).

Figure 52: Coarse sediment layer, dated to the timing of the 8.2 ka event by brown moss directly below. The occurrence of wood above indicates a warming afterwards.

The so called 8.2 ka event is a cold event recorded in numerous archives in the northern hemisphere (Alley et al., 1997; Alley and Ágústsdóttir, 2005; Rohling and Pälike, 2005; Thomas et al., 2007). In the Central and Eastern Alps, Nicolussi and Patzelt (2000) report advancing glaciers after 8400 cal BP. Several records suggest responses on this event in the Alps (Haas et al., 1998; Heiri et al., 2003; Ilyashuk et al., 2011; Nicolussi and Schlüchter, 2012; Wick and Tinner, 1997). Evidence for a marked 8.2 ka event in the Silvretta mountain range (Kromer Valley) by Kerschner et al. (2006), was confuted by Moran et al. (2015) later. Speleothem data of the Eastern Alps did not show a clear signal (Vollweiler et al., 2006), while a speleothem in the northern Central Alps (Kleinwalser Valley) did record a (clear) response (Wurth et al., 2004).

The combined evidence of palaeobotanical and vegetation proxies from Upper Las Gondas (Dietre et al. 2014) and the thick layers of coarse sediment in the Marmot Mire and Lower Las Gondas reported here, strongly suggest a response to the 8.2 ka event in the Fimba Valley. As the result of a glacier expansion of the closest (former) ice field to the southwest in front of the Fluchthorn was most likely the source of the coarse sediment. This is also suggested by the reconstructions of glacier extent at the end of the LIA and Pleistocene termination (Hertl, 2001). Shakesby et al. (2007) used a similar approach to reconstruct glacier expansion during the 8.2

ka event in a Norwegian stream-bank mire. It remains, however, unclear, if the high load of sediment was a direct result of a combined advance of the glacier and soil destabilisation due to vegetation withdrawal, or if it was transported because to the force of increased meltwater release.

The following period, until approximately 7600 cal BP, is characterised by interlayered mineral rich peat and silty sediment in the LLG record, indicating a continuous flushing with silty material. However, a small piece of wood embedded at 7850 cal BP suggests that the tree line had already moved up again after the 8.2 ka cold event. After 7500 cal BP, an almost undisturbed accumulation of peat is only interrupted by a silty layer at around 7300 cal BP, which would fit to the end of glacier recession reported for south-eastern Switzerland between 7450 and 6650 cal BP (Joerin et al., 2008). In both cases, a connection to glacier activity would be responsible. Another period of undisturbed peat accumulation thereafter suggests relatively warm and stable conditions, until a thick minerogenic layer, deposited at c. 6400 to 6200 cal BP interrupts this period. During this phase, the now incipient geochemical record of LLG (**Figure 53**) illustrates the high mineral input with a maximum MAR of 225 $g*m^{-2}*a^{-1}$ centred around 6300 cal BP. The almost synchronous date for the onset of peat accumulation directly after a coarse mineral bottom layer with angular gravel (mm to cm) in the LCM core (**Table 7**) suggests a common trigger. As the LCM mire is located on the eastern side of the Fimba Valley, it implies a mechanism, which is not just a small-scale or site-specific signal.

An anthropogenic impact as the cause behind the deposition and accumulation regimes of sediment and peat up to this point is rather unlikely. However, hunters and gatherers were present in the upper part of this valley and in neighbouring ones around 8.2 ka (Cornelissen and Reitmaier, 2016; Reitmaier, 2012). Reitmaier (2012) also showed archaeological evidence for human presence at about 7500 cal BP and between 6850 and 6500 cal BP. Moreover, a continuous phase of human activities in the valley was suggested after c. 7450 cal BP by Kothieringer et al. (2015) and Dietre et al. (2014). These studies observed an increasing human impact (fire, deforestation and maybe livestock) until around 6200 cal BP. This suggests that the sedimentation pulse observed in LLG after around 6400 cal BP was partly induced by these activities. However, a colder climate in the Fimba valley during this period is suggested by the Las Gondas pollen record (Dietre et al. (2014). Evidence from glaciers and dendrochronological studies also suggest cooler conditions in the Alps around this time (Bortenschlager, 2010; Haas et al., 1998; Ivy-Ochs et al., 2009; Joerin et al., 2008, 2006; Nicolussi and Patzelt, 2000). Some of these authors correlate this cooler phase with the Rotmoos-I phase, also known as the Piora-I oscillation. Similar to the LLG record, concurring silt layers were found by Wahlmüller (2002) in a mire at about 2000 m a.s.l. at Serfaus, 25 km northeast of the Fimba Valley (**Figure 23**).

Although the other local studies in the upper part of the Las Gondas Mire did present dendrochronological and pollen evidence for a colder climate, they did not document such distinct (coarse) mineral layers in their records, neither around 8200 nor 6300 cal BP. Again, this highlights the heterogeneity of the mire(s), but it also shows that the selection of the coring site can strongly influence the outcome of the study. In this case, the proximity of the LLG-core to the Aua da Gondas brook and with it the direct connection to the Fluchthorn glacier field probably made it more sensitive to glacial activities, corresponding to well-described cold events that triggered erosion. This sensitivity is illustrated by an ancient debris flow, coming from the Fluchthorn glacier field, passing by the LLG coring site and ending shortly downslope of it (aerial photo, **Figure 39**).

Despite the unavailability of geochemical data for most of the time period discussed in this section, the contemporaneous occurrence of prominent sediment layers, regional glacier progressions and evidence from pollen studies suggests a relationship. It is therefore concluded that several prominent cold events influenced the landscape and triggered glacial activity in the upper Fimba Valley, most prominently during the 8.2 ka event but also around 6300 cal BP, whereas human impact was rather negligible.

6.3.2 6200 to 2800 cal BP

After the preceding mineral layers of the cold period, an interval of low MAR 3 $g*m^{-2}*a^{-1}$ is observed in LLG from 6100 to 5100 cal BP and only a brief small deterioration shows up at 5400 cal BP in **Figure 53**. After sinking below 5 $g*m^{-2}*a^{-1}$ again, another rise of MAR shows up directly prior to 5000 cal BP and again at 4500 cal BP to 20 $g*m^{-2}*a^{-1}$. A period of increased MAR stretches from 3700 to 3500 cal BP, with a maximum of over 30 $g*m^{-2}*a^{-1}$. Two smaller peaks around 14 $g*m^{-2}*a^{-1}$ were then recorded at 3380 and 3170 cal BP but a level below 5 $g*m^{-2}*a^{-1}$ is kept until 2800 cal BP. Only a slightly elevated phase of almost 5 $g*m^{-2}*a^{-1}$ is centred around 2900 cal BP.

In good agreement with the palynological data (less tree, but no increase in cultural or pastoral pollen) and with the interpretation of Dietre et al. (2014), the MAR peak at 5400 cal BP could be related to the Rotmoos-II cold period. Another peak around 5000 cal BP is in line with reviews of major Alpine cold phases (CE-6) by Haas et al. (1998) or Ivy-Ochs et al. (2009). Thereafter, the Fimba Valley itself and neighbouring valleys to the south experienced an increasing impact of human activities due to the general transition from hunting to agro-pastoralism at c. 4800 cal BP (Bauerochse and Katenhusen, 1997; Dietre et al., 2017, 2014; Kothieringer et al., 2015). However, the MAR in LLG seems to be unaffected by the development at this point. Not much later, the peak at 4500 cal BP agrees well with a rise in pastoral and cultural indicators in the Las

Gondas Mire (Dietre et al., 2014) but also coincides with short glacier advances in the Central Alps (Joerin et al., 2006; Nicolussi and Patzelt, 2000).

During the Bronze Age, the first and highest of three MAR peaks around 3600 cal BP coincides with another cold period (Haas et al., 1998), also reflected in a glacier maximum of the Gepatschferner (Nicolussi and Patzelt, 2000), which is only 35 km to the east of the Fimba Valley (see **Figure 1**). Several radiocarbon dated archaeological finds from around the mire indicate human presence between approximately 4000 and 3600 cal BP (Reitmaier et al., 2018). However, the pollen record of Dietre et al. (2014) shows a phase of very low pollen influx and a trend to rather high percentages of tree pollen and a minimum of charcoal and pastoral indicators at the end of this phase (3500 cal BP). A decline of fire management in the neighbouring Lower Engadine Valley (**Figure 37**) towards 3650 cal BP was also suggested by Dietre et al. (2017). Hence, an anthropogenic cause behind the first MAR peak around 3600 cal BP signal is unlikely despite human presence. Thereafter, Hormes et al. (2001) suggested a warmer period with retreating glaciers and the two following MAR peaks in LLG during the Middle to Late Bronze Age coincided with rising pastoral indicators and a more open landscape, indicating an artificial lowering of the timber line, paired with increasing livestock grazing around the Las Gondas Mire (Bauerochse and Katenhusen, 1997; Dietre et al., 2014). Local archaeological evidence for human presence also exists for this period (Reitmaier et al., 2018). On the descent, south of the upper end of the Fimba Valley (**Figure 37**), an abri had been in use around 3480 to 3370 cal BP (Reitmaier, 2012). In this area, belonging to the Lower Engadin, Dietre et al. (2017) recorded a revival of fire management and agriculture from 3400 to 2800 cal BP. Reitmaier et al. (2018) demonstrated that a change in livestock management – vertical transhumance and a shift to the use of secondary animal products (dairy, wool, etc.) – happened in the same time interval and area. Not far from the eastern boundary of the Silvretta mountains, Wahlmüller (2002) documented stronger human impact, dated to around 3500 to 3350 cal BP. Further east (Oetz Valley, e.g. **Figure 23**), Festi et al. (2014) concluded that the onset of strong human impact (agro-pastoralism) began and prevailed in the Middle to Late Bronze Age. In the opposite direction, west of the Fimba Valley, studies supposed an increased agro-pastoralism before and around 3250 cal BP (Roepke et al., 2011; Roepke and Krause, 2013).

While some parts of the MM-core are chronologically less constrained, a first mineral peak appeared around 3500 cal BP (Si signal, **Figure 54**). In this case, the peak in MM could either correspond to the first, or to one of the latter MAR peaks in LLG. So far, the MM-core did not receive increased mineral content synchronously with MAR peaks in LLG during the previously suggested cold phases. This could be possibly due to the location of MM below another upstream mire, which is acting as a buffer for higher sediment loads. Furthermore, the nearby

water channel is not connected to the Fluchthorn glacier upslope. It is thus very likely that the mechanisms behind increased mineral input into LLG and MM are different from each other. Stream-bank mires like LLG seem to have primarily recorded a climatic, hydrological or geomorphological signal, at least in the older part of the core, while the concurrence of human activities and a higher mineral signal in MM or in the Upper Las Gondas Mire (Dietre et al., 2014) suggest that human impact is easier to track in these mire, because they integrate signals from a wider area. Towards 3000 cal BP, the profiles of both MM and LLG show a synchronously declining trend (**Figure** 53 and **Figure** 54), despite continuously recorded pastoral indicators in Las Gondas (Dietre et al., 2014) and the onset of an almost continuous phase with archaeological evidence of regional agro-pastoral land use in the Late Bronze Age (Carrer et al., 2016; Reitmaier et al., 2018). However, only subtle MAR fluctuations in LLG are possibly related to these human activities.

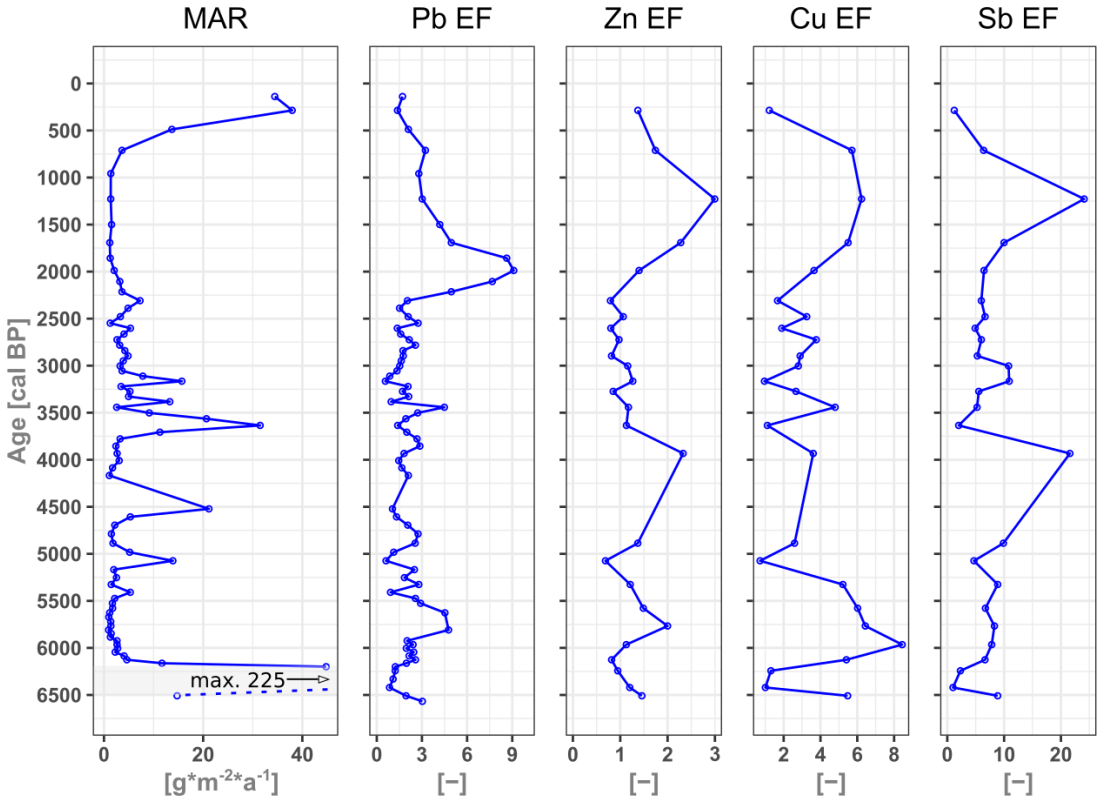

Figure 53: MAR, Pb EF, Zn EF, Cu EF, and Sb EF in LLG, derived from pXRF and ICP-MS.

After this increased human impact and strong landscape alteration in the upper Fimba Valley and elsewhere in the Central Alps, several studies suggest a slow cooling trend beginning after approximately 3300 cal BP, reflected in glacier progressions and descending tree lines (Haas et al., 1998; Ivy-Ochs et al., 2009; Nicolussi and Patzelt, 2000). Yet, it has to be mentioned that tree line reconstructions can no longer serve as an unambiguous proxy for climatic oscillations in the Central Alps since the Mid Bronze Age, because of strong anthropogenic deforestation at high

elevations (Nicolussi et al., 2005; Wick and Tinner, 1997). Following the suggestion of Nicolussi (2012), it can be assumed that also the tree line in the Fimba Valley was permanently lowered by the suggested widespread deforestation and land use since the Bronze Age. Even under lowered human impact and reduced grazing pressure, a recovery of tree cover at this altitude is very slow, especially during a cooling climate.

Besides variations in mineral input, the peat accumulation rate in LLG between roughly 6000 and 3000 cal BP was lower than before. Hence, generally drier conditions could have been responsible for a decreased peat growth and/or higher compaction and decomposition. A similar interpretation was made by Dietre et al. (2014) and Bauerochse and Katenhusen (1997), based on NPPs and pollen, in agreement with lower peat accumulation during that period recorded in a mire about 35 km to the west (Roepke et al., 2011).

In **Figure 53**, the EFs of Pb, Zn and Cu show only a very slight enrichment around 5700 cal BP. However, the fen character of LLG challenges the liability of everything but Pb as the only immobile element. Copper EF seems to be enriched below and above the mineral layer around 6300 cal BP, suggesting a post-depositional leaching from the silt into the peat layers. This is not the case for Pb, which has an EF of about 4.5 around 5750 cal BP. Altogether, the contemporaneously elevated EFs of Pb, Zn, and Cu suggest metallurgy in the region.

The next considerable signals are observed right after 4000 cal BP, although only for Zn EF and Sb EF. A short lived Pb EF peak (4.5) appears around 3450 cal BP, simultaneously to an increase of Cu EF. Probably due to the increased MAR around the Mid to Late Bronze Age, a higher amount of local sediment with a lower geological background Pb/Ti-ratio could have diluted and masked a higher atmospheric signal. However, because of widespread human activities and deforestation at that time, atmospheric soil dust from diffuse regional sources could have played a role as well.

When considering the proxies MAR and Pb and Cu EF in LLG plus increased mineral content in MM and matching it to evidence from archaeological and palynological studies, human impact can be suggested as the cause for the erosion peaks between 3500 and 3000 cal BP. For most of the previous pulses of increased erosion in LLG, the matching with documented glacier advances in the Central Alps indicates a causality between MAR increases and cold periods rather than human land use as a trigger. However, a combination of cooler climate and increasing pastoralism could have enhanced the observed erosion signals. It is, however, challenging to decipher this without further data.

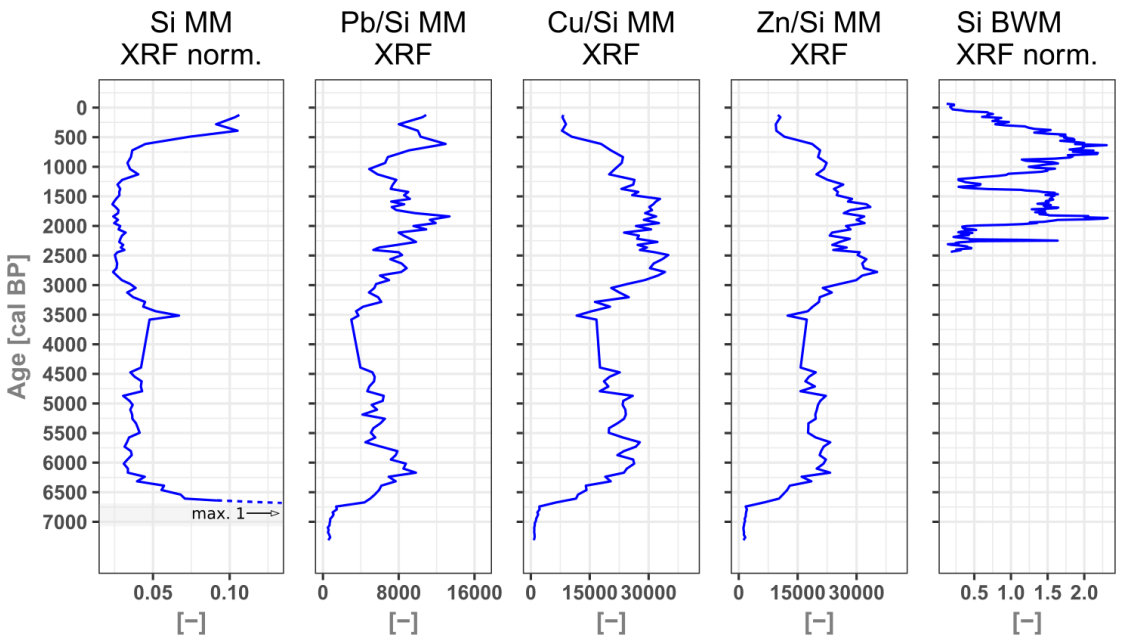

Figure 54: Si (normalised to total cps), Pb/Si, Cu/Si and Zn/Si in the MM-core, derived from XRF-core-scanning. The Si profile is clipped at 10 % of the maximum of the signal.

6.3.3 2800 to 1500 cal BP

The MAR in LLG stayed relatively low (< 3 $g*m^{-2}*a^{-1}$) between 3000 and 1000 cal BP. Fluctuations to values exceeding 5 and 7 $g*m^{-2}*a^{-1}$ are showing in the profile in **Figure 53** around 2600 and 2300 cal BP respectively. A declining trend set in afterwards and reached minimum values during the Roman period. Similar trends can be observed in the semi-quantitative Si-profile of the MM-core (**Figure 54**): Smaller fluctuations during the Late Iron Age are followed by a stable lower signal. A second increasing trend is parallel to MAR in LLG after 1200 cal CE and continues until the surface layers. A limiting factor in the following interpretations is the decreasing peat accumulation rate in LLG, which was steadily declining from 2800 cal BP onwards and hence affected the sample resolution.

A significant cooling in the Alps around the Early Iron Age was suggested by several studies (Haas et al., 1998; Ivy-Ochs et al., 2009; Joerin et al., 2006; Nicolussi, 2012; Nicolussi and Patzelt, 2000; Patzelt and Bortenschlager, 1973). But unlike earlier MAR signals in LLG, the input did not increase as strongly as earlier in response to the cooler climate. Only the small increase around 2600 cal BP would be in this range. Decreased anthropogenic erosion would be in good agreement with sinking charcoal values, rising tree pollen and decreased pastoral indicators in the first half of the Iron Age in the Las Gondas record of Dietre et al. (2014). Moreover, a decreased human activity in the Silvretta region during the Iron Age compared to the Bronze Age is suggested by Walser (2012). In contrast, the continuous use of an Iron Age pastoralist hut

was dated to the first half of the Iron Age (Carrer et al., 2016; Reitmaier et al., 2018). The slight increase of MAR, starting after 2500 cal BP and peaking at 2300 cal BP, is in line with palynological indicators for an intensified local land use around 2300 and 2000 cal BP (Bauerochse and Katenhusen, 1997). Furthermore, clearances in the Oetz Valley were suggested by Festi et al. (2014) between 2500 and 2100 cal BP. Archaeological sites are evidencing the existence of permanent pastoralist hut and pen structures not far below LLG at 2283 m a.s.l., radiocarbon dated to 2760-2460 cal BP and to 2620-2340 cal BP (Reitmaier, 2012; Reitmaier et al., 2013). This indicates a relation between human presence i.e. human land use and the observed initial erosion in LLG. However, the MAR signal is less strong when compared to the distinct peaks observed until the Bronze Age. This could possibly be explained by the already anthropogenically shaped landscape (absence or low cover of trees) and stabilisation of an extensive grassland or pasture system. Furthermore, the Iron Age hut, as the epicentre of impact, was not as elevated as the analysed mires, making its potential impact less severe. At this point, it has to be mentioned that the calibration of radiocarbon dates around the Mid Iron Age (2450 BP) is subject to high uncertainties due to the ^{14}C "Hallstatt plateau" (e.g. van der Plicht, 2005), which would affect both the age model in LLG (cf. **Table 14**) and most of the radiocarbon dates for the Iron Age hut (Reitmaier et al., 2018). This issue can explain inconsistencies in the comparison of the different studies and their findings.

The MAR decline by the end of the Iron Age corresponded with a generally lower land use in the upper valleys of the Silvretta Mountains during Roman times (Reitmaier, 2012; Walser, 2012). A decreased human impact at higher elevations elsewhere in the Central Alps was also suggested by Roepke and Krause (2013) and Walde (2006). These observations between 2500 BP and the end of the Roman period are in accordance with observations made in the Kleinwalser Valley and Piller Mire, although it is more pronounced in LLG. This is possibly due to its much higher elevation. In contrast, Dietre et al. (2014) found local palynological evidence for a continued pastoral activity around Las Gondas, whereas cultural indicators declined during the early Roman period. Towards the end of it, the same study, however, recorded increased openness and a return of cultural pollen (e.g. cereals).

No considerable EFs were documented until the Late Iron Age. However, increasing trends of Pb EF, Zn EF and Cu EF in LLG started after 2250 cal BP. For Sb, the EF started rising about 300 years later. While Pb EF reached a maximum of 9 around 2000 cal BP, a decline followed towards the Middle Ages. In contrast, Zn, Cu and Sb increased steadily. In MM, the Pb/Si ratio increased around 2250 cal BP as well, peaking around 1800 cal BP and declining thereafter. In contrast, the mineral sediment matrix in BWM impeded interpretation of metal enrichment.

In particular, the Pb EFs and Pb/Si in LLG and MM respectively, are correlating with the well-known and widely recorded peak of Roman mining activities (De Vleeschouwer et al., 2010b; Klaminder et al., 2003; Mighall et al., 2002; Shotyk et al., 2002). Both the increase and the decline are almost perfectly tracking the rise and fall of the Roman Empire. The generally rather low Pb EF, compared to HFL and Pi17, can be explained by the high input (content) of mineral matter, which diluted atmospheric input. Furthermore, potential spots of local mining and metallurgy in the Silvretta and adjacent regions where ores exist (Grutsch and Martinek, 2012; Hofmann and Wolkersdorfer, 2013; Tropper et al., 2011), were most probably too far away from the upper Fimba Valley to emit significant amounts of metals to get deposited in the Fimba Valley. Only the pan-European exploitation by the Romans released enough Pb into the atmosphere to reach this elevation and to be detectable in peatlands all over Europe.

Deciphering between climate and human impact as the trigger behind the relatively low erosion signals in the Fimba Valley during the Iron Age is challenging. Despite archaeological evidence for human presence, the period from 2800 cal BP to 450 cal CE shows an array of palynological and climatological evidence, pointing out to a climatic trigger behind slightly elevated MAR in the Early Iron Age, whereas local human activities can be suggested as the cause of a MAR increase during the Middle to Late Iron Age. Thereafter a reduced MAR coincides with decreased human impact at high elevations during Roman times. Aside from that, Roman mining and metallurgy are clearly visible by a distinctly increased Pb EF fingerprint.

6.3.4 450 cal CE until Modern Times

A low MAR around 1 $g*m^{-2}*a^{-1}$ was maintained until around 1000 cal CE in LLG. It then increased strongly and reached almost 40 $g*m^{-2}*a^{-1}$ around 1700 cal CE (**Figure 53**). In MM, the Si-profile started to increase after 700 cal CE (**Figure 54**). A second increase began parallel to LLG after 1200 cal CE and continued until the surface.

With the beginning of the Middle Ages, Bauerochse and Katenhusen (1997) saw signs of eutrophication in Las Gondas Mire and suggested livestock trampling damage on the mire's surface. Furthermore, their study documented intensification of land use around 1000 cal CE and again later at 1500 cal CE. Increasing cultural, pastoral and charcoal values were documented by Dietre et al. (2014) since the High Middle Ages and until recent times as well. A pen structure and a fireplace just a few hundred metres from Las Gondas were radiocarbon dated to 420-550 cal CE and to 940-1040 cal CE respectively (Reitmaier, 2012), which is evidence for human presence at this elevation and in line with the interpretations of Bauerochse and Katenhusen (1997). Despite these findings, increased erosion is not indicated in LLG earlier than

1000 cal CE, whereas the Si-content in MM started to rise around 750 cal CE. This could mean that the impact was rather low before the High Middle Ages.

The town of Ischgl at the mouth of the Fimba Valley exists at least since 1104 CE (Bauerochse and Katenhusen, 1997) and management of the Fimba Alp is documented for the first time at 1163 CE (Town of Ischgl, 2019). The whole Paznaun Valley experienced the immigration of Walser people around the 14th to 15th century CE (Krefeld and Klausmann, 1986; Rougier and Sanguin, 1981), which is almost parallel to the timing of documented Walser settlers in the Kleinwalser Valley. Their presence could have led to an increased demand for timber and pasture, as Bauerochse and Katenhusen (1997) argue. During the 15th to 17th century CE, Ischgl and the Fimba Valley (i.e. Fimbapass) became an important trading post and route to connect with the Upper Inn and Lower Engadin Valley, where the extent of deforestation culminated around the same time (Gobet et al., 2003). Back then, the Fimbapass was permanently crossed with pack horses and carts (Town of Ischgl, 2019). On the top of it, historical data proves that a strong deforestation took place everywhere in the Paznaun Valley, including the Fimba Valley, from the 16th century to 1800 cal CE to sustain mining activities in the region (Bauerochse and Katenhusen, 1997; Fromme, 1957). When looking at the accelerating upward trend of MAR in LLG and Si-signal in MM, these insights from historical and palynological data suggest a strong impact on the vulnerable soils of the upper Fimba Valley, which are most likely caused by the combination of the Walser arrival, deforestation, emerging trade and pastoralism.

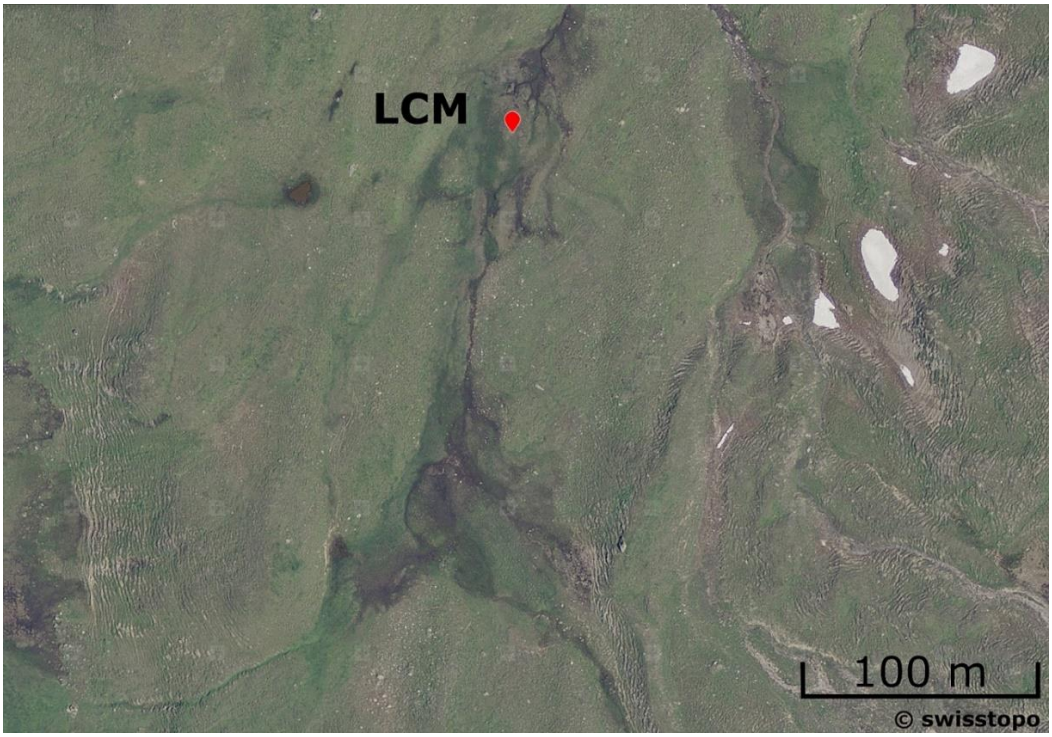

Figure 55: Erosional (stair-like) features from cattle grazing paths on the slopes of the upper Fimba Valley (>2400 m a.s.l.) around LCM (left, right and lower centre). (swisstopo, 2018b)

The results of Bauerochse and Katenhusen (1997) moreover indicated a slow cease of peat accumulation in their Las Gondas record since the Late Middle Ages, which is in line with the extremely low peat accumulation rates in the LLG profile. Especially in upland and riparian areas, cattle, and probably carts and horses too, are a strong eroding and compacting force (Trimble and Mendel, 1995). On mire surfaces, cattle trampling leads to disturbances, which can triple the decomposition in the affected upper layers (Urbina and Benavides, 2015), due to higher nutrient input and aeration. At the same time, it would also disturb the current vegetation and lead to surface erosion. A higher decomposition is also indicated by the increased S-content in the upper peat layers (not counting the mineral top layer). Grazing paths of cattle in the upper valley were already described by Pott et al. (1995). As a result of the suggested cattle impact, mineral sediment input, compaction and decomposition would have increased synchronously, whereas the peat accumulation rate decreased. Depending on the intensity of trampling, it could have even stopped or led to a surface erosion. This effect is suggested to be partly responsible for the developments in LLG from the Middle Ages to Modern Times. Nowadays, cattle is still omnipresent (illustrated in **Figure 55**), while the impact of carts and horses was replaced by touristic activities since the late 19th century (hiking, skiing and mountain biking).

In addition to an obviously strong human impact, a cooling climate could have played a role for the MAR as well. As indicated by much larger glaciers in the late 19th century around the Fluchthorn (Jacot-Guillarmod et al., 1896), the Little Ice Age (Matthews and Briffa, 2005) stopped travelling and freight hauling across the high passes (e.g. Jam Valley) already around the 18th century (Town of Ischgl, 2019) and led to a decline of local economy. This coincides with the simultaneously interrupted MAR increase in LLG and positive Si-content trend in MM. However, in contrast to other regions in the Central Alps (e.g. around the Piller Mire), cattle numbers increased, nonetheless, by 10 %, which happened uniquely in the Fimba Valley after the 19th century (Fromme, 1957). Beside pastoralism and trade, a third factor controlling the MAR could have been the colder climate at that time. The proxies investigated in this study do, however, not allow to disentangle climate from human impact, leaving the possibility of combined effects.

In terms of metal EFs in LLG, the Pb EF had been still higher than before the Roman peak, but a decreasing trend - to values that are equal to the sediment layer around 6300 cal BP - set in after around 1250 cal CE. Negative trends are also observed for Zn EF, Cu EF and Sb EF in **Figure 53**. MM on the other hand shows an increase of Pb/Si after 950 cal CE (**Figure 54**). A peak at approximately 1350 cal CE was followed by a decline until 1700 cal CE and another, smaller rise thereafter.

The decrease of Pb EF in LLG between Middle Ages and the 20th century is contrary to what would be expected for any mire in Europe. However, the time between 1800 cal CE and present is hardly covered by LLG and MM and the modern leaded gasoline peak, which was clearly visible in HFL, LAD and Pi17, is possibly not part of the core at all. Moreover, sediment input was strongly rising in LLG, parallel to increasing mining and metallurgy around the Silvretta (Hanneberg et al., 2009b; Hofmann and Wolkersdorfer, 2013; Neuhauser, 2015; Wolkersdorfer, 1991). The mineral materials consequently diluted any atmospheric input signal enriched in metals. Certain mechanisms could have played a role in the unexpected decrease of metal EFs. Indeed, Pb is physiochemically bound to organic matter (Vile et al., 1999) and could be released due to the suggested almost complete decomposition or partial erosion of surface peat layers (Rothwell et al., 2011, 2007). Without a considerable organic content at the surface, atmospherically deposited metals would not even have been retained in the first place. These effects should, however, be weaker in MM, as suggested by the relatively lower mineral signal and the higher peat accumulation rate in the upper layers and finally by the increase in Pb/Ti in the XRF-scanning data. Historical documentation also mentions the re-opening of silver mines close to Ischgl in the 16th century (Fromme, 1957). Iron and Cu deposits around Ischgl were also documented by Vavtar (1988). The observed Pb/Si ratio rise in MM could therefore be connected to these mining activities in the Paznaun Valley, although silver mining operations also intensified in the region east of the Fimba Valley (e.g. Imst, Platzer Valley; see **Figure 23**).

Altogether, the cores of the upper Fimba Valley are showing a strongly increasing anthropogenic impact from pastoralism, deforestation but also directly from freight hauling on the landscape of the upper Fimba Valley after around 1200 cal CE. However, not all of the recorded erosion signal can be completely ascribed to a human influence, as also the Little Ice Age could have interacted with land use and natural erosion in different ways.

6.4 Conclusions on the Fimba Valley

The longest record (LLG) of a total of four heterogeneous small-scale mires of the upper Fimba Valley at an elevation around 2400 m a.s.l. covers a radiocarbon dated time frame of over 10,000 years, in which longer episodes of peat growth appeared only after around 7500 cal BP. Geochemical data, from ICP-MS and pXRF for the LLG-core and XRF-core-scanning for MM is available for approximately the last 6500 years. Both the core descriptions as well as part of the geochemical data are coinciding with trends and events, indicated either from independent regional or local studies on climate, palynology, archaeology or historical information.

A comparison of this study's data to existing studies on the upper Fimba Valley shows that the onset of peat accumulation did not start synchronously and was probably controlled by rather local small-scale conditions and processes. The timing of certain layers, e.g. increased sediment content or coarse mineral grains in LLG, suggests a linkage to regionally – or globally – proven episodes of a colder climate (regional glacier activity). After such a layer around 9200 cal BP, the following 1000 years are indicating more stable and probably warmer conditions, with a tree line that was at or even above the elevation of 2350 m a.s.l. Subsequently, a prominent layer of coarse sediment was dated to around 8200 cal BP. Although its impact in the Alps is still under debate, the 8.2 ka cold event and its concurrence with the observed layer clearly point at a trans-regional climate response. From a local perspective, glacier activity on the glacier field below the Fluchthorn, west of the mire, is suggested to have been responsible for higher sediment input into LLG by the nearest meltwater channel that is coming from this glacier. Another cold event probably affected the upper Fimba Valley again, between c. 6400 and 6200 cal BP and an increase of MAR around 5400 and 5000 cal BP points at two more. Another signal at 4500 cal BP could have had, at least partly, an anthropogenic component. However, regional glacier advances at exactly this age are not allowing an unambiguous interpretation. In accordance with independent studies of the area, the same applies for the first of three temporary MAR increases during the Bronze Age. While the first one around 3600 cal BP points to a climate deterioration as a trigger, the following two at 3400 and 3200 cal BP are most likely caused by human land use, as they are coinciding with increased cultural and pastoral indicators. Despite the archaeologically proven presence of pastoralists around the mires, only subtle erosion signals appeared during the Iron Age, probably due to the stabilisation of extensive pasture systems after strong deforestation in the Mid to Late Bronze Age and a shift of the vegetation system. From Roman Times until High Middle Ages, neither LLG nor MM recorded increased erosion.

With the Late Middle Ages, a declining peat accumulation plus an increased MAR were probably caused by disturbances of both climate and a variety of human activities. While the Little Ice Age initiated glacier advances in the Central Alps, the Fimba Valley experienced heavy anthropogenic impact, consisting of heavy deforestation, livestock grazing and trade with the south. Indications for mining or metallurgy were observed in Roman Times and possibly after 1000 cal CE again, with a rather local to regional origin from operations around Ischgl and in the Paznaun Valley. However, a diluting effect of high sediment input combined with strong decomposition and metal release in LLG, probably masked and hampered the detection of metal EF signals.

The results from alpine small-scale mires of the upper Fimba Valley are demonstrating their great potential. However, several factors are a challenge for data interpretation. The cores from

different mires show very heterogeneous patterns in their sedimentation regimes and low peat accumulation rates are hampering high resolution sampling. Furthermore, the fen character of these mires and the resulting higher decomposition complicates the selection of material for radiocarbon dating. At the same time, more subtle geochemical information, like atmospheric metal input, could be diluted or completely overprinted by strong local sediment input. Hence, it aggravates the synchronisation to other cores or studies. Here, more than anywhere else, it is therefore important to investigate more than one core and to focus on robust age-depth models. In the field, it is important to understand basic geomorphological and hydrological factors before selecting a coring spot. Moreover, information from other disciplines is absolutely necessary to draw conclusions. Nevertheless, the mires of the Fimba Valley were able to indicate climatic impact on the alpine landscape, before human activities became strong enough to be a shaping factor.

7 Synthesis

7.1 Regression analysis comprising all samples

Three separate regression analyses were carried out for one mire in each of the three investigated valleys. In this chapter, samples from all three studied areas (cores HFL, Pi17 and LLG) that were measured by ICP-MS and pXRF (n=140), were combined within a single regression analysis. It allowed a more general assessment of the potential of pXRF in analysing peat samples. Furthermore, careful recommendations can be given for certain elements and their respective conversion/transfer functions to get quantitative values and, as far as possible, overcome some of the limitations of this technique. In the same fashion as in the site-specific regression analyses, **Figure 56** shows selected elements with the whole dataset of measurements, the coefficients of determination as well as the transfer functions.

1. Ti: Ti is best depicted by the polynomial function (2nd degree) for peat samples with a high mineral content or where higher mineral content can be expected (e.g. at the bottom, sediment, tephra). In addition to the samples that were classified as mineral samples before, three more samples of LLG were treated as mineral. These were in the transition zone of already high inorganic matter content with a Ti-concentration around 1000 mg*kg*$^{-1}$ (or around 2000 to 3000 pXRF raw) and where the regression curve started to get non-linear (cf. regression analysis LLG, chapter **6.2.3.1**). At least in this dataset, and to give another guide value, this threshold corresponds to a density of roughly 0.2 g*cm^{-3}, although other factors that are partly linked to the density as well should play a more important role (e.g. grain size, ash). Reaching above this range would be the case in mires at high elevations (mountains) or close to rivers. However, for most of the peat samples i.e. where Ti-concentrations are below 1000 mg*kg*$^{-1}$ (approx. 2000 raw), a linear function is appropriate. This would be the case in ombrotrophic and most other peat types.

2. Pb: Lead could be calibrated with a linear regression for samples with a Pb-concentration between approx. 2 mg*kg*$^{-1}$ up to at least 110 mg*kg*$^{-1}$ (or 175 pXRF raw). This behaviour appears to be almost independent of the type of site, peat, vegetation or geology. Only a negligible matrix effect, leading to a slightly underestimated concentration in mineral samples, can be observed. An anthropogenic Pb-contamination is, however, suggested to be linearly transformable and covered by the regression in **Figure 56**, if the samples are classified as peat.

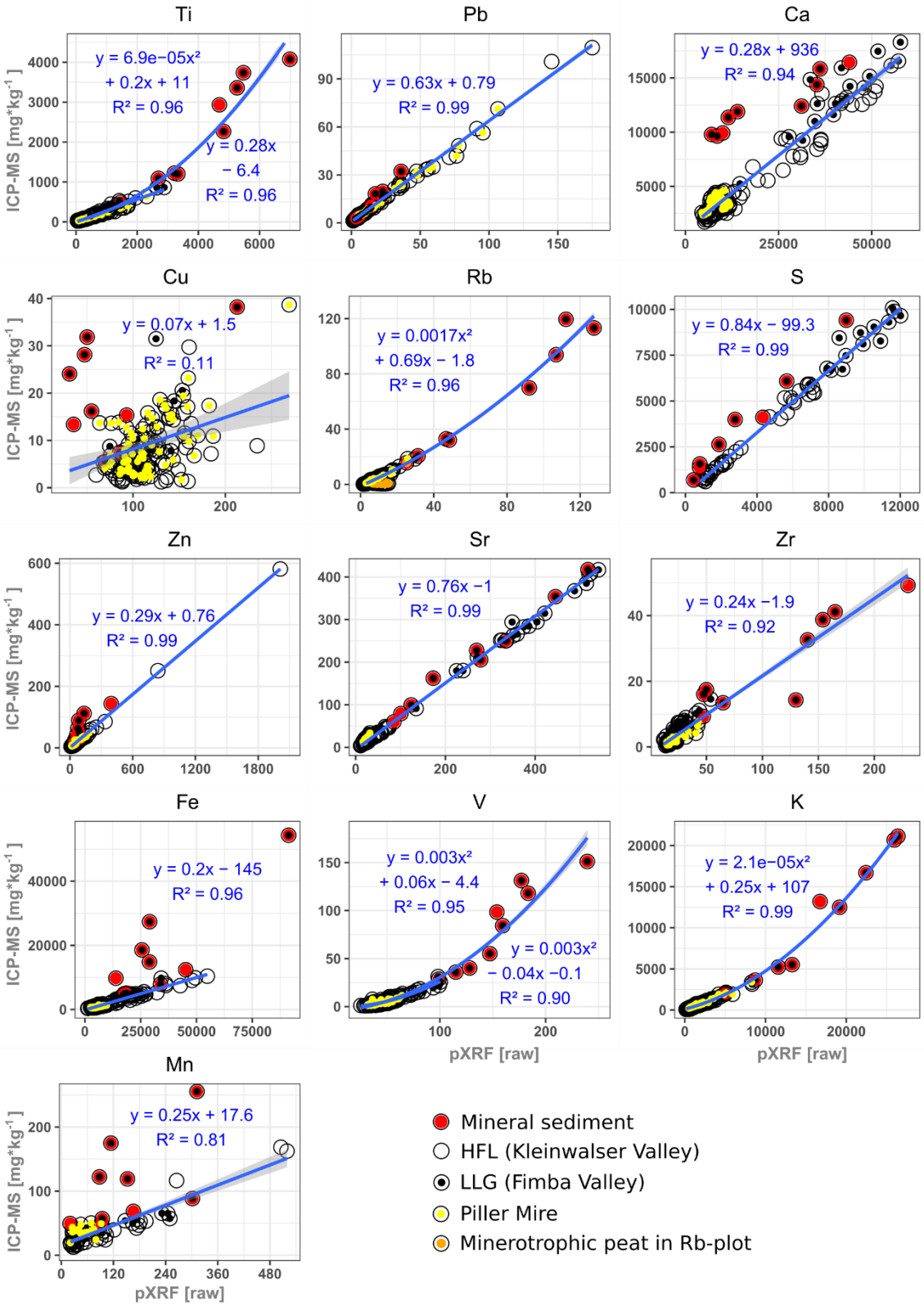

Figure 56: Regression analysis from three mire sites together (empty circles=HFL, orange dots=HFL minerotrophic, yellow dots=Pi17, black dots=LLG, red circles=mineral samples). Regression performed without mineral samples: (Ti), Ca, Cu, Zn, Fe, (V), Mn.

3. Ca: Calcium is scattered broadly around a linear regression, which is not clearly related to matrix differences. Also, site-specific effects are obvious when intercomparing LLG, Pi17 and HFL. Mineral and highly minerotrophic peat samples would be largely underestimated by the linear regression function for peat samples (**Figure 56**). The almost systematic offset of the mineral samples rather indicates that a separate function would be needed.

4. Rb: The consolidated Rb-measurements are represented by a polynomial function (2nd order), except for the minerotrophic part of HFL (**Figure 56**, orange). Despite of the fen/minerotrophic character of LLG with even higher concentrations than in HFL, the LLG samples do not show a similar effect. A difference between the two mires is that the mineral matter in LLG was probably deposited directly on its surface and is still existent in the form of mineral grains. In contrast, the HFL samples have a higher inorganic content due to enriched groundwater or remobilisation from the mineral bottom layers.

5. S: The linear regression's fit for S is excellent (R^2=0.99), even when including samples with high concentrations (e.g. LLG). Mineral samples were measured almost true to their real concentrations by pXRF, while the values for peat samples are only slightly too high. In other words, mineral samples appear to have an almost parallel, i.e. offset, regression curve to the peat samples. As discussed earlier, sulfur is a possible indicator for higher decomposition and a marker for the transition from minerotrophic to ombrotrophic conditions. Therefore, the successful measurement of S helps in the interpretation of other elements, like Cu or Zn.

6. Cu: Copper is not reliably quantified by pXRF in any of the analysed mires.

7. Zn: The pXRF device strongly overestimates the concentrations of Zn. A changing matrix effect between peat and mineral rich samples is obvious. But apart from that, even high Zn-values (e.g. anthropogenically enriched/contaminated) are measurable in peat and linearly transformable with the function given in **Figure 56**.

8. Sr: The regression analysis of Sr yields a similar transfer function for HFL and LLG. It is independent of the matrix and covers the sample range from mineral to ombrotrophic *Sphagnum* peat. It is therefore suggesting a general applicability of the given function. However, the ombrotrophic Pi17 core shows a slightly steeper slope (a) in **Figure 29** (yellow). Although a site-specific effect could be guessed, a look at the quality control of the ICP-MS results reveals that lower concentrations of Sr, Ca and Mn in CRMs were systematically measured higher than the certified concentrations during the analysing session of the Piller Mire samples (**Suppl. Table 1**, text grey highlighted). This could possibly be solved by recalibrating the ICP-MS results and re-doing the regression analysis. Therefore, the linear transfer function for Sr is suggested to be

universally valid for all peat samples in this study. At the same time, this issue does not compromise any of the interpretations concerning the trophic status of the affected Piller Mire, as the concentrations would be only slightly higher, and the trends would remain the same (chapter **5.2.3.2**). Based on these observations, Sr should be preferably selected against Ca when it comes to the detection of the point where minerotrophic conditions (i.e. groundwater influence) cease.

9. Zr: The determination coefficient for Zr (R^2=0.92) is promising. However, the scatter is relatively high, especially when operating with smaller concentrations, which could be due to the less pronounced peak shape of this element in the XRF spectrum. Without further interpretation, a site-specific effect seems to play a role in the Pi17-samples as well.

10. Fe: Iron is unreservedly measured in peat samples and values can be calibrated with the combined linear regression function. However, mineral samples need to be excluded, as they would be, similarly to Ca, strongly underestimated. Unlike for Ti or Rb, this matrix effect cannot be overcome via a polynomial regression function because the regression analysis indicated a non-continuous function (similar to Ca).

11. V: For V, the scatter is relatively high at very low concentrations but the combination into one single regression analysis indicates that a polynomial function (2nd order) can be used to quantify pXRF-results for this element. As for Ti, a higher number of samples in the transitional range between peat and mineral sediment would help to refine the equation of transformation. V could be an alternative, in case that Ti cannot be measured. There are indications for its immobility in peat (Cloy et al., 2011; Krachler et al., 2003; Shotyk, 1988). Furthermore, the profiles of V in this study are quite similar to the behaviour of Ti, which is at least suggesting a conservative behaviour. Its use is, however, limited by several factors: the relatively high standard deviation during pXRF-scanning, a larger scatter, a concentration close to the LOD, and a possible enrichment from modern oil combustion (Pacyna and Pacyna, 2001).

12. K: Like Ti, Rb and V, the measurements of K can be described by a polynomial regression function of 2nd order. The cross-plot in **Figure 56** furthermore suggests that a linear transformation function would work for samples with K-concentrations up to 5000 mg*kg^{-1} (~12500 pXRF raw); without any noteworthy site specific effects or limitations.

13. Mn: As mentioned above, an overestimation of Mn in the Pi17 samples could be due to a different calibration of the ICP-MS results. Aside from the calibration, concentrations that are close to a detection limit between 20 and 35 mg*kg^{-1} are resulting in a high scatter in this range and, moreover, all mineral samples are off the regression curve.

One of the general conclusions is, that the internal calibration of the pXRF is giving almost quantitative values for mineral samples like soil, moraine or fluvial/lacustrine sediment. In contrast, peat samples are yielding moderately to highly overestimated values. But as long as a series of samples consists of peat samples only, element specific linear regression functions can be applied for Ti, K, V, Pb, Zn, S, Sr, Fe, and, with some restrictions, for Rb, Zr, Ca and Mn. The behaviour of some elements was mostly dependant on the sample matrix (organic/inorganic) but site-specific effects could be another factor (e.g. geological background, vegetation). The most problematic issue occurs in peat samples with a strongly elevated mineral content. This results in a polynomial regression (2^{nd} degree) for some elements (e.g. Ti, K, Rb and V). Consequently, mires with recurring direct sediment influx, but also rich minerotrophic bottom peat layers that are enriched in mobile elements like Ca, can be affected. In turn, this result implies that these obvious limitations can be ignored in samples from ombrotrophic mires but also in most peat that is not directly bordering mineral layers. Either the dry bulk density or the Ti-concentration could help to decide, if the linear regression is still applicable: not only for Ti itself but also for K, Rb and V.

Although this case study cannot go into the details of the observed behaviour of the pXRF instrument, it demonstrates its great potential to analyse peat samples. While Shuttleworth et al. (2014) focussed on heavily contaminated peatlands, it is demonstrated here that this method works on peat samples with a very low Pb-concentration as well. Portable XRF is relatively time and cost efficient when compared to methods that require wet chemistry. Hence, it allows a high sampling resolution along a peat core. It furthermore circumvents the problems of heterogeneity and water content that are unavoidable with XRF core scanning. However, strong variations between mineral and organic content can bias the results if the regression analysis and transfer function is not adjusted accordingly. The point where the linear regression fails or changes to polynomial probably needs to be defined for every element individually. Finding an approximate criterion to define this range of transition, based on a larger dataset, would, however, be important for future studies to have calibrations available that are universally valid for geochemical peat analysis by pXRF.

7.2 Integrated chronological discussion

The integration of proxies and interpretation from various individual Alpine valleys can be achieved by taking into account several critical considerations. Signals of local climate can manifest in many ways depending on a large variety of factors like exposure, slope, elevation, geology, topography, etc. The same is true for human and environmental signals, which are both

influenced by climate themselves, but also depend on the landscape they live in. Mountain environments can be specifically attractive for humans to settle or to use the resources, like in the study areas presented in this work, for activities like agro-pastoralism, forestry and mining.

After having identified and interpreted signals of metallurgy and increased mineral input or erosion (and vegetation changes in the Kleinwalser Valley) from a rather local perspective, this chapter is going to consolidate the most important developments and events at all sites. Since the impact of both human land use and climate can influence the amount of erosion, the evaluation of this proxy's signal from a larger, more regional perspective can substantiate interpretations. Moreover, mining or metallurgical activities – as reflected in the EFs of e.g. Pb – can vary from mire to mire and from valley to valley. In general, a broader view is also helpful to assess the spatial significance and variability of all recorded signals. **Figure 57** summarises and illustrates the most important trends and events in all study areas and their interrelation with Central Alpine glacier advances and cultural information.

7.2.1 Early to Mid-Holocene: climate versus human impact

The geochemical data from peat records of the Fimba and Kleinwalser Valley stretch back to several hundreds of years before 6000 cal BP. However, the Fimba Valley's sediment record of LLG covers over 10,000 years. Even if the Early Holocene is only recorded in one of the sites (LLG) without having a corresponding sequence from the two other valleys, it allows interpretations that could be equally relevant for the Mid- and Late Holocene. As shown in **Figure 57** and discussed in the Fimba Valley chapter (chapter **6.3**), cold events, illustrated by the progressions of the glacier Gepatschferner glacier (Nicolussi and Patzelt, 2000) in the Tyrolean Central Alps (**Figure 1**), are matching almost perfectly to episodes of strongly increased MAR in the Fimba Valley (LLG). Following an approach that is basically similar to the one used by Shakesby et al. (2007) or Matthews et al. (2005), the most compelling evidence for glacier activity is a coarse-grained, but well dated layer within the timing of the 8.2 ka event. Only 2000 years later (within the uncertainty range of the age-depth model), the profiles of almost all investigated cores show a distinct peak of mineral matter input around the age of 6300 cal BP in the Fimba Valley, whereas the records in the Kleinwalser Valley (HFL, LAD) were just starting peat accumulation a few centuries later. Around this time window, a colder climate was reported from different proxies in the Central Alps (Joerin et al., 2008, 2006; Nicolussi and Patzelt, 2000; Wurth et al., 2004). It can therefore be concluded that strong and widespread natural climate deteriorations in the form of colder and wetter conditions occurred in the northern Central Alps between approximately 6400 to 6100 cal BP (see this study's age-depth models in chapters **4.2.2**, **5.2.2**

and **6.2.2**). This was reflected by increased erosion (sediment input), equally effective for (sub)alpine and montane environments at two spatially separated locations in the Central Alps. After this period, peat formation was (re)initiated synchronously in two different mires of the Kleinwalser and Fimba Valley. A link between cold phases and increased sediment input is, however, restricted to the glaciofluvial stream-bank mire LLG in the Fimba Valley. It is hence suggested that this coring site was sensitive to glacier activity upslope of the mire (see chapter **6.3**), similar to the findings in periglacial mires in Norway (Matthews et al., 2005; Shakesby et al., 2007). This interpretation would imply that specific high-elevation mires could be more prone to record climate fluctuations in general, because of a less stable vegetation and particularly by their vicinity to erosive forces of glaciers and meltwater runoff loaded with sediment.

As a result of generally smaller populations, potential impact and signals were probably faint and thus less easily detected in these mires. The first unmistakeable signal of human impact in the region shows up in the Kleinwalser Valley by a combined signal of pollen, charred wood and increased MAR, from 5700 to 5500 cal BP (**Figure 21**). These first landscape changes are followed by first indications for metallurgy (increased Pb EF) around 5450 cal BP. It is not surprising that these signals were recorded at a lower elevation and that they were close to the foreland of the Alps. It implies that a first occupation with stronger impact on the region had its origin in the northern Alpine Foreland. A temporarily warmer climate at that time, indicated by higher tree lines and receding glaciers (Hormes et al., 2001; Nicolussi et al., 2005; Schlüchter and Jörin, 2004), suggests that climate promoted this phase of human impact.

Evidence from the Piller Mire (chapter **5.3**) suggests subtle human induced erosion just after a possible cold phase recorded in the Fimba Valley at 4500 cal BP. Before and after this age, elevated metal EFs in the Piller Mire suggest metallurgy and maybe mining in the region. Around 4350 cal BP, the first simultaneous increase of Pb EF was recorded in north-western Tyrol (Piller) and in the Kleinwalser Valley, which indicates cultural activity spanning across valleys in the Central Alps. For the timing of another MAR peak after 4200 cal BP in the Piller Mire, no samples are available in the Fimba Valley records, but the concurrence with palynological anthropogenic indicators in the mire (Hubmann, 1994) point to human induced local deforestation and land use. In contrast, MAR in HFL remains on a low level, even though an increased Pb EF hints at recurring metallurgical activities in the region.

7.2.2 4200 to 2000 cal BP: rise of human land use /land-management

For several centuries after the onset of the Bronze Age, neither of the proxies shows any disturbances until c. 3650 cal BP, when for a short period glaciers advanced in the Central Alps (Nicolussi and Patzelt, 2000) and sediment input increased in the Fimba Valley. From this point, a strong pulse of human induced erosion is suggested for the Middle to Late Bronze Age. This happened all over the northern Central Alps with a simultaneous MAR peak at all investigated mire sites (LLG, MM, Pi17, HFL, LAD). The LLG profile suggests that this climax of human activities in the Fimba Valley around 3400 to 3200 cal BP is framed by colder phases (e.g. glacier progression, see **Figure 57**). However, the mineral input was generally higher during the Bronze Age in the upper Fimba Valley, as shown in the MM and LLG profiles. The same is true for the LAD profile in the Kleinwalser Valley, which can be explained by a higher sensitivity to landscape disturbances because of its position at the slope. In the Kleinwalser Valley, charred wood debris (HHA), dated to around 3400 cal BP, and the pollen signal illustrate a transition towards a human shaped landscape that developed from a precedent phase of probably patchy forest clearances, which opened the landscape for pastoralists (**Figure 21**). Then, with time and continued human impact, open forest was replaced by meadows and cultural pollen evidence agricultural activities. Similarly elevated patterns of agro-pastoral pollen indicators with increased charcoal are also documented in other studies at many sites in the (northern) Centrals Alps (e.g. Dietre et al., 2017, 2014; Festi et al., 2014; Hubmann, 1994; Roepke et al., 2011; Wahlmüller, 2002; Walde, 2006; Walde and Oeggl, 2004) but also in the northern Alpine Foreland (Stojakowits, 2014). A generally higher sediment input into lakes of the north-western Alps was induced by a mix of higher human impact and increased precipitation after 3500 cal BP (Arnaud et al., 2016). In the Eastern Alps (Central Austria), the establishment of Alpine pasture is suggested for a warm period between 3500 and 3200 cal BP (Schmidt et al., 2002). During this period, Della Casa (2013) saw technological and cultural triggers behind an increased permanent human occupation of the Central Alps and also Oeggl (2015) observed high human impact that had been independent from climate factors. Well-investigated Bronze Age settlements, e.g. in the Montafon (Western Austria), furthermore prove the existence of permanent, non-seasonal, occupation in the Central Alps (Krause, 2007; Schmidl and Oeggl, 2005b). In the Kleinwalser Valley, Leitner (2003) presented direct evidence for the presence of hunters and pastoralists not far from the analysed mire sites. From that moment on, also the cultic site at the Piller Mire has been used (Tschurtschenthaler and Wein, 1998, 1996).

As Roepke et al. (2011) suggested, initial phases of deforestation and pasture establishment are accompanied by slope destabilisation and erosion before the landscape stabilises again in

another system (e.g. pasture, grass/shrubland). This can be adopted as the mechanism behind the course of, relatively short but strongly, elevated MAR signals in all the sites.

The increased mineral input (soil dust or washed in sediment) into all mires during the Middle to Late Bronze Age probably diluted possible signals of metallurgy and mining (mainly for copper), which had been practiced extensively in the Eastern Alps (Goldenberg, 2015; O'Brien, 2015; Stöllner, 2015a). Around 5500 cal BP (chapter **4.3.2**), pollen indicators and elevated MAR came first in the Kleinwalser Valley, and not much later, an increased Pb EF was observed. Around the Piller Mire, a similar succession could be suggested in the Middle to Late Bronze Age. When populations began occupying a certain valley or region, large scale forest clearings opened the landscape and made it accessible, pasturable and arable. If these initial clearings were generated by using fire, as suggested in the Kleinwalser Valley, an uncontrolled destruction and destabilisation of large areas was likely. Over time, depending on the cultural background of people and on their knowledge and technology, they optimised the use of their surroundings and developed more complex and diverse skills and activities (e.g. mining, metallurgy) besides animal husbandry, hunting and gathering. Clearly in the Piller Mire, and more subtly in the Kleinwalser Valley, elevated EFs of Pb, Sb and Cu around 3200 cal BP (following a peak in MAR) support such an idea of human occupation in a specific valley or region. The combination of the own results with other studies (cf. references above) suggests that climatic factors were not directly triggering the observed signals during this period. Instead, cultural and technological factors could have played a role as well. Instead, it could have been the most distinct anthropogenic landscape deterioration of the Central Alps in prehistoric times.

After that, activities continued at a reduced pace until the onset of the Iron Age (2800 cal BP), as suggested by continuously occurring pastoral and agricultural pollen in regional and local studies (Dietre et al., 2017, 2014, 2012; Walde and Oeggl, 2004, 2003). However, a less intensive land use and a re-stabilisation of soils and (forest) vegetation were probably responsible for a decreasing erosion signal in all records. Although a correlation between cooling climate and reduced human impact in the mountains is not easy to establish, a slow cooling trend accompanied this development of decreasing anthropogenic indicators (Ivy-Ochs et al., 2009). A similar interpretation was made by Roepke and Krause (2013) for an observed decline of human activity south of the Kleinwalser Valley. The culmination of this cold period was dated to around 2600 cal BP, accompanied by glacier advances (Nicolussi, 2012). This coincided with a still low MAR in the Kleinwalser Valley and around the Piller Mire, and a small MAR rise in in the upper Fimba Valley. During this period of the Iron and Bronze Age, human activities in the mountains were probably less intense. The strongly elevated Pb EF in HFL around 2750 cal BP is,

however, pointing to metallurgical activities that included Pb-rich ores, close to the site at the northern boundary of the Central Alps, but without any indication for the source of the signal.

Until around 2500 cal BP, no significant MAR changes were recorded. While this low level remained stable in the Kleinwalser Valley, the eastern sites (LLG and Pi17) show a distinct rise in mineral inputs between 2400 and 2300 cal BP. This suggests that this region experienced a period of stronger human impact, reaching as high as the alpine zone. Again, a rather widespread human impact is supported by other studies in the Alps (Festi et al., 2014; Koinig et al., 2003; Moe et al., 2007). Except for a minor MAR response, the Kleinwalser Valley was most likely not affected by strong land use. However, elevated EFs of Pb (and Cu, Sb) point to regional mining or metallurgy and widespread regional land use is proven in other valleys of the Central Alps (Roepke et al., 2011; Roepke and Krause, 2013; Walde and Oeggl, 2004, 2003).

7.2.3 Roman period

In contrast to what could be expected from the technological power of the Roman Empire, their arrival and establishment of the Raetia province did not bring any significant increase in MAR. As hypothesised in other studies (e.g. Walde, 2006; Walser and Lambers, 2012), the reasons were probably cultural, which modified land use practice and settlement preferences. Nevertheless, this phase of forest recovery and reduced land use at higher elevations came to an end in the 3rd century cal CE, as suggested by the MAR reconstructions in the Kleinwalser Valley and Piller Mire. While the signal in the latter was rather short lived (**Figure 57**), the 3rd century cal CE was the onset of a longer lasting increased signal of mineral input in the Kleinwalser Valley. This coincided with increasing instability of the Roman Empire, especially close to its borders (e.g. Kleinwalser Valley), which could be interpreted as the return of local populations from agriculture in the valleys back to pastoralism at higher elevations. This change towards more erosive land use seems to have happened along with the slow decline of Roman power. What all peat records share, is a significant increase in Pb EF (or Pb/Si) around or right after 2000 cal BP (**Figure 57**). This peak in Pb is well known from other study sites (Allan et al., 2018; Marx et al., 2016; Shotyk, 2002) and hence serves as an independent time marker, which validates the age-depth models. Even though no direct archaeological or historical evidence is available to uncover a contribution of local mining activities (Bode et al., 2015), there are evidence and indicators for a Roman exploitation of existing ore resources in the Alps (Dolenz, 2015; Gleirscher, 2015b; Winckler, 2012).

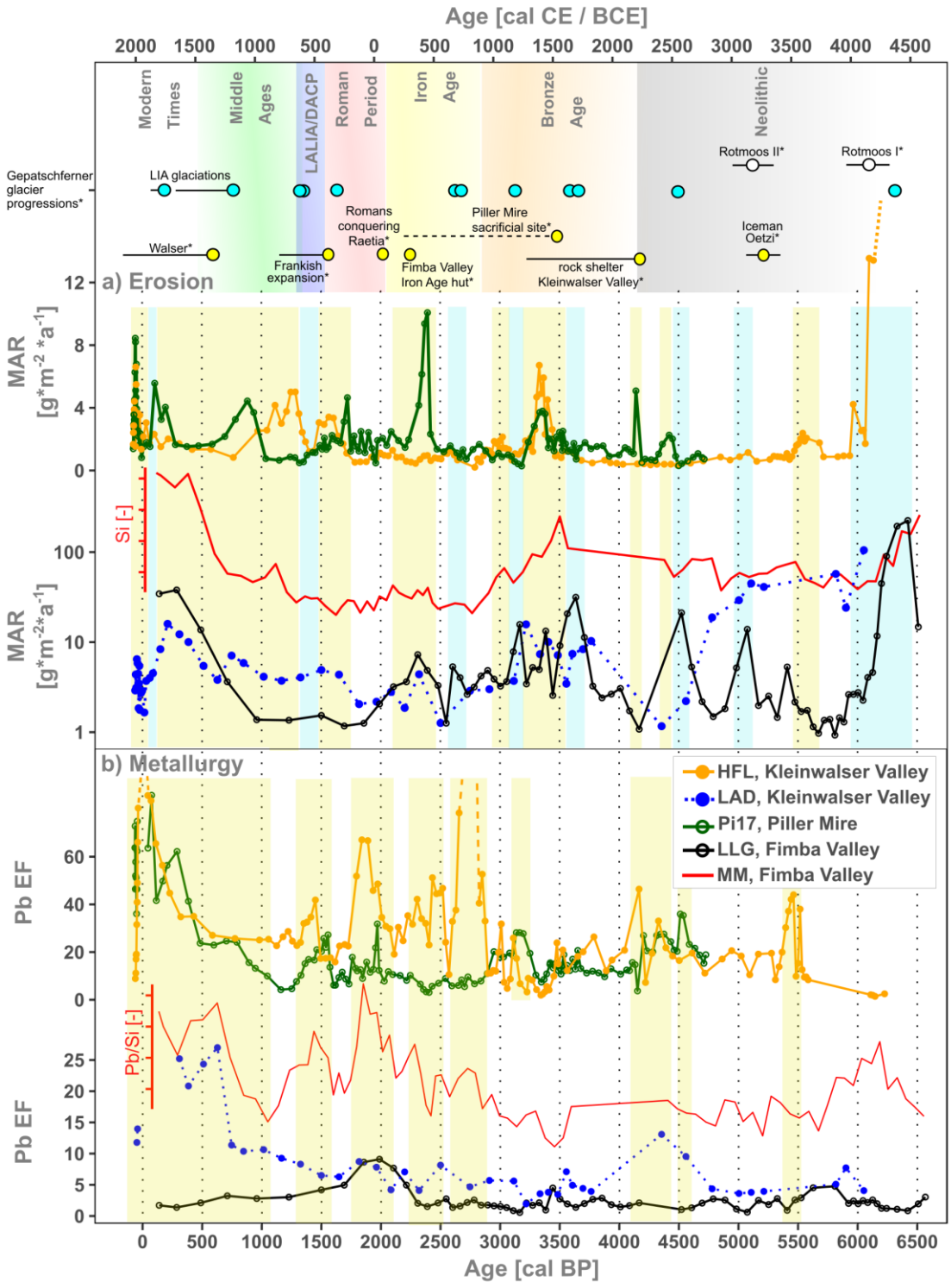

*Figure 57: Summarising plot for investigated sites HFL, LAD, Pi17, LLG, MM. Mineral input proxy MAR (logarithmic scale for LLG and LAD) and XRF Si-signal (a) and mining/metallurgy/contamination proxy Pb EF and XRF Pb/Si (b). Pb EF profiles are cut at EFs of 85 and 30. Suggested cold climate periods in light blue. Suggested anthropogenic signals in light yellow. * References in text.*

7.2.4 Middle Ages and Modern Times

After around 500 cal CE, a significant climatic shift towards cold and wet conditions is suggested to have either pushed human activities down to the lowlands or simply reduced anthropogenic pressure by a generally decimated population (McEvedy and Jones, 1978), as discussed in chapters **4.3.4** and **5.3.4**. This can be inferred from a decrease of MAR in the ombrotrophic cores of HFL and Pi17, where the timing coincides with LALIA and DACP (Büntgen et al., 2016; Helama et al., 2017). Furthermore, advancing glaciers were reported for this period across the Alps (Holzhauser et al., 2005; Nicolussi and Patzelt, 2000) concurrently to the significant population decrease (McEvedy and Jones, 1978). Lower land use is also supported by increasing forest cover and decreased agro-pastoral pollen indicators in the Kleinwalser Valley (HFL) and around the Piller Mire (Hubmann, 1994; Walde, 2006). A strong recovery of erosive land use, probably in the form of deforestation driven by growing monasteries (e.g. Friedmann and Stojakowits, 2017), occurred, however, in the Kleinwalser Valley (chapter **4.3.5**), whereas the Piller Mire and the Fimba Valley stayed rather undisturbed for several centuries.

The short, almost synchronous and similarly shaped increase of Pb EF around 500 cal CE in the Kleinwalser Valley and in Piller (Tyrol) as well as the Pb/Si peak in the Silvretta record (MM) can only partly be explained by a decreased mineral content. This Early Medieval Pb-peak is, so far, the only indicator for possible mining activity in the region during the time of the expansion of the Frankish Empire (Kaiser, 2010). The signal indicates mining or metallurgical activities on a regional scale, because Bränvall et al. (2001) documented a generally declining signal of anthropogenic lead deposition in Northern Europe between 400 and 900 cal CE.

While the Kleinwalser Valley experienced landscape changes and increasing mineral input, the more elevated and less accessible sites of the Fimba Valley and Piller Saddle lagged behind in this development after the Roman period. In the Piller Mire, a pulse of stronger erosion suggests a strong landscape deterioration in the surroundings from around 1000 to 1250 cal CE. The Fimba valley also recorded a higher mineral input starting at the same time, lasting until c. 1800 cal CE. In contrast, the MAR in HFL (Kleinwalser Valley) and on the Piller Saddle decreased after 1250 cal CE. To explain these contradictive trends, a link to a colder climate and progressing glaciers as harbingers of the LIA (Büntgen et al., 2011; Holzhauser et al., 2005; Matthews and Briffa, 2005; Nicolussi, 2012) is suggested. According to Büntgen et al. (2011), the “Great Famine” and “Black Death” were part of the consequences of a shift to a colder and wetter climate. And indeed, a severe drop in the populations of Austria, Germany and Switzerland (and Europe in general) was caused by the plague or “Black Death” (McEvedy and Jones, 1978) around 1350 CE (Herlihy, 1997), which is assumed to have decreased pressure on the landscape and led to a Europe-wide re-forestation (Yeloff and Van Geel, 2007). A generally declining trend in

mountain farming was already described by Bender (2010), but his results show also regional differences and another possible explanation for the contrasting trends: In Switzerland (Fimba Valley), the production of hard cheese (introduction of rennet) increased mountain farming, whereas parts of the Austrian Alps experienced reforestation to serve as hunting grounds (cf. chapter **4.3.5**, Kleinwalser Valley). While the combined effects of these events at that time reduced mineral input at lower elevations (Pi17, HFL and LAD temporarily), a combination of advancing glaciers and increasing or ongoing pastoralism (mountain dairy farming) could have induced higher mineral input into mires of the upper valleys, above the tree line (Fimba Valley).

A common cultural impact in the Kleinwalser and Fimba Valley was the immigration of the Walser people around 1300 to 1400 CE (Bauerochse and Katenhusen, 1997; Wagner, 1950). A trend to higher MARs was only subtle in HFL, but the mires that are closer to the more fragile slopes are clearly showing an increasing trend (LAD in Kleinwalser Valley, MM and LLG in Fimba Valley) during the respective period. Moreover, a more intensive use of less accessible areas at higher elevations for livestock grazing and/or timber harvest can be inferred from Wagner (1950) and Willand and Amann (2013). A high demand for wood was generated by mining and production of salt, metals and glass around Innsbruck or in the Allgaeu during Late Middle Ages and early Modern Times (Brandstätter et al., 2015; Kata, 1995).

Around 1500 cal CE, a lower mineral input continued in HFL and Pi17, which is in agreement with the general decrease of Alpine farming and population since the High Middle Ages (Bender, 2010; Lichtenberger, 1965). Meanwhile, the Fimba Valley mires experienced a maximum MAR before stagnating (end of record) on a high level until 1800 cal CE. Based on pollen (Bauerochse and Katenhusen, 1997; Dietre et al., 2014) and historical data (Town of Ischgl, 2019), human impact can be seen as the driving force behind this development. The MAR increase in Pi17 and LAD around 1750 cal CE is attributable attributed to local intensifications of land use, whereas the following decline at these sites coincides with another cold phase, expressed as glacier progressions and related to the Little Ice Age (Matthews and Briffa, 2005; Nicolussi and Patzelt, 2000). Moreover Bender (2010) reported an abandoning of many mountain farms due to this severe cold period. This ultimately stabilised the landscape and led to a, still ongoing, natural reforestation of pasture grounds since around 1850 CE in, for example, the Eastern Central Alps (Tasser et al., 2007). Economical numbers on agriculture and livestock for this interval and the regions around Fimba Valley and Piller Mire (Fromme, 1957) support the idea that reduced land use was probably responsible for a lower MAR (cf. chapters **5.3.5** and **6.3.4**). The Fimba Valley cores cannot resolve questions of land use later than around 1800 cal CE. However, another strong rise of (atmospheric) mineral input into the ombrotrophic peat sections of the

Kleinwalser Valley and Piller Mire was most likely connected to human activities, in form of local construction of infrastructure (tourism, power grids, roads) and peat mining.

Metallurgy and mining became more and more important (Brandstätter, 2015; Brandstätter et al., 2015; Hofmann and Wolkersdorfer, 2013) in the Montafon region and along the river Inn since the 10th century CE, which is reflected by the increase of the Pb EF at the sites of MM and Pi17, located further to the east (**Figure 57**). Although the LLG-profile exhibits an opposing trend, this contrasting behaviour can be explained by dilution effects and anthropogenic surface decomposition and erosion. A booming mining industry for mainly Pb and Ag along the Inn Valley, but also in the Paznaun, Kauner and Platzer Valley (**Figure 1** and **Figure 23**) south of the Piller Mire site is reflected by the increasing EFs (or ratio) around and after 1500 cal CE. The ombrotrophic upper sections of the Austrian sites recorded an ever accelerating Pb EF trend towards the 20th century cal CE. More detailed profiles of this recent part of the Pb EF signals recorded are given in **Figure 58**. This increasing trend in the Late Middle Ages was also observed in many other places in Europe (Brännvall et al., 1999; Mariet et al., 2016; Monna et al., 2004; Thevenon et al., 2011).

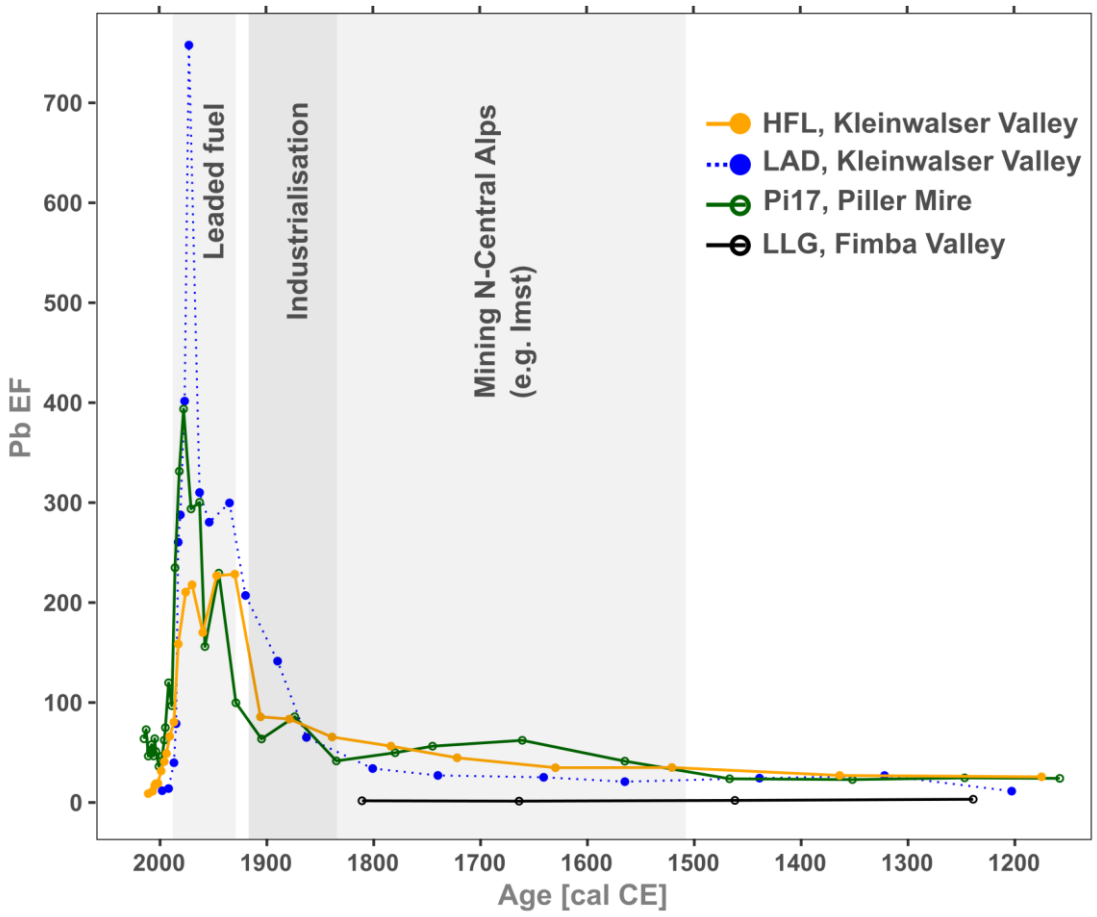

Figure 58: Pb EF since the Late Middle Ages of HFL, LAD, LLG and Pi17.

The industrialisation in Central Europe gained momentum after 1800 CE (Tilly, 2010) and is reflected in form of strongly increasing anthropogenic Pb input at about this time. A second increase around the middle 20th century can be attributed to the introduction of leaded gasoline. These similar trends at most of the investigated sites are, are in good agreement with other sites in Switzerland (Shotyk et al., 1998, 1996; Weiss et al., 1999) and in line with the global history of anthropogenic Pb-deposition (Marx et al., 2016). These studies are underlining that the sharp decline of Pb EF in the second half of the 20th century cal CE is corresponding to the fading out of atmospheric Pb-emissions after the ban of leaded gasoline in the 1980s (Pacyna and Pacyna, 2001). These independent studies and the simultaneous trends of Pb EF in the records (e.g. Roman signal, industrialisation) bring an extra chronological constrain in the age depth models of the three valleys.

7.2.5 Human impact and peat accumulation

Indicators for erosion, mining and metallurgy or for other anthropogenic or climatic developments are revealed by MAR and metal EFs. But as already mentioned earlier in the subchapters, also the peat accumulation rate can offer valuable information, even if more detailed investigations on this complex topic are needed. The rates in all mires ranged between 0.01 and 0.1 cm*a^{-1}. But there are common trends between the mires as well. LLG and HFL both show an extended period of relatively lower accumulation from 5500 to around 3500 cal BP with a minimum around 4500 cal BP. Following the interpretation of Dietre et al. (2014), drier conditions were responsible. Except for LAD, all investigated mires saw an almost simultaneous phase of very low peat accumulation (**Figure 59**): beginning the earliest after 2500 cal BP in the Fimba Valley (LLG) and the latest after around 700 cal CE in the Kleinwalser Valley (HFL), before reaching a minimum at approximately 1500 cal CE. Although colder summers, longer winters or droughts can act as a climate forcing behind such an observation, other mechanisms were additionally suggested here to explain this effect. In line with the findings of Sjögren et al. (2007), strong and long-term human impact can be suggested as the main responsible factor for this phase of reduced or ceased peat accumulation. In the Kleinwalser Valley and at the Piller Mire, partly still existing drainage could have played a role, but no date can be allocated to the initial instalment at the moment. Especially in the upper Fimba Valley, cattle trampling was probably the most important reason. Considering the Iron Age pastoral huts and pens (Reitmaier, 2012), the earlier decline in LLG could have been a consequence of this early phase of Alpine farming in the Fimba Valley.

In any case, both drainage and livestock trampling disturb upper peat layers, by inducing vegetation changes, oxygenating deeper layers and consequently leading to an enhanced decomposition. This is in line with elevated S-contents in the affected peat layers of all sites. Decomposition and mineralisation in the Fimba Valley (LLG) were so strong that an increasingly mineral layer formed towards the surface. Such a disturbance can affect buried peat layers and alter a signal or peat accumulation post-depositional. Putting an age to these suggested triggering impacts is therefore difficult.

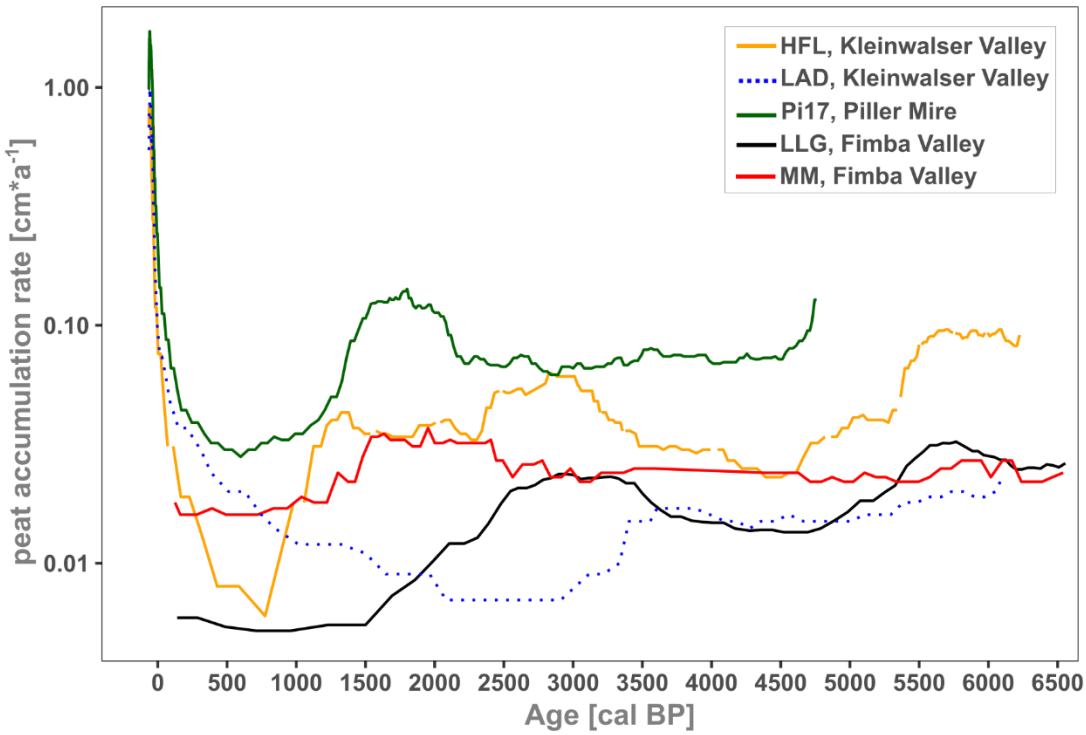

*Figure 59: Peat accumulation and growth rates [cm*a^{-1}] in the investigated mires HFL, LAD, Pi17, LLG, MM.*

Above these compacted layers, starting after 1900 cal CE, a strong growth boost of up to more than 1 cm*a^{-1} began in the lower elevated and ombrotrophic peatlands (HFL, LAD, Pi17). Even if the upmost part of an ombrotrophic bog grows much faster compared to the accumulation of peat, growth rates can benefit human activities like mowing, nature conservation measures or anything that changes the hydrological situation (cf. 4.3.5). Understanding the anthropogenic processes behind recent ombrotrophication and peat growth development in the Kleinwalser Valley actually attracted the attention of ongoing research (Schrautzer et al., in press, 2019), to which this study also contributed.

8 Conclusions and perspectives

8.1 Analytical development of pXRF

The methodological approaches of this study, the application and intercomparison of quantitative and semi-quantitative geochemical methods allow the calibration of results derived from a pXRF-device for a wide number of elements with ICP-MS and ICP-OES measurements of the same samples. A time and cost saving sampling of the peat cores is thereby made possible, resulting in a higher resolution. Due to the heterogeneity of samples, especially with respect to the mineral matter content, resulting from the respective mire types, their environment and vegetation, site-specific effects appear during analysis. A general result of this study is that elemental concentrations are significantly overestimated by pXRF. Regression analyses demonstrate that linear calibrations of pXRF measurements are possible within a peat matrix, whereas the addition of minerogenic samples introduces a matrix effect to the calibration functions for most elements. This effect manifests in such a way that the pXRF-measurements are getting closer to their real concentrations with rising mineral content. To reduce the uncertainty for less organic peat samples, more exact criteria for the point where the regression shifts from linear to polynomial shape should be defined in future studies. In addition to considering the dry bulk density or Ti-concentrations as guidance, the ash-content is proposed as a promising indicator to define this transition range. In any case, a thorough calibration of the pXRF-device should be carried out at an early stage of the study: either by another reliable independent method (e.g. ICP-MS or ICP-OES) or by a sufficient number of CRMs. Acquiring and developing more CRMs with an organic, peat-like matrix and a wider concentration range before using a pXRF-instrument is therefore highly recommended. Eventually, the development of universally valid calibrations for the geochemical pXRF-analysis of peat should be targeted.

The results that were obtained by regression analyses in this study demonstrate that it is possible to successfully quantify and reproduce potential geochemical palaeoenvironmental proxies by using pXRF in different types of dried and homogenised peat samples. Among these proxies are the elements Ti, Pb, Zn, S, K, Fe and Sr. With reservations, V, Rb, Mn and Zr can be quantified as well. Altogether, these results open new opportunities for future (palaeo)environmental or metal pollution studies in peatlands. This becomes particularly apparent when looking at the great advantages of pXRF. Relative to ICP-MS, both the sample preparation and analysis are fast and simple: The time and energy-consuming application of dangerous acids during sample processing and measurement becomes obsolete. Furthermore, pXRF is non-destructive, saving the material for other analyses. Relative to XRF-core-scanning, the preparation is, of course, slower, but effects of water content and surface irregularities are

circumvented. More importantly, the results of this work allow obtaining quantitative results and are thus a good compromise between ICP-MS and XRF-core-scanning.

Beside pXRF, the application of an XRF-core-scanner (Avaatech) on wet peat cores can be an effective tool to identify or confirm major geochemical signals, either of increased mineral content (Si preferred before Ti) or of anthropogenically enriched heavy metals like Pb or Zn.

8.2 Site specific factors and proxy sensitivity

Another major outcome of the present study is that the elevation of a mire and the exact position of it play an important role in what palaeoenvironmental or geochemical signals are recorded. At high elevations around or above the tree line, mires that are close to a smaller glacial meltwater discharge channel (proglacial stream-bank mires), could be more sensitive to record climate oscillations without or with only limited anthropogenic disturbance. However, the downside of this is, that a relatively higher mineral content, due to the geomorphologically very active environment in these high alpine valleys, dilutes and potentially masks airborne anthropogenic signals like (Pb) metal EFs. It is hence suggested that, at high elevations, detailed geochemical analysis is less important than detailed radiocarbon dating, age-depth models, field observations, core descriptions and sedimentology. Mires at lower elevations that are more sheltered or further away from glaciogenic erosion processes have a higher potential of detecting more subtle palaeoenvironmental signals. This is partly due to longer vegetation periods, which favours a higher peat accumulation rate and thus increases the potential resolution of sampling and chronology. Especially the problem of a decreasing resolution can be a severe issue at mire sites that are close to human settlements, where impacts like drainage, cattle trampling or even peat mining were or are disturbing factors. Nevertheless, despite their heterogeneity and certain limitations, the general qualification of mostly small-scale mountain mires as geoarchives of environmental change, climate, human impact, land use and land-cover, mining and metallurgy were demonstrated by the synchronicity of geochemical proxies with local pollen studies, archaeological findings, historical data, and regional palaeoclimate studies. This also underlines the need for further interdisciplinary, multi-proxy approaches in such sites to be able to validate and corroborate interpretations.

8.3 Multiproxy – multisite – multi disciplinary: the key to understanding a complex changing mountain environment

The study of multiple cores from three valleys the Central Alps revealed both regionally synchronous and locally different palaeoenvironmental changes that can be linked to climate or human impacts. This study contributes to understand and compare the responses of single valleys or a culturally and environmentally important region to either anthropogenic or climatic disturbances during the Holocene.

Colder and wetter conditions probably affected the high altitudes of the northern Central Alps around 8200 cal BP and again between c. 6450 and 6100 cal BP, triggering the subsequent onset of peat accumulation in the Kleinwalser Valley and increased sediment input in the Fimba Valley. Although, a response to the 8.2 ka event in the Alps is still under discussion, it appears to have affected the Fimba Valley. Cold periods with an influence on this valley are moreover suggested for periods around 5100, 4500, 3650, 3100 and 2600 cal BP. The first significant anthropogenic signal is detected in the Kleinwalser Valley around 5500 cal BP in the form of forest clearings, which lead to a patchy landscape opening and increased erosion. For the same period, the peat record also provides the earliest ever reported evidence for metallurgical or mining activities in this part of the periphery of the northern Central Alps, where ores are scarce. Another phase of increased land use is recorded between 4600 and 4000 cal BP around the Piller Mire, with simultaneously elevated metal(loid) EFs (also in the Kleinwalser Valley at 4200 cal BP), which is again earlier than the oldest archaeological evidence for metal production in this part of the Alps. The most drastic human impact in prehistoric times encompassed large parts of the northern Central Alps' landscape during the Middle to Late Bronze Age, between c. 3500 and 3000 cal BP. This work demonstrates that deforestation, the establishment of pasture management and agriculture led to a strong erosion of slopes and a large-scale transformation of the landscape. In particular in the Kleinwalser Valley, human impact was almost as strong as around 1850 CE. Decreasing human impact probably resulted in the recovery of forests and consequently reduced the fluxes of mineral matter by stabilising the soils around the Early Iron Age. Another period of increased land use started around 2500 cal BP in the area of the two eastern sites, related to pastoralism (Fimba Valley) or settlements and a cultic site (Piller Mire). In contrast, unassignable metallurgical activities were stronger around the Kleinwalser Valley over the Early and Middle Iron Age, whereas no local or direct impact on the landscape can be evidenced. While land use decreased in the whole region, the Roman lead mining peak is clearly visible in all sites around 2000 cal BP. Probably proceeding from the lowlands, the Kleinwalser Valley experienced the first visible anthropogenic impact again in the 3rd century cal CE. Not much later, a severe climate deterioration around 500 cal CE (LALIA and DACP) dramatically

interrupted human activities for more than a century. Larger landscape changes began, but were not contemporaneous, during the Middle Ages. In the upper Fimba Valley, increased mineral input could have been initiated by a mix of both colder climate (LIA) and more intensive land use. Episodes of a probably more erosive land use returned around 1750 cal CE and again in the second half of the 20th century (deforestation, pastoralism, drainage, infrastructure construction and tourism). From the Late Middle Ages onward, a successive intensification of regional mining and metallurgy was followed by emissions from industrialisation and fossil fuels, reflected in an ever-increasing Pb EF until 1980 cal CE. The characteristic pattern of Pb-emissions and enrichments in European sediment archives, provided an independent age-control for the 20th century CE together with the bomb-pulse radiocarbon dates. Besides documented erosion and metallurgy proxies, cattle trampling and drainage caused a high degree of decomposition and compaction. This affected peat layers at least since the Middle Ages until today, although strong peat growth was initiated again by changing land use practices and conservation measures after around 1950 cal CE.

Opening an environmental archive can provide long-term information on past environmental conditions, climate change and human impact, where archaeological findings are not as continuous or even lacking. Taking, for example, several signals of elevated Pb EF in prehistory or during Roman Times and in the Early Middle Ages, the signals presented here are suggesting several undocumented episodes of local or regional metallurgy and/or mining around the Kleinwalser Valley and the Piller Mire. The origin of these signals, however, could not be pinpointed or connected to any known archaeological sites in the study area and would require further investigation. Ideally, this would be in ombrotrophic mires in the vicinity of potential ore deposits. Detailed analysis of Pb-isotopes (e.g. $^{206}Pb/^{207}Pb$) in the peat samples and in natural local sediments and their comparison to signatures of the closest mines or ores would also be a strong tool to gaining knowledge on the origin of signals. A high-resolution pollen analysis on the same cores that are used for geochemistry could also be a valuable complement to find indicators for changes in land use connected to mining and smelting activities. Additional investigations on mires from neighbouring areas are, furthermore, needed. These could test the suggested climatic or anthropogenic signals derived from mineral input fluctuations that are less distinct than, for example, the extensive landscape transformations during the Mid to Late Bronze Age evidenced in this study.

As the chronological uncertainty in the uppermost peat layers is relatively high compared to precise historical data, ^{210}Pb-dating could help to refine the chronologies. This could thus test the interpretations of recent developments in the mire and thereby, for example, assess the

most recent human impact (e.g. drainage, mowing, grazing) and its effects on the mires' ecohydrology, peat growth and decay in mountainous environments.

In order to gain the full picture, there are many more research questions that should be addressed in the future. Nonetheless, the consolidation of this work's geochemical results with information from various other fields of scientific disciplines highlights the potential of using mountain mires in unveiling past developments of human activity. The investigated mires are not merely showing local human presence but are giving an idea about the character and extent of human impact on the Alpine landscape during different periods of the Late Holocene. Moreover, they are revealing previously unknown episodes of prehistoric to Medieval mining and/or metallurgic activities in the northern Central Alps, where polymetallic ores are found. Altogether, this study demonstrates the significance of pXRF-based geochemical studies in mountain mires and emphasises the strengths of this approach, ultimately making it an indispensable part of multidisciplinary, palaeoenvironmental studies in areas, where peatlands exist.

9 References

Allan, M., Pinti, D.L., Ghaleb, B., Verheyden, S., Mattielli, N., Fagel, N., 2018. Reconstruction of Atmospheric Lead Pollution During the Roman Period Recorded in Belgian Ombrotrophic Peatlands Cores. Atmosphere (Basel). 9, 253. https://doi.org/10.3390/atmos9070253

Alley, R.B., Ágústsdóttir, A.M., 2005. The 8k event: cause and consequences of a major Holocene abrupt climate change. Quat. Sci. Rev. 24, 1123–1149. https://doi.org/10.1016/j.quascirev.2004.12.004

Alley, R.B., Mayewski, P.A., Sowers, T., Stuiver, M., Taylor, K.C., Clark, P.U., 1997. Holocene climatic instability: A prominent, widespread event 8200 yr ago. Geology 25, 483–486.

Alpine-Convention, 2010. Alpine Convention Reference Guide. Alpine Signals 1, 2nd ed. Permanent Secretariat of the Alpine Convention, Innsbruck/Bolzano.

Amann, A., 2014. Alpgenossenschaften im Kleinwalsertal – Eine Vignette aus früherer Zeit“ Berichte aus Alpbüchern des Alters 1592 AD “, in: Laurinkari, J., Schediwy, R., Todev, T. (Eds.), Genossenschaftswissenschaft Zwischen Theorie Und Geschichte: Festschrift Für Prof. Dr. Johann Brazda Zum 60. Geburtstag. BoD – Books on Demand, pp. 49–63.

Amann, A., 2013a. Alpleben im Walsertal - ein kulturhistorischer Abriss, in: Amann, A., Willand, D. (Eds.), “Das Buoch Soll Kraft Und Macht Haben”. Alpbücher Im Kleinwalsertal 1541-1914. Brüüge, Riezlern/Kleinwalsertal, pp. 11–80.

Amann, A., 2013b. Kaleidoskop der Alpbücher, in: Willand, D., Amann, A. (Eds.), Das Buoch Soll Kraft Und Macht Haben". Alpbücher Im Kleinwalsertal 1541-1914. Brüüge, Riezlern/Kleinwalsertal, pp. 103–164.

Armit, I., Swindles, G.T., Becker, K., Plunkett, G., Blaauw, M., 2014. Rapid climate change did not cause population collapse at the end of the European Bronze Age. Proc. Natl. Acad. Sci. 111, 17045–17049. https://doi.org/10.1073/pnas.1408028111

Arnaud, F., Poulenard, J., Giguet-Covex, C., Wilhelm, B., Révillon, S., Jenny, J.-P., Revel, M., Enters, D., Bajard, M., Fouinat, L., Doyen, E., Simonneau, A., Pignol, C., Chapron, E., Vannière, B., Sabatier, P., 2016. Erosion under climate and human pressures: An alpine lake sediment perspective. Quat. Sci. Rev. 152, 1–18. https://doi.org/10.1016/j.quascirev.2016.09.018

Artioli, G., Angelini, I., Kaufmann, G., Canovaro, C., Dal Sasso, G., Villa, I.M., 2017. Long-distance connections in the Copper Age: New evidence from the Alpine Iceman’s copper axe. PLoS One 12, e0179263. https://doi.org/10.1371/journal.pone.0179263

Aubert, D., Le Roux, G., Krachler, M., Cheburkin, A., Kober, B., Shotyk, W., Stille, P., 2006. Origin and fluxes of atmospheric REE entering an ombrotrophic peat bog in Black Forest (SW Germany): Evidence from snow, lichens and mosses. Geochim. Cosmochim. Acta 70, 2815–2826. https://doi.org/10.1016/j.gca.2006.02.020

Babucke, V., 1995. Das frühe Mittelalter, in: Czysz, W., Dietrich, H., Weber, G. (Eds.), Kempten Und Das Allgäu. Führer Zu Archäologischen Denkmälern in Deutschland 30. Theiss, Stuttgart, pp. 70–78.

Bachnetzer, T., 2017. Prähistorischer Feuersteinbergbau im Kleinwalsertal, Vorarlberg. Silex- und Bergkristallabbaustellen in Österreich. Praearchos 5.

Bächtiger, K., 1982. Die Erzvorkommen und Lagerstätten Graubündens und der ehemalige Bergbau. Mitteilungen, Verein der Freunde des Bergbaues Graubünden 21, 2–12.

Barber, K.E., 1993. Peatlands as scientific archives of past biodiversity. Biodivers. Conserv. 2, 474–489. https://doi.org/10.1007/BF00056743

Barham, L.S., 2002. Systematic Pigment Use in the Middle Pleistocene of South-Central Africa. Curr. Anthropol. 43, 181–190. https://doi.org/10.1086/338292

Barker, M.L., 1982. Traditional Landscape and Mass Tourism in the Alps. Geogr. Rev. 72, 395. https://doi.org/10.2307/214593

Baron, S., Lavoie, M., Ploquin, A., Carignan, J., Pulido, M., De Beaulieu, J.L., 2005. Record of metal workshops in peat deposits: History and environmental impact on the Mont Lozère Massif, France. Environ. Sci. Technol. 39, 5131–5140. https://doi.org/10.1021/es048165l

Bartelheim, Martin, Eckstein, K., Huijsmans, M., Krauß, R., Pernicka, Ernst, 2002. Kupferzeitliche Metallgewinnung in Brixlegg, Österreich, in: Bartelheim, M., Pernicka, E., Krause, R. (Eds.), Die Anfänge Der Metallurgie in Der Alten Welt. Rahden, Westfalia: Verlag Marie Leidorf, Rahden, pp. 33–82.

Bätzing, W., 2015. Die Alpen: Geschichte und Zukunft einer europäischen Kulturlandschaft, 4th ed. C.H. Beck, Munich.

Bätzing, W., Perlik, M., Dekleva, M., 1996. Urbanization and depopulation in the Alps. Mt. Res. Dev. 335–350.

Bauerochse, A., Katenhusen, O., 1997. Reconstruction of Holocene landscape development and present vegetation of the Val Fenga (Tyrol/Grisons). Phytocoenologia 27, 353–453. https://doi.org/10.1127/phyto/27/1997/353

Bednarik, R.G., 1992. Early subterranean chert mining. The Artefact 15, 11–24.

Belokopytov, I.E., Beresnevich, V. V, 1955. Giktorf's peat borers. Torfyanaya Promyshlennost 8, 9–10.

Bender, O., 2010. Entstehung, Entwicklung und Ende der alpinen Bergbauernkultur. Über das Entsteh. und die Endlichkeit Phys. Prozesse, Biol. Arten und Menschl. Kult. 113–137.

Benedetti, M.F., Milne, C.J., Kinniburgh, D.G., Van Riemsdijk, W.H., Koopal, L.K., 1995. Metal Ion Binding to Humic Substances: Application of the Non-Ideal Competitive Adsorption Model. Environ. Sci. Technol. 29, 446–457. https://doi.org/10.1021/es00002a022

Beniston, M., 2005. Mountain climates and climatic change: an overview of processes focusing on the European Alps. Pure Appl. Geophys. 162, 1587–1606.

Bennett, P.C., Siegel, D.I., Hill, B.M., Glaser, P.H., 1991. Fate of silicate minerals in a peat bog. Geology 19, 328–331.

Benoit, J.M., Fitzgerald, W.F., Damman, A.W.H., 1998. The Biogeochemistry of an Ombrotrophic Bog: Evaluation of Use as an Archive of Atmospheric Mercury Deposition. Environ. Res. 78, 118–133. https://doi.org/10.1006/enrs.1998.3850

Bergström, A.-K., Jansson, M., 2006. Atmospheric nitrogen deposition has caused nitrogen enrichment and eutrophication of lakes in the northern hemisphere. Glob. Chang. Biol. 12, 635–643. https://doi.org/10.1111/j.1365-2486.2006.01129.x

Biester, H., Hermanns, Y.M., Martinez Cortizas, A., 2012. The influence of organic matter decay on the distribution of major and trace elements in ombrotrophic mires - a case study from the Harz Mountains. Geochim. Cosmochim. Acta 84, 126–136. https://doi.org/10.1016/j.gca.2012.01.003

Biester, H., Knorr, K.-H.H., Schellekens, J., Basler, A., Hermanns, Y.-M.M., 2014. Comparison of

different methods to determine the degree of peat decomposition in peat bogs. Biogeosciences 11, 2691–2707. https://doi.org/10.5194/bg-11-2691-2014

Bindler, R., 2006. Mired in the past - looking to the future: Geochemistry of peat and the analysis of past environmental changes. Glob. Planet. Change 53, 209–221. https://doi.org/10.1016/j.gloplacha.2006.03.004

Binnemans, K., Jones, P.T., Blanpain, B., Van Gerven, T., Pontikes, Y., 2015. Towards zero-waste valorisation of rare-earth-containing industrial process residues: a critical review. J. Clean. Prod. 99, 17–38. https://doi.org/10.1016/j.jclepro.2015.02.089

Blaauw, M., 2010. Methods and code for 'classical' age-modelling of radiocarbon sequences. Quat. Geochronol. 5, 512–518. https://doi.org/10.1016/j.quageo.2010.01.002

Blaauw, M., Christen, J.A., 2011. Flexible paleoclimate age-depth models using an autoregressive gamma process. Bayesian Anal. 6, 457–474. https://doi.org/10.1214/11-BA618

Bloemsma, M., Croudace, I., Daly, J.S., Edwards, R.J., Francus, P., Galloway, J.M., Gregory, B.R.B., Huang, J.-J.S., Jones, A.F., Kylander, M., Löwemark, L., Luo, Y., Maclachlan, S., Ohlendorf, C., Patterson, R.T., Pearce, C., Profe, J., Reinhardt, E.G., Stranne, C., Tjallingii, R., Turner, J.N., 2018. Practical guidelines and recent advances in the Itrax XRF core-scanning procedure. Quat. Int. https://doi.org/https://doi.org/10.1016/j.quaint.2018.10.044

Bode, M., Hanel, N., Rothenhöfer, P., 2015. Die Versorgung des Alpenraums mit Blei in römischer Zeit, in: Stöllner, T., Oeggl, K. (Eds.), Bergauf Bergab. 10.000 Jahre Bergbau in Den Ostalpen. Deutsches Bergbau-Museum Bochum, Bochum, pp. 389–394.

Boës, X., Rydberg, J., Martinez-Cortizas, A., Bindler, R., Renberg, I., 2011. Evaluation of conservative lithogenic elements (Ti, Zr, Al, and Rb) to study anthropogenic element enrichments in lake sediments. J. Paleolimnol. 46, 75–87. https://doi.org/10.1007/s10933-011-9515-z

Böning, P., Bard, E., Rose, J., 2007. Toward direct, micron-scale XRF elemental maps and quantitative profiles of wet marine sediments. Geochemistry, Geophys. Geosystems 8, n/a-n/a. https://doi.org/10.1029/2006GC001480

Bortenschlager, S., 2010. Vegetationsgeschichte im Bereich des Rotmoostales. Glaziale und periglaziale Leb. im Raum Obergurgl 77–92.

Boyle, J.F., 2000. Rapid elemental analysis of sediment samples by isotope source XRF. J. Paleolimnol. 23, 213–221. https://doi.org/10.1023/A:1008053503694

Bragg, O., Lindsay, R., 2003. Strategy and action plan for mire and peatland conservation in Central Europe. Wetlands International, Wageningen.

Brandstätter, K., 2015. Spätmittelalterlicher Bergbau im Ostalpenraum, in: Stöllner, T., Oeggl, K. (Eds.), Bergauf Bergab. 10.000 Jahre Bergbau in Den Ostalpen. Deutsches Bergbau-Museum Bochum, Bochum, pp. 419–424.

Brandstätter, K., Neuhauser, G., Anzinger, B., 2015. Waldnutzung und Waldentwicklung in der Grafschaft tirol im Spätmittelalter und der Frühen neuzeit, in: Stöllner, T., Oeggl, K. (Eds.), Bergauf Bergab. 10.000 Jahre Bergbau in Den Ostalpen. Deutsches Bergbau-Museum Bochum, Bochum, pp. 547–552.

Brännvall, M.-L., Bindler, R., Emteryd, O., Renberg, I., 2001. Four thousand years of atmospheric lead pollution in northern Europe: a summary from Swedish lake sediments.

J. Paleolimnol. 25, 421–435. https://doi.org/10.1023/A:1011186100081

Brännvall, M.L., Bindler, R., Renberg, I., Emteryd, O., Bartnicki, J., Billström, K., 1999. The medieval metal industry was the cradle of modern large-scale atmospheric lead pollution in northern Europe. Environ. Sci. Technol. 33, 4391–4395. https://doi.org/10.1021/es990279n

Breitenlechner, E., Goldenberg, G., Lutz, J., Oeggl, K., 2013. The impact of prehistoric mining activities on the environment: A multidisciplinary study at the fen Schwarzenbergmoos (Brixlegg, Tyrol, Austria). Veg. Hist. Archaeobot. 22, 351–366. https://doi.org/10.1007/s00334-012-0379-6

Bringemeier, L., Krause, R., Stobbe, A., Röpke, A., 2015. expansions of bronze age pasture farming and environmental changes in the northern alps (montafon, austria and prättigau, switzerland) – an integrated palaeoenv ironmental and archaeological approach, in: Kneisel, J., Corso, M.D., Kirleis, W., Scholz, H., Taylor, N., Tiedtke, V. (Eds.), The Third Food Revolution? Setting the Bronze Age Table: Common Trends in Economic and Subsistence Strategies in Bronze Age Europe. Verlag Dr. Rudolph Habelt GmbH, Bonn, pp. 181–200.

Brinson, M.M., Malvárez, A.I., 2002. Temperate freshwater wetlands: types, status, and threats. Environ. Conserv. 29, 115–133. https://doi.org/10.1017/S0376892902000085

Brown, K.A., 1985. Sulphur distribution and metabolism in waterlogged peat. Soil Biol. Biochem. 17, 39–45. https://doi.org/10.1016/0038-0717(85)90088-4

Brown, P.., Gill, S.., Allen, S.., 2000. Metal removal from wastewater using peat. Water Res. 34, 3907–3916. https://doi.org/10.1016/S0043-1354(00)00152-4

Büntgen, U., Myglan, V.S., Ljungqvist, F.C., McCormick, M., Di Cosmo, N., Sigl, M., Jungclaus, J., Wagner, S., Krusic, P.J., Esper, J., Kaplan, J.O., De Vaan, M.A.C., Luterbacher, J., Wacker, L., Tegel, W., Kirdyanov, A. V., 2016. Cooling and societal change during the Late Antique Little Ice Age from 536 to around 660 AD. Nat. Geosci. 9, 231–236. https://doi.org/10.1038/ngeo2652

Büntgen, U., Tegel, W., Nicolussi, K., McCormick, M., Frank, D., Trouet, V., Kaplan, J.O., Herzig, F., Heussner, K.U., Wanner, H., Luterbacher, J., Esper, J., 2011. 2500 years of European climate variability and human susceptibility. Science (80-.). 331, 578–582. https://doi.org/10.1126/science.1197175

Carcaillet, C., 1998. A spatially precise study of Holocene fire history, climate and human impact within the Maurienne valley, North French Alps. J. Ecol. 86, 384–396. https://doi.org/10.1046/j.1365-2745.1998.00267.x

Carlson, K.M., Curran, L.M., Asner, G.P., Pittman, A.M., Trigg, S.N., Marion Adeney, J., 2013. Carbon emissions from forest conversion by Kalimantan oil palm plantations. Nat. Clim. Chang. 3, 283–287. https://doi.org/10.1038/nclimate1702

Carrer, F., Colonese, A.C., Lucquin, A., Guedes, E.P., Thompson, A., Walsh, K., Reitmaier, T., Craig, O.E., 2016. Chemical analysis of pottery demonstrates prehistoric origin for high-altitude alpine dairying. PLoS One 11, 1–11. https://doi.org/10.1371/journal.pone.0151442

Casty, C., Wanner, H., Luterbacher, J., Esper, J., Böhm, R., 2005. Temperature and precipitation variability in the European Alps since 1500. Int. J. Climatol. 25, 1855–1880. https://doi.org/10.1002/joc.1216

Cerny, I., 1989. Die karbonatgebundenen Blei-Zink-Lagerstätten des alpinen und außeralpinen

Mesozoikums. Die Bedeutung ihrer Geologie, Stratigraphie und Faziesgebundenheit für Prospektion und Bewertung. Arch. Lagerstättenforsch. Geol. Bundesanst. 11, 5–125.

Chagué-Goff, C., Chan, J.C.H., Goff, J., Gadd, P., 2016. Late Holocene record of environmental changes, cyclones and tsunamis in a coastal lake, Mangaia, Cook Islands. Isl. Arc 25, 333–349. https://doi.org/10.1111/iar.12153

Chambers, F.M., Booth, R.K., De Vleeschouwer, F., Lamentowicz, M., Le Roux, G., Mauquoy, D., Nichols, J.E., van Geel, B., 2012. Development and refinement of proxy-climate indicators from peats. Quat. Int. 268, 21–33. https://doi.org/10.1016/j.quaint.2011.04.039

Chambers, F.M., Charman, D.J., 2004. Holocene environmental change: contributions from the peatland archive. The Holocene 14, 1–6. https://doi.org/10.1191/0959683604hl684ed

Chaney, R.L., Hundemann, P.T., 1979. Use of peat moss columns to remove cadmium from wastewaters. J. (Water Pollut. Control Fed. 51, 17–21.

Chawchai, S., Kylander, M.E., Chabangborn, A., Löwemark, L., Wohlfarth, B., 2016. Testing commonly used X-ray fluorescence core scanning-based proxies for organic-rich lake sediments and peat. Boreas 45, 180–189. https://doi.org/10.1111/bor.12145

Clark, J.S., Merkt, J., Muller, H., 1989. Post-Glacial Fire, Vegetation, and Human History on the Northern Alpine Forelands, South-Western Germany. J. Ecol. 77, 897. https://doi.org/10.2307/2260813

Cloy, J.M., Farmer, J.G., Graham, M.C., MacKenzie, A.B., 2011. Scottish peat bog records of atmospheric vanadium deposition over the past 150 years: comparison with other records and emission trends. J. Environ. Monit. 13, 58–65. https://doi.org/10.1039/C0EM00492H

Cloy, J.M., Farmer, J.G., Graham, M.C., MacKenzie, A.B., 2009. Retention of As and Sb in Ombrotrophic Peat Bogs: Records of As, Sb, and Pb Deposition at Four Scottish Sites. Environ. Sci. Technol. 43, 1756–1762. https://doi.org/10.1021/es802573e

Cooper, D.J., Wolf, E.C., Colson, C., Vering, W., Granda, A., Meyer, M., 2010. Alpine peatlands of the Andes, Cajamarca, Peru. Arctic, Antarct. Alp. Res. 42, 19–33. https://doi.org/10.1657/1938-4246-42.1.19

Cornelissen, M., Reitmaier, T., 2016. Filling the gap: Recent Mesolithic discoveries in the central and south-eastern Swiss Alps. Quat. Int. 423, 9–22. https://doi.org/10.1016/j.quaint.2015.10.121

Costanza, R., D'Arge, R., De Groot, R., Farber, S., Grasso, M., Hannon, B., Limburg, K., Naeem, S., O'neill, R. V, Paruelo, J., 1997. The value of the world's ecosystem services and natural capital. Nature 387, 253. https://doi.org/0.1038/387253a0

Couillard, D., 1994. The use of peat in wastewater treatment. Water Res. 28, 1261–1274. https://doi.org/10.1016/0043-1354(94)90291-7

Croudace, I.W., Rindby, A., Rothwell, R.G., 2006. ITRAX: description and evaluation of a new multi-function X-ray core scanner. Geol. Soc. London, Spec. Publ. 267, 51–63. https://doi.org/10.1144/GSL.SP.2006.267.01.04

Damman, A.W.H., 1978. Distribution and Movement of Elements in Ombrotrophic Peat Bogs. Oikos 30, 480. https://doi.org/10.2307/3543344

Dargie, G.C., Lewis, S.L., Lawson, I.T., Mitchard, E.T.A., Page, S.E., Bocko, Y.E., Ifo, S.A., 2017. Age, extent and carbon storage of the central Congo Basin peatland complex. Nature 542, 86–90. https://doi.org/10.1038/nature21048

Dart, P.B., 1971. On a further radiocarbon date for ancient mining in Southern Africa. S. Afr. J. Sci. 67, 10–11.

de Graaff, L.W.S., de Jong, M.G.G., Busnach, T., Seijmonsbergen, A.C., 2003. Geomorphologische Studie hinterer Bregenzerwald. Bericht an das Amt der Vorarlberger Landesregierung, Abt. Raumplanung und Baurecht Landhaus Bregenz. Amsterdam.

De Vleeschouwer, F., Chambers, F.M., Swindles, G.T., 2010a. Coring and sub-sampling of peatlands for palaeoenvironmental research. Mires Peat 7, 1–10. https://doi.org/10.1016/j.ssi.2010.01.014

De Vleeschouwer, F., Gérard, L., Goormaghtigh, C., Mattielli, N., Le Roux, G., Fagel, N., 2007. Atmospheric lead and heavy metal pollution records from a Belgian peat bog spanning the last two millenia: Human impact on a regional to global scale. Sci. Total Environ. 377, 282–295. https://doi.org/10.1016/j.scitotenv.2007.02.017

De Vleeschouwer, F., Le Roux, G., Shotyk, W., 2010b. Peat as an archive of atmospheric pollution and environmental change: A case study of lead in Europe. PAGES Mag. 18, 20–22. https://doi.org/10.22498/pages.18.1.20

De Vleeschouwer, F., van Vliët-Lanoé, B., Fagel, N., Richter, T., Boës, X., 2008. Development and application of high-resolution petrography on resin-impregnated Holocene peat columns to detect and analyse tephras, cryptotephras, and other materials. Quat. Int. 178, 54–67. https://doi.org/10.1016/j.quaint.2006.12.021

DeFries, R.S., Foley, J.A., Asner, G.P., 2004. Land-use choices: balancing human needs and ecosystem function. Front. Ecol. Environ. 2, 249–257. https://doi.org/10.1890/1540-9295(2004)002[0249:LCBHNA]2.0.CO;2

Della Casa, P., 2013. Switzerland and the Central Alps, in: Harding, A., Fokkens, H. (Eds.), The Oxford Handbook of the European Bronze Age. OUP Oxford, pp. 706–722.

Dertsch, R., 1974. Ortsnamensbuch des Landkreises Sonthofen. Historisches Ortsnamenbuch von Bayern. Schwaben. Bd. 7. Kommission für Bayerische Landesgeschichte, München.

Dieffenbach-Fries, H., 1981. Zur spät- und postglazialen Vegetationsentwicklung bei Oberstdorf (Oberallgäu) und im kleinen Walsertal (Vorarlberg). Technische Hochschule Darmstadt.

Dierßen, K., Dierßen, B., 2008. Moore, Ökologie Botanik. Ulmer.

Dietre, B., Anich, I., Reidl, D., Kappelmeyer, T., Haas, J.N., 2012. Erste Hirten und Bauern der Silvretta. Palynologie und Ethnobotanik Im Fimbertal und Paznaun, in: Reitmaier, T. (Ed.), Letzte Jäger, Erste Hirten - Hochalpine Archäologie in Der Silvretta. Archäologischer Dienst Graubünden, Chur, pp. 236–256.

Dietre, B., Walser, C., Kofler, W., Kothieringer, K., Hajdas, I., Lambers, K., Reitmaier, T., Haas, J.N., 2017. Neolithic to Bronze Age (4850–3450 cal. BP) fire management of the Alpine Lower Engadine landscape (Switzerland) to establish pastures and cereal fields. Holocene 27, 181–196. https://doi.org/10.1177/0959683616658523

Dietre, B., Walser, C., Lambers, K., Reitmaier, T., Hajdas, I., Haas, J.N., 2014. Palaeoecological evidence for Mesolithic to Medieval climatic change and anthropogenic impact on the Alpine flora and vegetation of the Silvretta Massif (Switzerland/Austria). Quat. Int. 353, 3–16. https://doi.org/10.1016/j.quaint.2014.05.001

Dise, N.B., 2009. Peatland response to global change. Science (80-.). 326, 810–811.

Dolenz, H., 2015. Die Goldbarrengießerei in der Stadt auf dem Magdalensberg - Einblicke in einen kaiserlich römischen Hightec-Betrieb, in: Stöllner, T., Oeggl, K. (Eds.), Bergauf

Bergab. 10.000 Jahre Bergbau in Den Ostalpen. Deutsches Bergbau-Museum Bochum, Bochum, pp. 383–388.

Dugmore, A.J., Larsen, G., Newton, A.J., 1995. Seven tephra isochrones in Scotland. The Holocene 5, 257–266. https://doi.org/10.1177/095968369500500301

Dumontet, S., Lévesque, M., Mathur, S.P., 1990. Limited downward migration of pollutant metals (Cu, Zn, Ni, and Pb) in acidic virgin peat soils near a smelter. Water. Air. Soil Pollut. 49, 329–342. https://doi.org/10.1007/BF00507072

Ebner, F., Cerny, I., Eichhorn, R., Götzinger, M., Paar, W.H., Prochaska, W., Weber, L., 1999. Mineral resources in the Eastern Alps and adjoining areas. Mitteilungen der Österreichischen Geol. Gesellschaft 92, 157–184.

Egger, H., Krenmayr, H.G., Mandl, G.W., Matura, A., Nowotny, A., Pascher, G., Pestal, G., Pistotnik, J., ROCKENSCHAUB M & SCHNABEL, W., 1999. Geologische Übersichtskarte der Republik Österreich 1: 1500000. Wien Geol. Bundesanstalt.

El Balti, N., Christ, L., Kempke, M., Martens, T., Bork, H.-R., Schrautzer, J., 2017. Die Moore im Kleinwalsertal – Aktueller Zustand und Entwicklungsmöglichkeiten. Ina. – Forsch. online 40, 46.

Erdtman, G., 1927. Literature on Pollen-statistics published before 1927. Geol. Föreningen i Stock. Förhandlingar 49, 196–211. https://doi.org/10.1080/11035892709447030

Festi, D., Putzer, A., Oeggl, K., 2014. Mid and late holocene land-use changes in the Ötztal alps, territory of the neolithic iceman “Ötzi.” Quat. Int. 353, 17–33. https://doi.org/10.1016/j.quaint.2013.07.052

Fink, J., von Klenze, H., 1891. Der Mittelberg. Geschichte, Landes- und Volkskunde des ehemaligen gleichnamigen Gerichtes (Reprint). Kösel, Kempten.

Firbas, F., 1923. Pollenanalytische Untersuchungen einiger Moore der Ostalpen. Lotos 71, 187–242.

Fitzsimons, S.J., Veit, H., 2001. Geology and geomorphology of the European Alps and the Southern Alps of New Zealand. Mt. Res. Dev. 21, 340–350. https://doi.org/10.1659/0276-4741(2001)021[0340:GAGOTE]2.0.CO;2

Fleitmann, D., Mudelsee, M., Burns, S.J., Bradley, R.S., Kramers, J., Matter, A., 2008. Evidence for a widespread climatic anomaly at around 9.2 ka before present. Paleoceanogr. Paleoclimatology 23.

Foley, J.A., DeFries, R., Asner, G.P., Barford, C., Bonan, G., Carpenter, S.R., Chapin, F.S., Coe, M.T., Daily, G.C., Gibbs, H.K., Helkowski, J.H., Holloway, T., Howard, E.A., Kucharik, C.J., Monfreda, C., Patz, J.A., Prentice, I.C., Ramankutty, N., Snyder, P.K., 2005. Global Consequences of Land Use. Science (80-.). 309, 570–574. https://doi.org/10.1126/science.1111772

Forel, B., Monna, F., Petit, C., Bruguier, O., Losno, R., Fluck, P., Begeot, C., Richard, H., Bichet, V., Chateau, C., 2010. Historical mining and smelting in the Vosges Mountains (France) recorded in two ombrotrophic peat bogs. J. Geochemical Explor. 107, 9–20. https://doi.org/10.1016/j.gexplo.2010.05.004

Fralick, P.W., Kronberg, B.I., 1997. Geochemical discrimination of clastic sedimentary rock sources. Sediment. Geol. 113, 111–124. https://doi.org/10.1016/S0037-0738(97)00049-3

Frank, C., Pernicka, E., 2012. Copper artefacts of the Mondsee group and their possible sources, in: Midgley, M.S., Sanders, J. (Eds.), Lake Dwellings after Robert Munro.

Proceedings from the Munro International Seminar: The Lake Dwellings of Europe. 22nd 23rd October 2010, University of Edinburgh. Sidestone press, Leiden, pp. 113–138.

Freeman, C., Evans, C.D., Monteith, D.T., Reynolds, B., Fenner, N., 2001. Export of organic carbon from peat soils. Nature 412, 785.

Frei, C., Schär, C., 1998. A precipitation climatology of the Alps from high-resolution rain-gauge observations. Int. J. Climatol. 18, 873–900. https://doi.org/10.1002/(SICI)1097-0088(19980630)18:8<873::AID-JOC255>3.0.CO;2-9

Frei, C., Schmidli, J., 2006. Das Niederschlagsklima der Alpen: Wo sich Extreme nahe kommen. promet 32, 61–67.

Friedmann, A., Stojakowits, P., 2017. Zur spät- und postglazialen Vegetationsgeschichte des Allgäu mit Alpenanteil. Kontrakpunkte: Festschrift für Manfred Rösch, Kontrakpunkte: Festschrift für Manfred Rösch, Universitätsforschungen zur prähistorischen Archäologie ; 300. Verlag Dr. Rudolf Habelt GmbH, Bonn, Bonn.

Fritz, A., 2000. Zur Vegetations-, Siedlungs und Klimageschichte des Millstätter Seentales. Carinthia II 110/160, 579–590.

Fritz, W., 1981. Kleinwalsertal einst und jetzt: heimatkundliche Betrachtungen. Verlag Walserdruck, Erich Stöckeler, Riezlern/Kleinwalsertal.

Fromme, G., 1957. Der Waldrückgang im Oberinntal (Tirol) Untersuchungen über das Ausmaß, die Ursachen und Folgeerscheinungen des Wald? rückganges in einem Gebirgslande sowie über die Aussichten der Wiederaufforstung von. Mitteilungen der Forstl. Bundesversuchsanstalt Mariabrunn 54, 3–222.

Gałka, M., Aunina, L., Feurdean, A., Hutchinson, S., Kołaczek, P., Apolinarska, K., 2017. Rich fen development in CE Europe, resilience to climate change and human impact over the last ca. 3500 years. Palaeogeogr. Palaeoclimatol. Palaeoecol. 473, 57–72. https://doi.org/10.1016/j.palaeo.2017.02.030

Gao, K., Pearce, J., Jones, J., Taylor, C., 1999. Interaction between peat, humic acid and aqueous metal ions. Environ. Geochem. Health 21, 13–26. https://doi.org/10.1023/A:1006592627852

Geiger, R., 1961. Überarbeitete Neuausgabe von Geiger, R. Köppen-Geiger/Klima der Erde.(Wandkarte 1 16 Mill.)–Klett-Perthes, Gotha.

Geological Survey of Austria, 2013. Geologie von Österreich - Posterkarte.

Givelet, N., Le Roux, G., Cheburkin, A., Chen, B., Frank, J., Goodsite, M.E., Kempter, H., Krachler, M., Noernberg, T., Rausch, N., 2004. Suggested protocol for collecting, handling and preparing peat cores and peat samples for physical, chemical, mineralogical and isotopic analyses. J. Environ. Monit. 6, 481–492.

Gleirscher, P., 2015a. Blei, der Glanz von Frög, in: Stöllner, T., Oeggl, K. (Eds.), Bergauf Bergab. 10.000 Jahre Bergbau in Den Ostalpen. Deutsches Bergbau-Museum Bochum, Bochum, pp. 369–372.

Gleirscher, P., 2015b. Keltisch-römischer Edelmetallbergbau in den Hohen Tauern?, in: Stöllner, T., Oeggl, K. (Eds.), Bergauf Bergab. 10.000 Jahre Bergbau in Den Ostalpen. Deutsches Bergbau-Museum Bochum, Bochum, pp. 373–376.

Gobet, E., Tinner, W., Hochuli, P.A., Van Leeuwen, J.F.N., Ammann, B., 2003. Middle to Late Holocene vegetation history of the Upper Engadine (Swiss Alps): the role of man and fire. Veg. Hist. Archaeobot. 12, 143–163.

Godwin, H., 1934. POLLEN ANALYSIS. AN OUTLINE OF THE PROBLEMS AND POTENTIALITIES OF THE METHOD. PART I. TECHNIQUE AND INTERPRETATION. New Phytol. 33, 278–305. https://doi.org/10.1111/j.1469-8137.1934.tb06815.x

Goldammer, J.G., Page, H., Prüter, J., 1997. Nutzung des Feuers in mittel- und nordeuropäischen Landschaften - Geschichte, Methoden, Probleme, Perspektiven, NNA Berichte. Feuereinsatz im Naturschutz. Niedersachsen.

Goldenberg, G., 2015. Prähistorische Kupfergewinnung aus Fahlerzen der Lagerstätte Schwaz-Brixlegg im Unterinntal, Nordtirol, in: Stöllner, T., Oeggl, K. (Eds.), Bergauf Bergab. 10.000 Jahre Bergbau in Den Ostalpen. Deutsches Bergbau-Museum Bochum, Bochum, pp. 151–163.

Goldscheider, N., 1998. Hydrogeologische Untersuchungen im alpinen Karstgebiet Gottesacker und Schwarzwassertal (Allgäu / Vorarlberg). Vor. Naturschau 4, 247–294.

Goodsite, M.E., Rom, W., Heinemeier, J., Lange, T., Ooi, S., Appleby, P.G., Shotyk, W., van der Knaap, W.O., Lohse, C., Hansen, T.S., 2001. High-resolution AMS 14 C dating of post-bomb peat archives of atmospheric pollutants. Radiocarbon 43, 495–515.

Gorham, E., 1995. The biogeochemistry of northern peatlands and its possible responses to global warming. Biot. Feed. Glob. Clim. Syst. Will Warm. Feed Warm. 169–187.

Grabherr, G., 2006. Die Via Claudia Augusta in Nordtirol, in: Walde, E., Grabherr, G. (Eds.), Via Claudia Augusta Und Römerstraßenforschung Im Östlichen Alpenraum. Athesia-Tyrolia Druck GmbH, Innsbruck, pp. 37–284.

Grabherr, G., Gottfried, M., Pauli, H., 2010. Climate change impacts in alpine environments. Geogr. Compass 4, 1133–1153.

Grosse-Brauckmann, G., 2002. Paläobotanische Befunde von zwei Mooren im Gebiet des Hohen Ifen, Vorarlberg (Österreich). Telma 32, 17–36.

Grutsch, C., Martinek, K.P., 2012. Die Nordtiroler Kupfererzvorkommen westlich von Schwaz als Rohstoffpotential der Bronzezeit, in: Oeggl, K., Schaffer, V. (Eds.), Die Geschichte Des Bergbaus in Tirol Und Seinen Angrenzenden Gebieten, Proceedings Zum 6. Milestone-Meeting Des SFB HiMAT Vom 3.-5.11.2011. innsbruck university press, Innsbruck, pp. 101–106.

Gulisano, G., 1995. Die Besiedlung des Kleinwalsertales und seiner angrenzenden Gebiete in Bayern und Vorarlberg von der Steinzeit bis zur Einwanderung der Walser. Archäologische Informationen 18, 53–65. https://doi.org/10.11588/ai.1995.1.35421

Gulisano, G., 1994. Neue mittelsteinzeitliche Fundplätze im oberen Illertal und im Kleinwalsertal. Archäologische Informationen 17, 79–84. https://doi.org/10.11588/ai.1994.1.35418

Haas, J.N., Richoz, I., Tinner, W., Wick, L., 1998. Synchronous holocene climatic oscillations recorded on the Swiss plateau and at timberline in the alps. Holocene 8, 301–309. https://doi.org/10.1191/095968398675491173

Haenssler, E., Nadeau, M.-J., Vött, A., Unkel, I., 2013. Natural and human induced environmental changes preserved in a Holocene sediment sequence from the Etoliko Lagoon, Greece: new evidence from geochemical proxies. Quat. Int. 308, 89–104.

Hammer, W., 1915a. Über Gelbbleierz im Oberinntal. Zeitschrift des Ferdinandeums für Tirol und Vor. 3, 270–277.

Hammer, W., 1915b. Über einige Erzvorkommen im Umkreis der Bündnerschiefer des

Oberinntales. Veröffentl. d. Museums Ferdinandeum 59, 63–94.

Hanneberg, A., Simon, P., Wolkersdorfer, C., 2009a. Galmei und schone Wulfenite: Der Blei-Zink-Bergbau rund um den Fernpass in Tirol. Lapis 34, 20.

Hanneberg, A., Simon, P., Wolkersdorfer, C., 2009b. Galmei und schöne Wulfenite: Der Blei-Zink-Bergbau rund um den Fernpass in Tirol. Lapis 34, 20.

Hansson, S. V., Rydberg, J., Kylander, M., Gallagher, K., Bindler, R., 2013. Evaluating paleoproxies for peat decomposition and their relationship to peat geochemistry. The Holocene 23, 1666–1671. https://doi.org/10.1177/0959683613508160

HDÖ, 1994. Die Niederschläge, Schneeverhältnisse und Lufttemperaturen in Österreich im Zeitraum 1981 – 1991. Beiträge zur Hydrographie Österreichs. Vienna.

Heiri, O., Lotter, A.F., Hausmann, S., Kienast, F., 2003. A chironomid-based Holocene summer air temperature reconstruction from the Swiss Alps. The Holocene 13, 477–484. https://doi.org/10.1191/0959683603hl640ft

Heiss, A.G., 2008. Weizen, Linsen, Opferbrote — Archäobotanische Analysen bronze- und eisenzeitlicher Brandopferplätze im mittleren Alpenraum (PhD-Thesis). Universität Innsbruck. https://doi.org/10.13140/RG.2.1.5185.5526

Helama, S., Jones, P.D., Briffa, K.R., 2017. Dark Ages Cold Period: A literature review and directions for future research. Holocene 27, 1600–1606. https://doi.org/10.1177/0959683617693898

Herbig, C., 2009. Recent archaeobotanical investigations into the range and abundance of Neolithic crop plants in settlements around Lake Constance and in Upper Swabia (south-west Germany) in relation to cultural influences. J. Archaeol. Sci. 36, 1277–1285. https://doi.org/10.1016/j.jas.2009.01.024

Herlihy, D., 1997. The Black Death and the transformation of the West. Harvard University Press.

Hertl, A., 2001. Untersuchungen zur spätglazialen Gletscher- und Klimageschichte der österreichischen Silvrettagruppe (PhD-Thesis). University of Innsbruck.

Heuberger, R., 1955. Der Bodenseeraum im Altertum, in: Büttner, H., Feger, O., Meyer, B. (Eds.), Aus Verfassungs- Und Landesgeschichte, Festschrift Für Theodor Mayer Zum 70. Geb. Band 2. Geschichtliche Landesforschung, Wirtschaftsgeschichte u. Hilfswissenschaften. Lindau/Konstanz, pp. 7–21.

Hofmann, J., Wolkersdorfer, C., 2013. Der historische Bergbau im Montafon, Montafoner Schriftenreihe. Heimatschutzverein Montafon, Schruns, Austria.

Hölzer, Adam, Hölzer, Amal, 1998. Silicon and titanium in peat profiles as indicators of human impact. The Holocene 8, 685–696. https://doi.org/10.1191/095968398670694506

Holzhauser, H., Magny, M., Zumbühl, H.J., 2005. Glacier and lake-level variations in west-central Europe over the last 3500 years. The Holocene 15, 789–801. https://doi.org/10.1191/0959683605hl853ra

Holzhauser, H., Zumbühl, H.J., 1996. To the history of the Lower Grindelwald Glacier during the last 2800 years-paleosols, fossil wood and historical pictorial records-new results. Zeitschrift fur Geomorphol. Suppl. 95–127.

Höppner, B., Bartelheim, M., Huijsman, M., Krauss, R., Martinek, K.-P., Pernicka, E., Schwab, R., 2005. Prehistoric copper production in the Inn Valley (Austria), and the earliest copper in

Cental Europe. Archaeometry 47, 293–315. https://doi.org/10.1111/j.1475-4754.2005.00203.x

Hormes, A., Müller, B.U., Schlüchter, C., 2001. The Alps with little ice: Evidence for eight holocene phases of reduced glacier extent in the Central Swiss Alps. Holocene 11, 255–265. https://doi.org/10.1191/095968301675275728

Hua, Q., 2009. Radiocarbon: a chronological tool for the recent past. Quat. Geochronol. 4, 378–390.

Hubmann, G., 1994. Palynologische Untersuchunger zweier Sedimentprofile aus dem Oberen Inntal, mit Augenmerk auf die anthropogene Beeinflussung (Diploma Thesis). University of Innsbruck.

Huttunen, A., Tolonen, K., 2006. Mire development history in Finland. Finl. L. mires.(Finnish Environ. 23) 79–88.

Iglesias, A., Lopez, R., Fiol, S., Antelo, J.M., Arce, F., 2003. Analysis of copper and calcium–fulvic acid complexation and competition effects. Water Res. 37, 3749–3755.

Ilyashuk, E.A., Koinig, K.A., Heiri, O., Ilyashuk, B.P., Psenner, R., 2011. Holocene temperature variations at a high-altitude site in the Eastern Alps: a chironomid record from Schwarzsee ob Sölden, Austria. Quat. Sci. Rev. 30, 176–191.

Impellitteri, C.A., Lu, Y., Saxe, J.K., Allen, H.E., Peijnenburg, W.J.G.M., 2002. Correlation of the partitioning of dissolved organic matter fractions with the desorption of Cd, Cu, Ni, Pb and Zn from 18 Dutch soils. Environ. Int. 28, 401–410.

Ivy-Ochs, S., Kerschner, H., Kubik, P.W., Schlüchter, C., 2006. Glacier response in the European Alps to Heinrich Event 1 cooling: the Gschnitz stadial. J. Quat. Sci. 21, 115–130. https://doi.org/10.1002/jqs.955

Ivy-Ochs, S., Kerschner, H., Maisch, M., Christl, M., Kubik, P.W., Schlüchter, C., 2009. Latest Pleistocene and Holocene glacier variations in the European Alps. Quat. Sci. Rev. 28, 2137–2149. https://doi.org/10.1016/j.quascirev.2009.03.009

Jacomet, S., 2009. Plant economy and village life in Neolithic lake dwellings at the time of the Alpine Iceman. Veg. Hist. Archaeobot. 18, 47–59. https://doi.org/10.1007/s00334-007-0138-2

Jacot-Guillarmod, C., Leuzinger, R., Bureau, S.E.T., (Wien), K.-K.M.-G.I., 1896. Samnaun. Topogr. Atlas der Schweiz [Kartenmaterial] 417,1896, Topographischer Atlas der Schweiz [Kartenmaterial] 417,1896.

Joerin, U.E., Nicolussi, K., Fischer, A., Stocker, T.F., Schlüchter, C., 2008. Holocene optimum events inferred from subglacial sediments at Tschierva Glacier, Eastern Swiss Alps. Quat. Sci. Rev. 27, 337–350. https://doi.org/10.1016/j.quascirev.2007.10.016

Joerin, U.E., Stocker, T.F., Schlüchter, C., 2006. Multicentury glacier fluctuations in the Swiss Alps during the Holocene. Holocene 16, 697–704. https://doi.org/10.1191/0959683606hl964rp

Johnston, C.A., 1991. Sediment and nutrient retention by freshwater wetlands: effects on surface water quality. Crit. Rev. Environ. Sci. Technol. 21, 491–565.

Jones, J.M., Hao, J., 1993. Ombrotrophic peat as a medium for historical monitoring of heavy metal pollution. Environ. Geochem. Health 15, 67–74. https://doi.org/10.1007/BF02627824

Jowsey, P.C., 1966. an Improved Peat Sampler. New Phytol. 65, 245–248. https://doi.org/10.1111/j.1469-8137.1966.tb06356.x

Kadlec, R.H., 1997. An autobiotic wetland phosphorus model. Ecol. Eng. 8, 145–172.

Kaiser, R., 2010. Das römische Erbe und das Merowingerreich, Enzyklopädie deutscher Geschichte. De Gruyter.

Kalnicky, D.J., Singhvi, R., 2001. Field portable XRF analysis of environmental samples. J. Hazard. Mater. 83, 93–122. https://doi.org/10.1016/S0304-3894(00)00330-7

Kappelmeyer, T., 2014. 7500 Jahre lokale und regionale Floren3 und Vegetationsentwicklung im Umkreis des Unteren Butterwiesenmoores (Fimbertal, Kanton Graubünden, Schweiz) im archäologischen und paläoklimatologischen Kontext. Leopold Franzens Universität Innsbruck.

Kapustová, V., Pánek, T., Hradecký, J., Zernitskaya, V., Hutchinson, S.M., Mulková, M., Sedláček, J., Bajer, V., 2018. Peat bog and alluvial deposits reveal land degradation during 16th-and 17th-century colonisation of the Western Carpathians (Czech Republic). L. Degrad. Dev. 29, 894–906. https://doi.org/10.1002/ldr.2909

Kata, B., 1995. Das Allgäu in Mittelalter und früher Neuzeit. Spätmittelalterliche und neuzeitliche Glashütten im Allgäu, in: Czysz, W., Dietrich, H., Weber, G. (Eds.), Kempten Und Das Allgäu. Führer Zu Archäologischen Denkmälern in Deutschland 30. Theiss, Stuttgart, pp. 95–98.

Kathrein, Y., 2012. Die Namen in der Silvretta, in: Reitmaier, T. (Ed.), Letzte Jäger, Erste Hirten - Hochalpine Archäologie in Der Silvretta. Archäologischer Dienst Graubünden, Chur, pp. 101–110.

Kempter, H., Görres, M., Frenzel, B., 1997. Ti and Pb concentrations in rainwater-fed bogs in Europe as indicators of past anthropogenic activities. Water. Air. Soil Pollut. 100, 367–377.

Kerndorff, H., Schnitzer, M., 1980. Sorption of metals on humic acid. Geochim. Cosmochim. Acta 44, 1701–1708.

Kerschner, H., Hertl, A., Gross, G., Ivy-Ochs, S., Kubik, P.W., 2006. Surface exposure dating of moraines in the Kromer valley (Silvretta Mountains, Austria)-evidence for glacial response to the 8.2 ka event in the Eastern Alps? The Holocene 16, 7–15. https://doi.org/10.1196/0959683606hl902rp

Kilian, R., Hohner, M., Biester, H., Wallrabe-Adams, H.J., Stern, C.R., 2003. Holocene peat and lake sediment tephra record from the southernmost Chilean Andes (53-55 S). Rev. Geol. Chile 30, 23–37.

Kinniburgh, D.G., van Riemsdijk, W.H., Koopal, L.K., Borkovec, M., Benedetti, M.F., Avena, M.J., 1999. Ion binding to natural organic matter: competition, heterogeneity, stoichiometry and thermodynamic consistency. Colloids Surfaces A Physicochem. Eng. Asp. 151, 147–166.

Kivinen, E., Pakarinen, P., 1981. Geographical distribution of peat resources and major peatland complex types in the world. Suomalainen tiedeakatemia.

Klaminder, J., Renberg, I., Bindler, R., Emteryd, O., 2003. Isotopic trends and background fluxes of atmospheric lead in northern Europe: analyses of three ombrotrophic bogs from south Sweden. Global Biogeochem. Cycles 17.

Klavins, M., Silamikele, I., Nikodemus, O., Kalnina, L., Kuske, E., Rodinov, V., Purmalis, O., 2009.

Peat properties, major and trace element accumulation in bog peat in Latvia. Baltica 22, 37–49.

Koinig, K., Shotyk, W., Lotter, A., Ohlendorf, C., 2003. 9000 Years of Geochemical Evolution of Lithogenic Major and Trace Elements in the Sediment of an alpine lake – the role of climate, vegetation, and land- use history. J. Paleolimnol. 4, 307–320. https://doi.org/10.1023/a:1026080712312

Koppisch, D., 2012. Torfbildung, in: Joosten, H., Succow, M. (Eds.), Landschaftsökologische Moorkunde. Schweizerbart Science Publishers, Stuttgart, Germany, pp. 9–17.

Koster, E.A., Favier, T., 2005. Peatlands, Past and Present, in: Koster, E.A. (Ed.), The Physical Geography of Western Europe, Oxford Regional Environments. OUP Oxford, pp. 161–182.

Kothieringer, K., Walser, C., Dietre, B., Reitmaier, T., Haas, J.N., Lambers, K., 2015. High impact: early pastoralism and environmental change during the Neolithic and Bronze Age in the Silvretta Alps (Switzerland/Austria) as evidenced by archaeological, palaeoecological and pedological proxies. Zeitschrift für Geomorphol. Suppl. Issues 59, 177–198.

Krachler, M., Mohl, C., Emons, H., Shotyk, W., 2003. Two thousand years of atmospheric rare earth element (REE) deposition as revealed by an ombrotrophic peat bog profile, Jura Mountains, Switzerland. J. Environ. Monit. 5, 111–121. https://doi.org/10.1039/b208355h

Krachler, M., Mohl, C., Emons, H., Shotyk, W., 2002. Analytical procedures for the determination of selected trace elements in peat and plant samples by inductively coupled plasma mass spectrometry. Spectrochim. Acta - Part B At. Spectrosc. 57, 1277–1289. https://doi.org/10.1016/S0584-8547(02)00068-X

Kralj, P., Veber, M., 2003. Investigations into nonspectroscopic effects of organic compounds in inductively coupled plasma mass spectrometry. Acta Chim. Slov. 50, 633–644.

Krause, R., 2007. The prehistoric settlement of the inneralpine valley of Montafon in Vorarlberg (Austria). Preist. Alp. 12, 119–136.

Krause, R., 1987. Early tin and copper metallurgy in south-western Germany at the beginning of the Early Bronze Age, in: Old World Archaeometallurgy: Proceedings of the International Symposium “Old World Archaeometallurgy,” Heidelberg. pp. 25–32.

Krefeld, T., Klausmann, H., 1986. Romanische und rätoromanische Reliktwörter im Arlberggebiet, in: Holtus, G., Ringger, K. (Eds.), RAETIA ANTIQUA ET MODERNA, W. Theodor Elwert Zum 80. Geburtstag. Max Niemeyer Verlag, Tübingen, pp. 121–146.

Kutschera, W., Patzelt, G., Wild, E.M., Haas-Jettmar, B., Kofler, W., Lippert, A., Oeggl, K., Pak, E., Priller, A., Steier, P., Wahlmüller-Oeggl, N., Zanesco, A., 2014. Evidence for Early Human Presence at High Altitudes in the Ötztal Alps (Austria/Italy). Radiocarbon 56, 923–947. https://doi.org/10.2458/56.17919

Kylander, M.E., Muller, J., Wüst, R.A.J., Gallagher, K., Garcia-Sanchez, R., Coles, B.J., Weiss, D.J., 2007. Rare earth element and Pb isotope variations in a 52 kyr peat core from Lynch’s Crater (NE Queensland, Australia): Proxy development and application to paleoclimate in the Southern Hemisphere. Geochim. Cosmochim. Acta 71, 942–960. https://doi.org/10.1016/j.gca.2006.10.018

Le Roux, G., Aubert, D., Stille, P., Krachler, M., Kober, B., Cheburkin, A., Bonani, G., Shotyk, W., 2005. Recent atmospheric Pb deposition at a rural site in southern Germany assessed using a peat core and snowpack, and comparison with other archives. Atmos. Environ. 39, 6790–6801. https://doi.org/10.1016/j.atmosenv.2005.07.026

Le Roux, G., De Vleeschouwer, F., 2010. Preparation of peat samples for inorganic geochemistry used as palaeoenvironmental proxies. Mires Peat 7, 1–9.

Le Roux, G., Weiss, D., Grattan, J., Givelet, N., Krachler, M., Cheburkin, A., Rausch, N., Kober, B., Shotyk, W., 2004. Identifying the sources and timing of ancient and medieval atmospheric lead pollution in England using a peat profile from Lindow bog, Manchester. J. Environ. Monit. 6, 502–510. https://doi.org/10.1039/B401500B

Leitner, W., 2015. Jägerische Archäologie im Hochgebirge, in: Stöllner, T., Oeggl, K. (Eds.), Bergauf Bergab. 10.000 Jahre Bergbau in Den Ostalpen. Deutsches Bergbau-Museum Bochum, Bochum, pp. 53–57.

Leitner, W., 2007. Der Weg der Feuersteine . Spuren zum ältesten Bergwerk Europas | Online-Artikel. Walserheimat 81, 6–7.

Leitner, W., 2003. Der Felsüberhang auf der Schneiderkürenalpe - Ein Jäger- und Hirtenlager der Vorzeit. Bergschau 1–32.

Leitner, W., Bachnetzer, T., Staudt, M., 2011. Die Anfänge des Abbaus mineralischer Rohstoffe in der Steinzeit, in: Goldenberg, G., Töchterle, U., Oeggl, K., Krenn-Leeb, A. (Eds.), Archäologie Österreichs Spezial. Forschungsprogramm HiMAT. Neues Zur Bergbaugeschichte Der Ostalpen. Wien, pp. 19–29.

Lichtenberger, E., 1965. Das Bergbauernproblem in den Österreichischen Alpen Perioden und Typen der Entsiedlung (The Problem of Mountain Farming in the Austrian Alps). Erdkunde 19, 39–57.

Liese-Kleiber, H., 1993. Settlement and landscape history at the Federsee, south-west Germany, as reflected in pollen diagrams. Veg. Hist. Archaeobot. 2, 37–46. https://doi.org/10.1007/BF00191704

Limpens, J., Berendse, F., Blodau, C., Canadell, J.G., Freeman, C., Holden, J., Roulet, N., Rydin, H., Schaepman-Strub, G., 2008. Peatlands and the carbon cycle: from local processes to global implications-a synthesis. Biogeosciences 5, 1475–1491.

Liritzis, I., Zacharias, N., 2011. Portable XRF of archaeological artifacts: current research, potentials and limitations, in: X-Ray Fluorescence Spectrometry (XRF) in Geoarchaeology. Springer, pp. 109–142.

Livingstone, D.A., 1955. A lightweight piston sampler for lake deposits. Ecology 36, 137–139.

Lomas-Clarke, S.H., Barber, K.E., 2007. Human impact signals from peat bogs–a combined palynological and geochemical approach. Veg. Hist. Archaeobot. 16, 419–429.

Longman, J., Veres, D., Wennrich, V., 2018. Utilisation of XRF core scanning on peat and other highly organic sediments. Quat. Int. 0–1. https://doi.org/10.1016/j.quaint.2018.10.015

Loveluck, C.P., McCormick, M., Spaulding, N.E., Clifford, H., Handley, M.J., Hartman, L., Hoffmann, H., Korotkikh, E. V, Kurbatov, A. V, More, A.F., Sneed, S.B., Mayewski, P.A., 2018. Alpine ice-core evidence for the transformation of the European monetary system, AD 640–670. Antiquity 1–15. https://doi.org/10.15184/aqy.2018.110

Lowe, L.E., Bustin, R.M., 1985. Distribution of sulphur forms in six facies of peats of the Fraser River Delta. Can. J. Soil Sci. 65, 531–541.

Löwemark, L., Chen, H.F., Yang, T.N., Kylander, M., Yu, E.F., Hsu, Y.W., Lee, T.Q., Song, S.R., Jarvis, S., 2011. Normalizing XRF-scanner data: A cautionary note on the interpretation of high-resolution records from organic-rich lakes. J. Asian Earth Sci. 40, 1250–1256. https://doi.org/10.1016/j.jseaes.2010.06.002

Lutz, J., Pernicka, E., 2013. Prehistoric copper from the Eastern Alps. Open J. Archaeom. 1, 25. https://doi.org/10.4081/arc.2013.e25

Lutz, J., Schwab, R., 2015. Eisenzeitliche Nutzung alpiner Kupferlagerstätten, in: Stöllner, T., Oeggl, K. (Eds.), Bergauf Bergab. 10.000 Jahre Bergbau in Den Ostalpen. Deutsches Bergbau-Museum Bochum, Bochum, pp. 113–116.

Ma, W., Tobin, J.M., 2004. Determination and modelling of effects of pH on peat biosorption of chromium, copper and cadmium. Biochem. Eng. J. 18, 33–40.

Ma, W., Tobin, J.M., 2003. Development of multimetal binding model and application to binary metal biosorption onto peat biomass. Water Res. 37, 3967–3977.

Mackensen, M., 1995. Die spätrömische Grenze im Gebiet von Cambidano-Kempten, in: Czysz, W., Dietrich, H., Weber, G. (Eds.), Kempten Und Das Allgäu. Führer Zu Archäologischen Denkmälern in Deutschland 30. Theiss, Stuttgart, pp. 61–69.

Magny, M., Galop, D., Bellintani, P., Desmet, M., Didier, J., Haas, J.N., Martinelli, N., Pedrotti, A., Scandolari, R., Stock, A., Vannière, B., 2009. Late-Holocene climatic variability south of the Alps as recorded by lake-level fluctuations at Lake Ledro, Trentino, Italy. Holocene 19, 575–589. https://doi.org/10.1177/0959683609104032

Maltby, E., Proctor, M.C.F., 1996. Peatlands: their nature and role in the biosphere.

Mann, M.E., 2002. Medieval Climatic Optimum. Encycl. Glob. Environ. Chang. 1, 514–516.

Mansel, K., 1989. Ein latènezeitlicher Schlüssel mit Stierplastik aus Sonthofen im Allgäu. Germania 67, 572–587.

Mariet, A.-L., Bégeot, C., Gimbert, F., Gauthier, J., Fluck, P., Walter-Simonnet, A.-V., 2016. Past mining activities in the Vosges Mountains (eastern France): Impact on vegetation and metal contamination over the past millennium. The Holocene 26, 1225–1236. https://doi.org/10.1177/0959683616638419

Martínez Cortizas, A., López-Merino, L., Bindler, R., Mighall, T., Kylander, M.E., 2016. Early atmospheric metal pollution provides evidence for Chalcolithic/Bronze Age mining and metallurgy in Southwestern Europe. Sci. Total Environ. 545–546, 398–406. https://doi.org/10.1016/j.scitotenv.2015.12.078

Marx, S.K., Rashid, S., Stromsoe, N., 2016. Global-scale patterns in anthropogenic Pb contamination reconstructed from natural archives. Environ. Pollut. 213, 283–298.

Matthews, J.A., Berrisford, M.S., Quentin Dresser, P., Nesje, A., Olaf Dahl, S., Elisabeth Bjune, A., Bakke, J., John, H., Birks, B., Lie, Ø., Dumayne-Peaty, L., Barnett, C., 2005. Holocene glacier history of Bjørnbreen and climatic reconstruction in central Jotunheimen, Norway, based on proximal glaciofluvial stream-bank mires. Quat. Sci. Rev. 24, 67–90. https://doi.org/10.1016/j.quascirev.2004.07.003

Matthews, J.A., Briffa, K.R., 2005. The “Little Ice Age”: Re-evaluation of an evolving concept. Geogr. Ann. Ser. A Phys. Geogr. 87, 17–36. https://doi.org/10.1111/j.0435-3676.2005.00242.x

McClymont, E., Pendall, E., Nichols, J.E., 2010. Stable isotopes and organic geochemistry in peat: Tools to investigate past hydrology, temperature and biogeochemistry. PAGES news 18, 15–18. https://doi.org/10.1002/jqs.1295.Mitchell

McEvedy, C., Jones, R., 1978. Atlas of world population history. Penguin Books Ltd, Harmondsworth, Middlesex, England.

McLennan, S.M., 2001. Relationships between the trace element composition of sedimentary rocks and upper continental crust. Geochemistry, Geophys. Geosystems 2. https://doi.org/10.1029/2000GC000109

Mejía-Piña, K.G., Huerta-Diaz, M.A., González-Yajimovich, O., 2016. Calibration of handheld X-ray fluorescence (XRF) equipment for optimum determination of elemental concentrations in sediment samples. Talanta 161, 359–367. https://doi.org/10.1016/j.talanta.2016.08.066

Merbeler, J., 1995. Erzbergbau und Verhüttung im Starzlachtal, in: Czysz, W., Dietrich, H., Weber, G. (Eds.), Kempten Und Das Allgäu. Führer Zu Archäologischen Denkmälern in Deutschland 30. Theiss, Stuttgart, pp. 149–152.

Mighall, T.M., Grattan, J.P., Timberlake, S., Lees, J.A., Forsyth, S., 2002. An atmospheric pollution history for lead–zinc mining from the Ystwyth Valley, Dyfed, mid-Wales, UK as recorded by an upland blanket peat. Geochemistry Explor. Environ. Anal. 2, 175–184.

Mighall, T.M., Timberlake, S., Foster, I.D.L., Krupp, E., Singh, S., 2009. Ancient copper and lead pollution records from a raised bog complex in Central Wales, UK. J. Archaeol. Sci. 36, 1504–1515. https://doi.org/10.1016/j.jas.2009.03.005

Mingram, J., Negendank, J.F.W., Brauer, A., Berger, D., Hendrich, A., Köhler, M., Usinger, H., 2007. Long cores from small lakes - Recovering up to 100 m-long lake sediment sequences with a high-precision rod-operated piston corer (Usinger-corer). J. Paleolimnol. 37, 517–528. https://doi.org/10.1007/s10933-006-9035-4

Moe, D., Fedele, F.G., Maude, A.E., Kvamme, M., 2007. Vegetational changes and human presence in the low-alpine and subalpine zone in Val Febbraro, upper Valle di Spluga (Italian central Alps), from the Neolithic to the Roman period. Veg. Hist. Archaeobot. 16, 431–451. https://doi.org/10.1007/s00334-006-0088-0

Monna, F., Petit, C., Guillaumet, J.-P., Jouffroy-Bapicot, I., Blanchot, C., Dominik, J., Losno, R., Richard, H., Lévêque, J., Chateau, C., 2004. History and Environmental Impact of Mining Activity in Celtic Aeduan Territory Recorded in a Peat Bog (Morvan, France). Environ. Sci. Technol. 38, 665–673. https://doi.org/10.1021/es034704v

Moore, P., Webb, J., Collinson, M., 1991. Pollen Analysis. Blackwell Scientific Publications Ltd, Oxford.

Moore, P D, 2013. European Mires, in: Moore, Peter D. (Ed.), . Academic Press, pp. 1–10. https://doi.org/10.1016/C2013-0-11194-4

Moran, A.P., Kerschner, H., Ochs, S.I., 2015. Redating the moraines in the Kromer Valley (Silvretta Mountains) – New evidence for an early Holocene glacier advance. Holocene 26, 655–664. https://doi.org/10.1177/0959683615612571

Muller, J., Kylander, M., Martinez-cortizas, A., Wu, R.A.J., Weiss, D., Blake, K., Coles, B., Garcia-sanchez, R., 2008. The use of principle component analyses in characterising trace and major elemental distribution in a 55 kyr peat deposit in tropical Australia : Implications to paleoclimate 72, 449–463. https://doi.org/10.1016/j.gca.2007.09.028

Naturpark Kaunergrat, 2000. Naturwanderführer durch die Piller Moore.

Nesbitt, H.W., Markovics, G., 1997. Weathering of granodioritic crust, long-term storage of elements in weathering profiles, and petrogenesis of siliciclastic sediments. Geochim. Cosmochim. Acta 61, 1653–1670. https://doi.org/https://doi.org/10.1016/S0016-7037(97)00031-8

Neuhauser, G., 2015. ,,Argentifodinam seu montem dictum Mùntafùne ,, - 1000 Jahre Bergbau im südlichen Vorarlberg, in: Stöllner, T., Oeggl, K. (Eds.), Bergauf Bergab. 10.000 Jahre Bergbau in Den Ostalpen. Deutsches Bergbau-Museum Bochum, Bochum, pp. 447–454.

Nicolussi Castellan, S., Tomedi, G., Lachberger, R., 2008. Das bronzezeitliche Haus von Fließ-Silberplan, in: Oeggl, K., Schaffer, V. (Eds.), Die Geschichte Des Bergbaus in Tirol Und Seinen Angrenzenden Gebieten. Proceedings Zum 3. Milestone Meeting Des SFB HiMAT. p. 2008.

Nicolussi, K., 2012. Jahrringdaten zur nacheiszeitlichen Waldverbreitung in der Silvretta, in: Reitmaier, T. (Ed.), Letzte Jäger, Erste Hirten - Hochalpine Archäologie in Der Silvretta. Archäologischer Dienst Graubünden, Chur, pp. 87–98.

Nicolussi, K., Kaufmann, M., Patzelt, G., Van Der Plicht, J., Thurner, A., 2005. Holocene tree-line variability in the Kauner Valley, Central Eastern Alps, indicated by dendrochronological analysis of living trees and subfossil logs. Veg. Hist. Archaeobot. 14, 221–234. https://doi.org/10.1007/s00334-005-0013-y

Nicolussi, K., Patzelt, G., 2000. Untersuchungen zur holozänen Gletscherentwicklung von Pasterze und Gepatschferner (Ostalpen). Zeitschrift für Gletscherkd. und Glazialgeol. 36, 1–87.

Nicolussi, K., Schlüchter, C., 2012. The 8.2 ka event—Calendar-dated glacier response in the Alps. Geology 40, 819–822.

Niedermayr, G., Auer, C., Berger, A., Bernhard, F., Bojar, H.-P., BRANDSTÄTTER, F., Fink, R., Hollerer, C.E., Kolitsch, U., MÖRTL, J., Postl, W., Prasnik, H., Schabereiter, H., Schillhammer, H., Steinwender, C., Strobl, M., Walter, F., Taucher, J., 2014. Neue Mineralfunde aus Österreich LXIII. Carinthia II 204, 65–146.

Nieminen, T.M., Ukonmaanaho, L., Shotyk, W., 2002. Enrichment of Cu, Ni, Zn, Pb and As in an ombrotrophic peat bog near a Cu-Ni smelter in Southwest Finland. Sci. Total Environ. 292, 81–89.

Novák, M., Adamová, M., Wieder, R.K., Bottrell, S.H., 2005. Sulfur mobility in peat. Appl. Geochemistry 20, 673–681. https://doi.org/10.1016/j.apgeochem.2004.11.009

Novak, M., Zemanova, L., Voldrichova, P., Stepanova, M., Adamova, M., Pacherova, P., Komarek, A., Krachler, M., Prechova, E., 2011. Experimental evidence for mobility/immobility of metals in peat. Environ. Sci. Technol. 45, 7180–7187. https://doi.org/10.1021/es201086v

Nowotny, A., Pestal, G., Rockenschaub, M., 1993. Der geologische Bau des nördlichen Silvrettamasse und die Problematik der geologischen Stellung der Zone von Puschlin. Geol. des Oberinntaler Raumes - Schwerpkt. Blatt 144 Landeck. Arbeitstagung Geol. Bundesanstalt Österreich 55–91.

Nriagu, J.O., 1983. Lead and lead poisoning in antiquity, Lead and lead poisoning in antiquity. John Wiley, New York.

O'Brien, W., 2015. Prehistoric Copper Mining in Europe: 5500-500 BC. Oxford University Press.

Oblinger, H., 2002. Rohstoffe aus Schwabens Boden und ihre geologischen Grundlagen. Berichte des Naturwissenschaftlichen Vereins für Schwaben e.V. 106, 2–31.

Oblinger, H., 1996. Blei- und Zinkerz am Roßkopf (Ostrachtal/Allgäuer Alpen). Berichte des Naturwissenschaftlichen Vereins für Schwaben e.V. 100, 85–90.

Oeggl, K., 2015. Vegetationsgeschichte und Landnutzung, in: Stöllner, T., Oeggl, K. (Eds.),

Bergauf Bergab. 10.000 Jahre Bergbau in Den Ostalpen. Deutsches Bergbau-Museum Bochum, Bochum, pp. 43–49.

Oeggl, K., Nicolussi, K., 2009. Prähistorische Besiedlung von zentralen Alpentälern in Bezug zur Klimaentwicklung, in: Roland Psenner, Reinhard Lackner, A.B. (Ed.), Klimawandel in Österreich: Die Letzten 20.000 Jahre ... Und Ein Blick Voraus. innsbruck university press, pp. 77–86.

Ohlendorf, C., Wennrich, V., Enters, D., 2015. Experiences with XRF-scanning of long sediment records, in: Croudace, I.W., Rothwell, R.G. (Eds.), Micro-XRF Studies of Sediment Cores: Applications of a Non-Destructive Tool for the Environmental Sciences (Developments in Paleoenvironmental Research). Springer, pp. 351–372.

Pacyna, J.M., Pacyna, E.G., 2001. An assessment of global and regional emissions of trace metals to the atmosphere from anthropogenic sources worldwide. Environ. Rev. 9, 269–298. https://doi.org/10.1139/er-9-4-269

Page, S.E., Baird, A.J., 2016. Peatlands and global change: response and resilience. Annu. Rev. Environ. Resour. 41, 35–57. https://doi.org/10.1146/annurev-environ-110615-085520

Page, S.E., Siegert, F., Rieley, J.O., Boehm, H.-D. V, Jaya, A., Limin, S., 2002. The amount of carbon released from peat and forest fires in Indonesia during 1997. Nature 420, 61.

Päivänen, J., Vasander, H., 1994. Carbon balance in mire ecosystems, in: World Resource Review. pp. 102–111.

Palmer, P.T., Jacobs, R., Baker, P.E., Ferguson, K., Webber, S., 2009. Use of field-portable XRF analyzers for rapid screening of toxic elements in FDA-regulated products. J. Agric. Food Chem. 57, 2605–2613.

Patzelt, G., Bortenschlager, S., 1973. 1973: Die postglazialen Gletscherund Klimaschwankungen in der Venedigergruppe (Hohe Tauern, Ostalpen). Zeitschrift für Geomorphologie Neue Folge 16, Supplement, 25-72.

Pernicka, E., Frank, C., 2015. Das Kupfer der Mondseegruppe, in: Stöllner, T., Oeggl, K. (Eds.), Bergauf Bergab. 10.000 Jahre Bergbau in Den Ostalpen. Deutsches Bergbau-Museum Bochum, Bochum, pp. 77–83.

Piotrowska, N., Blaauw, M., Mauquoy, D., Chambers, F.M., 2011. Constructing deposition chronologies for peat deposits using radiocarbon dating. Mires Peat 7, 1–14.

Piotrowska, N., De Vleeschouwer, F., Sikorski, J., Pawlyta, J., Fagel, N., Le Roux, G., Pazdur, A., 2010. Intercomparison of radiocarbon bomb pulse and 210Pb age models. A study in a peat bog core from North Poland. Nucl. Instruments Methods Phys. Res. Sect. B Beam Interact. with Mater. Atoms 268, 1163–1166.

Pöll, J., 1998. Urgeschichte und Römerzeit in Landeck, in: Baeck, P. (Ed.), Stadtbuch Landeck. Landeck, pp. 53–66.

Poto, L., Gabrieli, J., Crowhurst, S., Agostinelli, C., Spolaor, A., Cairns, W.R.L., Cozzi, G., Barbante, C., 2015. Cross calibration between XRF and ICP-MS for high spatial resolution analysis of ombrotrophic peat cores for palaeoclimatic studies. Anal. Bioanal. Chem. 407, 379–385. https://doi.org/10.1007/s00216-014-8289-3

Pott, R., Hüppe, J., Remy, D., Bauerochse, A., Katenhusen, O., 1995. Paläoökologische Untersuchungen zu holozänen Waldgrenzschwankungen im oberen Fimbertal (Val Fenga, Silvretta, Ostschweiz). Phytocoenologia 25, 363–398. https://doi.org/10.1127/phyto/25/1995/363

Prohaska, T., Hann, S., Latkoczy, C., Stingeder, G., 1999. Determination of rare earth elements U and Th in environmental samples by inductively coupled plasma double focusing sectorfield mass spectrometry (ICP-SMS). J. Anal. At. Spectrom. 14, 1–8. https://doi.org/10.1039/a806720a

R Core Team, 2017. R: A Language and Environment for Statistical Computing.

Rabassa, J., Coronato, A., Heusser, C.J., Roig Juñent, F., Borromei, A., Roig, C., Quattrocchio, M., 2006. Chapter 6 The peatlands of Argentine Tierra del Fuego as a source for paleoclimatic and paleoenvironmental information. pp. 129–144. https://doi.org/10.1016/S0928-2025(06)09006-7

Radivojević, M., Rehren, T., Pernicka, E., Šljivar, D., Brauns, M., Borić, D., 2010. On the origins of extractive metallurgy: new evidence from Europe. J. Archaeol. Sci. 37, 2775–2787.

Ravansari, R., Lemke, L.D., 2018. Portable X-ray fluorescence trace metal measurement in organic rich soils: pXRF response as a function of organic matter fraction. Geoderma 319, 175–184. https://doi.org/10.1016/j.geoderma.2018.01.011

Reimer, P.J., Bard, E., Bayliss, A., Beck, J.W., Blackwell, P.G., Ramsey, C.B., Buck, C.E., Cheng, H., Edwards, R.L., Friedrich, M., Grootes, P.M., Guilderson, T.P., Haflidason, H., Hajdas, I., Hatté, C., Heaton, T.J., Hoffmann, D.L., Hogg, A.G., Hughen, K.A., Kaiser, K.F., Kromer, B., Manning, S.W., Niu, M., Reimer, R.W., Richards, D.A., Scott, E.M., Southon, J.R., Staff, R.A., Turney, C.S.M., van der Plicht, J., 2013. IntCal13 and Marine13 Radiocarbon Age Calibration Curves 0–50,000 Years cal BP. Radiocarbon 55, 1869–1887. https://doi.org/10.2458/azu_js_rc.55.16947

Reitmaier, T., 2017. Prähistorische Alpwirtschaft. Eine archäologische Spurensuche in der Silvretta (CH/A), 2007–2016., in: Archäologie Schweiz 100. Archäologie Schweiz, Basel, pp. 7–53.

Reitmaier, T., 2012. Letzte Jäger, erste Hirten, in: Reitmaier, T. (Ed.), Letzte Jäger, Erste Hirten - Hochalpine Archäologie in Der Silvretta. Archäologischer Dienst Graubünden, Chur, pp. 9–65.

Reitmaier, T., Doppler, T., Pike, A.W.G., Deschler-Erb, S., Hajdas, I., Walser, C., Gerling, C., 2018. Alpine cattle management during the Bronze Age at Ramosch-Mottata, Switzerland. Quat. Int. 484, 19–31. https://doi.org/10.1016/j.quaint.2017.02.007

Reitmaier, T., Lambers, K., Walser, C., Zingman, I., Haas, J.N., Dietre, B., Reidl, D., Hajdas, I., Nicolussi, K., Kathrein, Y., 2013. Alpine Archäologie in der Silvretta. Archäologie Schweiz 36, 4–15.

Remy, D., 2012. Waldgrenze und Waldgrenzschwankungen in der Silvretta / Zentralalpen - Funde von Pinus cembra oberhalb der potentiellen Waldgrenze im Oberen Fimbertal. Berichte der Reinhold-Tüxen Gesellschaft e.V. 24, 61–75.

Revelle, R., Suess, H.E., 1957. Carbon dioxide exchange between atmosphere and ocean and the question of an increase of atmospheric CO2 during the past decades. Tellus 9, 18–27.

Richter, T.O., van der Gaast, S., Koster, B., Vaars, A., Gieles, R., de Stigter, H.C., De Haas, H., van Weering, T.C.E., 2006. The Avaatech XRF Core Scanner: technical description and applications to NE Atlantic sediments. Geol. Soc. London, Spec. Publ. 267, 39–50. https://doi.org/10.1144/GSL.SP.2006.267.01.03

Ringqvist, L., Öborn, I., 2002. Copper and zinc adsorption onto poorly humified Sphagnum and Carex peat. Water Res. 36, 2233–2242. https://doi.org/10.1016/S0043-1354(01)00431-6

Roepke, A., Krause, R., 2013. High montane-subalpine soils in the Montafon Valley (Austria, northern Alps) and their link to land-use, fire and settlement history. Quat. Int. 308–309, 178–189. https://doi.org/10.1016/j.quaint.2013.01.022

Roepke, A., Stobbe, A., Oeggl, K., Kalis, A.J., Tinner, W., 2011. Late-Holocene land-use history and environmental changes at the high altitudes of St Antönien (Switzerland, Northern Alps): Combined evidence from pollen, soil and tree-ring analyses. The Holocene 21, 485–498. https://doi.org/10.1177/0959683610385727

Rogora, M., Mosello, R., Arisci, S., Brizzio, M.C., Barbieri, A., Balestrini, R., Waldner, P., Schmitt, M., Stähli, M., Thimonier, A., Kalina, M., Puxbaum, H., Nickus, U., Ulrich, E., Probst, A., 2006. An Overview of Atmospheric Deposition Chemistry over the Alps: Present Status and Long-term Trends. Hydrobiologia 562, 17–40. https://doi.org/10.1007/s10750-005-1803-z

Rohling, E.J., Pälike, H., 2005. Centennial-scale climate cooling with a sudden cold event around 8,200 years ago. Nature 434, 975.

Rösch, M., 1996. Archäobotanische Untersuchungen in der spätbronzezeitlichen Ufersiedlung Hagnau-Burg (Bodenseekreis), Siedlungsarchäologie im Alpenvorland IV. Die Spätbronzezeit am nordwestlichen Bodensee Taucharchäologische Untersuchungen in Hagnau und Unteruhldingen 1982-1989. Theiss, Stuttgart.

Rösch, M., 1993. Prehistoric land use as recorded in a lake-shore core at Lake Constance. Veg. Hist. Archaeobot. 2, 213–232. https://doi.org/10.1007/BF00198163

Rösch, M., 1992. Human impact as registered in the pollen record: some results from the western Lake Constance region, Southern Germany. Veg. Hist. Archaeobot. 1, 101–109. https://doi.org/10.1007/BF00206090

Rothwell, J.J., Evans, M.G., Liddaman, L.C., Allott, T.E.H., 2007. The role of wildfire and gully erosion in particulate Pb export from contaminated peatland catchments in the southern Pennines, U.K. Geomorphology 88, 276–284. https://doi.org/10.1016/j.geomorph.2006.11.011

Rothwell, J.J., Taylor, K.G., Ander, E.L., Evans, M.G., Daniels, S.M., Allott, T.E.H., 2009. Arsenic retention and release in ombrotrophic peatlands. Sci. Total Environ. 407, 1405–1417. https://doi.org/10.1016/j.scitotenv.2008.10.015

Rothwell, J.J., Taylor, K.G., Chenery, S.R.N., Cundy, A.B., Evans, M.G., Allott, T.E.H., 2010. Storage and behavior of As, Sb, Pb, and Cu in ombrotrophic peat bogs under contrasting water table conditions. Environ. Sci. Technol. 44, 8497–8502. https://doi.org/10.1021/es101150w

Rothwell, J.J., Taylor, K.G., Evans, M.G., Allott, T.E.H., 2011. Contrasting controls on arsenic and lead budgets for a degraded peatland catchment in Northern England. Environ. Pollut. 159, 3129–3133. https://doi.org/10.1016/j.envpol.2011.05.026

Rougier, H., Sanguin, A.-L., 1981. Deux zones franches au cœur des Alpes Centrales: Livigno et Samnaun. Rev. géographie Alp. 69, 543–560.

Røyset, J., Ryum, N., 2005. Scandium in aluminium alloys. Int. Mater. Rev. 50, 19–44. https://doi.org/10.1179/174328005X14311

Rubel, F., Brugger, K., Haslinger, K., Auer, I., 2017. The climate of the European Alps: Shift of very high resolution Köppen-Geiger climate zones 1800-2100. Meteorol. Zeitschrift 26, 115–125. https://doi.org/10.1127/metz/2016/0816

Sahraoui, H., Hachicha, M., 2017. Effect of soil moisture on trace elements concentrations using portable x-ray fluorescence spectrometer. J. Fundam. Appl. Sci. 9, 468–484.

Sapkota, A., Cheburkin, A.K., Bonani, G., Shotyk, W., 2007. Six millennia of atmospheric dust deposition in southern South America (Isla Navarino, Chile). The Holocene 17, 561–572.

Sapkota, A., Krachler, M., Scholz, C., Cheburkin, A.K., Shotyk, W., 2005. Analytical procedures for the determination of selected major (Al, Ca, Fe, K, Mg, Na, and Ti) and trace (Li, Mn, Sr, and Zn) elements in peat and plant samples using inductively coupled plasma-optical emission spectrometry. Anal. Chim. Acta 540, 247–256. https://doi.org/10.1016/j.aca.2005.03.008

Schach, C., Minsinger, S., 1849. Geognostische Karte Tirols 1:115.200.

Schellekens, J., Bindler, R., Martínez-Cortizas, A., McClymont, E.L., Abbott, G.D., Biester, H., Pontevedra-Pombal, X., Buurman, P., 2015. Preferential degradation of polyphenols from Sphagnum–4-Isopropenylphenol as a proxy for past hydrological conditions in Sphagnum-dominated peat. Geochim. Cosmochim. Acta 150, 74–89.

Schlüchter, C., Jörin, U., 2004. Holz-und Torffunde als Klimaindikatoren. Alpen ohne Gletscher? Die Alpen 80, 34–47.

Schmidl, A., Oeggl, K., 2005a. Land Use in the Eastern Alps During the Bronze Age — an Archaeobotanical Case Study of a Hilltop Settlement in the Montafon (Western Austria) 2, 455–470.

Schmidl, A., Oeggl, K., 2005b. Subsistence strategies of two Bronze Age hill-top settlements in the eastern Alps—Friaga/Bartholomäberg (Vorarlberg, Austria) and Ganglegg/Schluderns (South Tyrol, Italy). Veg. Hist. Archaeobot. 14, 303–312. https://doi.org/10.1007/s00334-005-0088-5

Schmidt-Thomé, P., 1960. Zur Geologie und Morphologie des Ifengebirgsstockes (Allgäu): Erläuterungen zur topographisch-morphologischen Kartenprobe VI 3: Alpiner Karst und Bergsturz (On the Geology and Morphology of the Hohe Ifen). Erdkunde 14, 181–195.

Schmidt, R., Koinig, K.A., Thompson, R., Kamenik, C., 2002. A multi proxy core study of the last 7000 years of climate and alpine land-use impacts on an Austrian mountain lake (Unterer Landschitzsee, Niedere Tauern). Palaeogeogr. Palaeoclimatol. Palaeoecol. 187, 101–120.

Schneeberger, N., Bürgi, M., Hersperger, A.M., Ewald, K.C., 2007a. Driving forces and rates of landscape change as a promising combination for landscape change research—An application on the northern fringe of the Swiss Alps. Land use policy 24, 349–361. https://doi.org/10.1016/j.landusepol.2006.04.003

Schneeberger, N., Bürgi, M., Kienast, P.D.F., 2007b. Rates of landscape change at the northern fringe of the Swiss Alps: Historical and recent tendencies. Landsc. Urban Plan. 80, 127–136. https://doi.org/10.1016/j.landurbplan.2006.06.006

Schofield, J.E., Edwards, K.J., Mighall, T.M., Martínez Cortizas, A., Rodríguez-Racedo, J., Cook, G., 2010. An integrated geochemical and palynological study of human impacts, soil erosion and storminess from southern Greenland since c. AD 1000. Palaeogeogr. Palaeoclimatol. Palaeoecol. 295, 19–30. https://doi.org/10.1016/j.palaeo.2010.05.011

Schönberger, H., 1969. The Roman frontier in Germany: an archaeological survey. J. Rom. Stud. 59, 144–197. https://doi.org/10.2307/299853

Schrautzer, J., Bork, H.-R., Christ, L., El-Balti, N., Martens, T., Kempke, M., von Scheffer, C., Unkel, I., n.d. Classification, ecological characterization and development of montane

mires. Phytocoenologia - J. Veg. Ecol.

Shakesby, R.A., Smith, J.G., Matthews, J.A., Winkler, S., Dresser, P.Q., Bakke, J., Dahl, S.-O., Lie, Ø., Nesje, A., 2007. Reconstruction of Holocene glacier history from distal sources: glaciofluvial stream-bank mires and a glaciolacustrine sediment core near Sota Sæter, Breheimen, southern Norway. The Holocene 17, 729–745. https://doi.org/10.1177/0959683607080514

Shand, C.A., Wendler, R., 2014. Portable X-ray fluorescence analysis of mineral and organic soils and the influence of organic matter. J. Geochemical Explor. 143, 31–42. https://doi.org/10.1016/j.gexplo.2014.03.005

Shaw, G., Williams, A.M., 1994. Critical issues in tourism: a geographical perspective. Blackwell Publishers.

Shotyk, W., 2002. The chronology of anthropogenic, atmospheric Pb deposition recorded by peat cores in three minerogenic peat deposits from Switzerland. Sci. Total Environ. 292, 19–31. https://doi.org/10.1016/s0048-9697(02)00030-x

Shotyk, W., 1996a. Natural and anthropogenic enrichments of As, Cu, Pb, Sb, and Zn in ombrotrophic versus minerotrophic peat bog profiles, Jura Mountains, Switzerland. Water. Air. Soil Pollut. 90, 375–405. https://doi.org/10.1007/BF00282657

Shotyk, W., 1996b. Peat bog archives of atmospheric metal deposition: geochemical evaluation of peat profiles, natural variations in metal concentrations, and metal enrichment factors. Environ. Rev. 4, 149–183. https://doi.org/10.1139/a96-010

Shotyk, W., 1988. Review of the inorganic geochemistry of peats and peatland waters. Earth Sci. Rev. 25, 95–176. https://doi.org/10.1016/0012-8252(88)90067-0

Shotyk, W., Cheburkin, A.K., Appleby, P.G., Fankhauser, A., Kramers, J.D., 1996. Two thousand years of atmospheric arsenic, antimony, and lead deposition recorded in an ombrotrophic peat bog profile, Jura Mountains, Switzerland. Earth Planet. Sci. Lett. 145, E1–E7. https://doi.org/10.1016/S0012-821X(96)00197-5

Shotyk, W., Krachler, M., 2004. Atmospheric deposition of silver and thallium since 12370 14 C years BP recorded by a Swiss peat bog profile, and comparison with lead and cadmium. J. Environ. Monit. 6, 427–433.

Shotyk, W., Krachler, M., Chen, B., 2004. Antimony in recent, ombrotrophic peat from Switzerland and Scotland: Comparison with natural background values (5,320 to 8,020 14 C yr BP) and implications for the global atmospheric Sb cycle. Global Biogeochem. Cycles 18. https://doi.org/10.1029/2003GB002113

Shotyk, W., Krachler, M., Martinez-Cortizas, A., Cheburkin, A.K., Emons, H., 2002. A peat bog record of natural, pre-anthropogenic enrichments of trace elements in atmospheric aerosols since 12 370 14 C yr BP, and their variation with Holocene climate change. Earth Planet. Sci. Lett. 199, 21–37. https://doi.org/10.1016/S0012-821X(02)00553-8

Shotyk, W., Nesbitt, H.W., Fyfe, W.S., 1992. Natural and antropogenic enrichments of trace metals in peat profiles. Int. J. Coal Geol. 20, 49–84. https://doi.org/https://doi.org/10.1016/0166-5162(92)90004-G

Shotyk, W., Weiss, D., Appleby, P.G., Cheburkin, A.K., Frei, R., Gloor, M., Kramers, J.D., Reese, S., Van der Knaap, W.O., 1998. History of atmospheric lead depostion since 12,37014C yr BP from a Peat bog, Jura Mountains, Switzerland. Science (80-.). 281, 1635–1640. https://doi.org/10.1126/science.281.5383.1635

Shotyk, W., Weiss, D., Kramers, J.D., Frei, R., Cheburkin, A.K., Gloor, M., Reese, S., 2001. Geochemistry of the peat bog at Etang de la Gruère, Jura Mountains, Switzerland, and its record of atmospheric pb and lithogenic trace metals (Sc, Ti, Y, Zr, and REE) since 12,37014C yr bp. Geochim. Cosmochim. Acta 65, 2337–2360. https://doi.org/10.1016/S0016-7037(01)00586-5

Shuttleworth, E.L., Evans, M.G., Hutchinson, S.M., Rothwell, J.J., 2014. Assessment of lead contamination in peatlands using field portable XRF. Water. Air. Soil Pollut. 225. https://doi.org/10.1007/s11270-013-1844-2

Sigl, M., Winstrup, M., McConnell, J.R., Welten, K.C., Plunkett, G., Ludlow, F., Büntgen, U., Caffee, M., Chellman, N., Dahl-Jensen, D., 2015. Timing and climate forcing of volcanic eruptions for the past 2,500 years. Nature 523, 543. https://doi.org/10.1038/nature14565

Sjögren, P., Knaap, W.O. Van Der, Leeuwen, J.F.N. Van, Andrič, M., Grünig, a, 2007. The occurrence of an upper decomposed peat layer, or "kultureller Trockenhorizont", in the Alps and Jura Mountains. Mires Peat 2, 1-14 ST-The occurrence of an upper decomposed p. https://doi.org/Mires and Peat, Volume 2 (2007), Article 05, http://www.mires-and-peat.net/, ISSN 1819-754X

Sjörs, H., 1980. Peat on earth: multiple use or conservation? Ambio 303–308.

Springhorn, R., 2007. Geology of the Engadine Window, especially the upper Val Fenga (East Switzerland) [Geologie des Engadiner Fensters unter besonderer Berücksichtigung des oberen Val Fenga (Ost-Schweiz)]. Zeitschrift der Dtsch. Gesellschaft für Geowissenschaften 158, 67–87. https://doi.org/10.1127/1860-1804/2007/0158-0067

State of Tyrol, 2019a. Aerial photography 2010 [WWW Document]. Laser- & Luftbildatlas Tirol. URL https://portal.tirol.gv.at/LBAWeb/luftbilduebersicht.show (accessed 2.28.19).

State of Tyrol, 2019b. digitales Geländemodell / digital elevation model [WWW Document]. TIRIS. URL https://maps.tirol.gv.at/ (accessed 9.27.18).

State of Tyrol, 2019c. Aerial photography 1974 [WWW Document]. Laser- & Luftbildatlas Tirol. URL https://portal.tirol.gv.at/LBAWeb/luftbilduebersicht.show (accessed 2.28.19).

State of Vorarlberg, 2018a. VoGIS, Vorarlberg Atlas [WWW Document]. Urmappe 1857. URL http://vogis.cnv.at/ (accessed 8.17.18).

State of Vorarlberg, 2018b. Aerial photo 1980. VoGIS.

Staudt, M., 2011. Rätisches Haus in Wenns. Fundbericihte aus Österreich 49, 144–165.

Staudt, M., Tomedi, G., 2015. Zur Besiedlungsgeschichte der Ostalpen in der Mittel-bis Spätbronzezeit: Bestand, Kolonisation und wirtschaftlicher Neuanfang in der mittleren und späten Bronzezeit in Nordtirol, in: Stöllner, T., Oeggl, K. (Eds.), Bergauf Bergab. 10.000 Jahre Bergbau in Den Ostalpen. Deutsches Bergbau-Museum Bochum, Bochum, pp. 135–144.

Steiner, G.M., 2005. Die Moorverbreitung in Österreich. Moore von Sib. bis Feuerland. Stapfia 85, 55–96.

Stetzenbach, K.J., Amano, M., Kreamer, D.K., Hodge, V.F., 1994. Testing the Limits of ICP-MS: Determination of Trace Elements in Ground Water at the Part-Per-Trillion Level. Groundwater 32, 976–985.

Stivrins, N., Ozola, I., Gałka, M., Kuske, E., Alliksaar, T., Andersen, T.J., Lamentowicz, M., Wulf, S., Reitalu, T., 2017. Drivers of peat accumulation rate in a raised bog: impact of drainage,

climate, and local vegetation composition. Mires Peat 19, UNSP 08. https://doi.org/10.19189/MaP.2016.OMB.262

Stojakowits, P., 2014. Pollenanalytische Untersuchungen zur Rekonstruktion der Vegetationsgeschichte im südlichen Iller-Wertach-Jungmoränengebiet seit dem Spätglazial (PhD-Thesis). Universität Augsburg.

Stöllner, T., 2015a. Der Mitterberg als Großproduzent für Kupfer in der Bronzezeit, in: Stöllner, T., Oeggl, K. (Eds.), Bergauf Bergab. 10.000 Jahre Bergbau in Den Ostalpen. Deutsches Bergbau-Museum Bochum, Bochum, pp. 175–186.

Stöllner, T., 2015b. die alpinen Kupfererzreviere: Aspekte ihrer zeitlichen, technologischen und wirtschaftlichen Entwicklung im zweiten Jahrtausend vor christus, in: Stöllner, T., Oeggl, K. (Eds.), Bergauf Bergab. 10.000 Jahre Bergbau in Den Ostalpen. Deutsches Bergbau-Museum Bochum, Bochum, pp. 99–104.

Stöllner, T., Oeggl, K., 2015. Bergauf Bergab. 10.000 Jahre Bergbau in den Ostalpen. Deutsches Bergbau-Museum Bochum, Bochum.

Succow, M., 2012. Kurzer Abriß der Nutzungsgeschichte mitteleuropäischer Moore, in: Joosten, H.. M.S.H. (Ed.), Landschaftsökologische Moorkunde. Schweizerbart Science Publishers, Stuttgart, Germany, pp. 404–406.

Suter, P.J., Hafner, A., Glauser, K., 2005. Lenk-Schnidejoch. Funde aus dem Eis–ein vor-und frühgeschichtlicher Passübergang. Archäologie im Kant. Bern 6, 499–522.

Swindles, G.T., De Vleeschouwer, F., Plunkett, G., 2010. Dating peat profiles using tephra : stratigraphy , geochemistry and chronology 7, 1–9.

swisstopo, 2018a. GeoCover datasets V2 1:25000, Compilation, Samnau-Ischgl, nr.1179. Geocover.

swisstopo, 2018b. SWISSIMAGE Orthofoto [WWW Document]. SWISSIMAGE. URL https://map.geo.admin.ch/ (accessed 1.28.18).

Sydow, W., 1995. Der hallstattzeitliche Bronzehort von Fliess im Oberinntal, Tirol, Fundberichte aus Österreich, Materialhefte A. Berger.

Tahvanainen, T., 2011. Abrupt ombrotrophication of a boreal aapa mire triggered by hydrological disturbance in the catchment. J. Ecol. no-no. https://doi.org/10.1111/j.1365-2745.2010.01778.x

Tasser, E., Walde, J., Tappeiner, U., Teutsch, A., Noggler, W., 2007. Land-use changes and natural reforestation in the Eastern Central Alps. Agric. Ecosyst. Environ. 118, 115–129. https://doi.org/https://doi.org/10.1016/j.agee.2006.05.004

Theurillat, J.-P., Guisan, A., 2001. Potential impact of climate change on vegetation in the European Alps: a review. Clim. Change 50, 77–109.

Thevenon, F., Guédron, S., Chiaradia, M., Loizeau, J.-L., Poté, J., 2011. (Pre-) historic changes in natural and anthropogenic heavy metals deposition inferred from two contrasting Swiss Alpine lakes. Quat. Sci. Rev. 30, 224–233. https://doi.org/10.1016/j.quascirev.2010.10.013

Thomas, E.R., Wolff, E.W., Mulvaney, R., Steffensen, J.P., Johnsen, S.J., Arrowsmith, C., White, J.W.C., Vaughn, B., Popp, T., 2007. The 8.2 ka event from Greenland ice cores. Quat. Sci. Rev. 26, 70–81.

Tilly, R.H., 2010. Industrialization as an historical process [WWW Document]. Eur. Hist. Online.

URL www.ieg-ego.eu/tillyr-2010-en (accessed 1.23.19).

Tinner, W., Ammann, B., 2001. Timberline paleoecology in the Alps. Pages News 9, 9–11.

Tinner, W., Kaltenrieder, P., 2005. Rapid responses of high-mountain vegetation to early Holocene environmental changes in the Swiss Alps. J. Ecol. 93, 936–947.

Tinner, W., Lotter, A.F., Ammann, B., Conedera, M., Hubschmid, P., Van Leeuwen, J.F.N., Wehrli, M., 2003. Climatic change and contemporaneous land-use phases north and south of the Alps 2300 BC to 800 AD. Quat. Sci. Rev. 22, 1447–1460. https://doi.org/10.1016/S0277-3791(03)00083-0

Tjallingii, R., Röhl, U., Kölling, M., Bickert, T., 2007. Influence of the water content on X-ray fluorescence corescanning measurements in soft marine sediments. Geochemistry, Geophys. Geosystems 8, 1–12. https://doi.org/10.1029/2006GC001393

Töchterle, U., 2015. Die Besiedlungsgeschichte der Ostalpen in der Früh- bis Mittelbronzezeit: Kolonisation und wirtschaftlicher Neuanfang. Teil 2, in: Stöllner, T., Oeggl, K. (Eds.), Bergauf Bergab. 10.000 Jahre Bergbau in Den Ostalpen. Deutsches Bergbau-Museum Bochum, Bochum, pp. 129–134.

Tolonen, K., 1984. Interpretation of changes in the ash content of ombrotrophic peat layers. Bull. Geol. Soc. Finl. 56, 207–219.

Tomedi, G., 2012. Der mittelbronzezeitliche Schatzfund vom Piller., in: Hansen, S., Neumann, D., Vachta, T. (Eds.), Hort Und Raum: Aktuelle Forschungen Zu Bronzezeitlichen Deponierungen in Mitteleuropa. Walter de Gruyter, Berlin, pp. 151–168.

Tomedi, G., 2002a. Zur Datierung des Depotfundes vom Piller 4.

Tomedi, G., 2002b. Hinweise zu einem lokalen Bronzehandwerk aus dem Depotfund vom Moosbruckschrofen am Piller. Archaeo Tirol. Kleine Schriften 4 - Schriften zur Archäologischen Landeskd. Tirols 4, 77–82.

Tomedi, G., Castellan, S.N., Lachberger, R., 2009. Denkmalschutzgrabungen am bronzezeitlichen Haus von Fliess-Silberplan, Jahresbericht. Das Zentrum für Alte Kulturen. Innsbruck, Austria.

Tomedi, G., Staudt, M., Töchterle, U., 2013. Zur Bedeutung des prähistorischen Bergbaus auf Kupfererze im Raum Schwaz-Brixlegg, in: Oeggl, K., Schaffer, V. (Eds.), Cuprum Tyrolense - 5550 Jahre Bergbau Und Kupferverhüttung in Tirol. Edition Tirol, pp. 55–70.

Town of Ischgl, 2019. Abriss der Chronik [WWW Document]. URL http://www.ischgl.tirol.gv.at/Abriss_der_Chronik (accessed 1.25.19).

Trimble, S.W., Mendel, A.C., 1995. The cow as a geomorphic agent — A critical review, in: Hupp, C.R., Osterkamp, W.R., Howard, A.D. (Eds.), Biogeomorphology, Terrestrial and Freshwater Systems. Elsevier, Amsterdam, pp. 233–253. https://doi.org/https://doi.org/10.1016/B978-0-444-81867-6.50019-8

Tropper, P., Bechter, D., Zambanini, J., Kaindl, R., Vavtar, F., Lutz, J., 2011. Montangeschichte, Mineralogie, Geochemie und Petrologie der Kupferlagerstätte Bartholomäberg/Silbertal (Montafon, Vorarlberg). Geo. Alp 8, 20–44.

Tschurtschenthaler, M., Wein, U., 1998. Das Heiligtum auf der Pillerhöhe und seine Beziehungen zur Via Claudia Augusta, in: Walde, E. (Ed.), Via Claudia : Neue Forschungen. Innsbruck : Inst. für Klassische Archäologie, Innsbruck, pp. 227–259.

Tschurtschenthaler, M., Wein, U., 1996. Kontinuität und Wandel eines alpinen Heiligtums im

Laufe seiner 1.800-jährigen Geschichte. Archäologie Österreichs 5, 14–28.

Unkel, I., Fernandez, M., Björck, S., Ljung, K., Wohlfarth, B., 2010. Records of environmental changes during the Holocene from Isla de los Estados (54.4 S), southeastern Tierra del Fuego. Glob. Planet. Change 74, 99–113.

Urbina, J.C., Benavides, J.C., 2015. Simulated small scale disturbances increase decomposition rates and facilitates invasive species encroachment in a high elevation tropical Andean peatland. Biotropica 47, 143–151.

Valese, E., Conedera, M., Held, A.C., Ascoli, D., 2014. Fire, humans and landscape in the European Alpine region during the Holocene. Anthropocene 6, 63–74. https://doi.org/10.1016/j.ancene.2014.06.006

Van Breemen, N., 1995. How Sphagnum bogs down other plants. Trends Ecol. Evol. 10, 270–275. https://doi.org/10.1016/0169-5347(95)90007-1

Van der Knaap, W.O., van Leeuwen, J.F.N., Ammann, B., 2004. The first rise and fall of Fagus sylvatica and interactions with Abies alba at Faulenseemoos (Weiss Plateau) 6900–6000 cal yr BP. Acta Palaeobot 44, 249–266.

van der Plicht, J., 2005. Radiocarbon, the Calibration Curve and Scythian Chronology, in: Marian Scott, E., Alekseev, A.Y., Zaitseva, G. (Eds.), Impact of the Environment on Human Migration in Eurasia. Springer Netherlands, Dordrecht, pp. 45–61.

Van Geel, B., 1978. A palaeoecological study of Holocene peat bog sections in Germany and the Netherlands, based on the analysis of pollen, spores and macro-and microscopic remains of fungi, algae, cormophytes and animals. Rev. Palaeobot. Palynol. 25, 1–120.

Vanneste, H., De Vleeschouwer, F., Martínez-Cortizas, A., von Scheffer, C., Piotrowska, N., Coronato, A., Le Roux, G., 2015. Late-glacial elevated dust deposition linked to westerly wind shifts in southern South America. Sci. Rep. 5. https://doi.org/10.1038/srep11670

Vavtar, F., 1988. Die Erzanreicherungen im Nordtiroler Stubai-, Ötztal- und Silvrettakristallin, in: Archiv Für Lagerstättenforschung. Archiv für Lagerstättenforschung. Geologisches Bundesamt Österreich, Wien, pp. 103–153.

Vermeersch, P., Paulissen, E., 1993. Palaeolithic chert quarrying and mining in Egypt.

Véron, A., Goiran, J.P., Morhange, C., Marriner, N., Empereur, J.Y., 2006. Pollutant lead reveals the pre-Hellenistic occupation and ancient growth of Alexandria, Egypt. Geophys. Res. Lett. 33, L06409. https://doi.org/10.1029/2006GL025824

Viehweider, B., Feichter-Haid, A., Koch Waldner, T., Masur, A., 2013. Mining-related land use changes since the Neolithic in the region of Kitzbühel (Tyrol). Metalla 20, 52–55.

Vile, M. a, Wieder, R.K., Novák, M., 1999. Mobility of Pb in Sphagnum -derived peat 35–52.

Vitt, D.H., Chee, W.-L., 1990. The relationships of vegetation to surface water chemistry and peat chemistry in fens of Alberta, Canada. Vegetatio 89, 87–106.

Völk, H.R., 2001. Geomorphologie des Kleinwalsertales und seiner Gebirgsumrahmung. Landschaftsformen zur Eiszeit und Nacheiszeit unter Einbeziehung der geologischen Verhältnisse. Vor. Naturschau 10, 7–95.

Vollweiler, N., Scholz, D., Mühlinghaus, C., Mangini, A., Spötl, C., 2006. A precisely dated climate record for the last 9 kyr from three high alpine stalagmites, Spannagel Cave, Austria. Geophys. Res. Lett. 33, 1–5. https://doi.org/10.1029/2006GL027662

von Gümbel, C.W., 1861. Geognostische Beschreibung des Königreichs Bayern: Geognostische

Beschreibung des bayerischen Alpengebirges und seines Vorlandes. bayer. Staatsministerium der der Finanzen., Gotha.

von Klebelsberg, R., 1939. Nutzbare Bodenvorkommnisse in Nordtirol. Veröff. d. Museum Ferdinandeum Innsbruck, Bd 19, 1–56.

von Raiser, J.N., 1830. Der Ober-Donau-Kreis des Königreichs Bayern unter den Römern. Die Römer-Male von Augusta rauracum bis Augusta Vindelicorum: 1. Kranzfelder, Augsburg.

von Srbik, R., 1929. Überblick des Bergbaues von Tirol und Vorarlberg in Vergangenheit und Gegenwart. Bericht des naturwissenschaftlich - medizinischen Vereins zu Innsbruck 41, 113–277.

Vorren, K.-D., Mørkved, B., Bortenschlager, S., 1993. Human impact on the Holocene forest line in the Central Alps. Veg. Hist. Archaeobot. 2, 145–156. https://doi.org/10.1007/BF00198585

Wagner, G., 1950. Rund um Hochifen und Gottesackergebiet. Verlag der Hohenloheschen Buchhandlung Ferdinand Rau, Öhringen.

Wahlmüller, N., 2002. Die Komperdellalm im Wandel der Jahrtausende. Ein Beitrag zur Vegetationsund Besiedlungsgeschichte des Oberen Gerichts, in: Klien, R. (Ed.), Serfaus. Athesia-Tyrolia Druck GmbH, Innsbruck: Gemeinde Serfaus, pp. 71–83.

Walde, C., 2006. Die Vegetations-und Siedlungsgeschichte im Oberen Gericht-Pollenanalytische Untersuchungen des Plemun-Weihers (Fließ, Tirol), in: Walde, E., Grabherr, G. (Eds.), Via Claudia Augusta Und Römerstraßenforschung Im Östlichen Alpenraum. Ikarus 1. Innsbruck University Press, pp. 394–407.

Walde, C., Oeggl, K., 2004. Neue Ergebnisse zur Siedlungsgeschichte am Tannberg. Die Pollenanalysen aus dem Körbersee. Walserheimat Vor. , Tirol und Liechtenstein 75, 4–7.

Walde, C., Oeggl, K., 2003. Blütenstaub enthüllt 3000-jährige Siedlungsgeschichte im Tannberggebiet. Walserheimat Vor. , Tirol und Liechtenstein 73, 1–6.

Walser, C., 2012. Kalt-Warm. Klima und Besiedlungsdynamik in der Silvretta, in: Reitmaier, T. (Ed.), Letzte Jäger, Erste Hirten - Hochalpine Archäologie in Der Silvretta. Archäologischer Dienst Graubünden, Chur, pp. 205–218.

Walser, C., Lambers, K., 2012. Human Activity in the Silvretta Massif and Climatic Developments throughout the Holocene. Landsc. Archaeol. Proc. Int. Conf. Held Berlin, 6th - 8th June 2012 (eTopoi. J. Anc. Stud. Spec. Vol. 3) 3, 55–62.

Wang, M., Moore, T.R., Talbot, J., Riley, J.L., 2015. The stoichiometry of carbon and nutrients in peat formation. Global Biogeochem. Cycles 29, 113–121. https://doi.org/10.1002/2014GB005000

Wardenaar, E.C.P., 1987. A new hand tool for cutting peat profiles. Can. J. Bot. 65, 1772–1773.

Weber, L., 1997. Die neue Metallogenetische Karte von Osterreich 1: 500 000 unter Einbeziehung der Industrieminerale und Energierohstoffe. Bhm-b. und Huttenmann. Monatshefte 142, 420–424.

Weber, L., Cerny, I., Ebner, F., Fritz, I., Göd, R., Götzinger, M.A., Gräf, W., Paar, W.H., Prohaska, W., Sachsenhofer, R.F., 1997. Metallogenetische Karte von Österreich 1: 500.000. Arch. für Lagerstättenforsch.

Weber, M., 1995. Die frühe und mittlere römische Kaiserzeit, in: Czysz, W., Dietrich, H., Weber, G. (Eds.), Kempten Und Das Allgäu. Führer Zu Archäologischen Denkmälern in

Deutschland 30. Theiss, Stuttgart, pp. 49–60.

Weiss, D., Shotyk, W., Appleby, P.G., Kramers, J.D.A.N.D., Cheburkin, A.K., Weiss, D., Shotyk, W., Appleby, P.G., Kramers, J.D.A.N.D., Cheburkin, A.K., Weiss, D., Shotyk, W., Appleby, P.G., Kramers, J.D.A.N.D., Cheburkin, A.K., 1999. Atmospheric Pb deposition since the industrial revolution recorded by five Swiss peat profiles: Enrichment factors, fluxes, isotopic composition, and sources. Environ. Sci. Technol. 33, 1340–1352. https://doi.org/10.1021/es980882q

Weiss, D., Shotyk, W., Cheburkin, A.K., Gloor, M., Reese, S., 1997. Atmospheric Lead Deposition from 12,400 to ca. 2,000 yrs BP in a Peat Bog Profile, Jura Mountains, Switzerland. Water. Air. Soil Pollut. 100, 311–324. https://doi.org/10.1023/A:1018341029549

Weltje, G.J., Bloemsma, M.R., Tjallingii, R., Heslop, D., Röhl, U., Croudace, I.W., 2015. Prediction of geochemical composition from XRF core scanner data: a new multivariate approach including automatic selection of calibration samples and quantification of uncertainties, in: Micro-XRF Studies of Sediment Cores. Springer, pp. 507–534.

Weltje, G.J., Tjallingii, R., 2008. Calibration of XRF core scanners for quantitative geochemical logging of sediment cores: theory and application. Earth Planet. Sci. Lett. 274, 423–438.

Wick, L., Tinner, W., 1997. Vegetation Changes and Umbertine Fluctuations in the Central Alps as Indicators of Holocene Climatic Oscillations. Arct. Alp. Res. 29, 445–458. https://doi.org/10.2307/1551992

Willand, D., Amann, A., 2013. “Das Buoch soll Kraft und Macht haben”. Alpbücher im Kleinwalsertal 1541-1914. Brüüg, Riezlern/Kleinwalsertal.

Winckler, K., 2012. Die Alpen im Frühmittelalter: die Geschichte eines Raumes in den Jahren 500 bis 800. Böhlau.

Wolkersdorfer, C., 1991. Geschichte des Bergbaus im westlichen Mieminger Gebirge/Tirol. Aufschluss 42, 359–379.

Woodland, W.A., Charman, D.J., Sims, P.C., 1998. Quantitative estimates of water tables and soil moisture in Holocene peatlands from testate amoebae. Holocene 8, 261–273. https://doi.org/10.1191/095968398667004497

Wurth, G., Niggemann, S., Richter, D.K., Mangini, A., 2004. The Younger Dryas and Holocene climate record of a stalagmite from Hölloch Cave (Bavarian Alps, Germany). J. Quat. Sci. 19, 291–298. https://doi.org/10.1002/jqs.837

Wyllie, D.C., 2014. Rock fall engineering. CRC Press.

Yeloff, D., Van Geel, B., 2007. Abandonment of farmland and vegetation succession following the Eurasian plague pandemic of ad 1347–52. J. Biogeogr. 34, 575–582.

Yu, Z., Loisel, J., Brosseau, D.P., Beilman, D.W., Hunt, S.J., 2010. Global peatland dynamics since the Last Glacial Maximum 37, 1–5. https://doi.org/10.1029/2010GL043584

Zaccone, C., Cocozza, C., Cheburkin, A.K., Shotyk, W., Miano, T.M., 2008. Distribution of As, Cr, Ni, Rb, Ti and Zr between peat and its humic fraction along an undisturbed ombrotrophic bog profile (NW Switzerland). Appl. Geochemistry 23, 25–33. https://doi.org/10.1016/j.apgeochem.2007.09.002

Zacher, W., 1990. Geologische Karte von Österreich: Blatt 113 Mittelberg 1:50000. Geologische Bundesanstalt, Wien.

ZAMG, 2018. ZAMG [WWW Document]. Klimadaten von Österreich, 1971 - 2000. URL http://www.zamg.ac.at/fix/klima/oe71-00/klima2000/klimadaten_oesterreich_1971_frame1.htm (accessed 9.24.18).

Zemmer-Plank, L., 1992. Ein Waffenopfer der Fritzens-Sanzeno-Kultur in Wenns im Pitztal. Veröffentlichungen des Tiroler Landesmuseum 72, 231–249.

Zerbe, S., Steffenhagen, P., Parakenings, K., Timmermann, T., Frick, A., Gelbrecht, J., Zak, D., 2013. Ecosystem service restoration after 10 years of rewetting peatlands in NE Germany. Environ. Manage. 51, 1194–1209. https://doi.org/10.1007/s00267-013-0048-2

Zhou, P., Yan, H., Gu, B., 2005. Competitive complexation of metal ions with humic substances. Chemosphere 58, 1327–1337.

Zoller, H., Erny-Rodmann, C., Punchakunnel, P., 1996. The history of vegetation and land use in the Lower Engadine (Switzerland). Pollen records of the last 13000 years. Natl. der Schweiz.

Zwicker, U., 1989. Untersuchungen zur Herstellung von Kupfer und Kupferlegierungen im Bereich des östlichen Mittelmeeres (3500-1000 v. Chr.), in: Hauptmann, A., Pernicka, E., Wagner, G.A. (Eds.), Old world archaeometallurgy : proceedings of the International Symposium “Old World Archaeometallurgy,” Heidelberg 1987. Selbstverlag des Deutschen Bergbau-Museums, Bochum, pp. 191–201.

10 Annex

*Suppl. Table 1: Quality control by measurements of organic CRMs by ICP-MS. Element concentrations. certified concentrations (Cert.in mg*kg^{-1}) and deviations from the certified value (Dev in %). Values in orange are indicative or informative. Grey highlighted columns = separate ICP-MS run. NA = no value.*

	Unit	GBW 07603 (a)	GBW 07603 (b)	GBW 07603 (c)	GBW 07603 (d)	NIST 1515 (a)	NIST 1515 (b)	NIST 1515 (c)	NIST 1547a (a)	NIST 1547a (b)	NJV 941 (a)	NJV 941 (b)	NJV 941 (c)	NJV 941 (d)	NJV 942 (a)	NJV 942 (b)	NJV 942 (c)	NJV 942 (d)
Al	[mg*kg^{-1}]	1701.1	1777.8	1854.4	2004.0	277.1	266.1	300.8	242.9	265.2	1014.0	855.6	849.7	1635.7	832.6	820.1	809.0	838.4
Cert.	[mg*kg^{-1}]	2000	2000	2000	2000	286	286	286	249	249	900	900	900	900	950	950	950	950
Dev	[%]	-14.9	-11.1	-7.3	0.2	-3.1	-7.0	5.2	-2.4	6.5	12.7	-4.9	-5.6	81.8	-12.4	-13.7	-14.8	-11.7
As	[mg*kg^{-1}]	0.89	0.88	0.91	1.02	0.21	0.21	0.20	0.14	0.12	2.53	2.50	2.61	2.73	0.51	0.52	0.54	0.52
Cert.	[mg*kg^{-1}]	1.25	1.25	1.25	1.25	NA	NA	NA	0.06	0.06	NA	NA	NA	NA	NA	NA	NA	NA
Dev	[%]	-29.0	-29.5	-27.3	-18.0	NA	NA	NA	133.1	96.0	NA	NA	NA	NA	NA	NA	NA	NA
Ca	[mg*kg^{-1}]	16143	16696	15914	17037	14216	13900	15210	14652	15324	8766	8743	8689	9272	1262	1232	1181	1695
Cert.	[mg*kg^{-1}]	16800	16800	16800	16800	15250	15250	15250	15600	15600	10200	10200	10200	10200	1200	1200	1200	1200
Dev.	[%]	-3.9	-0.6	-5.3	1.4	-6.8	-8.8	-0.3	-6.1	-1.8	-14.1	-14.3	-14.8	-9.1	5.2	2.7	-1.6	41.3
Cr	[mg*kg^{-1}]	2.4	2.2	3.6	3.5	0.6	0.5	0.9	1.3	2.1	2.0	1.2	1.7	2.1	1.4	1.4	1.2	2.2
Cert.	[mg*kg^{-1}]	2.6	2.6	2.6	2.6	0.3	0.3	0.3	1	1	NA	NA	NA	NA	NA	NA	NA	NA
Dev	[%]	-9.5	-15.4	36.9	34.3	84.5	74.4	188.1	32.9	107.2	NA	NA	NA	NA	NA	NA	NA	NA
Cu	[mg*kg^{-1}]	5.84	5.64	5.51	5.35	5.09	5.00	4.74	3.38	3.16	1.48	1.36	1.66	1.29	1.47	1.33	1.38	1.38
Cert.	[mg*kg^{-1}]	6.6	6.6	6.6	6.6	5.69	5.69	5.69	3.75	3.75	2	2	2	2	1.7	1.7	1.7	1.7
Dev	[%]	-11.4	-14.6	-16.6	-19.0	-10.6	-12.1	-16.6	-9.8	-15.9	-26.0	-32.2	-16.8	-35.3	-13.3	-22.0	-18.9	-18.9
Fe	[mg*kg^{-1}]	1000.	1052.8	650.3	670.2	80.9	75.6	75.3	224.3	205.0	3108.3	3068.7	3184.3	2192.22	1063.9	1016.8	993.6	701.8
Cert.	[mg*kg^{-1}]	1070	1070	1070	1070	82.7	82.7	82.7	219.8	219.8	3900	3900	3900	3900	1300	1300	1300	1300
Dev	[%]	-6.5	-1.6	-39.2	-37.4	-2.1	-8.6	-9.0	2.1	-6.7	-20.3	-21.3	-18.4	-43.8	-18.2	-21.8	-23.6	-46.0
K	[mg*kg^{-1}]	9081	9384	9353	10076	14767	14506	16388	21993	24180	297	164	153	792	267	246	217	248
Cert.	[mg*kg^{-1}]	9200	9200	9200	9200	16100	16100	16100	24300	24300	NA	NA	NA	NA	NA	NA	NA	NA
Dev	[%]	-1.3	2.0	1.7	9.5	-8.3	-9.9	1.8	-9.5	-0.5	NA	NA	NA	NA	NA	NA	NA	NA

	Unit	GBW 07603 (a)	GBW 07603 (b)	GBW 07603 (c)	GBW 07603 (d)	NIST 1515 (a)	NIST 1515 (b)	NIST 1515 (c)	NIST 1547a (a)	NIST 1547a (b)	NJV 941 (a)	NJV 941 (b)	NJV 941 (c)	NJV 941 (d)	NJV 942 (a)	NJV 942 (b)	NJV 942 (c)	NJV 942 (d)
Mn	[mg*kg^{-1}]	59.23	62.50	64.61	67.42	47.07	46.97	80.95	87.28	96.48	28.52	28.82	28.71	46.68	7.57	8.17	8.04	11.41
Cert.	[mg*kg^{-1}]	61	61	61	61	54	54	54	98	98	36	36	36	36	8	8	8	8
Dev	[%]	-2.9	2.5	5.9	10.5	-12.8	-13.0	49.9	-10.9	-1.6	-20.8	-19.9	-20.3	29.7	-5.3	2.2	0.5	42.6
Nd	[mg*kg^{-1}]	0.95	0.87	0.83	0.95	15.06	15.66	15.84	6.61	6.49	0.76	0.71	0.80	0.80	0.75	1.61	0.75	0.73
Cert.	[mg*kg^{-1}]	1	1	1	1	17	17	17	7	7	NA	NA	NA	NA	NA	NA	NA	NA
Dev	[%]	-5.4	-12.6	-17.1	-5.3	-11.4	-7.9	-6.8	-5.6	-7.3	NA	NA	NA	NA	NA	NA	NA	NA
Ni	[mg*kg^{-1}]	1.42	1.51	2.03	2.12	1.06	0.94	1.02	0.77	1.24	1.78	1.36	1.88	2.31	0.91	0.87	1.26	1.06
Cert.	[mg*kg^{-1}]	1.7	1.7	1.7	1.7	0.936	0.936	0.936	0.69	0.69	NA	NA	NA	NA	NA	NA	NA	NA
Dev	[%]	-16.3	-11.4	19.7	24.4	13.1	0.1	8.6	12.2	79.1	NA	NA	NA	NA	NA	NA	NA	NA
Pb	[mg*kg^{-1}]	47.32	48.60	46.38	48.76	0.44	0.49	0.50	0.86	0.83	2.09	2.11	2.10	2.71	9.48	9.13	9.48	8.72
Cert.	[mg*kg^{-1}]	47	47	47	47	0.47	0.47	0.47	0.87	0.87	2.4	2.4	2.4	2.4	10.1	10.1	10.1	10.1
Dev.	[%]	0.7	3.4	-1.3	3.8	-5.7	3.7	7.2	-1.1	-4.5	-13.1	-11.9	-12.6	13.1	-6.1	-9.6	-6.2	-13.7
Rb	[mg*kg^{-1}]	3.8	3.9	3.9	4.1	8.7	8.8	9.4	17.4	18.1	0.8	0.4	0.4	2.0	0.6	0.8	0.7	0.7
Cert.	[mg*kg^{-1}]	4.5	4.5	4.5	4.5	10.2	10.2	10.2	19.7	19.7	NA	NA	NA	NA	NA	NA	NA	NA
Dev	[%]	-16.1	-12.8	-14.3	-9.2	-14.6	-13.8	-7.5	-11.6	-8.0	NA	NA	NA	NA	NA	NA	NA	NA
S	[mg*kg^{-1}]	6777.9	8012.2	NA	NA	1708.2	1752.3	NA	1528.2	NA	2690.2	2867.1	NA	NA	1931.4	1923.6	NA	NA
Cert.	[mg*kg^{-1}]	7300	7300	7300	7300	NA	NA	NA	NA	NA	2900	2900	2900	2900	2170	2170	2170	2170
Dev	[%]	-7.2	9.8	NA	NA	NA	NA	NA	NA	NA	-7.2	-1.1	NA	NA	-11.0	-11.4	NA	NA
Sb	[mg*kg^{-1}]	0.083	0.095	0.083	0.077	0.017	0.011	0.007	0.018	0.023	0.047	0.045	0.050	0.047	0.138	0.152	0.151	0.143
Cert.	[mg*kg^{-1}]	0.095	0.095	0.095	0.095	NA	NA	NA	NA	NA	NA	NA	NA	NA	NA	NA	NA	NA
Dev	[%]	-12.2	0.5	-12.4	-18.8	NA	NA	NA	NA	NA	NA	NA	NA	NA	NA	NA	NA	NA
Sc	[mg*kg^{-1}]	0.38	0.32	0.55	0.58	0.06	0.00	0.11	0.08	0.16	0.23	0.17	0.18	0.40	0.19	0.14	0.17	0.32
Cert.	[mg*kg^{-1}]	0.32	0.32	0.32	0.32	0.03	0.03	0.03	0.04	0.04	NA	NA	NA	NA	NA	NA	NA	NA
Dev	[%]	19.9	-0.6	71.2	79.8	94.8	-98.0	280.4	107.0	301.0	NA	NA	NA	NA	NA	NA	NA	NA

	Unit	GBW 07603 (a)	GBW 07603 (b)	GBW 07603 (c)	GBW 07603 (d)	NIST 1515 (a)	NIST 1515 (b)	NIST 1515 (c)	NIST 1547a (a)	NIST 1547a (b)	NJV 941 (a)	NJV 941 (b)	NJV 941 (c)	NJV 941 (d)	NJV 942 (a)	NJV 942 (b)	NJV 942 (c)	NJV 942 (d)
Sm	[mg*kg^{-1}]	0.19	0.18	0.16	0.19	2.66	2.70	2.79	1.03	1.03	0.14	0.15	0.14	0.14	0.12	0.32	0.12	0.12
Cert.	[mg*kg^{-1}]	0.19	0.19	0.19	0.19	3	3	3	1	1	NA	NA	NA	NA	NA	NA	NA	NA
Dev	[%]	-0.5	-4.7	-14.1	-0.4	-11.3	-10.0	-7.1	3.0	2.6	NA	NA	NA	NA	NA	NA	NA	NA
Sr	[mg*kg^{-1}]	238.0	247.2	238.6	247.2	22.3	22.4	37.1	50.4	56.2	32.0	31.8	32.28	53.5	15.9	15.1	15.8	24.3
Cert.	[mg*kg^{-1}]	246	246	246	246	25.1	25.1	25.1	53	53	NA	NA	NA	NA	NA	NA	NA	NA
Dev	[%]	-3.2	0.5	-3.0	0.5	-11.2	-10.7	47.7	-4.9	6.1	NA	NA	NA	NA	NA	NA	NA	NA
Ti	[mg*kg^{-1}]	92.1	90.2	92.0	93.4	13.3	12.4	13.4	24.1	24.6	34.5	33.6	27.1	26.9	51.8	115.2	49.6	49.5
Cert.	[mg*kg^{-1}]	95	95	95	95	NA	NA	NA	NA	NA	NA	NA	NA	NA	NA	NA	NA	NA
Dev.	[%]	-3.0	-5.1	-3.2	-1.7	NA	NA	NA	NA	NA	NA	NA	NA	NA	NA	NA	NA	NA
V	[mg*kg^{-1}]	1.98	2.07	2.33	2.39	0.24	0.19	0.29	0.33	0.36	1.47	1.27	1.29	1.41	1.16	1.29	1.16	1.20
Cert.	[mg*kg^{-1}]	2.4	2.4	2.4	2.4	0.254	0.254	0.254	0.367	0.367	NA	NA	NA	NA	NA	NA	NA	NA
Dev	[%]	-17.5	-13.7	-3.0	-0.5	-7.1	-26.5	13.7	-9.2	-1.1	NA	NA	NA	NA	NA	NA	NA	NA
Zn	[mg*kg^{-1}]	53.94	56.67	53.52	55.30	11.31	11.22	11.83	16.95	17.14	6.04	6.47	11.46	42.99	8.14	7.44	8.17	7.68
Cert.	[mg*kg^{-1}]	55	55	55	55	12.45	12.45	12.45	17.97	17.97	NA	NA	NA	NA	NA	NA	NA	NA
Dev	[%]	-1.9	3.0	-2.7	0.5	-9.2	-9.9	-5.0	-5.7	-4.6	NA	NA	NA	NA	NA	NA	NA	NA
Zr	[mg*kg^{-1}]	1.96	2.12	2.16	2.44	0.13	0.15	0.16	0.57	0.72	1.06	1.16	0.86	1.68	1.58	2.35	1.41	1.35
Cert.	[mg*kg^{-1}]	NA	NA	NA	NA	NA	NA	NA	NA	NA	NA	NA	NA	NA	NA	NA	NA	NA
Dev	[%]	NA	NA	NA	NA	NA	NA	NA	NA	NA	NA	NA	NA	NA	NA	NA	NA	NA

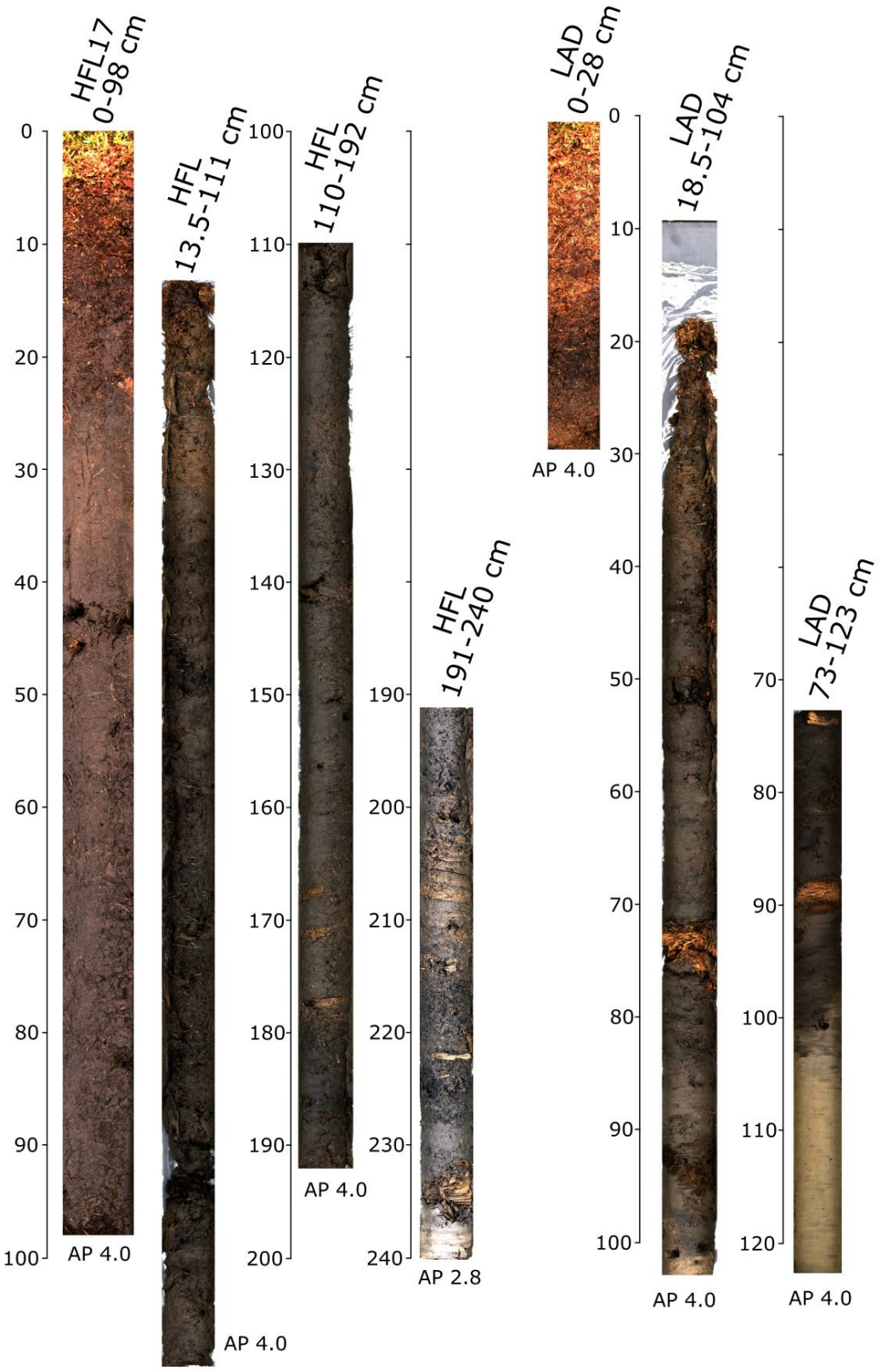

Suppl. Figure 1: Line-scans of Kleinwalser Valley core-sequences (HFL, LAD). AP= line-scan camera aperture.

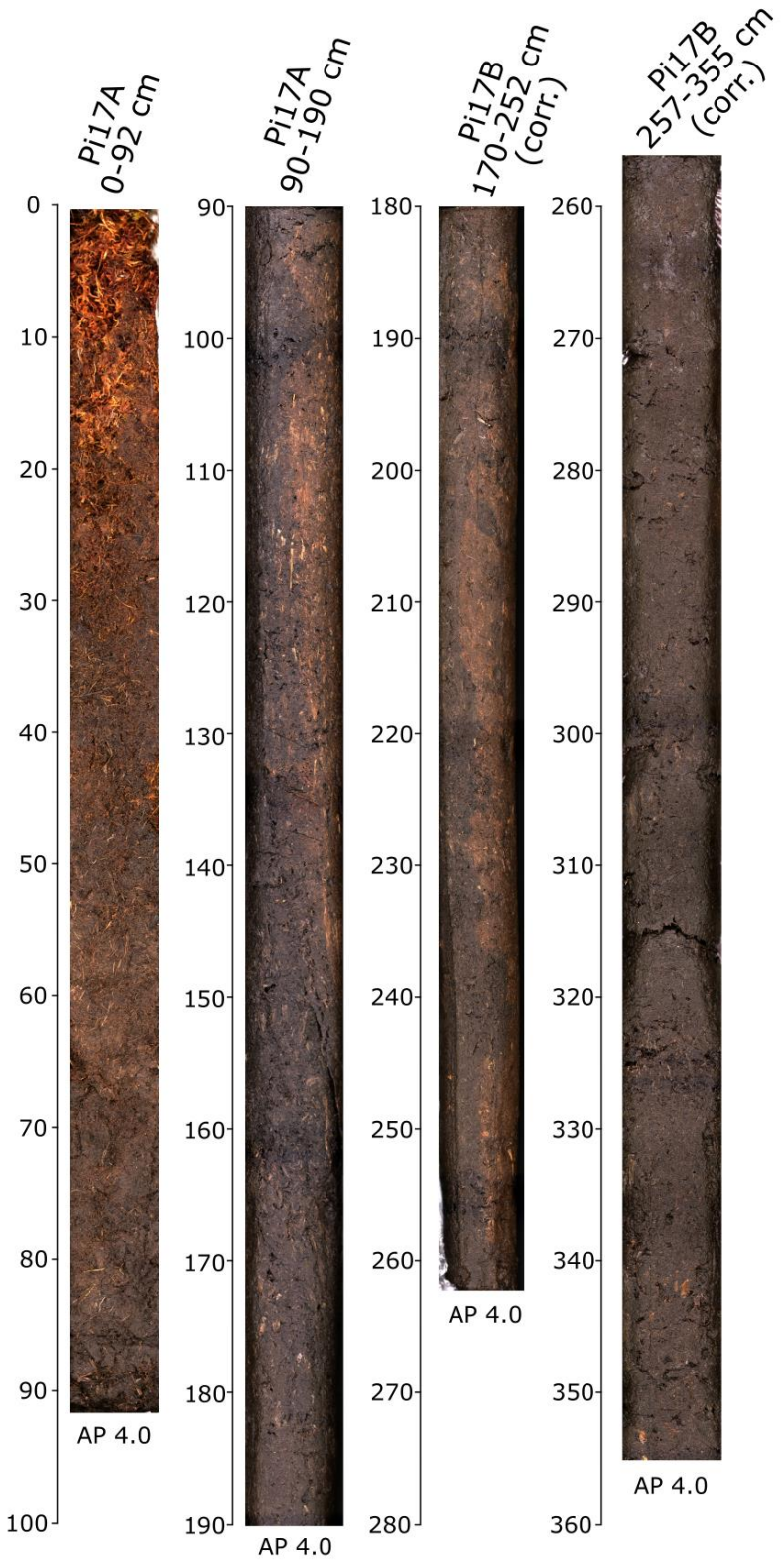

Suppl. Figure 2: Line-scans of a composite Pi17 core-sequences, with corrected depths for the lower part of core B. AP= line-scan camera aperture.

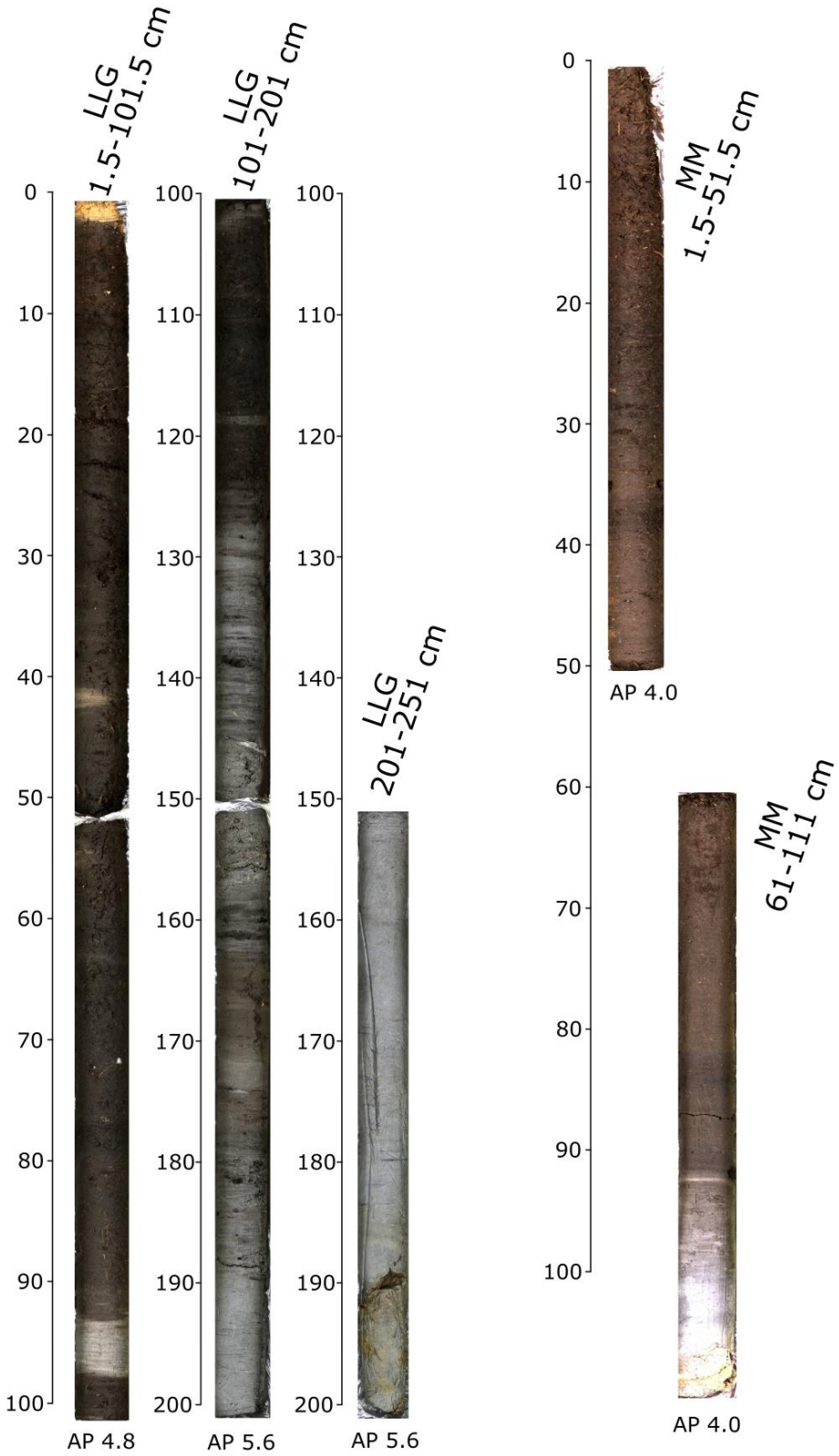

Suppl. Figure 3: Line-scans of Fimba Valley core-sequences (LLG, MM). AP= line-scan camera aperture.

Declaration

Herewith, the author of this dissertation (Clemens von Scheffer) declares and confirms the following:

1. Apart from the supervisors‘ guidance, the content and design of the thesis is all the doctoral researcher’s own work, only using the sources listed.
2. The thesis has been submitted neither partially nor wholly as part of a doctoral examination procedure to another examining body and has not been published or submitted for publication.
3. The thesis has been prepared subject to the Rules of Good Scientific Practice of thee German Research Foundation.
4. No academic degree has ever been withdrawn.

Date, signature